

UNIVERSITÉ DE MONTRÉAL

ANALYSE MÉCANIQUE ET THERMIQUE DES  
ADHÉSIFS ET DES JOINTS COLLÉS

MOHAMED OUDDANE  
DÉPARTEMENT DE GÉNIE MÉCANIQUE  
ÉCOLE POLYTECHNIQUE DE MONTRÉAL

THÈSE PRÉSENTÉE EN VUE DE L'OBTENTION  
DU DIPLÔME DE PHILOSOPHIEA DOCTOR (Ph.D)  
(GÉNIE MÉCANIQUE)

Décembre 1997

©Mohamed Ouddane, 1997



National Library  
of Canada

Acquisitions and  
Bibliographic Services

395 Wellington Street  
Ottawa ON K1A 0N4  
Canada

Bibliothèque nationale  
du Canada

Acquisitions et  
services bibliographiques

395, rue Wellington  
Ottawa ON K1A 0N4  
Canada

*Your file* *Votre référence*

*Our file* *Notre référence*

The author has granted a non-exclusive licence allowing the National Library of Canada to reproduce, loan, distribute or sell copies of this thesis in microform, paper or electronic formats.

The author retains ownership of the copyright in this thesis. Neither the thesis nor substantial extracts from it may be printed or otherwise reproduced without the author's permission.

L'auteur a accordé une licence non exclusive permettant à la Bibliothèque nationale du Canada de reproduire, prêter, distribuer ou vendre des copies de cette thèse sous la forme de microfiche/film, de reproduction sur papier ou sur format électronique.

L'auteur conserve la propriété du droit d'auteur qui protège cette thèse. Ni la thèse ni des extraits substantiels de celle-ci ne doivent être imprimés ou autrement reproduits sans son autorisation.

0-612-33017-6

UNIVERSITÉ DE MONTRÉAL

ÉCOLE POLYTECHNIQUE DE MONTRÉAL

Cette thèse intitulée

ANALYSE MÉCANIQUE ET THERMIQUE  
DES ADHÉSIFS ET DES JOINTS COLLÉS

présentée par : OUDDANE Mohamed  
en vue de l'obtention du diplôme de: Philosophica Doctor  
a été dûment acceptée par le jury d'examen constitué de:

M. Bernard SANSCHAGRIN, Ph.D., président  
M. Rachid BOUKHILI, Ph.D. membre et directeur de recherche  
M. Raymond GAUVIN, D.Sc.A., membre et co-directeur de recherche  
M. Bohislav FISA, Ph.D, membre  
M. Johanne DENAULT, Ph.D, membre

À mes parents  
À mes amis

## REMERCIEMENTS

Je tiens à exprimer ma vive reconnaissance à mon directeur de thèse, le professeur Rachid Boukhili, qui a accepté de diriger mon travail et pour ces nombreux conseils et discussions fructueuses tout au long de ce travail. Je lui exprime aussi ma gratitude pour le temps qu'il a consacré et pour l'aide qu'il m'a apportée dans la rédaction de ce mémoire. Je désire remercier le professeur Raymond Gauvin, codirecteur du Centre de recherche appliquée sur les polymères, et lui exprimer ma profonde reconnaissance pour l'accueil qu'il m'a réservé au sein de son équipe et son appui continué durant la durée de ce travail.

Je ne voudrais surtout pas oublier de mentionner les membres du CRASP pour leur contribution respective dans l'accomplissement de ce travail. Qu'il me soit permis de remercier tout particulièrement les techniciens du laboratoire de génie mécanique, en particulier monsieur François Morin, pour leur disponibilité et leurs conseils. Je remercie également M. François Robitaille, Benoit Goulet et Mohamed Abousaleh pour leurs encouragements et assistance pour la réalisation de ce travail.

Mes remerciements vont également à messieurs Bernard Sanschagrin et Bohuslav Fisa, tous deux professeurs au département de génie mécanique, et madame Johanne Denault, chercheuse à l'Institut des Matériaux Industriels, pour avoir accepté de faire partie du jury d'examen de cette thèse.

Finalement, je tiens à remercier les organismes qui ont contribué financièrement à

la réalisation de ce travail tels le CRSNG et le fonds FCAR.

## RÉSUMÉ

Au cours des dernières années, d'énormes efforts ont été consacrés pour le développement de nouvelles méthodes d'essai, ainsi que pour améliorer la durabilité des assemblages collés sous diverses conditions. Souvent, des problèmes pratiques sont soulevés sur la souhaitabilité des adhésifs, surtout pour les applications externes. Généralement, ces problèmes peuvent survenir à cause des changements climatiques de basses températures à moyennes. Définitivement, deux importants critères sont requis lors de la caractérisation mécanique des assemblages collés, soit la fiabilité des résultats et la simplicité de l'essai expérimental. Il est vraisemblable que ces critères sont irréconciliables dans la pratique. Par conséquent, deux principaux volets sont élaborés dans la présente étude, soit l'analyse mécanique et thermique des adhésifs et des joints collés.

Les adhésifs qui font l'objet de cette étude sont à base d'époxy modifié par ajout de deux types de charges: billes de verre (GB) et poudre céramique d'alumine (ACP) dont le taux volumique ( $V_f$ ) varie entre 0 et 30%. L'analyse mécanique et l'analyse thermique étaient effectuées sur l'adhésif sous forme de "Bulk" et sous forme de différents joints collés.

Dans la première phase, un montage de torsion est proposé pour mesurer les propriétés mécaniques des joints collés, adaptable aux machines de traction/compression conventionnelles, et en même temps génère des résultats fiables. Le mécanisme pour créer la torsion est basé sur deux barres servant de levier et disposées en croix, induisant un couple en vertu de leur mouvement de rotation opposé; chacune des deux barres s'insère dans une

des extrémités du spécimen. Pour des fins de validation, des jauges de déformation sont installées sur des spécimens pour détecter les déformations principales durant le chargement et par conséquent les contraintes parasites qui peuvent fausser les résultats. Finalement, deux méthodes d'essais normalisés, joints à mi-épaisseur et joints annulaires, sont effectuées en parallèle pour des fins de comparaison. L'étude de l'effet du taux de charge sur la résistance au cisaillement ( $\tau_u$ ) déterminé par des essais standard sur joint à mi-épaisseur (shear lap test) a montré qu'en augmentant le taux de charge,  $\tau_u$  augmente, atteint un maximum, puis chute pour de grands volumes de charge. La même tendance est obtenue avec le montage proposé avec, cependant, des valeurs de  $\tau_u$  plus élevées. Sachant que l'essai de joint à mi-épaisseur sous-estime la valeur de  $\tau_u$ , il était conclu que le montage de torsion développé est fiable et se trouve donc validé.

Dans une seconde phase, l'analyse mécanique dynamique (DMA), des essais de traction, joints à mi-épaisseur et joints annulaires en torsion ont été effectués concurremment pour élaborer l'effet de la quantité de la charge sur les caractéristiques de l'adhésif et des joints collés à base d'époxy. Il a été observé que le module élastique,  $E'$ , la température de transition vitreuse,  $T_g$ , des adhésifs étudiés sont augmentés avec l'ajout des charges. Par contre, la capacité d'amortissement maximale,  $\tan \delta$ , diminue significativement avec la quantité de la charge incorporée. Il est évident que l'ajout de charges a pour effet d'augmenter le module élastique et la réduction de la résistance mécanique. Quant aux essais de cisaillement des joints collés à mi-épaisseur et annulaire, la résistance mécanique de ces derniers augmente, atteint un maximum, puis chute pour de grand volume de charge. Ce maximum atteint dépend du type de la charge, il est de l'ordre de 10% de volume d'alumine



et de l'ordre de 20% de volume de billes de verre. Afin d'expliquer les comportements observés, le concept de rupture adhésive versus cohésive a été utilisé. Il a été remarqué que l'allure générale du comportement de la fraction surfacique de la rupture cohésive en fonction du volume de la charge ajoutée est le même que celui observé dans le cas de la résistance mécanique. En d'autres termes, la fraction surfacique de la rupture cohésive augmentait avec le volume de la charge, atteint un maximum, puis chute pour de grand volume de la charge. Curieusement, le maximum atteint est semblable à celui obtenu pour la résistance mécanique. Ces résultats confirment que le niveau atteint de la résistance mécanique des joints collés est relativement lié à la rupture cohésive produite.

Finalement, l'effet du type et de la quantité de la charge sur la performance et la durabilité des joints collés exposés à un environnement humide et chaud est étudié en utilisant concurremment l'essai de cisaillement à mi-épaisseur et l'analyse thermomécanique (TMA). Une méthodologie basée sur la TMA est proposée pour prédire la résistance mécanique des assemblages collés ayant subi un vieillissement. Il a été trouvé que les joints collés chargés d'alumine montrent une résistance mécanique relative supérieure à ceux à base de billes de verre. Ceux des joints collés non chargés ont retenu après vieillissement près de 85% de la résistance mécanique initiale. L'incorporation des charges d'alumine a amélioré la résistance mécanique relative de près de 100%. Par contre, l'ajout de billes de verre a réduit la résistance mécanique relative de près de 65%. Afin d'expliquer ces comportements, le coefficient d'expansion thermique (CTE) de joints miniatures est mesuré sous les mêmes conditions. L'utilisation de l'analyse thermomécanique dans ce cas a établi l'effet néfaste de l'humidité absorbée sur les adhésifs et les joints collés. Généralement, l'augmentation du

CTE des joints est en parfait accord avec la résistance mécanique relative des joints à mi-épaisseur après le vieillissement. En effet, l'augmentation du CTE semble induire des contraintes résiduelles qui, à leur tour, réduisent la résistance mécanique des joints collés. De la même manière, il a été trouvé que les adhésifs à base de billes de verre sont beaucoup plus susceptibles à l'eau chaude que les adhésifs chargés d'alumine, confirmant ainsi la réduction de la résistance mécanique de leurs joints collés.

## ABSTRACT

In the past years a considerable research effort has been directed toward the development of experimental methods of testing adhesive bonded joints, as well as, to improve the durability of the assembled constructions under various conditions. Many industries have reported some practical problems related either to the service life or the performance of adhesive bonded joints for outdoor applications where temperature changes are considerable. Some problems might arise from thermal cycling of environmental weathering from low to moderate temperatures. Actually, two main requirements are needed when dealing with mechanical characterization of bonded joints: the reliability of the results and ease of testing. It seems that reliability and ease of testing are irreconcilable in practice. The purpose of this work is two fold; mechanical and thermal analysis of adhesive bonded constructions.

In the present study, an epoxy based adhesive is used and modified by incorporating two types of fillers; glass beads (GB) and an alumina ceramic powder (ACP) with a volume content ( $V_f$ ) varying from 0 to 30%. The mechanical and thermal analysis were undertaken on Bulk adhesives and bonded joints of either step lap and Lap joint specimens.

First, the design of a simple torsion fixture for bonded joints is proposed which is adaptable to conventional testing machines, and at the same time gives reliable results. This is achieved by transforming a compression movement of a conventional machine, to a

torsional one on the bonded joints. The mechanism to create torsional loading on a bulk specimen or a bonded joint is based on the torque generated by two lever arms in a cross configuration moving in opposite rotational directions. The rotation of the lever arms is provided by the axial displacement of the cross-head of the uniaxial testing machine. Strain gaged specimens are tested to detect for possible extraneous stresses. Finally, experiments on bonded joints are performed and compared to step lap shear test. It is observed that both experiments showed the same trend, i.e, the shear strength increased as the filler content increased, reaching a maximum and then vanished. As a matter of fact, it can be argued that the proposed torsion apparatus is satisfactory for measuring the strength of napping ring bonded joints.

It seemed interesting to conduct a full analysis of the previous adhesives used in the first part of this work. Accordingly, dynamic mechanical analysis (DMA), tensile, step lap, and torsion shear tests are used concurrently to investigate the effect of filler content on the bulk, and adhesive joints properties of an epoxy based adhesives. It is shown from the DMA results, that the storage modulus,  $E'$ , and glass transition temperature,  $T_g$ , of the bulk material improve with filler content, while the maximum damping capacity,  $\tan \delta$ , decreases significantly. As expected, it is found that the tensile modulus increased, and the tensile strength decreased as the filler content increased. However, the shear strength, as measured with the bonded joints, is significantly improved with the introduction of fillers. This improvement reached a maximum at an intermediate filler content and then started to decrease. Furthermore, the maximum reached depends on the type of filler used, it is at 10%

volume for ACP filler, and nearly at 20% volume for glass beads. In order to explain these behaviors an adhesive versus cohesive failure concept is used. Interestingly, it is found that the general trend for the fraction of cohesive fracture surface is similar to that of the shear strength. In other terms, the fraction of cohesive fracture surface increased with the filler content, reaching a maximum and then decreased.

Finally, the effect of filler type and content on the performance and durability of adhesive bonded joints upon exposure to hot water is investigated, using concurrently step lap shear and thermo mechanical analysis (TMA) experiments. A TMA based approach is proposed in order to predict the strength of the bonded constructions. The same types of fillers used in the previous work are added to an epoxy adhesive. It is found that alumina filled adhesives showed a higher strength retention when compared to glass beads systems. The unfilled system retained about 85% of its initial strength, the introduction of alumina filler improved the strength retention to almost 100%, whereas, the addition of glass beads filler decreased the strength retention to about 65%. In order to explain such behaviors, the coefficient of thermal expansion (CTE) of small scale bonded joints are measured for the same conditions. It is demonstrated that valuable information can be extracted from TMA measurements. Generally, the increase of the CTE of the bonded joints are found to be in agreement with the strength retention of the step lap joints after exposure. The increase of the CTE of the bonded joints resulting from exposure to hot water seemed to increase the stresses, which in turn, affected the overall strength. Similarly, bulk adhesive results showed that GB filled systems are more susceptible to water than ACP filled ones, which in turn confirmed the decrease in strength of GB filled bonded constructions.

## TABLES DES MATIÈRES

<b>REMERCIEMENTS.....</b>	<b>v</b>
<b>RÉSUMÉ.....</b>	<b>vii</b>
<b>ABSTRACT.....</b>	<b>xi</b>
<b>TABLES DES MATIÈRES.....</b>	<b>xiv</b>
<b>LISTE DES TABLEAUX.....</b>	<b>xix</b>
<b>LISTE DES SIGLES ET ABRÉVIATIONS.....</b>	<b>xx</b>
<b>LISTE DES FIGURES.....</b>	<b>xxiv</b>
<b>CHAPITRE 1: INTRODUCTION GÉNÉRALE.....</b>	<b>1</b>
1.1 INTRODUCTION.....	1
1.2 REVUE BIBLIOGRAPHIQUE.....	5
1.2.1 Principes de l'adhésion.....	5
1.2.2 Mécanismes ou principes théoriques de l'adhésion.....	6
1.2.3 Analyse mécanique des joints collés.....	8
1.2.3.1 Essai de cisaillement par traction.....	9
1.2.3.2 Essai de pelage.....	10
1.2.3.3 Essai de clivage.....	10
1.2.3.4 Essai de cisaillement par torsion.....	11
1.2.4 Techniques pour prédire la résistance d'un joint collé.....	11
1.2.5 Appareil de torsion pour des joints collés.....	13
1.2.6 Prédiction de la résistance mécanique par les techniques d'analyse thermique.....	14

1.2.7 Appareils d'analyse thermique.....	16
1.2.7.1 DSC.....	16
1.2.6.2 DMA.....	16
1.2.6.3 TMA.....	17
1.3 SYNTHÈSE DES ARTICLES ET LIEN AVEC L'ENSEMBLE DES TRAVAUX.....	18
RÉFÉRENCES.....	29
<b>CHAPITRE II : MECHANICAL AND THERMAL ANALYSIS OF</b>	
<b>ADHESIVES BONDED JOINTS: A REVIEW.....</b>	<b>32</b>
2.1 ABSTRACT.....	33
2.2 INTRODUCTION.....	34
2.3 ADHESIVES AND ADHESION.....	34
2.3.1 Bonding mechanisms.....	35
2.3.2 Possible defects in adhesive joints.....	37
2.3.3 Requirements for a good bond.....	38
2.4 MECHANICAL ANALYSIS OF ADHESIVE JOINTS.....	39
2.4.1 Basic mechanical testing.....	39
2.4.2 Joint design analysis.....	41
2.4.2.1 Tensile shear.....	41
2.4.2.2 Peel test.....	42
2.4.2.3 Cleavage test.....	43
2.4.2.4 Axisymmetric joints.....	43
2.4.3 Analysis techniques to predict joint strength.....	45
2.4.3.1 Analysis methods of lap joints stress analysis.....	47

2.4.3.2 Stress analysis methods of axisymmetric joints.....	48
2.4.4 Torsion shear apparatus.....	50
<b>2.5 PREDICTION OF MECHANICAL PROPERTIES BY THERMAL</b>	
<b>ANALYSIS TECHNIQUES.....</b>	<b>53</b>
2.5.1 Indirect relationship between thermal properties and mechanical performance .....	53
2.5.2 The use of TMA to investigate the thermal properties.....	56
2.5.3 Thermal effects on adhesive joints.....	58
2.6.2 Analysis of bonded joints under thermal effects.....	59
2.6 CONCLUSIONS.....	61
2.7 ACKNOWLEDGMENTS.....	62
2.8 REFERENCES.....	63
<b>CHAPITRE III : PROPOSAL OF A TORSION SHEAR FIXTURE FOR</b>	
<b>BONDED JOINTS.....</b>	<b>88</b>
3.1 ABSTRACT.....	88
3.2 INTRODUCTION.....	89
3.3 PROPOSAL OF A TORSION FIXTURE.....	93
3.4 Experimental validation of the proposed torsion fixture.....	96
3.5 Results and Discussions.....	97
3.6 APPLICATION TO THE CASE OF BONDED JOINTS.....	100
3.6.1 Materials.....	100
3.6.2 Specimens preparation.....	100
3.6.3 Shear test procedures.....	101



3.7 BONDED JOINT RESULTS AND DISCUSSION.....	102
3.8 CONCLUSION.....	103
3.9 ACKNOWLEDGMENT.....	104
3.10 REFERENCES.....	105
<b>CHAPITRE IV : THE EFFECT OF FILLER CONTENT ON THE MECHANICAL PROPERTIES OF EPOXY BASED ADHESIVES.....</b>	<b>124</b>
4.1 ABSTRACT.....	124
4.2 INTRODUCTION.....	125
4.3 EXPERIMENTAL PROCEDURE.....	127
4.3.1 Materials.....	127
4.3.2 Specimens preparation.....	127
4.3.3 Mechanical Evaluation.....	128
4.4 RESULTS AND DISCUSSION.....	129
4.4.1 DMA results.....	129
4.4.2 Lap shear vs. Torsion shear results.....	132
4.5 CONCLUSION.....	136
4.6 ACKNOWLEDGMENT.....	137
4.7 REFERENCES.....	138
<b>CHAPITRE V : MOISTURE ABSORPTION EFFECT OF ADHESIVE FILLED BONDED JOINTS.....</b>	<b>157</b>
5.1 ABSTRACT.....	157
5.2 INTRODUCTION.....	158
5.3 EXPERIMENTAL PROCEDURE.....	159

5.3.1 Materials.....	159
5.3.2 Specimens preparation.....	160
5.3.3 TMA procedure.....	161
<b>5.4 RESULTS AND DISCUSSION.....</b>	<b>161</b>
5.4.1 Bulk adhesives.....	161
5.4.2 TMA results.....	164
5.4.3 Bonded joints.....	167
<b>5.5 CONCLUSION.....</b>	<b>170</b>
<b>5.6 ACKNOWLEDGMENTS.....</b>	<b>171</b>
<b>5.7 REFERENCES.....</b>	<b>172</b>
<b>DISCUSSION GÉNÉRALE.....</b>	<b>192</b>
<b>CONCLUSION GÉNÉRALE.....</b>	<b>196</b>
<b>BIBLIOGRAPHIE.....</b>	<b>199</b>

**LISTE DES TABLEAUX**

**Table 3.1 Results of the torsion and tensile tests.**

**Table 4.1 Properties of fillers and the matrix.**

## LISTE DES SIGLES ET ABRÉVIATIONS

A	aire effectif
ACP	particules d'alumine
CaCo <sub>3</sub>	carbonate de calcium
CTE	coefficient d'expansion thermique
d	épaisseur d'adhésif
D <sub>i</sub>	coefficient de diffusion, représentant celui des particules et de la matrice respectivement
DGEBA	éther de diglycidyl bisphénole de type A
e	épaisseur d'adhésif
E	module élastique
E'	module élastique obtenu par DMA
E''	module de perte obtenu par DMA
E' <sub>c</sub> /E' <sub>1</sub>	module relatif
E' <sub>i</sub>	module élastique obtenu par DMA, avec l'indice i= c, 1, 2 représentant respectivement l'adhésif chargé, la matrice époxy et les particules d'alumine
ou billes	de verre
F	surface totale à coller
F <sub>a</sub>	force axiale appliquée sur le roulement
FEM	méthode d'éléments finis
(FFV) <sub>TR</sub>	fraction de volume de vide à la température de référence
G <sub>a</sub>	module de cisaillement de l'adhésif

$G_A$	module de cisaillement apparent
$G' / G'_i$	module relatif
$G'_i$	module de cisaillement obtenu par DMA, avec l'indice $i = c, 1$ représentant respectivement l'adhésif chargé et la matrice époxy
$G_T$	module de cisaillement obtenu par l'essai de traction
GB	billes de verre
$h_i$	épaisseur d'adhésif
$l$	longueur de recouvrement
$M$	couple de torsion
$M_m$	augmentation de la masse après l'essai d'immersion à l'eau en fonction du temps
$r$	rayon de joint cylindrique plein ou annulaire
$R$	force radiale appliquée
$r_o$	rayon externe du joint annulaire
$r_m$	rayon moyen
$r_i$	rayon interne du joint annulaire
$P$	force appliquée de la machine de traction/compression traditionnelle
PTFE	poly tétra fluoroéthylène
ST	température de service
$t$	épaisseur de l'adhérent
$t^{1/2}$	racine carrée de temps
$T$	couple de torsion
Tan $\delta$	capacité d'amortissement interne

$t_i$	épaisseur, $i = \text{Al.}, \text{adh.}, \text{T}$ représentant respectivement l'aluminium, adhésif
et	l'épaisseur totale
$T_g$	température de transition vitreuse
$T_R$	température de référence
V125	versamide (agent de cuisson à base d'amine)
$V_f$	fraction volumique de la charge incorporée
$V_m$	vitesse verticale de la machine de traction/compression traditionnelle
$\alpha_i$	coefficient d'expansion thermique, $i = c, m, f$ représentant respectivement l'adhésif chargé, matrice et particules
$\alpha_g$	coefficient d'expansion thermique au-dessous de la température de transition vitreuse
$\alpha_L$	coefficient d'expansion thermique au-dessus de la température de transition vitreuse
$\alpha_i^j$	coefficient d'expansion thermique dans un joint, $i = g, L$ représente au-dessous et au-dessus de la température de transition vitreuse $T_g$
$\alpha_i^k$	coefficient d'expansion thermique $i = g, L$ et $k = \text{Al.}, \text{adh.}$ représente l'aluminium et adhésif respectivement
$\gamma_{r\theta}$	déformation en cisaillement du joint annulaire
$\epsilon$	déformation axiale maximale
$\Delta\alpha$	$\alpha_L - \alpha_g$
$\Delta h_{\text{resid.}}$	chaleur exotherme résiduelle
$\Delta M$	incrément de poids

$\Delta t^{1/2}$	incrément de la racine carrée de temps
$\Delta T$	$(T_R - T_g)$
$\Delta \tau / \tau$	variation de contrainte dans un tube annulaire cylindrique
$\theta$	angle formé entre les deux barres de levier
$\mu$	coefficient de frottement
$\nu_i$	coefficient de Poisson, $i = m, f$ représentant respectivement la matrice et particule
$\sigma_i^{ult}$	contrainte ultime nominale en traction dans un joint en butée d'épaisseur $2h_i$
$\sigma_x, \sigma_y, \sigma_z$	contraintes selon les axes $x, y, z$
$\tau_1$	contrainte ultime de l'adhérent
$\tau_B$	contrainte ultime de l'adhésif
$\tau_{r\theta}$	contrainte de cisaillement ultime du joint annulaire
$\tau_{r\theta \max}$	contrainte de cisaillement maximale agissant sur le bord extrême du joint annulaire
$\tau_u$	contrainte de cisaillement
$\tau_{us1}$	contrainte ultime dans un joint en butée dans le cas d'une rupture cohésive dans l'adhésif
$\tau_{us2}$	contrainte ultime dans un joint tubulaire à recouvrement dans le cas d'une rupture cohésive dans l'adhésif
$\tau_{ut}$	contrainte ultime dans les joints précédents lorsque la rupture est adhésive
$\tau_{z\theta}$	contrainte de cisaillement en torsion
$\phi_2$	fraction volumique de la charge ajoutée
$\phi_m$	fraction volumique maximale de la charge ajoutée
$\omega$	vitesse de rotation

**LISTE DES FIGURES**

- Figure 2.1 Good and poor wetting by an adhesive spreading across a surface [10].
- Figure 2.2 Some typical joints used in testing.
- Figure 2.3 Stress distribution in a single lap joint, comparison between closed form solution with finite element (FE) results. A) shear stresses b) normal stresses [34].
- Figure 2.4 Load path in a) undeformed and b) deformed joint,  $k$ =bending moment factor [5].
- Figure 2.5 a) Step lap geometry, b) Stresses in step lap joint [5].
- Figure 2.6 Basic peel tests [31].
- Figure 2.7 Wedge crack test specimen configuration.
- Figure 2.8 Butt or napping ring specimen geometry.
- Figure 2.9 Circular butt joint: a) annular; b) solid [65].
- Figure 2.10 Joints geometry for strength prediction [68].
- Figure 2.11 Upper steel frame diagram [71].
- Figure 2.12 Diagram showing the mechanism of the proposed torsion fixture [71].
- Figure 2.13 Shear strength as a function of filler content in the case of ACP filler adhesive [71].
- Figure 2.14 Shear strength as a function of filler content in the case of glass beads filler adhesive [71].
- Figure 2.15 Conversion and lap shear strength of adhesive Evo-Tech TE as a function



of curing time at 120°C [78].

- Figure 2.16 Relative strength retention vs. percentage increase of CTE [87].
- Figure 2.17 Temperature dependence of strength of aluminum lap joint using epoxy adhesive compared to mechanical properties of the adhesive [90].
- Figure 2.18 Effect of the coefficient of thermal expansion ratio's on principle stress distribution in adhesive rectangular butt joint [100].
- Figure 3.1 Diagram showing the mechanism of the proposed torsion fixture.
- Figure 3.2 Upper steel frame diagram.
- Figure 3.3 A photograph showing the strain gages mounted on the validation specimen also shown a 45° failure direction.
- Figure 3.4 Finite element model of the validation specimen.
- Figure 3.5 Axial, transverse and shear strains as a function of time (bending in the xz plane).
- Figure 3.6 Axial, transverse and shear strains as a function of time (bending in the yz plane).
- Figure 3.7 Transverse strain vs. axial strain curve .
- Figure 3.8 Tensile stress vs. strain curve.
- Figure 3.9 Step lap specimens (all dimensions are in mm).
- Figure 3.10 Napkin ring specimen (all dimension are in mm).
- Figure 3.11 Shear strength as a function of filler content in the case of ACP.
- Figure 3.12 Shear strength as a function of filler content in the case of glass beads.
- Figure 3.13 Relative modulus as a function of filler content in the case of ACP.

- Figure 3.14 Relative modulus as function of filler content in the case of glass beads.
- Figure 3.15 Torsion shear stress versus torsion shear strain (comparison between bulk adhesive and bonded joint).
- Figure 3.16 Torsion shear stress vs. torsion shear strain in the case of alumina filled adhesive.
- Figure 3.17 Torsion shear stress vs. torsion shear strain in the case of glass beads filled adhesive..
- Figure 4.1 Step lap shear and napping ring specimens.
- Figure 4.2 Storage modulus and damping capacity as a function of temperature for ACP.
- Figure 4.3 Storage modulus and damping capacity as a function of temperature for glass beads.
- Figure 4.4 Glass transition temperature as a function of filler content.
- Figure 4.5 Loss modulus as a function of temperature for ACP.
- Figure 4.6 Loss modulus as a function of temperature for glass beads.
- Figure 4.7 Relative modulus as a function of filler content (comparison between the theoretical prediction and experimental results) .
- Figure 4.8 Step lap shear strength as a function of filler content.
- Figure 4.9 Torsion shear strength as a function of filler content.
- Figure 4.10 Fraction of cohesive fracture surface as a function of filler content (step lap shear test).
- Figure 4.11 Fraction of cohesive fracture surface as a function of filler content (torsion shear test).

- Figure 4.12 Tensile stress versus tensile strain obtained from bulk adhesives.
- Figure 4.13 Schematic drawing showing how fillers affect adhesion.
- Figure 4.14 Fraction of cohesive fracture surface versus step lap shear strength.
- Figure 4.15 Fraction of cohesive fracture surface versus torsion shear strength.
- Figure 4.16 Torsion shear stress versus torsion shear strain (comparison between bulk adhesive and bonded joint).
- Figure 5.1 Step lap shear and TMA specimen geometries.
- Figure 5.2 Percentage weight gain vs. square root of time for ACP filled bulk adhesives.
- Figure 5.3 Percentage weight gain vs. square root of time for GB filled bulk adhesives.
- Figure 5.4 Apparent diffusion coefficient as a function of filler content.
- Figure 5.5 Volume increase of bulk adhesives as a function of filler content .
- Figure 5.6 Dimension change as a function of temperature.
- Figure 5.7 Glass transition temperature as a function of ACP filler content.
- Figure 5.8 Glass transition temperature as a function of GB filler content.
- Figure 5.9 Glassy coefficient of thermal expansion (CTE) as a function of ACP filler content (bulk adhesives).
- Figure 5.10 Glassy coefficient of thermal expansion (CTE) as a function of GB filler content (bulk adhesives).
- Figure 5.11 Rubbery coefficient of thermal expansion (CTE) as a function of ACP filler content (bulk adhesives).
- Figure 5.12 Rubbery coefficient of thermal expansion (CTE) as a function of GB filler

content (bulk adhesives).

- Figure 5.13 Coefficient of thermal expansion as a function of ACP filler content and bondline thickness, a) glassy CTE, b) rubbery CTE, (comparison between theoretical prediction and experiment).
- Figure 5.14 Coefficient of thermal expansion as a function of GB filler content and bondline thickness, a) glassy CTE, b) rubbery CTE, (comparison between theoretical prediction and experiment).
- Figure 5.15 Relative strength retention as a function of filler content.
- Figure 5.16 Percentage increase of CTE as a function of filler content.
- Figure 5.17 Relative strength retention vs. percentage increase of CTE.

# CHAPITRE I

## INTRODUCTION GÉNÉRALE

### 1.1 Introduction

Les progrès scientifiques et technologiques réalisés ces dernières années ont contribué à l'amélioration des techniques de fabrication dans tous les secteurs industriels. Ainsi, le développement de nouveaux matériaux et l'évolution remarquable réalisés dans le domaine de l'adhésion et des adhésifs ont amené de nombreuses industries, pour des raisons techniques et économiques, à utiliser le collage comme procédé d'assemblage ou plutôt remplacer les assemblages mécaniques déjà existants; certains types d'adhésifs sont même employés pour des pièces structurales importantes d'avions militaires modernes.

Vu la grande performance des adhésifs, l'assemblage par collage est désormais usuel dans de nombreux domaines tels que l'industrie de l'automobile où on a recours au collage non seulement du métal au métal, mais aussi du polymère au métal. Il remplace dans certains cas des méthodes plus conventionnelles, telles que le soudage ou le rivetage, et ce même pour des applications où la solidité est un paramètre critique. Dans de nombreux cas industriels, où a recours au collage de différents type de matériaux, l'assemblage de structures faisant généralement à des températures élevées. Lors du refroidissement à la température ambiante, des contraintes résiduelles se développent dans le joint à cause de la différence du coefficient d'expansion thermique (CTE) des substrats. Ainsi, l'adhésion est un aspect multidisciplinaire qui fait appel à plusieurs notions de chimie de surface, physique,

chimie des polymères et l'analyse des contraintes et de la rupture.

Il nous est apparu intéressant de commencer une recherche analogue sur les collages des structures, dont deux principaux axes seront étudiés, soient les analyse mécanique et thermique des adhésifs et des joints collés à base d'époxyde.

Tel que souligné dans plusieurs ouvrages scientifiques, les propriétés des adhésifs font en sorte qu'il est fortement recommandé de solliciter un joint collé en cisaillement et d'éviter la traction. En conséquence, les essais de cisaillement revêtent une importance particulière. En pratique, deux importants critères sont requis dans l'assemblage des structures par l'intermédiaire des colles: la fiabilité des résultats expérimentaux et la simplicité de la méthode d'essai. Cependant, ces critères semblent irréconciliables dans les joints collés. La résistance ultime en cisaillement des joints collés est généralement obtenue par le test standard de cisaillement à simple recouvrement. Toutefois, cette méthode d'essai est caractérisée par un cisaillement non uniforme et par la présence d'autres contraintes normales au plan de joint. D'autre part, la détermination de la résistance et de la rigidité en cisaillement des joints collés est obtenue par l'essai de cisaillement en torsion. Principalement, l'essai consiste en l'application d'un couple de torsion sur un joint annulaire mince d'adhésif par l'intermédiaire d'une force agissant sur un bras de levier; la contrainte de cisaillement est alors uniforme puisque les effets de bord, associés aux joints à recouvrement, sont éliminés. Cependant, le montage expérimental de torsion n'est pas disponible pour tous les laboratoires, ce qui entrave l'utilisation usuelle de cette méthode d'essai.

Entre autres, deux méthodes sont généralement utilisées pour caractériser les adhésifs et joints collés. La première, la plus usuelle, étant l'analyse mécanique des joints collés sur des films minces tel que le joint à simple recouvrement. Une caractérisation mécanique est plus simple sur les adhésifs en tant que matériau que sur les joints collés. Ceci est dû au fait que de grandes déformations se produisent dans le matériau en "bulk" que sur une mince épaisseur d'adhésif. L'utilisation des deux analyses en parallèle s'avère très intéressante dans plusieurs cas. L'utilisation des méthodes d'analyse mécanique et d'analyse thermique sont de plus en plus appropriées à une bonne caractérisation des adhésifs et des joints collés. En particulier, si ces dernières sont utilisées concurremment dans le but de trouver un lien entre les propriétés mécaniques et thermiques, c'est précisément à ce type d'étude que nous nous intéresserons. Notre but est premièrement de développer un montage expérimental de torsion qui s'adapte à des machines de traction/compression conventionnelles et en même temps générant des résultats fiables. En deuxième lieu, l'utilisation concurrente des méthodes d'analyse mécanique dynamique, l'analyse thermomécanique et le test de cisaillement sur les joints collés seront le sujet de notre étude.

Cette thèse se présente sous forme d'une thèse par articles scientifiques. Les quatre articles sont présentés de façon intégrale incluant les références aux chapitres 2 à 5. Le premier article est une version anglaise plus complète que celle présentée dans la revue bibliographique chapitre 1. Le reste des articles comprend une introduction qui présente une revue de la littérature pertinente suivie des procédures expérimentales utilisées, de la présentation des résultats, leur discussion et finalement d'une conclusion. Au début de notre thèse, un rappel sur les principes d'adhésion des matériaux, les mécanismes d'adhésion qui

régissent la performance des joints collés sont donnés. On rappellera également les principales méthodes de mesure de la résistance mécanique, les méthodes d'analyse des joints collés et la prédiction de la résistance mécanique par les techniques d'analyse thermique. Enfin, les appareils d'analyse mécanique dynamique et thermomécanique seront présentés.



## **1.2 Revue bibliographique**

### **1.2.1 Principes de l'adhésion**

Cette section est consacrée à une introduction sur les phénomènes d'adhésion et à un bref rappel des principaux modèles théoriques qui ont été élaborés afin d'expliquer ce phénomène. La technique de collage consiste à assembler deux matériaux en appliquant entre eux un adhésif. Ce produit peut se présenter sous forme liquide, pâteuse ou en film. Les films de colle constituent la forme la plus évoluée des adhésifs à performance élevée et donc la plus largement sélectionnée pour les collages structuraux.

L'adhésion peut être définie comme étant un phénomène interfacial dans lequel des forces physiques et/ou chimiques se créent entre deux surfaces mises en contact. En d'autres termes, la force d'adhésion est une mesure du degré d'attraction entre deux parties à coller. Quatre conditions sont à satisfaire pour l'obtention d'une liaison solide [1]:

- la propreté des surfaces à assembler: ceci peut être obtenu par un traitement de surface approprié, physique ou chimique;
- la colle doit mouiller toute la surface à coller;
- la colle doit subir une polymérisation ou une réticulation nécessaire pour entraîner son bon durcissement;

Entre autres, deux modes de rupture caractérisent un joint collé: rupture adhésive et cohésive.

La première correspond à une rupture au niveau de l'interface colle/substrat, la seconde correspond à une rupture à travers la colle et donc concerne les caractéristiques de la colle.

En pratique, les deux modes se produisent en même temps en proportion de 40% cohésive et 60% adhésive [2].

### **1.2.2 Mécanismes ou principes théoriques de l'adhésion**

Si la mécanique de la cohésion du joint collé, bien que complexe, est en voie d'être maîtrisée, celle de l'adhésion, très liée au vieillissement, reste du domaine de l'empirisme. Ceci dit, de nombreuses études ont été proposées pour mieux comprendre les lois régissant les phénomènes d'adhésion et essayer de les expliquer.

**Théorie mécanique.** Cette théorie attribue l'origine de l'adhésion à l'accrochage de l'adhésif à la surface des substrats dans les aspérités, les cavités, les pores et les trous [1,3].

**Théorie physique de l'adsorption.** Selon cette théorie, l'adhésion est le résultat d'un contact moléculaire entre les deux matériaux et les liaisons de surface qui se développent. Ce phénomène est connu aussi sous la notion de mouillage et fait appel à la tension superficielle entre le substrat et l'adhésif. Généralement, le mouillage des surfaces à coller s'explique par des critères thermodynamiques, comme élaborés dans la référence [4]. Zisman et al. [5] ont pu développer une méthode empirique pour la détermination de la tension superficielle des surfaces solides par extrapolation des angles de contact. Vraisemblablement, une adhésion permanente est le résultat des forces d'attraction moléculaire. Également, des liaisons chimiques peuvent être à l'origine des liaisons cohésive et adhésive. Ces liaisons sont d'origine ioniques, covalentes, métalliques et des liaisons de Van Der Waals [1].

**Théorie de la diffusion.** Cette théorie repose sur le phénomène de diffusion et considère l'adhésion comme étant le résultat de l'interdiffusion des molécules entre les deux surfaces de polymères en contact [1]. Cette théorie concerne principalement les assemblages entre deux polymères.

**Théorie électrostatique,** En l'absence de groupes réactifs, le mécanisme dominant l'adhésion est l'attraction électrostatique polaire entre l'adhésif et l'adhérent. Ce sont des forces dispersives ou liaisons de London qui se produisent par l'interaction permanente de deux dipôles. En effet, ces liaisons d'attraction entre le substrat et l'adhésif contribuent d'une manière très significative à produire une rupture cohésive dans la colle [6-7].

**Théorie de la faible zone (weak boundary layer W.B.L).** Cette théorie basée sur l'hypothèse, dite des zones de faible cohésion (W.B.L), indique que la rupture d'un assemblage collé ne peut être adhésive, mais se produit toujours dans une zone de faible cohésion, située plus ou moins proche de l'interface. Cette théorie ne constitue pas, en soi, une théorie de l'adhésion mais elle peut fournir une explication de certaines ruptures de joints collés.

En résumé, l'adhésion peut être examinée à l'aide de différentes théories. Cependant, aucune d'entre elles n'est capable, à elle seule, d'expliquer de manière pleinement satisfaisante la totalité des phénomènes observés. En général, ce sont plutôt plusieurs de ces mécanismes qui entrent en jeu dans le phénomène d'adhésion. Néanmoins, quelles que soient

les théories prises en compte, les forces d'adhésion d'un adhésif sur un substrat dépendent essentiellement de la compatibilité chimique substrat/adhésif, de l'aptitude de ce dernier à mouiller le substrat et de la propreté et la régularité des surfaces qui entrent en contact. De petites quantités d'impuretés, des gaz adsorbés ou de légères couches d'oxyde auront pour effet de modifier considérablement les forces d'adhésion.

### **1.2.3 Analyse mécanique des joints collés**

Les paramètres déterminant la force et l'efficacité d'un collage sont extrêmement nombreux puisqu'il faut tenir compte des matériaux, des préparations de surface, de la nature de l'adhésif, de la géométrie de l'assemblage et du type de sollicitation, de la durée de vie, des effets de fatigue et du vieillissement. Généralement, la performance d'un assemblage collé est soit obtenue par la détermination des caractéristiques de la colle ou par des tests sur le joint à la rupture ou encore les deux ensemble. Dans l'analyse d'un joint collé, il est fortement recommandé de déterminer le module élastique, le module de cisaillement, le coefficient de Poisson, la déformation et la contrainte de cisaillement ultime. La résistance à la rupture d'un joint collé dépend, en partie, de la nature de l'environnement et des efforts qu'il subit sous sollicitation. Les quatre principaux types de chargement auxquels il peut être soumis sont: la traction, le cisaillement, le clivage et le pelage.

### 1.2.3.1 Essai de cisaillement par traction

Dans le cas d'un joint travaillant sous tension, les contraintes sont perpendiculaires au plan du joint et les forces sont ainsi distribuées uniformément sur l'intégralité de la surface. L'application des contraintes de cisaillement a également pour effet une répartition uniforme des forces sur la totalité de la surface du joint, mais dans ce cas, elles s'exercent parallèlement au plan du joint. Ainsi, tout l'adhésif contribue à la résistance de la structure collée.

Le joint à simple recouvrement constitue un type d'essai normalisé, cet essai demeure un outil de comparaison entre les adhésifs puisque la distribution des contraintes n'est pas uniforme le long du recouvrement et à travers l'épaisseur de l'adhésif [8-21]. Par ailleurs, plusieurs facteurs ont une influence sur la résistance en cisaillement par traction de cet assemblage. En plus des méthodes de mise en oeuvre, de préparation des surfaces et des caractéristiques physico-chimique de l'adhésif, la résistance du joint dépend d'autres variables liées aux dimensions de l'assemblage et à l'épaisseur de joint collé.

L'augmentation de la déformation du joint avec la charge dépend de la rigidité du substrat. La distorsion particulièrement importante aux extrémités engendre des forces de décollement dans la direction normale au plan du joint. Ces efforts sont principalement engendrés par la présence d'un couple causé par le fait que les forces de traction ne sont pas alignées avec le centre du joint [14,22-23]. L'utilisation du joint à simple recouvrement à mi-épaisseur est en effet une des solutions pour permettre d'éviter ces efforts indésirables. De

plus, le joint à double recouvrement est très courant dans les assemblages collés permettant ainsi l'optimisation des efforts du pelage aux extrémités. En effet, cet assemblage n'est pas soumis aux moment de flexion, contrairement au joint à simple recouvrement. Toutefois, le phénomène de concentration de contraintes aux extrémités du joint est toujours présent, en raison des déformations différentielles du substrat et de l'adhésif.

### **1.2.3.2 Essai de pelage**

L'essai de pelage, tout comme celui du joint à simple recouvrement, ne peut être utilisé que sur une base comparative puisque les contraintes ne sont pas uniformes. Plusieurs formes de pelage existent pour déterminer la performance des adhésifs structuraux dont l'essai de pelage en T, qui est le plus utilisé. Comme le clivage, le pelage favorise également la concentration de contraintes sur une mince ligne d'adhésif et ainsi seule une faible partie de celui-ci supporte la charge, le reste ne supportant aucun effort [23]. L'essai de pelage connu sous le nom "Boeing Wedge Test" simule d'une manière quantitative les forces et les effets d'environnement d'un joint collé à l'interface entre le substrat et l'adhésif. Il représente ainsi l'essai le plus utilisé pour prédire la durabilité des assemblages collés et le contrôle de la qualité des traitements de surface.

### **1.2.3.3 Essai de clivage**

Ce type d'essai est rarement énuméré dans les publications et ouvrages scientifiques. Cependant, il est plus pratique de tester l'adhésif en clivage pour déterminer sa résistance

à supporter des contraintes d'arrachement et sa durabilité avant l'assemblage final [24].

#### **1.2.3.4 Essai de cisaillement par torsion**

Dans l'essai de cisaillement en torsion, le joint est soumis à une contrainte de cisaillement pure, sans les complications apportées par des contraintes bi et tri-axiale additionnelles. En effet, le spécimen ne subit pas de changements dimensionnels engendrés par des déformations différentes entre le substrat et l'adhésif et par l'effet de Poisson. Le joint annulaire bout à bout est considéré comme le plus précis pour déterminer la résistance et la rigidité en cisaillement d'adhésifs structuraux. Pour des raisons pratiques, le joint tubulaire est appelé à un grand développement dans le domaine du génie civil car il permet de remplacer les techniques de liaison de tubes de distribution de fluides telles que le brasage, le soudage ou le soudo-brasage [25-28]. Plusieurs ouvrages techniques ont été consacrés à l'étude de ce type de joint. Entre autres, Lubkin et al. [29], Adams et al.[30] sont parmi les premiers à étudier le joint tubulaire en torsion. Les contraintes ont été analysées de la même manière que celles d'un joint à simple recouvrement

#### **1.2.4 Techniques pour prédire la résistance d'un joint collé**

Une meilleure connaissance de la distribution des contraintes et déformations dans un joint collé, ainsi que les facteurs qui les influencent, permettent d'en optimiser la résistance mécanique. Une revue rapide des ouvrages techniques révèle qu'il existe trois méthodes largement acceptées qui sont utilisées pour prédire la performance des joints collés.

La première approche fait appel à une analyse élasto-plastique des contraintes et déformations exprimées par des solutions analytiques rapprochées. Ainsi, la rupture du joint est considérée de se produire pour une déformation en cisaillement critique d'adhésif [15,31]. L'autre approche utilise la méthode des éléments finis et considère que les matériaux ont un comportement élasto-plastique et l'adhésif ne contient aucun défaut. Il a été suggéré que le critère de la contrainte maximale donne de meilleurs résultats pour des adhésifs fragiles. Par contre, le critère de la déformation principale serait la meilleure approche pour les adhésifs ductiles [8]. L'analyse mécanique linéaire élastique de la rupture [LEFM] est l'une des approches proposées pour la mesure de la ténacité des adhésifs en mode I, mode II et le mode mixte I et II [32]. Anderson et De Vries [33] ont utilisé le taux de relâchement d'énergie critique et une fissure de longueur prédéterminée dans l'adhésif pour suggérer une relation entre ces paramètres et la résistance à la rupture des joints circulaires en butée. Récemment, Reedy et al. [34-35] ont élaboré une approche basée sur le facteur d'intensité de contrainte dans le contexte de la théorie d'élasticité. Ce critère de rupture suggère que la résistance d'un joint collé en butée ( $\sigma_1^{ult}$ ) d'épaisseur quelconque ( $2h_1$ ) peut être estimée en connaissant la résistance ultime du joint ( $\sigma_2^{ult}$ ) dont l'épaisseur est ( $2h_2$ ) par la simple relation suivante:

$$\sigma_{t_2}^{ult} = \sigma_{t_1}^{ult} (h_1/h_2)^{1/3} \quad (1)$$

où  $2h_i$  est l'épaisseur du joint,  $\sigma_i^{ult}$  est la contrainte ultime en traction et l'indice  $i=1,2$  identifie deux joints de différentes épaisseurs. Cependant, cette relation est valable pour des joints de faible épaisseur lorsque le coefficient de Poisson de l'adhésif est entre 0.3 et 0.4, les substrats sont relativement rigides, et un écoulement très faible se produit à l'interface.



### 1.2.5 Appareil de torsion pour des joints collés

Les appareils de torsion destinés à déterminer la résistance mécanique ainsi que le module de rigidité en cisaillement des adhésifs sont conçus de manière à ne pas induire des contraintes transverses, de clivage ou des efforts de flexion sur des joints annulaires à parois minces. Les montages existants utilisent habituellement un bras de levier ou un système à pignon entraîné par des chaînes pour créer un moment de torsion sur le joint collé annulaire. La différence entre les deux diamètres interne et externe constituant le joint annulaire à paroi mince doit être choisie de telle sorte que la variation de contraintes  $\Delta\tau/\tau$  (equation 2) ne doit pas dépasser 10%.

$$\frac{\Delta\tau}{\tau} = \frac{\tau_{ro} - \tau_{ri}}{\tau} = \frac{F}{2A} \quad (2)$$

où  $\tau_{ro}$  et  $\tau_{ri}$  sont des contraintes à la paroi externe et interne respectivement, F est l'aire totale de la surface collée et A est l'aire effective.

Généralement, les montages proposés sont conçus de telle manière qu'ils sont adaptables à des machines d'essai standard comme celui développé par Bossler et al.[36] ou celui adopté par ASTM E229 [37].

### 1.2.6 Prédiction de la résistance mécanique par les techniques d'analyse thermique

Dans le but de relier les propriétés thermiques à la performance mécanique des adhésifs et des joints collés, une revue des travaux publiés sur l'analyse thermique de ces derniers est discutée dans la section suivante. Il est bien connu que la méthode d'analyse calorimétrique (DSC) et la méthode dynamique mécanique (DMA) sont actuellement très utilisées pour étudier la cuisson des adhésifs. Ils permettent ainsi l'obtention des formulations d'adhésifs optimales pour une meilleure performance. Toutefois, on s'attarde dans ce chapitre sur un certain nombre d'ouvrages consacrés à ce sujet afin d'élucider l'importance des méthodes d'analyse thermique.

Brett [38] a utilisé la méthode de la chaleur résiduelle (DSC) afin de relier la résistance des joints collés au degré de cuisson. Il a été conclu que le mode de rupture est cohésif lorsque le degré de cuisson est entre 70-90% et change en rupture adhésive au dessus des 90%. Perker et al. [39] ont trouvé que la résistance d'un joint diminue lorsque la chaleur résiduelle exothermique diminue. Un critère basé sur un minimum de chaleur résiduelle en conjonction avec les paramètres de la cinétique de cuisson a été proposé pour évaluer la durée de vie des adhésifs à différentes températures au dépôt. Il a été démontré que les lots d'adhésifs peuvent être utilisés ou rejetés en se basant sur la chaleur résiduelle et la résistance ultime du joint collé. D'autre part, Pitrone [40] a conduit des expériences de DMA pour évaluer l'effet de traitement de surface par des apprêts organo-silanes sur la qualité de l'interface à coller. En utilisant des joints miniatures, il a pu trouver une relation quantitative entre la capacité d'amortissement interne,  $\tan \delta$ , obtenue par la DMA et la résistance

mécanique ultime obtenue par pelage. Ludbrook et al. [41] ont utilisé la DSC en conjonction avec la DMA, et le joint à simple recouvrement pour l'étude des adhésifs à base d'époxy. Leur étude a révélé que l'évolution de la résistance mécanique avec le temps est semblable à celle du degré de cuisson obtenu par la DSC. Cependant, une tentative de corrélérer le module d'élasticité obtenu par la DMA à la résistance mécanique pour différentes températures n'a pas donné des résultats satisfaisants. Toutefois, l'évolution des deux propriétés définies précédemment en fonction de la température a montré une bonne concordance. Sanborn et al.[42] ont utilisé la DSC et un dilatomètre en quartz en conjonction avec le joint à simple recouvrement pour étudier l'effet du cyclage thermique sur les propriétés mécaniques des adhésifs époxydes. Il a été rapporté que le cyclage thermique produit un changement dans la structure de la résine, se traduisant par une augmentation de la température de transition vitreuse  $T_g$ . Cette augmentation de  $T_g$  est attribuée à une réticulation additionnelle, réduisant la mobilité locale des segments moléculaires et diminuant ainsi le coefficient d'expansion thermique (CTE) des spécimens. En effet, ce changement dans la structure de la résine a pour effet de réduire la résistance mécanique des joints collés, entre 5 à 30% de réduction selon la température de l'essai. De Nève et al. [43] ont examiné l'effet de l'humidité et du vieillissement sur les propriétés mécaniques des adhésifs époxydes en utilisant la DMA. Ils ont démontré que la température de transition vitreuse,  $T_g$ , et la capacité d'amortissement interne,  $\tan \delta$ , diminuent lorsque les spécimens subissent un vieillissement.

## **1.2.7 Appareils d'analyse thermique**

### **1.2.7.1 DSC**

Les instruments de mesure en DSC se partagent en deux grandes catégories: ceux basés sur la mesure du flux de chaleur DSC (Du Pont 910 et Mettler DSC 20 ou 30) et ceux basés sur la mesure de la puissance compensée DSC (Perkin-Elmer et Setarum 101). Le type d'instrument utilisé dans la présente étude est une DSC Du Pont 910. La sensibilité de la cellule pour la mesure du flux de la chaleur est de  $0.01 \text{ mW cm}^{-1}$  et les valeurs d'enthalpie sont calculées avec une précision de  $\pm 0.35\%$  en utilisant l'analyseur thermique 2000 adapté d'un logiciel de traitement de données.

L'analyse calorimétrique (DSC) s'est révélée très utile pour la détermination des paramètres de la cinétique de cuisson et la chaleur dégagée des matériaux thermodurcissables. Actuellement, il existe deux méthodes d'analyse: la méthode isotherme et la méthode dynamique. Une revue exhaustive des deux méthodes ainsi que de la théorie de calcul des paramètres de la cinétique de cuisson sont données dans la référence [44].

### **1.2.7.2 DMA**

L'analyse mécanique dynamique est une forme de spectroscopie mécanique dynamique appartenant à la famille d'analyse thermique, offrant un moyen rapide pour étudier le comportement viscoélastique des adhésifs étudiés. Les essais d'analyse mécanique

dynamique sont réalisés avec un appareil de marque Du Pont DMA 983 pour déterminer le module élastique,  $E'$ , le module de perte,  $E''$ , et la capacité d'amortissement interne,  $\tan \delta$ . L'échantillon est soumis à une faible oscillation 0.3 mm en mode de fréquence fixe (1 Hz) en fonction de la température et du temps. Un LVDT (Linear Variable Displacement Transducer) mesure la position du bras mobile, ainsi le comportement de l'échantillon est contrôlé par le transducteur. La différence entre le signal d'entrée et le signal du LVDT donne l'angle de phase, utile pour calculer le module élastique et la capacité d'amortissement.

### 1.2.7.3 TMA

Le dilatomètre ou l'analyseur thermomécanique (TMA) est un des instruments les plus courants pour déterminer le changement dimensionnel qu'il soit volumique ou linéaire en fonction de la température. Les essais d'analyse thermomécanique sont réalisés à l'aide d'un analyseur de marque TMA 2940 de Du Pont pour déterminer le coefficient d'expansion thermique des adhésifs et des joints collés. Le changement de volume ou de dimension des spécimens est détecté par un LVDT attaché à la sonde. Un four, entourant l'échantillon et la sonde, permet le chauffage et le refroidissement durant l'essai. Les mesures de changement dimensionnel sont obtenues avec une précision de l'ordre de 0.1  $\mu\text{m}$ . D'autres propriétés peuvent être obtenues avec l'instrument TMA, telles que la température de transition vitreuse  $T_g$ , et l'état de cuisson des résines en utilisant la sonde de pénétration.

### 1.3 SYNTHÈSE DES ARTICLES ET LIEN AVEC L'ENSEMBLE DES TRAVAUX

Les quatre articles présentés dans ce mémoire traitent des adhésifs en touchant à deux principaux aspects: l'analyse mécanique et thermique des adhésifs et des joints collés. Leur présentation est chronologique dans le but de refléter l'évolution des idées et la pertinence de l'analyse concurrente de la caractérisation mécanique des adhésifs et des joints collés ainsi que l'analyse thermique de ces derniers.

Le premier article résume l'ensemble des travaux effectués sur l'analyse mécanique et thermique des adhésifs et des joints collés. En premier lieu, une critique des principales méthodes utilisées pour déterminer la résistance mécanique des joints collés est donnée. En vue de clarifier les points forts et les inconvénients de chaque méthode d'essai, une géométrie ainsi qu'une brève analyse de contraintes sont présentées. En particulier, l'essai de joint à simple recouvrement et l'essai de cisaillement en torsion ont été étudiés en détail. Par la suite, une analyse thermique des adhésifs et des joints collés est présentée afin de montrer la pertinence de ces méthodes dans la caractérisation des adhésifs. Entre autres, les ouvrages techniques consacrés à ce type d'analyse sont discutés, en particulier pour les techniques d'analyse thermique telles que la DSC, DMA et TMA. Par ailleurs, ces techniques d'analyse ont été utilisées pour prédire la résistance mécanique des adhésifs et des joints collés. Un résumé de la revue bibliographique équivalente au premier article est donné dans le chapitre 1 de ce travail.

Suite à cette recherche pertinente élaborée dans une partie du premier article, il nous

est apparu essentiel de développer ou plutôt de proposer un montage expérimental de torsion ayant pour spécificité la simplicité de l'essai expérimental et son adaptabilité aux machines de traction/compression traditionnelles. Le mécanisme pour créer la torsion est basé sur deux barres servant de levier, disposées en croix induisant un couple en vertu de leurs mouvements de rotation opposés; chacune des deux barres s'insérant dans une des extrémités du spécimen. Les travaux de validation consistaient à vérifier si le montage proposé induit des contraintes de flexion ou de clivage pouvant fausser les résultats de la résistance mécanique des joints collés. Dans un premier temps, des jauges de déformation ( $0^\circ/90^\circ$ ) sont installées sur des spécimens de validation dans les directions y et z et d'autres ( $\pm 45^\circ$ ) pour détecter les déformations principales durant le chargement. Ces jauges permettront de mesurer les déformations axiale, transverse et de cisaillement. La taille de ces déformations montrera l'état de contraintes ainsi que leurs amplitudes durant dans l'essai en question. Les essais préliminaires sur les spécimens de validation ont montré des ruptures en torsion typique à  $45^\circ$  de la direction principale. Toutefois, ces résultats ont révélé que les déformations parasites dans les deux plans xz et yz représentent dans les cas extrêmes 3% et 4% de la déformation en cisaillement respectivement. À titre de comparaison, des essais de traction sur le même type de matériau ont été effectués. Les modules de rigidité en cisaillement de ces derniers ont été calculés et comparés à ceux mesurés sur les spécimens de validation. La valeur moyenne du module de rigidité en cisaillement dans le cas des spécimens de traction est de l'ordre de 1059 MPa, celle des spécimens en torsion est de l'ordre de 958 MPa. Relativement, une différence de l'ordre de 9% est enregistrée entre les deux types d'essais. Cette différence est principalement causée par des pertes mécaniques par frottement non enregistrées lors de chargement dans les roulements et le bloc

d'alignement. Cependant, les efforts de flexion parasites, aussi petits soient-ils, peuvent contribuer à cette différence. En résumé, les résultats obtenus dans les deux types d'essais sont du même ordre de grandeur. En effet, une variation de l'ordre de 9% dans la mesure du module de rigidité en cisaillement suggère que le montage proposé est acceptable. Il est évident que ces contraintes parasites enregistrées dans le cas des spécimens de validation disparaîtront presque complètement dans le cas des joints annulaires. En effet, deux méthodes d'essais normalisées, joints à mi-épaisseur et joints annulaires, ont été effectuées en parallèle. Le but de cette partie du travail consiste à vérifier la fiabilité du montage proposé en comparant les résultats obtenus avec ceux des joints à mi-épaisseur. Les détails de cette étude sont donnés dans le troisième article proposé. Pour atteindre l'objectif de ce travail, deux types de charges sont ajoutés à un système d'adhésif: résine époxyde/polyamide. Il a été remarqué que le comportement de la résistance mécanique pour les deux types d'expérience en variant le type et le volume de la charge augmentait, atteint un maximum, puis chute pour de grands volumes de la charge. Ou encore, une autre remarque importante observée est que la résistance mécanique des joints annulaires testés avec le montage proposé montre de plus grandes valeurs que ceux des joints à mi-épaisseur. Il est évident que le joint à mi-épaisseur génère de faible résistance mécanique dû aux contraintes d'arrachements élevées présentes sur les extrémités du joint. Ceci veut dire que le montage proposé est assez fiable pour mesurer la résistance mécanique des adhésifs. Une autre évidence de la fiabilité du montage proposé peut être montrée en comparant le module de rigidité en cisaillement mesuré par deux méthodes d'essai différentes. Il a été trouvé que les modules de rigidité en cisaillement des différents



adhésifs chargés obtenus avec la DMA sont en parfait accord avec ceux obtenus sur des joints annulaires testés avec le montage proposé. Cet accord montre la validité et la fiabilité du montage proposé.

Enfin, le quatrième chapitre montre l'effet du type de charge ainsi que le volume de ces derniers sur les propriétés mécaniques des adhésifs et des joints collés. L'analyse mécanique dynamique (DMA), des essais de traction, joints à mi-épaisseur et joints annulaires en torsion ont été effectués en parallèle pour étudier l'effet de la quantité de la charge sur les caractéristiques de l'adhésif et des joints collés à base d'époxy. Ces derniers sont renforcés avec deux types de charge, une poudre céramique d'alumine (ACP) et des billes de verre (GB), dont le volume ( $V_f$ ) varie de 0 à 30%. Dans la première phase, les caractéristiques des adhésifs chargés, telles que le module élastique,  $E'$ , le module de perte,  $E''$ , la capacité à l'amortissement  $\tan \delta$ , et la température de transition vitreuse,  $T_g$ , sont déterminés avec la technique DMA. Il a été observé que la température de transition vitreuse,  $T_g$ , augmentait avec le volume de la charge, mais que cette dernière n'est pas affectée par le type de la charge (ACP ou GB), contrairement à  $E'$  et  $\tan \delta$ . Les charges ACP contribuent à l'augmentation du module de l'adhésif d'une manière plus prononcée que les charges GB. Ceci peut être expliqué en terme de la micromécanique, car le module d'ACP est au moins quatre fois plus grand que celui des billes de verre. Les modules relatifs ( $G'_c / G'_l$ ), où  $G'$  est le module de rigidité en cisaillement et les indices  $c$  et  $l$  représentent respectivement l'adhésif chargé et la matrice époxy/polyamide, obtenus expérimentalement sont comparés à ceux obtenus par le modèle de Kerner modifié et ceci en fonction du volume de la charge

ajouté. Il a été trouvé que les deux comportements de module relatif étaient très similaires. Cet accord entre les résultats expérimentaux et ceux obtenus par la prédiction n'est pas surprenant, car l'équation de Kerner est développée pour des systèmes avec une symétrie de particules sphériques et une continuité à l'interface entre la matrice et la charge. Probablement une des importantes caractéristiques observées est le changement de  $\tan \delta$  avec la quantité de la charge incorporée, particulièrement au-dessus de la température de transition vitreuse. Malgré que les adhésifs étudiés ne sont pas conçus pour résister à des températures élevées, le changement dans  $\tan \delta$  aux hautes températures est remarquable, puisque c'est une indication de l'arrangement microstructural entre les particules et le polymère. L'aspect microstructural concerne en particulier l'interface charge/polymère et les agglomérats. Une amélioration de l'interface réduit le mouvement interfacial entre les particules et le polymère qui, à son tour, fait diminuer la capacité d'amortissement,  $\tan \delta$ . Par contre, la formation des agglomérats favorise le frottement entre particules, induisant une augmentation de  $\tan \delta$ . Pour les deux types de charge étudiés, il a été remarqué que  $\tan \delta$  diminue dans les deux cas avec l'augmentation du volume de la charge. Cependant, cette diminution est très prononcée dans le cas d'époxy/ACP comparativement à époxy/GB et peut être expliquée en considérant la définition de  $\tan \delta = E''/E'$ . En effet, des particules d'alumine plus rigides contribuent à diminuer  $\tan \delta$  en augmentant  $E'$ . Mais cette considération seule ne suffit pas pour expliquer la différence observée dans  $\tan \delta$  pour les deux types de charges. Par conséquent, on peut prétendre que l'excès d'amortissement obtenu dans le cas des billes de verre est le résultat d'une mauvaise interface particule/époxy et/ou l'existence d'agglomérats de charge.

Quant aux essais de cisaillement des joints collés à mi-épaisseur et annulaires, la résistance mécanique de ces derniers augmentait, atteint un maximum, puis chute pour de grand volume de la charge. Ce même comportement a été souligné dans les ouvrages techniques sans explication. Ce maximum atteint dépend du type de la charge, il est de l'ordre de 10% de volume dans le cas d'alumine et de l'ordre de 20% de volume dans le cas des billes de verre. Afin d'expliquer les comportements observés, le concept rupture adhésive versus rupture cohésive a été utilisé. Il a été remarqué que l'allure générale du comportement de la fraction surfacique de la rupture cohésive en fonction du volume de la charge ajoutés est le même que celui observé dans le cas de la résistance mécanique. En d'autres termes, la fraction surfacique de la rupture cohésive augmentait avec le volume de la charge, atteint un maximum, puis chute pour de grand volume de la charge. Curieusement, le maximum atteint est semblable à celui obtenu pour la résistance mécanique. Ces résultats confirment que le niveau atteint de la résistance mécanique des joints collés est relativement lié à la rupture cohésive produite. Par conséquent, la meilleure résistance mécanique des joints collés chargés avec l'ACP peut être maintenant expliquée par le fait qu'au même niveau de charge, l'ACP contribue plus à une rupture cohésive que GB. De cette interprétation découlent les questions suivantes: 1) Quelles sont les considérations qui font que l'ACP contribue plus à une rupture cohésive que les GB ? 2) Est-ce que la résistance d'un tel adhésif dépend seulement de la fraction surfacique de la rupture cohésive ou dépend elle d'autres propriétés physiques de la charge incorporée ? Le fait que l'addition d'une certaine quantité de charge résulte en l'amélioration de la résistance mécanique de joint en favorisant une rupture cohésive mérite une explication. Ceci est particulièrement important puisqu'il est connu que l'incorporation des charges inertes a pour effet de réduire la résistance mécanique des

polymères et ceci a été vérifié par des essais de traction sur les mêmes types d'adhésifs chargés. Évidemment, il a été trouvé que l'augmentation du volume de la charge a pour effet de réduire la résistance mécanique des adhésifs chargés. Pour expliquer le fait que l'incorporation des charges, d'une part, réduit la résistance mécanique des adhésifs et, d'autre part, améliore la résistance mécanique des joints collés, le mécanisme suivant a été proposé. L'adhésif non chargé, contenant une grande quantité de bulles d'air, qui émerge à l'interface durant la fabrication du joint a pour effet de réduire la résistance mécanique des joints collés par deux mécanismes: 1) en réduisant l'aire effective de la surface à coller, 2) en servant de sites préférentiels pour l'initiation de la rupture. Lorsque les charges sont ajoutées, il est possible que les particules occupent l'espace de ces bulles d'air. Ces particules ayant été mouillées par l'adhésif sont maintenant capables d'adhérer mieux à l'interface à coller. Dans le cas où le volume de charges est excessif, un niveau de saturation est atteint et le joint ne peut plus supporter un excès de charge et une résistance mécanique faible est enregistrée.

Idéalement, il est préférable d'obtenir des ruptures cohésives dans les assemblages collés, puisque seulement la performance et les caractéristiques de l'adhésif sont testées. Par conséquent, l'utilisation du concept rupture cohésive/adhésive dans l'analyse des joints collés est très importante. Si on construit une courbe reliant la résistance mécanique des joints collés en fonction de la fraction surfacique de la rupture cohésive, on pourra extrapoler le cas idéal de 100% rupture cohésive. Ce cas correspond à un matériau parfait sans défauts, c'est-à-dire qu'on obtient la performance d'un adhésif avec une résistance mécanique optimale. Ceci est réalisé par une simple extrapolation de la courbe linéaire de la résistance mécanique versus la fraction surfacique de la rupture cohésive. Les résultats de cette

extrapolation sont présentés pour les deux types d'essais de cisaillement, que ce soit pour les joints à mi-épaisseur ou pour les joints annulaires. Selon cette relation linéaire trouvée entre les deux paramètres, 100% rupture cohésive pour un adhésif parfait doit montrer une résistance mécanique d'environ 31 MPa pour l'essai de cisaillement sur des joints à mi-épaisseur et 40 MPa pour l'essai de cisaillement sur des joints annulaires. Afin de prédire la résistance mécanique de l'adhésif en utilisant les résultats de l'extrapolation où vice versa, des essais de torsion sur l'adhésif sont effectués avec le montage proposé et comparés aux essais de torsion sur des joints annulaires. Les résultats de ces essais ont montré que le module trouvé par les deux types d'expérience est du même ordre de grandeur. Par contre, la résistance mécanique du joint annulaire est beaucoup plus faible que celle obtenue pour l'essai de torsion sur l'adhésif.

L'autre volet de ce mémoire consiste à déterminer l'effet synergique de l'humidité et de la température sur les mêmes types d'adhésifs auparavant analysés. L'effet du type et de la fraction volumique de la charge sur la performance et la durabilité des assemblages collés a été examiné en utilisant concurremment l'essai de cisaillement à mi-épaisseur et l'analyse thermomécanique (TMA). En plus, une approche basée sur l'analyse thermomécanique a été développée pour prédire la résistance mécanique des assemblages collés. Pour réaliser cette étude, trois types de spécimens ont été utilisés. Il s'agit des joints à mi-épaisseur, des joints miniatures pour mesurer l'expansion thermique et tout changement qui pourrait surgir durant l'exposition à une température humide et des échantillons d'adhésif pour déterminer les caractéristiques physiques telles que le coefficient de diffusion (D) et le coefficient d'expansion thermique (CTE).

La première étape consistait à déterminer le coefficient de diffusion apparent,  $D$ , pour les adhésifs étudiés. Pour ce faire, trois spécimens de chaque formulation ont été submergés dans l'eau bouillante et le pourcentage de poids gagné ( $M_m$ ) en fonction de la racine carrée du temps ( $t^{1/2}$ ) a été établi. Il a été observé que le système époxy/bille de verre est beaucoup plus perméable à l'eau que l'époxy/alumine. Théoriquement, il a été établi que le coefficient de diffusion apparent diminue avec la quantité de charge ajoutée. Ceci est logique puisque la quantité d'eau absorbée par les charges ACP et GB est négligeable et que le modèle est établi en supposant une interface parfaite entre les particules et la matrice. Malheureusement, cette tendance n'est pas respectée pour les systèmes étudiés et le désaccord est plus prononcé dans le cas des billes de verre que l'alumine. Les raisons de tel désaccord est le résultat des bulles d'air qui accompagnent l'ajout des charges et que l'interface particule/matrice peut servir de sites préférentiels pour la diffusion d'eau. Donc, selon cette explication, le système époxy/ACP posséderait une meilleure interface que celle d'époxy/GB et ceci est en parfait accord avec le précédent travail effectué sur les mêmes adhésifs en relation avec les propriétés mécaniques.

D'autre part, le CTE des adhésifs a été obtenu avec l'appareil TMA. Pour ce faire, on a utilisé la méthode recommandée dans la littérature. Il a été trouvé que l'expansion thermique au-dessus et au-dessous de la température de transition vitreuse ( $T_g$ ) des adhésifs chargés diminue avec le volume des charges ajoutées. Toutefois, différents modèles théoriques ont été appliqués sans succès, sauf celui de Kerner qui générerait des résultats semblables à ceux trouvés par l'expérience. Une importante pénétration a été observée dans les environs de  $T_g$  sur les courbes de changement dimensionnel versus température.

Cependant, cette pénétration a tendance à disparaître avec les joints miniatures. Une comparaison des résultats de la température de transition vitreuse obtenue par les deux types d'essais, c'est-à-dire sur des joints miniatures et sur les adhésifs, a révélé que les valeurs trouvées sont très proches. Une fois encore, ces mêmes résultats ont été obtenus avec l'analyse DMA. Cependant, les expériences effectuées sur les adhésifs submergés dans l'eau chaude ne sont pas exploitables, puisque ces derniers ont montré des irrégularités dans le comportement changement dimensionnel versus la température.

Comme suggéré auparavant, afin de mesurer le coefficient d'expansion thermique des joints collés, on a utilisé des joints miniatures pour des raisons d'adaptabilité avec l'appareil TMA. Au moins cinq éprouvettes ont été testées pour la reproductibilité des résultats. Vu que ces spécimens sont sensibles au changement de l'épaisseur de l'adhésif, la variation de ce paramètre a permis de voir le comportement de CTE en fonction de la fraction volumique de la charge ajoutée et de l'épaisseur de l'adhésif. Les résultats de ces essais ont montré que l'expansion thermique des joints collés diminue avec le volume de la charge incorporé et augmente avec l'épaisseur de l'adhésif, et ce pour des températures au-dessus ou au-dessous de la température de transition vitreuse,  $T_g$ . Un modèle théorique basé sur la loi des mélanges et tenant compte des différents paramètres influençant le coefficient d'expansion thermique des joints a été proposé. Il a été trouvé que ce modèle prédit bien l'expansion thermique des joints collés au-dessous de la température de transition vitreuse et qu'il existe un désaccord au-dessus de  $T_g$ . Afin de corriger cette différence, on a incorporé un facteur correcteur qui prédit bien l'expansion thermique des différentes formulations des joints collés.

Dans la deuxième partie de ce travail, afin de prédire la résistance mécanique des joints collés exposés à une température humide, on a évalué la résistance mécanique relative des joints à mi-épaisseur. Cinq échantillons ont été testés avant et après la submersion à l'eau. Les résultats de cette étude ont révélé que les joints collés à base d'époxy/GB sont plus sensibles à l'eau que ceux à base d'époxy/ACP. Afin d'expliquer ces comportements, le CTE des joints miniatures exposés à une température humide est comparé à la résistance mécanique relative des joints à mi-épaisseur. Effectivement, le CTE des joints époxy/GB exposés à l'eau chaude a subi une augmentation plus marquée que celui des joints époxy/ACP. En termes de contraintes résiduelles, ceux qui montrent un CTE plus élevé sont plus susceptibles d'avoir une résistance mécanique plus faible. Une même tendance a été observée entre la résistance mécanique relative et le pourcentage d'augmentation de CTE. En d'autres termes, cela veut dire qu'il existe une relation de proportionnalité entre ces deux propriétés mesurées. En fait, si une courbe est tracée entre la résistance mécanique relative et le pourcentage d'augmentation de CTE, une relation linéaire sera trouvée entre les deux. Selon cette courbe, il a été remarqué que les joints qui ont subi une forte augmentation de CTE ont subi un sévère endommagement lors de l'exposition ce qui fut le cas des joints à base d'époxy/GB.



**RÉFÉRENCES**

- 1 E. M. Petrie, *Plastics and adhesives as adhesives*, Handbook of Plastics and Elastomers, ed. C. A. Harper, McGraw-Hill, NY, 1975
- 2 R. B. Thompson and D. O. Thompson, *J. Adhes. Sci. Tech.*, V.5, N.8, 1991, p. 583
- 3 L. H. Lee, "Adhesive Bonding", ed. L. H. Lee, Plenum Press NY, 1991
- 4 D. H. Ridge, "Physical Chemistry of Adhesion, Willey- Interscience, 1971
- 5 W. A. Zisman, "Adhesion and Cohesion", ed. P. Weiss, 1962
- 6 H. F. Mark, *Adhesives Age*, V.22, N.7, 1979, p.35
- 7 H. F. Mark, *Adhesives Age*, V.22, N.9, 1979, p.45
- 8 R.D. Adams and William C.Wake, "Structural adhesive joint in engineering", Elsevier Applied Science Pub., London and NY, 1984, p.14
- 9 O. Volkersen, *Construction Métallique*, N.4, 1965, p.3
- 10 J. M. Giraud, *Matériaux et Techniques*, 1980, p.255
- 11 M. Halioui and J. P. Lieurade, *Matériaux et Techniques*, 1991, p. 17
- 12 C. Kassapoglou and J. C. Adelmann, *SAMPE Quart.*, V.24, N.1, 1992, p.19
- 13 F. Erdogan and M. Ratwani, *Journal of Composite Materials*, V.5, 1971, p.378
- 14 L. J. Hart-Smith, Technical report, NASA CR1122 36, 1973
- 15 M. Y. Tsai and J. Morton, *J.Strain Analy.*, V. 29, N. 1, 1994, p.137
- 16 R. D. Adams and J. A. Harris, *Int. J. Adhes. Adhes.*, V. 7, N.2, 1987, p.69
- 17 V. Mallick, " Stress Analysis of Metal/CFRP Adhesive Joints Subjected to the Effects of Thermal Stress ", Ph.D Dissertation Univ. Bristol, UK, 1989
- 18 M. Goland, E. Reissner, *J. Appl.Mech.*, V.11, 1944, p.A17

- 19 K. Mori and T. Sugibayashi, Nippon Kikai Gakkai Ronbunshi, PartA V. 55, N.519, 1989, p.2211
- 20 F.E. Penado and R.K Dropele, Adhesives and Sealant " Engineered Materials Handbook", ASM Int. V.3, 1990, p.477
- 21 K. Mori and T. Sugibayashi, JSME Int. J., Series 1, V. 33, N. 3, 1990, p.349
- 22 T. A. Osswald, "Adhesives and Sealants, Engineered Materials Handbook", ASM Int. V.3, 1990, p.325
- 23 L. J. Hart-Smith and E. W. Thrall, Adhesive Bonding of Aluminium Alloys, ed. E. W. Thrall and R. W. Shanon, Marcel Dekker, 1985, p.241
- 24 R.D. Adams, Adhesives and Sealants: Engineered Materials Handbook, ASM Int., V.3, 1990, p.325
- 25 C. O'reilly, SAE Trans. J. Mater.Manufac., Section 5, V.55, 1990, p.839.
- 26 Y. Delmas, "Contribution à l'étude théorique et expérimentale du collage de tubes métalliques par l'intermédiaire de résines époxydiques", Thesis Université de Reims,1985.
- 27 E. D. Reedy, JR. and T. R. Guess, Int. J. Fract., V.63, 1993, p.351, also SED-V.14, Wind Energy, ASME 1993
- 28 Y. Gilibert and A . Rigolot, Mech. Res. Comm., V.8, N.5, 1981, p.269
- 29 J. L. Lubkin, E. Reissner, Trans. ASME, 1956, p. 1213
- 30 R.D. Adams, J. Coppendale, J. Adhes., V.9, 1977, p.11
- 31 L.J. Hart-Smith, Join. Compos. Mater., ASTM STP 749, ed. K.T. Kedward, Philadelphia, PA, 1981, p.3
- 32 K. M. Liechti, "Adhesive and Sealant, Engineered Materials Handbook", ASM Int.

- V.3, 1990, p.335
- 33 G. P. Anderson and K. L. devries, *Int. J. Fract.*, V.39, 1989, p.191
- 34 E. D. Reedy, JR., *Int. J.Solid Struct.*, V.30, N.6, 1993, p.767
- 35 E. D. Reedy, JR. and T. R. Guess, *Int. J. Solid Struct.*, V.30, N.21, 1993, p.2029
- 36 R. C. Bossler, M. C. Franzblau and J. L. Rutherford, *J. Sci. Inst: J. Phys. E. ,* V.21, 1968, p.829
- 37 *Standard Test Method for Shear Strength and Modulus of Structural Adhesives, E229-70.*
- 38 C. L. Brett, *J. Appl. Polym. Sci*, V.20, 1976, p.1431
- 39 B. G. Perker and C. Hart-Smith, *Modern Plast.*, 1979, p.58
- 40 L. R. Pitrone, *5th Int. Joint Military/Government Industry Symposium on Structural Adhesive bonding*, Dover New Jersey, 1987, p. 359
- 41 B. D. Ludbrook and R. J. Whitwood, *Int. J. Adhes. Adhes.*, V.12, N.3, 1992, p.138
- 42 J. A. Sanborn and D. E. Morel, JR., *J. Reinf. Plast. Compos.*, V.27, N.2, 1988, p.155
- 43 B. De Nève and M.E.R. Shanahan, *Int J. Adhes. Adhesi.*, V.12, N.3, 1992, p.191
- 44 R.B. Prime, *Thermal characterisation of polymeric materials*, ed. E.A. Turi, Academic Press NY, 1985, p.435

## CHAPITRE II

### MECHANICAL AND THERMAL ANALYSIS OF BONDED JOINTS- A REVIEW

#### 2.1 Abstract

Two major requirements are needed when dealing with mechanical characterization of bonded joints: the reliability of the results and ease of testing. Numerous testing methods have been developed in order to measure the strength of bonded constructions. Therefore, this paper reviews basic mechanical tests, methods to predict joint strength and some thermal techniques used to relate the thermal properties to the performance of adhesive bonded constructions. From this review, it seems that reliability and ease of testing are irreconcilable in practice. Actually, in most cases drawbacks of given analysis methods shadows its advantage.

## 2.2 Introduction

Adhesives, which have existed for thousands of years, have only gained special importance in recent decades. Recognition of the merits of adhesive bonded joints has led to an ever increasing amount of interest in adhesive bonding. Consequently, adhesion science is an extremely active area of research today. According to Irving [1], many industrial experts predicted, it would be only a matter of time before adhesive bonding would be used much more extensively than it is now. The subject of adhesive bonding is truly multi-disciplinary, involving aspects of surface chemistry and physics, polymer chemistry, stress and fracture analysis. General reviews of the subject are given by Kinloch [2-4], Adams and Wake [5] and more recently Lee [6]. The present review criticizes some of the basic mechanical standard testing methods and shows the importance of the thermal methods used to relate the thermal properties to the mechanical ones. In addition, this work brings light of the importance of the torsion shear test in producing reliable results compared to the popular single lap shear test.

At present, adhesives are widely used in thousands of operations in automotive applications, involving metal-to-metal, plastic-to-plastic and plastic-to-metal applications [1]. Polymeric composites such as GFRP (Glass Fibre Reinforced Plastics) and CFRP (Carbon Fibre Reinforced Plastics) bonded to metal counterparts are also widely used in aerospace applications. Despite the benefits of adhesive bonded joints, no universal theory of adhesion has been adopted confirming that adhesion science is a complex and controversial subject. Nevertheless, there are many situations where the advantages far

outweigh the disadvantages. In such cases it becomes the responsibility of the engineer or designer concerned whether or not to use adhesives. Therein lies the problem of whether or not to choose an adhesive and the problem of its suitability to do a specific job. As a consequence, this paper first reviews mechanisms of adhesion, basic mechanical testing and joint design analysis with particular emphasis on the techniques to predict the joint strength. Furthermore, some of the work devoted to relate the mechanical strength to the thermal properties is discussed.

### **2.3 Adhesives and Adhesion**

Adhesive bonding is the process of uniting materials with the aid of an adhesive; a substance capable of holding such materials together by surface attachment. The major function of adhesives is for mechanical fastening. Sealing and insulating is another function of adhesives. The adhesive in properly prepared joint provides full contact with mating surfaces, it forms a barrier to fluids that do not attack or soften it. Furthermore, adhesive can be used to resist corrosion and vibration and many advantages that are listed in ref. [7-9].

Adhesive bonding is not a panacea for assembling all products. The fact that there are so many variations in available formulations makes selection of the optimum adhesive for a particular application more difficult than selecting a mechanical fastening system. These variations also complicate control procedures on incoming materials, assembly processing and testing of the finished product [10]. Although adhesives can produce structures that are more reliable than those joined by conventional methods, adhesive bonded

structures must be carefully designed and used under conditions that do not exceed the known operational limitations of the adhesive. Such limitations include types and magnitudes of stresses and environmental factors such as temperature, humidity, salt environment, or the pressure of other vapors or liquids.

### **2.3.1 Bonding mechanisms**

The actual mechanism of adhesive attachment is not yet fully understood. The following are some of the theories suggested in the literature. Sometimes, these mechanisms occur individually or simultaneously.

**Mechanical theory:** According to this theory, in order to function properly the adhesive must penetrate cavities on the surface of the substrate and displace the trapped air at the interface. Mechanical interlocking can certainly be a significant factor in most adhesive joining, although the roughness and porosity of the substrate and their effects on stress distribution in the interfacial region can be other significant factors [6,9].

**Adsorption theory:** This theory states that adhesion results from molecular contact between two materials and the surface forces that develops. This phenomenon is known as wetting and is related to the surface tension of the substrate and that of the adhesive. Good wetting results when the adhesive flows into the valleys and crevices on the substrate surface as shown in figure 2.1 [9].

Having the adhesive in a liquid state is not sufficient to assure that it will wet and adhere to the substrate to which it is applied. Thermodynamic criteria for wetting and spreading have been investigated and a detailed review is given in ref. [11]. Zisman and co-workers [12] have developed an empirical method for determining a critical surface tension of solid surfaces by extrapolating contact angles. After intimate contact is achieved between the adhesive and adherent through wetting, it is believed that permanent adhesion results primarily through forces of molecular attraction. Four chemical bonds are thought to be involved in adhesion and cohesion. These are: electrostatic bonds, covalent bonds, metallic bonds and Van Der Waal's forces [9].

**Diffusion theory:** This theory suggests that adhesion is developed through the inter diffusion of molecules in the adhesive and adherents when both are long chain polymers [9]. Obviously, this does not apply to metal substrates.

**Electrostatic theory:** By far the dominating adhesion mechanisms especially in the absence of reactive groups, is the electrostatic attraction of the polar groups of the adhesive to the adherent and to each other. These are primarily dispersion forces (London forces) arising from the interaction of permanent dipoles. These forces provide much of the attraction between the adhesive and adherent and contribute significantly to the cohesive strength of the adhesive polymers [13-14].



### 2.3.2 Possible defects in adhesive joints

The possible defects, flaws or discontinuities listed below, can occur in adhesive bonded structures and generate failure [15-17]. It is important to mention that adhesive bonded joints can show two modes of failure depending on the path of the fracture. The cohesive failure corresponds to failure in the bulk of the adhesive, while the adhesive failure is associated with failure between the adhesive and adherent, generally at the interface. Operationally, a bond is often characterized as having particular fractions of these two modes, e.g., 40% cohesion and 60% adhesion failure typically for the adhesives studied [18].

**Void.** A void is any area that should contain, but does not contain adhesive. They are found in a variety of shapes and sizes usually at random locations within the bondline. Voids in the adhesive are similar to porosity except that the individual defect volume can be much greater. They are caused by air or gases becoming trapped by the pattern of laying the adhesive being applied. Large voids cannot be caused by volatile unless there is something wrong with the formulation of the adhesive system.

**Unbonds or disbonds.** Areas where the adhesive attaches only one adherent are termed unbonds or disbonds. They are caused by inadequate surface preparation, contamination, or improperly applied pressure. This also may be considered as a weak boundary layer occurring in the adhesive or adherent if an impurity concentrates near the bonding surface and forms a weak attachment to the substrate. A weak boundary layer can originate from the

adhesive, the adherents, the environment, or a combination of any of these factors. From a review of some related work to the mechanisms of adhesion, it is considered that the weak boundary layer (W.B.L) is one of the main mechanisms that is responsible for the failure of the bonded joints [9].

**Porosity.** Many adhesive bondlines have some degree of porosity, which may be dispersed or localized. Porosity is defined as a group of small voids clustered together or in lines. It is usually caused by trapped volatile and is also associated with thick (single layer adhesive) bondline that did not have enough pressure applied during the cure cycle. The reduced bond strength in these porous areas is directly related to its frequency and/or severity.

**Porous or frothy fillets.** This condition results from too-high heat up rate during curing, this defect is visually detectable and should also be seen in the test specimen processed within the production parts. Finally, there is others numerous known defects given in the literature such as lack of fillets, adhesive flash and so on.

### **2.3.3 Requirements for a good bond**

The basic requirements for good adhesive bonds are the following [9].

- Cleanliness of surfaces; this can be achieved by a special treatments that generally involve physical or chemical processes or a combination of both [19].
- Wetting, (see figure 2.1) generally for a good bond to occur, the adhesive must wet the whole surface to be bonded, and this is achieved if the roughness of the adherents are

controlled through abrasion and chemical treatment of the surfaces.

-Solidification; the liquid adhesive, once applied, must be capable of being converted into a solid.

- Proper choice of adhesive; a number of consideration must be taken into account when selecting the adhesive to be used for a particular application. The general areas of concern to the design engineer when selecting adhesives to be used are: 1) the materials to be bonded, 2) service requirements, 3) production requirements, and 4) costs [8].

-Good joint design; the adhesive joint should be designed to take advantage of the desirable properties of adhesives and to minimize their shortcomings.

## **2.4 Mechanical analysis of adhesive joints**

### **2.4.1 Basic mechanical testing**

The mechanical performance of adhesives are usually determined on bulk specimens, adhesively bonded joints or both. Testing bulk adhesives is easier than testing films because much larger deformations can be attained which in turn, are much easier to measure. On the other hand, mechanical testing of adhesive bonded constructions is the most useful tool to measure the strength of the joint. In the design and strength analysis of bonded joints, the major requirements are the elastic shear and tensile modulus. Also necessary are the Poisson's ratio, the ultimate shear strain, and the ultimate shear stress. Usually, strain measurements are an important facet in the adhesive bonded joint analysis. However, the selection of specimen configuration is another one in which the adhesive bond should be

subjected to a pure shear stress without the complication of biaxial or triaxial stresses in the bond [20]. The effects of individual factors, such as bondline thickness, material strength properties, thickness of adherents, on the strength of the bonded joint cannot always and unequivocally be distinguished, since these factors are interdependent to a varying degree [21].

Often, it is not necessary to test a whole component or structure in order to ascertain the likely behavior under load. For instance, if an aluminum sheet is bonded into a structure, it is usually only the quality of the adhesive to be assessed. Sometimes this is done nondestructively on the component, but there are severe uncertainties about the success of most, if not all, current nondestructive tests for adhesive bonds [22].

There are four basic types of loading an adhesive joint: tensile, shear, peel and cleavage (figure 2.2). The most frequently used standard test is the single lap and its derivatives figure 2.2.b, c. From the point of view testing, the lap shear configuration has gained much popularity because of its simplicity. As can be seen in the forthcoming discussion, none of the testing standard configurations of bonded joints has gained a full confidence in term of reliability except thin walled axisymmetric joint loaded in torsion. However, the latter seems irreconcilable with simplicity, since it requires a particular testing apparatus, which is not available for all laboratories. The following presents a detailed discussion of the main standard tests known to date.

## **2.4.2 Joint design analysis**

### **2.4.2.1 Tensile shear**

Tensile shear strength is most widely adopted as a measure of the ultimate shear strength of an adhesive bond loaded in tension. In this type of loading, the forces act in the plane of the adhesive layer. The single lap joint is the most commonly used adhesive joint configuration and has been best studied so far. The precise analysis of simple lap is very complicated because of the interaction between each of the three potential failure modes: adherent yielding, adhesive peel, and adhesive shear. In addition, the stress distribution along the overlap length and through thickness is non uniform, which would affect the reliability of the measured joint strength [5, 23-34]. The fact that the directions of the two forces illustrated in figure 2.3 are not colinear would create a bending in addition to the in-plane tension. The stress distribution as reported by many authors is shown in figure 2.4. The results show a comparative study between a closed form solutions as given by Golland and Reissner [32] and the finite element method for both shear and normal stresses. It is clearly shown that there is a good agreement between the two methods and the stresses are higher at the edges of the single lap specimen where failure would initiate.

The use of step lap joint figure 2.5.a is an alternative test method of the single lap joint, in which the undesirable bending effect is avoided. However, the stress distributions are almost not changed as illustrated in figure 2.5.b [27, 35-36]. Double laps joint are

probably the most desirable joints transferring loads between two members. The loads in the adherent parts can be in tension, compression, or in plane shear. However, the stresses are not uniform along the overlap length and through adhesive thickness, and there is the further difficulty of making two bondlines of the same thickness uniform [37].

#### **2.4.2.2 Peel test**

Peel tests are the most selective for measuring the surface treatment quality differences. Uniformity of peel strength values for a given adhesive in contrast to lap shear test system made the peel test an attractive way to measure the properties of adhesive bonded joints. Various forms of peel tests are used to assess the performance of structural adhesives. In fact, the configuration of this test intentionally stresses the adhesive in a very small region, subjecting it to a large tensile stress, whereas there is usually a complex stress state present. This stress state is not easily assessed, and peel is normally used to compare adhesives rather than to measure their properties [36]. Figure 2.6 shows different types of peel tests. The most commonly used is the T-peel test as shown in figure 2.6.d

The wedge crack test method known as Boeing Wedge Test simulates in a qualitative manner the forces and environmental effects on an adhesively bonded joint at the adhesive-adherent interface (figure 2.7). It has proven to be highly reliable in determining and predicting the environmental durability of adherent surface preparations. The test has been used in controlling surface preparation operations and in screening surface preparations, primer, and adhesive systems for durability. The test yields information on crack growth rate

and can indicate whether the fracture is between the adhesive and the substrate or wholly within the adhesive [38].

#### **2.4.2.3 Cleavage test**

Cleavage strength is very rarely quoted in reference works. In this type of test (figure 2.2.e) severe localized loading occurs on one side of the joint only, while the other side is merely loaded. This type of test is usually performed to investigate the ability of the bonded joint to withstand further processing after assembly [22].

#### **2.4.2.4 Axisymmetric joints**

Axisymmetric joints also with square or rectangular adherents, are widely used specimens for testing the response of adhesives to shear, tensile and compressive stresses. Butt joints or napkin ring, as specified by ASTM E229 (figure 2.8), can provide an apparently convenient mean for determining the mechanical properties of structural adhesives. The test is used to measure the modulus of rigidity and elasticity and Poisson's ratio. The advantage of using butt joints is that the adhesive is tested in the thin film form as used in most joints, thus overcoming any possible objection to bulk specimen. On the face of it, the stress distribution is simple, however, end effects are once again a problem. As stated by Adams and Wake [5], "if joints are to be loaded to failure and if the failure stress is to mean anything, then it must be true stress and not a convenient but misleading approximation."

In practice, most structural adhesives exhibit considerable plastic deformation when subjected to shear stresses, and it is quite probable that the small volume of the adhesive near the adherents corner will yield without causing premature failure of the joint when loaded in torsion. However, this small volume known as spew fillet makes the joint stiffer in torsion and this would lead to an overestimation of the shear modulus of the adhesive. Consequently, it is advisable to remove any spew fillet present on the test specimen. This can be largely avoided by using close-fitting spacers of PTFE films during the curing process. Extraneous deformation in the metallic components of the joints have been reported and corrected to measure the shear modulus of the epoxy adhesive, which agreed well with those obtained from the bulk specimens [39]. Such correction is obtained using special extensometers which measures the annular displacement of the adherents and that of the adhesive. The adhered material properties effects have been investigated by Sugibayashi et al. [40]. It was concluded that the tensile joint strength decreased when the difference in Young's modulus of the dissimilar adherents is larger. This decrease has been attributed to the stress distribution at the interface between the adhesive layer and the adhered.

For practical purposes, tubular lap joints have apparently gained place in the adhesion science. The growing interest of such joints in the field of civil engineering has made the subject expanding towards new applications such as irrigation tubes and wind turbine blades usually made with light weight materials, such as polymer matrix composites and aluminum. Actually, traditional joining techniques, such as welding, are frequently inapplicable, and it can be argued that adhesive bonding is often the best method for joining such materials [41-44]. Lubkin et al. [45], and Adams et al.[46] were probably among the first authors whom



studied the tubular lap joints loaded in torsion. The stresses were analyzed in similar manner as those obtained in the case of single lap joints. The analysis of tubular lap joints in torsion made of composite materials have been also investigated by Hipol [47], Chon [48] and Graves et al. [49] using closed form solutions. Alwar et al. [50] on the other side, have used FEM to investigate the effect of viscoelastic behavior of the adhesive on the strength of the tubular lap joints loaded in tension. It was found that not only the elastic stresses are different at different adhesive thickness levels but also the viscoelastic response showed considerable variation from one level to another. A large reduction of the order of 57%, was noticed in the normal stress and an even larger reduction of 62% in the shear stress over three decades of time. The same authors [51] have reported an analysis using FEM on tubular lap joints assuming linear elastic adherents and nonlinear biaxial stress-strain law in the adhesive. The constants appearing in the nonlinear law were obtained from uniaxial tension test data. The stress-strain relationship, however, was assumed to be time-independent. They have demonstrated that for low stress levels, of the order of 12% of the fracture stress, the nonlinear stresses were as much as 15% lower in shear and 8% in peel than the linear stresses.

#### **2.4.3 Analysis techniques to predict joint strength**

A review of the published literature suggests that there are three widely accepted methods for predicting the strength of bonded joints. The first approach uses a closed form solutions and elastic-plastic analysis for bond stress and strain. Joint failure is predicted to occur at a critical adhesive shear strain [52]. In another approach, a detailed finite element

analysis of the joint is performed with the adhesive modeled as an unflawed (uncracked), elastic-plastic material. It has been suggested that a maximum principal stress criterion works best for brittle adhesives, while a maximum principal strain condition should be used for toughened adhesives [5]. Linear elastic fracture mechanics concepts have also been applied to bonded joints. A variety of adhesively bonded fracture specimens have been developed to measure the mode I, mode II and mixed mode I and II adhesive fracture toughness [53]. For instance, it has been reported by Anderson and De Vries [54] that a method that utilizes both a critical energy release rate and an inherent flaw size has successfully correlated the failure of butt tensile joints. In addition to those methods for predicting joint failure and strength of adhesive bonded specimen, a new approach that is based on an interface corner stress intensity factor has been investigated within the context of elasticity theory by Reedy et al. [55-56]. This fracture criterion suggests that the strength of an adhesively bonded butt joint loaded in tension can be estimated from strength data for a joint having different bond thickness by the simple relationship.

$$\sigma_{t_2}^{ult} = \sigma_{t_1}^{ult} (h_1/h_2)^{1/3} \quad (1.1)$$

Where  $2h_i$  is the bond thickness,  $\sigma_i^{ult}$  is the nominal butt tensile strength and subscript  $i = 1, 2$  identifies the two joints with differing bond thickness. This relation applies only to thin bonds when the adhesive Poisson's ratio is between 0.3 and 0.4, the adherents are relatively stiff, and small scale yielding conditions occur at the interface corner.

### 2.4.3.1 Analysis methods of lap joint stress analysis

Knowledge of the stresses and strains in an adhesive joint is necessary to an understanding of joint strength. Broadly speaking, there have been two approaches to the problem. The first is the analytical, or closed form approach in which an exact mathematical solution for the stress condition is attempted. Usually, under simplifying assumptions, the closed form solution is presented. Goland and Reissner [32] have developed one-dimensional elasticity solutions based on the work of Volkerson [57] for two limiting cases: 1) the adhesive is homogeneous, thin and stiff, the axial stress is zero, and stresses do not vary through the adhesive layer; 2) the adhesive layer is soft and flexible mainly due to the deformation of the adhesive layer, the axial stress is zero, and stresses do not vary through the adhesive thickness. In the first case, the peel stress was found to be very high at the edge of the joint, while the shear stress is zero. In the second case, the maximum values of the peel and shear stresses occurred at the edge of the joint.

Erdogan and Ratwani [27] have presented an analytical solution based on a one-dimensional model for calculating stresses in stepped lap joints. One adherend was treated as isotropic and the second as orthotropic, and linear elastic behavior was assumed. The through thickness variation of the stresses in both, the adherends and the adhesive, was neglected. It was found that the shear and peel stresses were higher at the adhesive edge near the orthotropic adherent.

Several analytical solutions exist, each has been proposed on the basis of the imposed

assumptions [28,32,58-61]. A detailed review of the analytical aspect is given by Mallick [31] and Reedy [62]. The other approach is to use numerical methods such as the finite element method (FEM). FEM has gained universal acceptance since it facilitates more complete analyzes than otherwise possible. In finite element methods all possible cases have been treated, these include elasto-plasticity, and nonlinear analysis.

#### 2.4.3.2 Stress analysis methods of axisymmetric joints

From the literature review, the same methods of analyzes of lap joint have been used for annular joint. Kuenzi and Stevens [63], Bossler et al. [64] have used this configuration subjected to torsion load to obtain shear stress-strain curves. The shear stress distribution in the adhesive calculated from simple elasticity theory is given by:

$$\tau_{r\theta} = \frac{2Tr}{\pi (r_o^4 - r_i^4)} \quad (2.2)$$

Where  $\tau_{r\theta}$  is the shear stress at a radius  $r$ , caused by an applied torque  $T$ , while  $r_i$  and  $r_o$  are the inner and outer radii of the annulus.

Usually, when bonding the specimen, a small amount of the adhesive is squeezed out to form a spew fillet as is shown in figure 2.9, and this may modify the stress distribution given by equation 2.2. Adams et al. [65] have studied solid and annular butt joint loaded in torsion and tension, and have examined the effects of adherent flexibility in spew fillet. Under torsion load and taken with equation 2.2, it is predicted that the stress increases

linearly from zero at the center to a maximum at the outside. The magnitude of the applied torque has been selected to give a unit shear stress at the outside of the joint. The same torque was then applied to a similar joint having two different sizes of spew fillet. It was found that the spew fillet has reduced the general level of stress and introduced a stress concentration near the adherent corners. Related works, based on numerical computations, have been carried out by Sawa et al. [66] Nakano et al. [67] to investigate the stress distribution and displacements in adhesive butt joint subjected to a torsional load. It should be noted that the solution takes into account the adherent and the adhesive rigidity and the thickness of the adhesive. It was found that the singularity of the stress increased at the inner and outer circumferences of the interface with an increase in the ratio of shear modulus of the adhesive to that of the adherent ( $G_{\text{Adhesive}}/G_{\text{Adherent}}$ ). The increase of the maximum shear stress of the joint was noticed when the ratio ( $G_{\text{Adhesive}}/G_{\text{Adherent}}$ ) is small. Experimental prediction on the nominal ultimate shear stresses of adhesive bonded circular and rectangular joints (figure 2.10) has been reported by Matsui [68]. Based on the experimental results, he proposed a failure criterion for both cohesive and adhesive failure. For cohesive failure in the adhesive, the ultimate strength of butt adhesive joint is given by equation 2.3.

$$\tau_{us1} = 6.25 \tau_1 (G_a/E)(t/d)[1 - (t/D)]^2 \quad (2.3)$$

For the case of cohesive failure in tubular lap joint, the ultimate strength is given by equation 2.4.

$$\tau_{us2} = 6.25 \tau_1 (G_a/E)(2t/d) \quad (2.4)$$

The adhesive failure occurs when the ultimate shear stress equal to that of the bulk adhesive strength.

$$\tau_{ur} = \tau_B \quad (2.5)$$

Where  $G_a$  is the shear modulus of the adhesive,  $E$  is the tensile modulus of adherent,  $t$  is the thickness of the adherent,  $d$  is the thickness of the adhesive,  $l$  is the length of overlap,  $D$  is the mean diameter,  $\tau_B$  is the shear strength of the adhesive,  $\tau_1$  is the shear strength of the adherent and  $\tau_u$  is the shear stress.

#### 2.4.4 Torsion shear apparatus

The torsion shear apparatus must be designed to ensure that no bending or cleavage loads are imposed on the napkin ring specimens which must be subjected to a pure shear. The adherents consists of two thin walled tubes and some specifications are imposed to make the two tubes concentric. The thickness of the adherent tubes must be designed to ascertain that the variation  $\Delta\tau/\tau$  (equation 2.6) between the inner and outer radii of the tube is at least equal 10% [69].

$$\Delta\tau/\tau = (F/2A) \quad (2.6)$$

Where  $F$  is the total bonded area of the annular joint and  $A$  is the effective area given by:

$$\begin{aligned}
 F &= \pi(r_o^2 - r_i^2) \\
 A &= \pi r_m^2
 \end{aligned}
 \tag{2.7}$$

And  $r_i$  is the inner radii,  $r_o$  is the outer radii,  $r_m$  is the mean radii.

Broadly speaking, the torsion shear apparatus is designed to operate with standard machines commercially available. Historically, the torsion apparatus has been developed by Bossler et al. in 1968 [64]. Other design has been also proposed by ASTM E229 [70]. As a summary, the loading mechanism of the torsion shear apparatus proposed by Bossler [64] is transmitted to the torsion shear specimen through a yoke that is connected to the load cell through a universal joint. The yoke is attached to the specimen via two chains that pass through two pulleys before fastening to a torsion sprocket. The torsion sprocket is bolted to the movable adherent by four bolt, 90° apart. Since the yoke is free to move, the load is distributed equally between the two chains, ensuring that the sprocket is subjected to a pure torsion. The fixed adherent is bolted to the back plate and the entire apparatus is bolted to the machine cross head. Recently, a new fixture for bonded joints loaded in torsion has been proposed [71]. This fixture is designed to be fitted to any uniaxial testing machine with the aid of some clamping accessories (figure 2.11). The mechanism to create a torsion loading on a bulk specimen or a bonded joint is based on the torque generated by two lever arms in a cross configuration moving in opposite rotational directions. The rotation of the lever arms is provided by the axial displacement of the cross-head of the uniaxial testing machine. The specimen is inserted between the two lever arms through

cross grooves and a centering pin as shown in figure 2.12.a. To accomplish a perfect rotation movement, the lever arms are laid on needle bearings hold by lower and upper shafts (figure 2.11). The shafts came with a lower and upper steel frames that can be connected to an uniaxial testing machine. Moreover, clamping accessories are designed to hold the upper and lower frames aligned and at the same time avoid the frames to rotate during loading. In figure 2.12.b a detailed mechanism of equilibrium forces acting on the system is shown. The force applied by the uniaxial machine is transferred to the needle bearings supported by the steel shafts and give rise to two concurring forces:

$$\begin{aligned} R &= P/2 \cos \theta \\ F_a &= \mu (P/2 \sin \theta) \end{aligned} \quad (2.8)$$

where  $\mu$  is the coefficient of friction,  $P/2$  is the half force applied by the machine and  $\theta$  is the angle between the segment BC and the horizontal base.

The angular speed in this case based on cinematic relationships, is given by:

$$\omega = \frac{V_m \cdot \cos^2 \theta}{d} \quad (2.9)$$

Where  $\omega$  is the rotational speed and  $V_m$  is the cross head speed of the machine.

Results of both the proposed fixture compared to the step lap shear test is shown in figures 2.13 and 2.14 for two different types of filler used. It is shown from the figures that the general trend of the shear strength in both experiments increases with filler content, reaches a maximum and then starts to decrease. It is clear that the shear strength measured



with the proposed torsion shear fixture is higher than that measured with the conventional step lap specimen. This is not surprising, since it is well known that step lap joints produce lower joint strengths [25].

## **2.5 Prediction of mechanical properties by thermal analysis techniques**

A review of the published work related to the thermal analysis of adhesively bonded joints in attempt to predict the performance and durability of bonded structures is discussed in the following section. Differential scanning calorimetry (DSC) and dynamic mechanical analysis (DMA) were extensively used to investigate the cure of adhesives. They are used to help to formulate and to obtain the optimum adhesive properties.

### **2.5.1 Indirect relationship between thermal properties and mechanical performance**

In the early seventies, Brett [72] has used a residual DSC technique, the isothermal method 2, to correlate bond strengths with degree of cure. The bond strength data showed a good correlation with the residual exotherm for both isothermal and isochronal curing (isochronal curing means curing at constant time). Storage of assembled adhesive joints at room temperature prior to elevated temperature cure has caused deterioration of the bond strength and concomitant reduction of the residual exotherm, indicating that premature curing had a deleterious effect on the adhesive bond. Based on the DSC results, Brett has concluded that the bond failure was cohesive in the range of 70-90% cure and become

adhesive above 90% cure.

Perker et al. [73] have found that the lap shear strength of an epoxy film adhesive decreased as the residual exotherm decreased. Cure kinetics as measured by DSC, has been used to determine the minimum  $\Delta H_{\text{resid}}$  (Residual heat exotherm) that corresponds to the minimum bond strength. It has also been shown that film adhesive lots could be accepted or rejected on the basis of residual exotherm as well as lap shear strength. Zukas et al. [74] have used high performance liquid chromatography (HPLC), size exclusion chromatography (SEC) and thermogravimetric analysis (TGA) to establish the lot-to-lot consistency of the adhesive components composition. The thermal, dynamic mechanical, and rheological properties as a function of cure has been monitored by DSC, torsional braid analysis (TBA) and parallel plate rheometer. In a separate work, the effects of curing conditions on the mechanical behavior of bulk adhesives have been reported by Hahn et al. [75], and Lee et al. [76]. DSC and TGA analyzes have been performed to understand the effects of curing conditions on the cross linking and the thermal degradation. It has been shown that better thermal and mechanical properties can be attained by adequate curing conditions. On the other hand, Lee et al. [76] have demonstrated the complexity of the cure chemistry and have showed the effects of processing conditions on the thermomechanical properties and the reliability of the UV curable epoxies. Pitrone [77] has conducted DMA experiments to assess the interfacial adhesion quality resulting from the application of various organofunctional silane primers. Using small-scale laminated joints, he correlated the internal damping capacity,  $\text{Tan } \delta$ , obtained from DMA results with the floating roller peel mechanical test. Ludbrook et al. [78] have demonstrated the usefulness of the DSC and DMA to determine

the cure of reactive adhesives. The data obtained from DSC results showed a good correlation with the build-up of mechanical strength (figure 2.15). The degree of conversion as a function of time and temperature showed the same behavior as the lap shear strength versus curing time and temperature. On the other hand, DMA yielded a measure of modulus as a function of temperature which is useful to correlate the mechanical performance to service temperature. Whilst not related directly to adhesive joint strength, both modulus and strength behave similarly particularly for brittle adhesives as function of temperature. Sanborn et al. [79] have used a DSC and a quartz dilatometer instruments in conjunction to lap shear test to investigate the effect of thermal cycling on the mechanical properties of epoxy adhesives. It was found that thermal cycling produced a change in the physical structure of the resin resulting in a significant increase in the glass transition temperature  $T_g$ . This increase was attributed to the additional increase of crosslinking, thus reducing the local segment mobility, which in turn reduced the CTE of the thermally cycled samples. On the other hand, this thermal cycling produced 5 to 30 percent decrease in mechanical strength depending on the test temperature. De Nève et al. [80] have examined the effect of humidity and ageing time on the physical properties of epoxy adhesives using DMA. They showed that the glass transition temperature  $T_g$  and  $\tan \delta$  decreased as the ageing time increased. Fillers effect, on the other hand, have been investigated using a DSC in conjunction with TMA by Kaelble et al. [81-82]. They showed that an aluminum flake filler in an epoxy-phenolic adhesive is inert. Apparent activation energies, calculated from the variation in peak reaction temperatures with heating rate, were identical for the filled and unfilled systems. The heats of reactions for the two systems were in proportion to filler loading. At fast heating rates a cavitation process in the unfilled adhesive has been observed just above 100°C. This

phenomenon, which results in a void formation in the adhesive, has not been observed in the metal filled adhesive. In addition to reducing void formation, the metal filler provided higher modulus and better fracture toughness in the cured adhesive.

### 2.5.2 The use of TMA to investigate the thermal properties

TMA instrument has appeared to be a useful tool in characterizing polymers. However, its merits can go beyond its usual use. The information embodied in the TMA results can be used as a basis of determining the service temperature as well as the toughness of materials. This is shown by the two examples presented herein. Based on the free volume principle, Aharoni [83-84] has presented an empirical model relating the notional reference temperature ( $T_R$ ) at which the material would lose coherent strength in the absence of prior decomposition ( $T_R > T_g$ ), and the fractional free volume at that temperature,  $(FFV)_{TR}$ :

$$\Delta T = T_R - T_g = \frac{0.113 (T_R/T_g - 1)^{1/3}}{\Delta\alpha} \quad (2.10)$$

$$(FFV)_{TR} = \Delta\alpha \Delta T.$$

where  $\Delta\alpha = (\alpha_L - \alpha_g)$  is the change in volumetric expansion at the temperature of transition  $T_g$ ,  $\alpha_L$  is the CTE at the rubbery state and  $\alpha_g$  is the CTE at the glassy state. Aharoni [83] has reported an approximately linear empirical correlation between  $(FFV)_{TR}$  and  $(T_R - 2T_g)$ , within various polymer families especially for epoxy resin systems. The apparent correlation obtained from this linear relation appeared more convincing than that between the Simha-Boyer approximation of the free energy ( $\Delta\alpha \cdot T_g$ ) and  $T_g$  which has been reported for epoxy resins [85]. However, the obtained empirical correlation is relatively insensitive to

experimental values. According to the measured coefficients of thermal expansions and  $T_g$  for each epoxy system, it was concluded that the obtained results are sufficiently not accurate for close analysis of  $T_R$  and  $(FFV)_{TR}$ . Later, Burton [86] has reported series of experiments on toughened epoxy resins. It has been concluded that at a given  $T_g$ , polymers that have high value of  $(\alpha_L - \alpha_g)$  would show the greatest toughness. Recently, using TMA instrument, it is reported that the increase of the coefficient of thermal expansion upon absorption of water by the bonded joints; showed the same trend as the relative strength retention of the step lap shear specimens [87]. The expansion stresses expressed by equation 2.11 upon exposure to hot water led to the decrease of the overall strength of the bonded joints. It is conclusive that both properties are proportionally linked. A relationship between the percentage increase of CTE and the relative strength retention for both alumina and glass beads filled bonded joints is indicated in figure 2.16. It is shown that the relative increase of CTE is in general agreement with the measured strength retention. The higher increase of CTE in these joints specially in the case of glass beads filled bonded joints, produced higher stresses, which in turn induced lower strength retention.

$$\sigma_x = \sigma_y = \int_{T_r}^{T_p} \frac{E(T) \alpha^j dT}{1 - \nu(T)} \quad (2.11)$$

and  $\sigma_z = 0$ .

where  $\alpha^j$  is the CTE of the bonded joint in the glassy and/or rubbery state,  $E$  is the modulus,  $\nu$  is the Poisson ratio, and  $T$  is the temperature.

### 2.5.3 Thermal effects on adhesive joints

An adhesive bonded joint has three main elements: the adherents, the interface and/or interphase, and the adhesive. In fact, a little is known about the effect of temperature on the interface. Comyn [88] has reported some of the aspects that influence the behavior as well as the strength of adhesives. Some of which will be discussed in the next section. The effect of temperature on the strength of some aluminum alloy joints bonded with epoxy adhesives has been investigated by Brewis et al. [89-90]. In the case of the epoxide-polyamide adhesive FM 1000 (Cynamid), modulus and tensile strength were measured on bulk samples of the cured adhesive in the range of 16 to 85°C, and a considerable decrease in the modulus was observed at the glass transition temperature (40°C). The strengths of single lap joints were measured over temperature range of -60°C to 95°C, and decreased as the temperature increased. It was reported that the joints have maximum strength at sub-zero temperatures. As the temperature rises, joints become weaker and the mode of failure become 100% cohesive. The same authors have reported a study on epoxy adhesives based on DGEBA and di(1-aminopropyl-3-ethoxy) ether. It was shown that joint strengths are controlled by the mechanical properties of the adhesive, and that bulk properties dominate interfacial properties in controlling the strengths of these joints as shown in figure 2.17. The same conclusion on the dependence of joint strength on temperature has been drawn by several authors (Adams, Pilakoutas, Mori et al.) [91-95]. They have also showed that the strength upon temperature changes affected the stress distribution of the bonded joints, which, in turn as noted previously affected the joint strength. The service temperatures (ST) for some epoxy adhesives depend mainly on the functionality of the curing agent. For instance, epoxy

adhesive cured with polyamide have ST of 65°C. Those cured with aliphatic amines have ST of 100°C, with aromatic amines ST of 150°C, and 175°C for those cured with acid anhydrides.

#### **2.5.4 Analysis of bonded joints under thermal effects**

In an adhesive joint, the mismatch between the properties of the adhesive and that of the adherent may lead to significant stress concentrations in response to externally applied loads or residual strains. These stress concentrations may have significant effects on the properties of the joint, especially on its strength. This stress concentration also depends on the physical dimensions of the joint. Many reports and papers have been published on the thermal stresses in joints. As in the case of stress analysis discussed in section 2.4.3.1, investigations of thermal stresses in joints fall into two broad areas. The first approach uses closed form solutions such as the work of Rossettos et al. [96-97]. In their work, they have taken into account the thermal mismatch between the adhesive and the adherent and assumed that the adhesive may expand due to temperature change. A modified shear lag model was adopted to obtain the closed form solution. The second, probably the most widely used approach is the use of finite element method (FEM). Harison and Harison [98] have used the FEM to calculate the stress near the ends of an adhesive layer of uniform thickness subjected to shrinkage stresses, and shear loads. The interfacial shear stresses, due to shrinkage stresses, or applied tension have been found to be greater in adhesive materials with low Poisson's ratios than with those of high Poisson's ratios. Actually, this is somewhat logical since a large Poisson ratios may denote ductility and ductile materials accommodate large

deformations at lower stresses. The obtained results using FEM [98] yielded useful information about the mechanical behavior of joints. However, these results do not provide the information necessary on the residual stresses arising as a result of the mismatch in the thermal expansion coefficients. The effect of mismatched CTE's of the adherents to that of the adhesive on the stress distribution of adhesive bonded joints have been studied and reported by Kirchner et al. [99] and Kawada et al. [100]. As the ratio of mismatched CTE of the adherent to that of the adhesive increased, the stresses generated by temperature change decreased (figure 2.18). They were tensile near the end of the interface and compressive around its center [100]. More recent investigations on thermal stresses in adhesively bonded joints arising from temperature fields and internal stresses generated in cooling and shrinkage processes have been examined through boundary element method (BEM), FEM and photo elastic experiments [31,99-110]. It is generally believed that thermal stresses are compressive or (negative) on heating and tensile or (positive) on cooling in adhesive joints. They depend on the geometry of the body and its adhesive elastic and thermal parameters such as Young's modulus, thermal expansion coefficient, the Poisson's ratio, and the temperature distribution [104-111].

The wide spread use of composites in many areas create a need to join them to other substrate such as metal parts. For instance, CFRP are extensively used for drive shafts of power transmissions, robot arms, and truss structures for spacecraft. However, the thermal expansion coefficients of FRPs are much different than those of metals. As a consequence, thermal stresses are generated in the adhesive joint during heating and cooling [31,93-95,112-116]. In a separate work, Sato et al. [112] and O'Callaghan et al. [113] have



investigated thermal effects in which metal was bonded to either CFRP or SMC composites respectively. FEM technique was conducted by Sato [112] in order to predict the strength of CFRP/metal shaft joints under temperature changes. Both room and low temperatures (-70°C) were investigated under mixed loads (tensile and shear) on bonded shaft steel and CFRP adherents. It was found that the strength of the joint in the steel adherent increased as the temperature decreased and the thermal stresses generated were higher at the edge of the adhesive layer. On the other hand O'Callaghan [113] has reported that the stress distribution showed a considerable dependency upon varying the stiffness of the composite adherent. It was concluded that an adequate design of the adherent SMC composite would minimize the peel and shear stresses significantly in both thermal and applied mechanical loads.

## **2.6 Conclusions**

The need to characterize adhesive bonded joints to withstand either an external applied load or environmental conditions seems to be of extreme importance. Several test methods have been developed to evaluate specific mechanical properties. However, it is conclusive that these test methods presented difficulties to achieve the two main requirements; ease of testing and reliable results. At present, shear testing of adhesive bonded joint is achieved under tension or compression loading of either single or step lap joints. This approach meets the requirements of ease of testing, however, its reliability is questionable because of the non-uniform stress distribution. The contrary is seen for the torsion testing method, i.e., the method is reliable but the experiment is difficult which has prevented its widespread and popularity.

Thermal characterization have been so far used to evaluate the performance and shelf life of bulk adhesives. However, correlations between the mechanical properties of bonded joints and the thermal properties of bulk adhesives do not seem convincing, even though, qualitative agreements have been obtained using DSC and DMA. In addition, it is seen that TMA technique is useful to characterize thermoset materials and evaluate the performance of curing resins. In respect of what has been found using TMA to measure the performance of bonded joints under moisture effects, it is believed that TMA technique can be used to understand the behavior of adhesives as well as to relate them to their mechanical performance.

## **2.7 Acknowledgments**

The authors wish to thank the Natural Sciences and Engineering Research Council of Canada (NSERC) and Fonds pour la Formation des Chercheurs et de l'Aide à la Recherche (FCAR).

## 2.8 References

- 1 B. Irving, *J. Welding*, V.73, N.9, 1994, p.51
- 2 A. J. Kinloch, *J. Mater. Sci.*, V.15, 1980, p.2141
- 3 A. J. Kinloch, " A fracture mechanics approach to the failure of structural joints ",  
*Development in Adhesive 2*, ed. A. J. Kinloch, 1981, p.83
- 4 A. J. Kinloch, *J. Mater. Sci.*, V.17, 1982, p.617
- 5 R.D. Adams and William C.Wake, "Structural adhesive joint in engineering",  
*Elsevier Applied Science Pub.*, London and NY, 1984, p.14
- 6 L. H. Lee, "Adhesive Bonding", ed. L. H. Lee, *Plenum Press NY*, 1991
- 7 L. H. Sharpe, *Machine Design*, V.38, N.19, 1966, p.179
- 8 *Society of Manufacturing Engineers, Adhesives in modern Manufacturing*, ed. E. J. Bruno, 1970
- 9 E. M. Petrie, *Plastics and adhesives as adhesives, Handbook of Plastics and Elastomers*, ed. C. A. Harper, *McGraw-Hill*, NY, 1975
- 10 E. M. Landrock, " Introduction", *Adhesive Technology Handbook*, ed. A. H. Landrock, *Park Ridge, New Jersey, Noyes Pub.*, 1985. p.1
- 11 D. H. Ridge, "Physical Chemistry of Adhesion, *Willey- Interscience*, 1971
- 12 W. A. Zisman, "Adhesion and Cohesion", ed. P. Weiss, 1962
- 13 H. F. Mark, *Adhesives Age*, V.22, N.7, 1979, p.35
- 14 H. F. Mark, *Adhesives Age*, V.22, N.9, 1979, p.45
- 15 M. T. Clark, "Definition and Nondestructive detection of critical adhesive bondline flaws", *AFML-TR-78-108*, U.S. air force materials Laboratory, 1978
- 16 E. Segal and J. L. Rose, *Research Techniques in Nondestructive testing*, V. IV, ed. R. S. Sharpe *Academic Press Inc. London*, 1980, p.275.

- 17 D. J. Hagemaiier, Adhesives and Sealants: Engineered Materials Handbook, ASM Int., V.3, 1990, p.743
- 18 R. B. Thompson and D. O. Thompson, J. Adhes.Sci.Tech., V.5, N.8, 1991, p. 583
- 19 E. H. Landrock, Adhesive Technology Handbook, ed. A.H. Landrock, Park Ridge, New Jersey, Noyes Pub., 1985, p.54
- 20 E. J. Hughes, W. Althof and R. B. Krieger, Adhesive Bonding of Aluminium Alloys, ed. E. W. Thrall and R. W. Shanon, Marcel Dekker, 1985, p.141
- 21 S. Semerdjier, " Metal to Metal Adhesive Bonding ", ed. S. Semerdjier Business Books London, 1970, p.55
- 22 R. D. Adams, Engineered Materials Handbook, ASM Int. V.3, 1990, p.325
- 23 O. Volkersen, Construction Métalique, N.4, 1965, p.3
- 24 J. M. Giraud, Matériaux et Techniques, 1980, p.255
- 25 M. Halioui and J. P. Lieurade, Matériaux et Techniques, 1991, p. 17
- 26 C. Kassapoglou and J. C. Adelman, SAMPE Quart., V.24, N.1, 1992, p.19
- 27 F. Erdogan and M. Ratwani, Journal of Composite Materials, V.5, 1971, p.378
- 28 L. J. Hart-Smith, Technical report, NASA CR1122 36, 1973
- 29 M. Y. Tsai and J. Morton, J.Strain Analy., V. 29, N. 1, 1994, p.137
- 30 R. D. Adams and J. A. Harris, Int. J. Adhes. Adhes., V. 7, N.2, 1987, p.69
- 31 V. Mallick, " Stress Analysis of Metal/CFRP Adhesive Joints Subjected to the Effects of Thermal Stress ", Ph.D Dissertation Univ. Bristol, UK, 1989
- 32 M. Goland, E. Reissner, J. Appl.Mech., V.11, 1944, p.A17
- 33 K. Mori and T. Sugibayashi, Nippon Kikkai Gakkai Ronbunshi, PartA V. 55, N.519, 1989, p.2211
- 34 F.E. Penado and R.K Dropele, Adhesives and Sealant " Engineered Materials Handbook", ASM Int. V.3, 1990, p.477

- 35 K. Mori and T. Sugibayashi, *JSME Int. J., Series 1, V. 33, N. 3, 1990, p.349*
- 36 T. A. Osswald, "Adhesive and Sealant, *Engineered Materials Handbook*", ASM Int. V.3, 1990, p.325
- 37 L. J. Hart-Smith and E. W. Thrall, *Adhesive Bonding of Aluminium Alloys*, ed. E. W. Thrall and R. W. Shanon, Marcel Dekker, 1985, p.241
- 38 A. Marceau and E. W. Thrall, in *Adhesive Bonding of Aluminium Alloys*, ed. E. W. Thrall and R.W. Shanon, Marcel Dekker 1985, p.177
- 39 M. P. Zanni-deffarges and M.E.R. Shanahan, *Int. J. Adhes.Adhes.*, V.13, N.1, 1993, p.41
- 40 T. Sugibayashi,, K. Matsuo, H. Kyogoku and K. Ikegami, *Nippon Kikkai Gakkai Ronbunshi, Trans. J. Soc. Mech. Eng., Part A, V. 52, N.476, 1989, p.1043*
- 41 C. O'reilly, *SAE Trans. J. Mater.Manufac., Section 5, V.55, 1990, p.839.*
- 42 Y. Delmas, "Contribution à l'étude théorique et expérimentale du collage de tubes métalliques par l'intermédiaire de résines époxydiques", Thesis Université de Reims,1985.
- 43 E. D. Reedy, JR. and T. R. Guess, *Int. J. Fract.*, V.63, 1993, p.351, also SED-V.14, *Wind Energy, ASME 1993*
- 44 Y. Gilibert and A . Rigolot, *Mech. Res. Comm.*, V.8, N.5, 1981, p.269
- 45 J. L. Lubkin, E. Reissner, *Trans. ASME*, 1956, p. 1213
- 46 R.D. Adams, J. Coppedale, *J. Adhes.*, V.9, 1977, p.11
- 47 P. J. Hipol, *J. Compos. Mater.*, V. 18, N.4, 1984, p.298
- 48 C. T. Chon, *J. Compos. Mater.*, V.16, N.4, 1982, p.268
- 49 S. R. Graves and D. F. Adams, *J. Compos. Mater.*, V.15, N.3, 1981, p.211
- 50 R.S. Alwar, Y.R. Nagaraja, *J. Adhes.*, V.8, 1976, p.79
- 51 Y. R. Nagaraja and R. S. Alwar, *J. Adhes.*, V.10, 1979, p.97.

- 52 L.J. Hart-Smith, *Join. Compos. Mater.*, ASTM STP 749, ed. K. T. Kedward, Philadelphia, PA, 1981, p. 3
- 53 K. M. Liechti, "Engineered Materials Handbook", *ASM Int.* V.3, 1990, p.335
- 54 G. P. Anderson and K. L. devries, *Int. J. Fract.*, V.39, 1989, p.191
- 55 E. D. Reedy, JR., *Int. J.Solid Struct.*, V.30, N.6, 1993, p.767
- 56 E. D. Reedy, JR. and T. R. Guess, *Int. J. Solid Struct.*, V.30, N.21, 1993, p.2029
- 57 O. Volkersen, *Die nietkraftverteilung in zugbeansprochten nietverbindungen mit konstanten laschenquerschnitten*, *Luftfahrtforschung*, V.15, 1938, p.41
- 58 J. N. Reedy and S. Roy, "Adhesive Bonding", ed. L. H. Lee, Plenum Press NY, 1991, p.359
- 59 D. J. Allman, *Quart. J. Mech. Appl. Math.*, V.XXX part 4, 1977, p.415
- 60 F. Delale, F. Erdogan and M. N. Aydinoglu, *J. Compos. Mater.*, V.15, 1981, p.249
- 61 Harwell report AEREG 411, " A computer program for the non-linear stress analysis of adhesively bonded single lap joints, 1986
- 62 W. J. Renton and J. R. Vinson, *J. Appl. Mech. Trans. ASME*, 1977, p.101
- 63 E. W. Kuenzi and G. H. Stevens, *US Forest products Service Research Note FLP-011*, US Dept. of Agric., Madison Wisconsin, 1963
- 64 R. C. Bossler, M. C. Franzblau and J. L. Rutherford, *J. Sci. Inst: J. Phys. E.* , V.21, 1968, p.829
- 65 R.D. Adams, J. Coppendale and N.A. Peppiatt, *J.Strain Analy.*, V.13, N.1, 1978, p.1
- 66 T. Sawa, Y. Nakano and K. Temma, *J. Adhes.*, V.24, 1987, p.245
- 67 Y. Nakano, T. Sawa and S. Arai, *Int. J. Adhes.Adhes.*, V.9, N.2, 1989, p.83.
- 68 K. Matsui, *Int. J. Adhes. Adhes.*, V.11, N.2, 1991, p.11
- 69 C. F. Kollbrunner and K. Basler, " Torsion in structures, An engineering approach, Springer-Verlag New York, Heidelberg Berlin 1969, p.1

- 70 Standard Test Method for Shear Strength and Modulus of Structural Adhesives, E229-70.
- 71 M. Ouddane, R. Boukhili and R. Gauvin, submitted to J. Mater. Sci., May 1997
- 72 C. L. Brett, J. Appl. Polym. Sci, V.20, 1976, p.1431
- 73 B. G. Perker and C. Hart-Smith, Modern Plast., 1979, p.58
- 74 W. X. Zukas and H. H. Wong, ANTEC 1987, p.1051
- 75 O. Hahn and X. S. Yi, Weld. World, V.25, N.7/8, 1987, p.152
- 76 C. J. Lee, 6th Int.SAMPE Electronics Conference, 1992, p.500
- 77 L. R. Pitrone, 5th Int. Joint Military/Government Industry Symposium on Structural Adhesive bonding, Dover New Jersey, 1987, p. 359
- 78 B. D. Ludbrook and R. J. Whitwood, Int. J. Adhes. Adhes., V.12, N.3, 1992, p.138
- 79 J. A. Sanborn and D. E. Morel, JR., J. Reinf. Plast. Compos., V.27, N.2, 1988, p.155
- 80 B. De Nève and M.E.R. Shanahan, Int J. Adhes. Adhesi., V.12, N.3, 1992, p.191
- 81 D. H. Kealble and E. H. Cirlin, J. Polym. Sci., Part C 35, 1971, p.79
- 82 D. H. Kealble and E. H. Cirlin, J. Polym. Sci., Part C 35, 1971, p.101
- 83 S. M. Aharoni, J. Macromol. Sci. Phys. V.B10, N4, 1974, p.663
- 84 S. M. Aharoni, J. Macromol. Sci. Phys. V.B9, N4, 1974, p.699
- 85 S.V. Petryayev, Y.M. Blyakhmam, D.A.P. Lipenok, E.M. Gvirts and P.Y. Gofman, Polym. Sci., USSR, V.14, 1972, p.1821
- 86 B. L. Burton, SAMPE J., V.24, 1988, p.27
- 87 M. Ouddane, R. Boukhili, R. Gauvin, Submitted to Polym. Compos., August 1997
- 88 J. Comyn, Adhesives and Sealants: Engineered Materials Handbook, ASM Int., V.3, 1990, p.616
- 89 D. M. Brewis, J. Comyn and R. J. A. Shalash, Int. J. Adhes. Adhes., V.2, 1982, p.215
- 90 D. M. Brewis, J. Comyn and R. J. A. Shalash, Polym., V.24, 1983, p.67

- 91 R.D. Adams , J. Coppendale, V. Mallick and H. Al-hamdan, *Int. J. Adhes. Adhes.*, V.12, N.3, 1992, p.185
- 92 Y. Nakano, F. Nakagawa, and T. Sawa, EEP-V.4-1, *Advances in Electronic Packaging ASME* 1993, p.11
- 93 T. Mori, Q. Yu, S. Takahana and M. Shiratori, *JSME Int., Series I: V.34, N.2, 1991*, p.257
- 94 R. D. Adams and V. Mallick, *J. Adhes.*, V.43, 1993, p.17
- 95 K. Pilakoutas, S. Hafeez and S. Dritos, *Mater.Struct./ Matériaux et Construction*, V. 27, N.173,1994, p.527
- 96 J. N. Rossettos, Y. Peng, and H. Neyeb-Hashemi, M-DV.29, *Plast. Plast. Compos.: Mater. Proper., Part perform. Proc. Simul. ASME*, 1991, p.259
- 97 J. N. Rossettos, Y. Peng, and H. Neyeb-Hashemi, *J. Eng. Mater.Tech., Trans. ASME*, V.116, 1994, p. 533
- 98 N. L. Harison and W. J. Harison, *J. Adhes.*, V.3, 1972, p. 195
- 99 H. P. Kirchner, J. C. Conway, JR., and A. Esegall, *J. Am. Ceram. Soc.* V.70, N. 2, 1987, p.104
- 100 H. Kawada and K. Ikegami, *JSME int. Series 1: Solid Mech., Strength Mater.*, V.35, N.2, 1992, p152
- 101 R.D. Adams and V. Mallick, *J. Adhes.*, V.38, 1992, p.199
- 102 E. W. Huang, *SPIE*, V.1303, *Advances in Optical Structure Systems*, 1990, p.58
- 103 G. K. Hu, D. Baptiste and D. Francois, *Euromat Advanced Structural material*, V.II, combridge UK, 1991, p.493
- 104 Y. Suzuki, *JSME int. , Series I: V.30, N.265, 1987*, p.1042
- 105 T. Hattori, *JSME Int. , Series I:V. 34, N.3, 1991*, p.326
- 106 K. Mori and T. Sugibayashi, *JSME Int. ,Series I: V.33, N.3, 1990*, p.349



- 107 D. Chen and S. Sheng, *Trans. ASME, J. Appl. Mech.*, V.57, 1990, p.78
- 108 J. W. Sawyer and P. A. Cooper, *AIAA J.*, V.19, N.11, 1981, p.1443
- 109 Y. Nakano, T. Sawa and F. Nakagawa, *JSME Int., Series I*: V.35, N.2, 1987, p.145
- 110 F. Nakagawa, Y. Nakano, T. Sawa, *JSME Int., Series A*: V.37, N.3, 1994, p.238
- 111 D. M. Mazenko, G. A. Jensen and P. J. McCormick, *SAMPE J.*, V.23, N.3, 1987, p.28
- 112 C. Sato and K. Ikegami, *JSME Int., Series A*: V.37, N.3, 1994, p.282
- 113 P. O'Callaghan and K. Callaway, 31st AIAA/ASME/ASCE/AHS/ASC Struct., Struct. Dyna. Mater. Conference, Part 2, 1990, p.1234
- 114 Q. Yu, M. Shiratori and T. Mori, *JSME Int., Series A*: V.36, N.1, 1993, p.43
- 115 H. E. Williams, *J. Therm. Stress*, V.8, 1985, p.183
- 116 T. Mori, Q. Yu and M. Shiratori, *Mechanical behavior of materials, Part VI*, V.3, Kyoto Japan, 1991, p.41

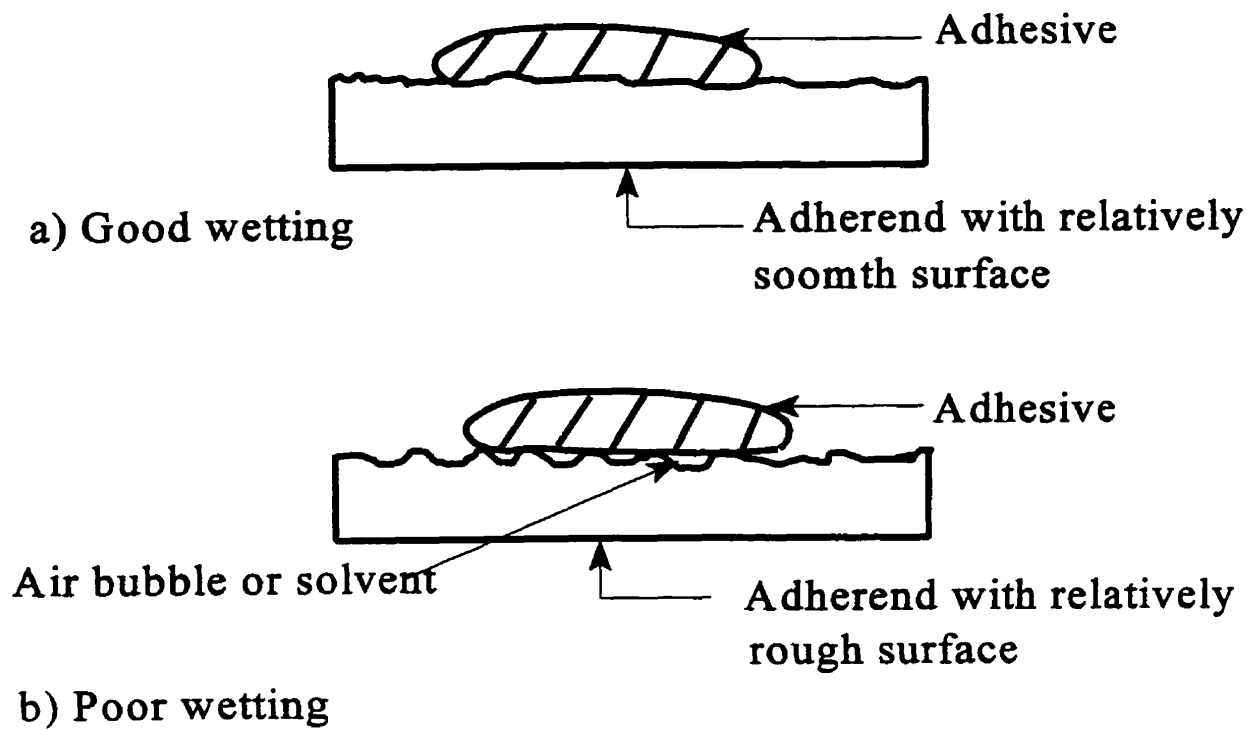


Figure 2.1 Good and poor wetting by an adhesive spreading across a surface [10].

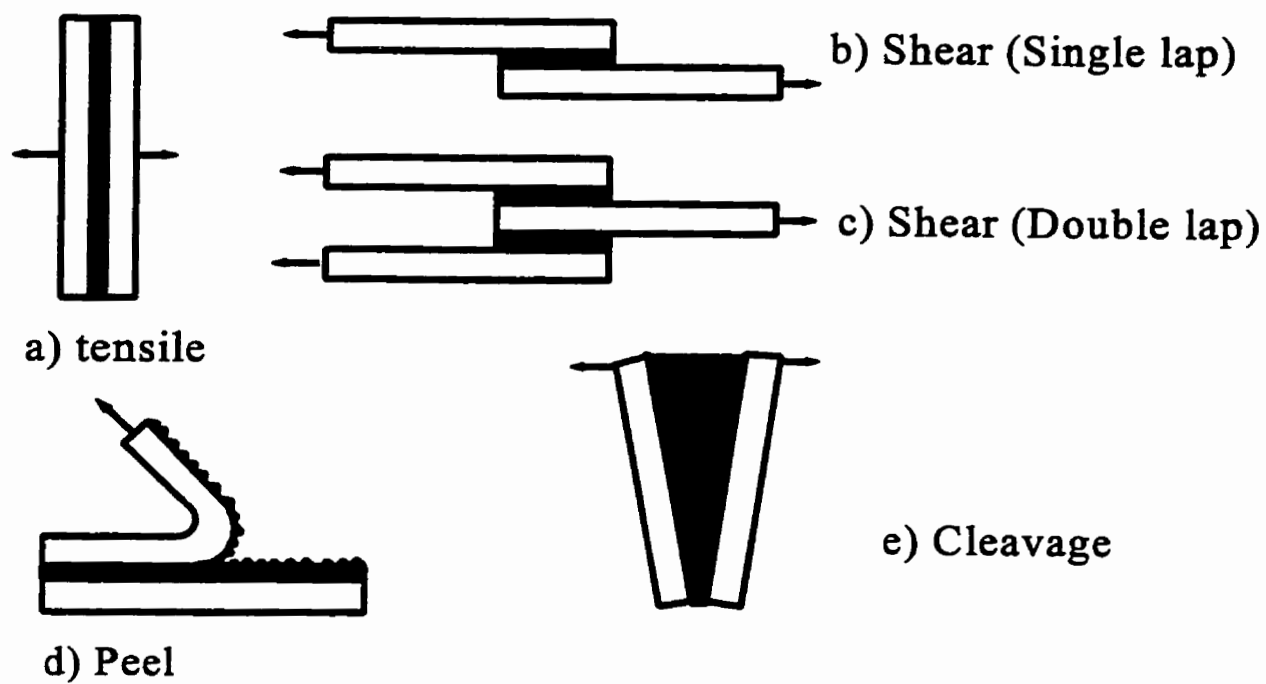


Figure 2.2 Some typical joints used in testing.

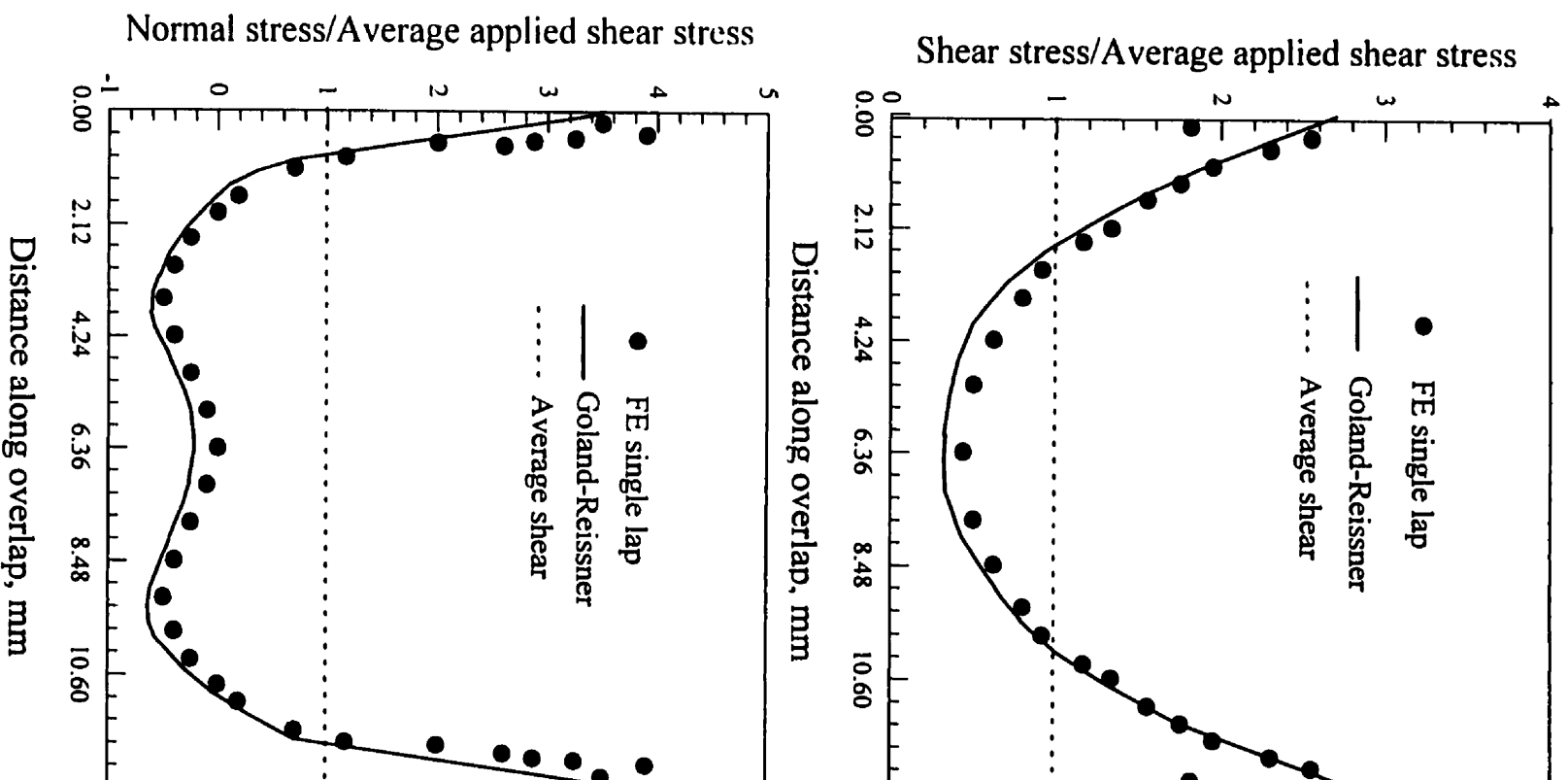


Figure 2.3 Stress distribution in a single lap joint, comparison between closed form solution with finite element (FE) results. A) shear stresses b) Normal stresses [34].

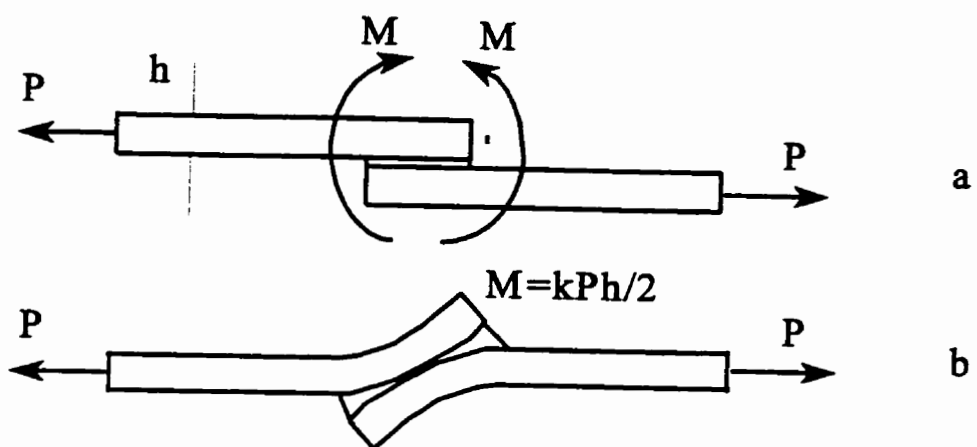


Figure 2.4 Load path in a) undeformed and b) deformed joint,  $k$  = bending moment factor[5].

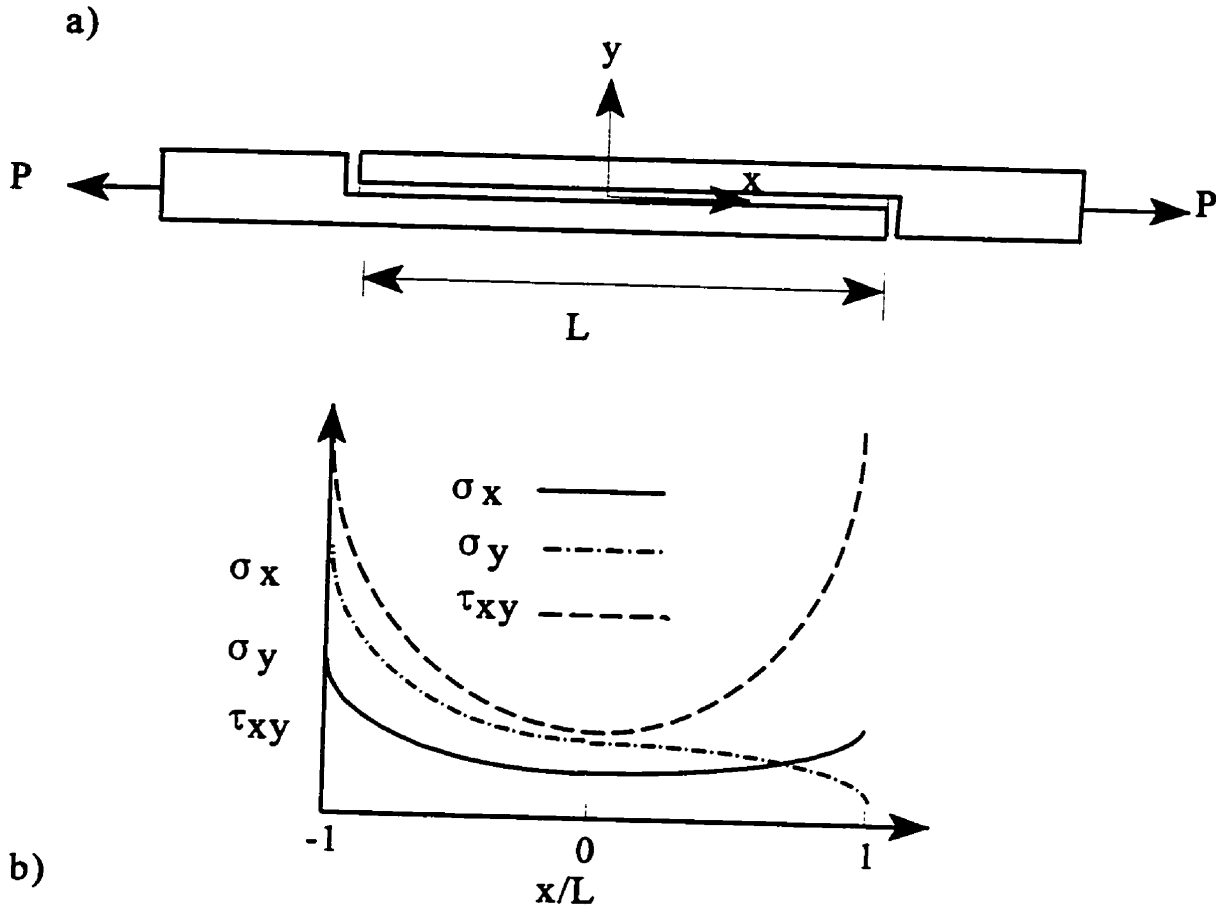


Figure 2.5 a) Step lap geometry, b) Stresses in step lap joint [5].

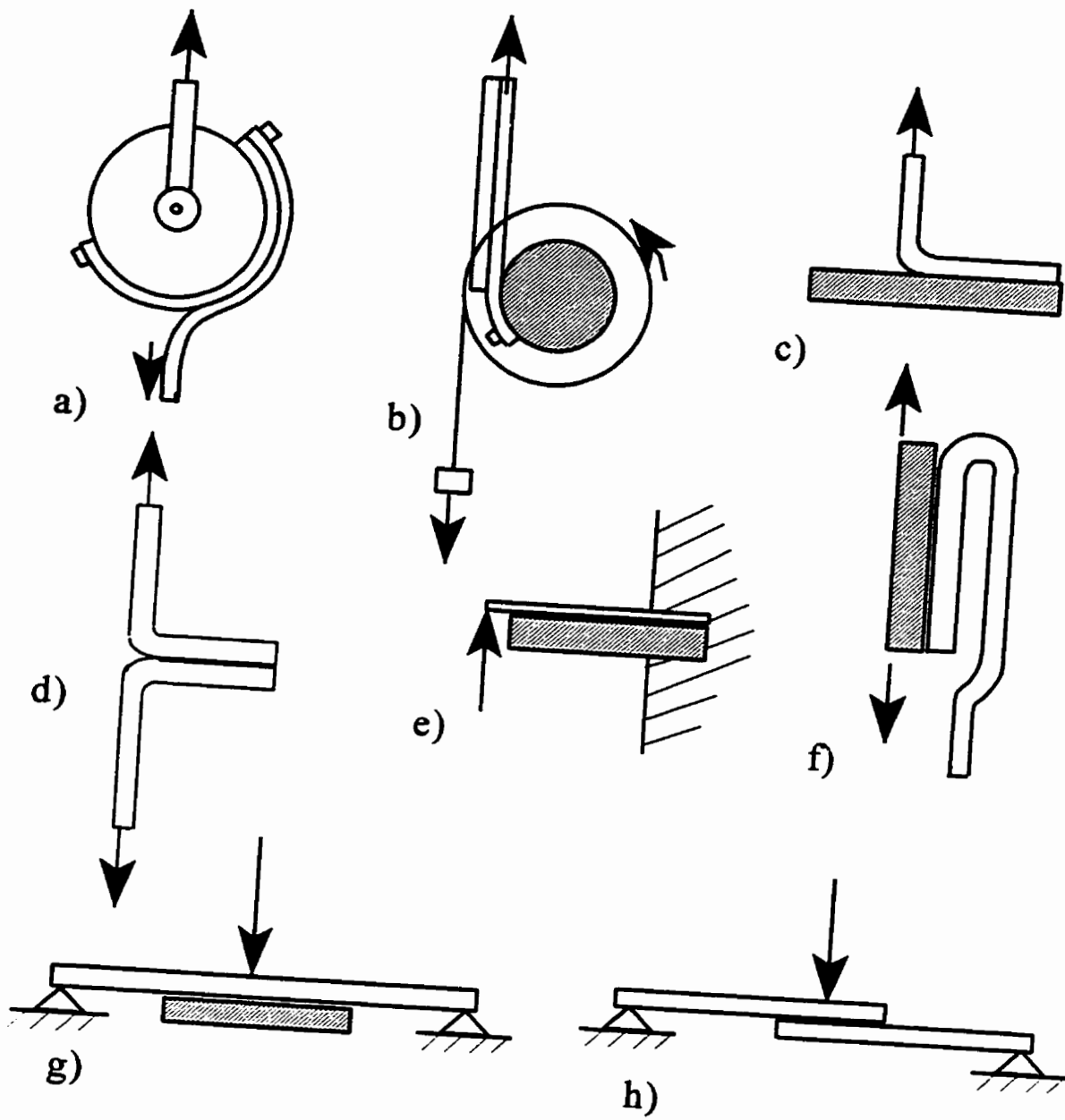


Figure 2.6 Basic peel tests [31].

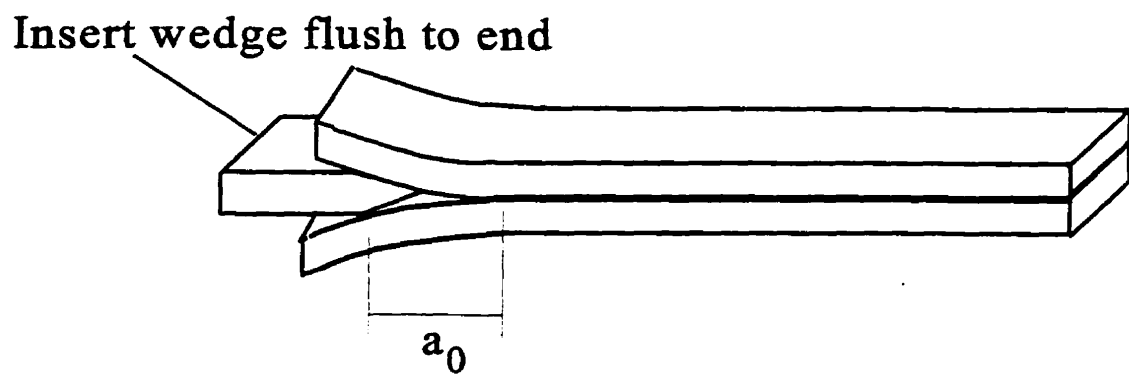


Figure 2.7 Wedge crack test specimen configuration.



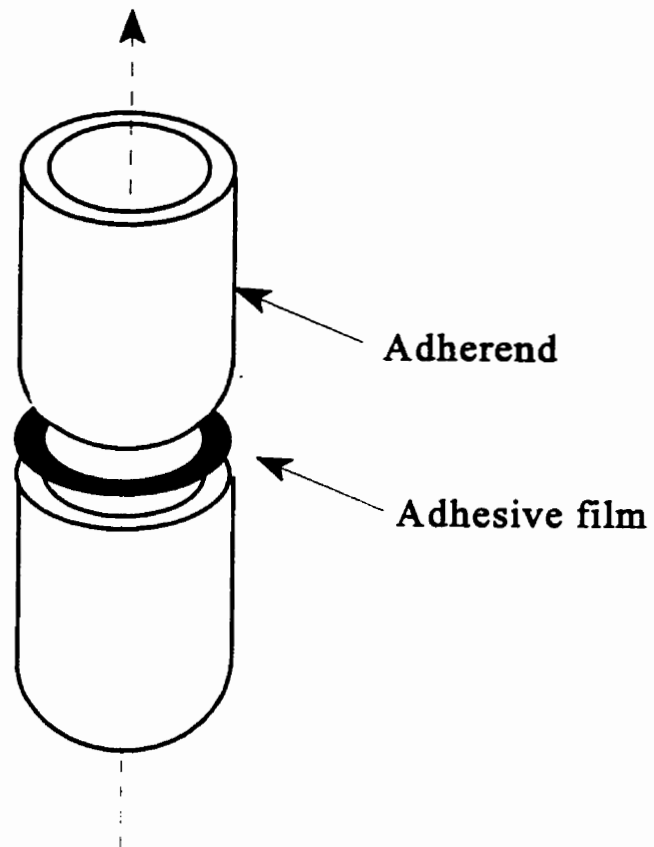


Figure 2.8 Butt or napping ring specimen geometry.

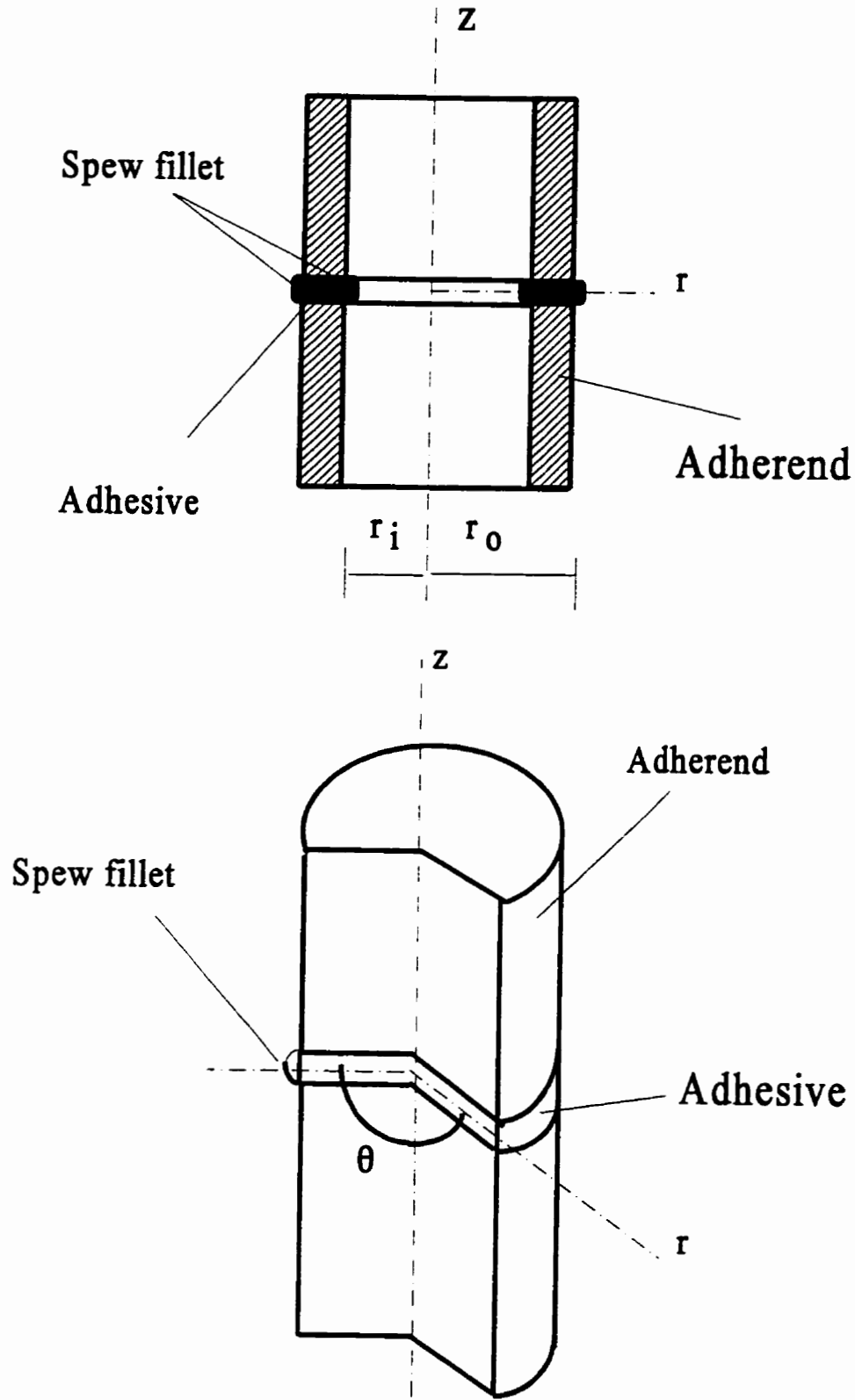


Figure 2.9 Circular butt joint: a) annular; b) solid [65].

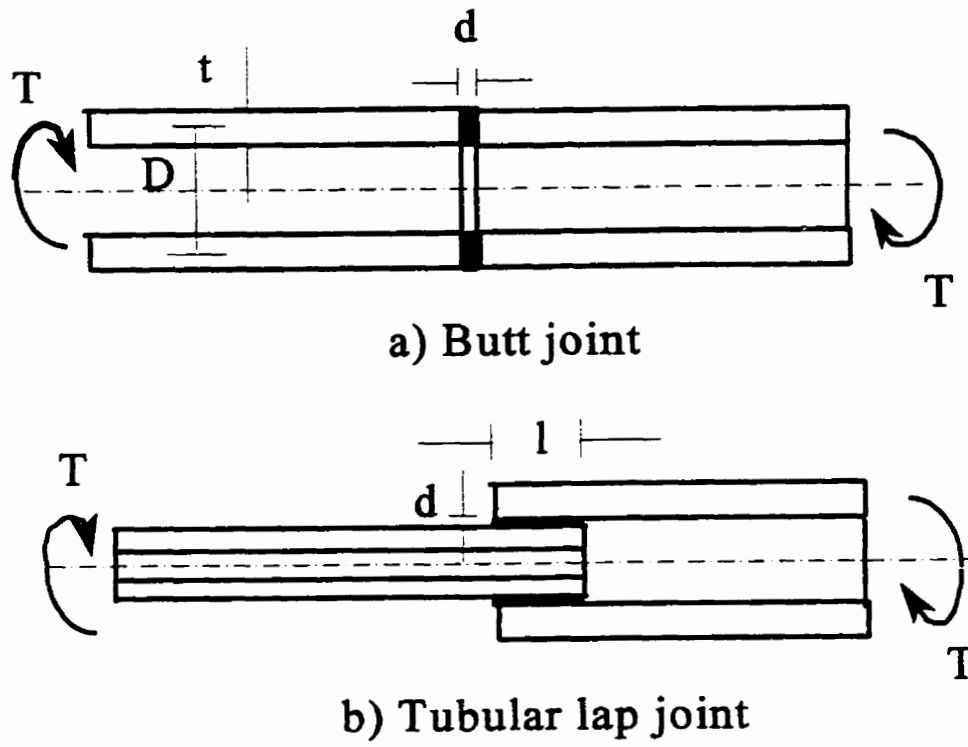


Figure 2.10 Joints geometry for strength prediction [68].

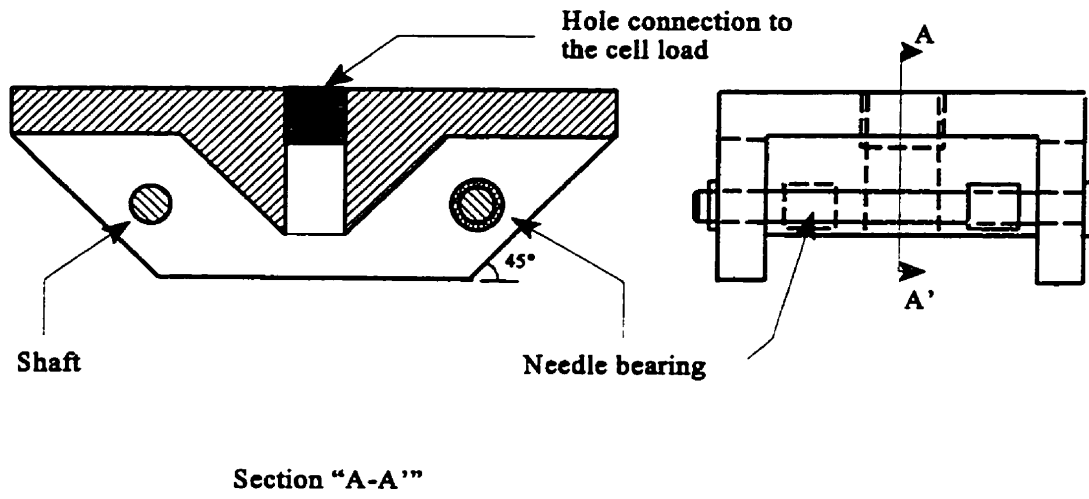


Figure 2.11 Upper steel frame diagram [71]

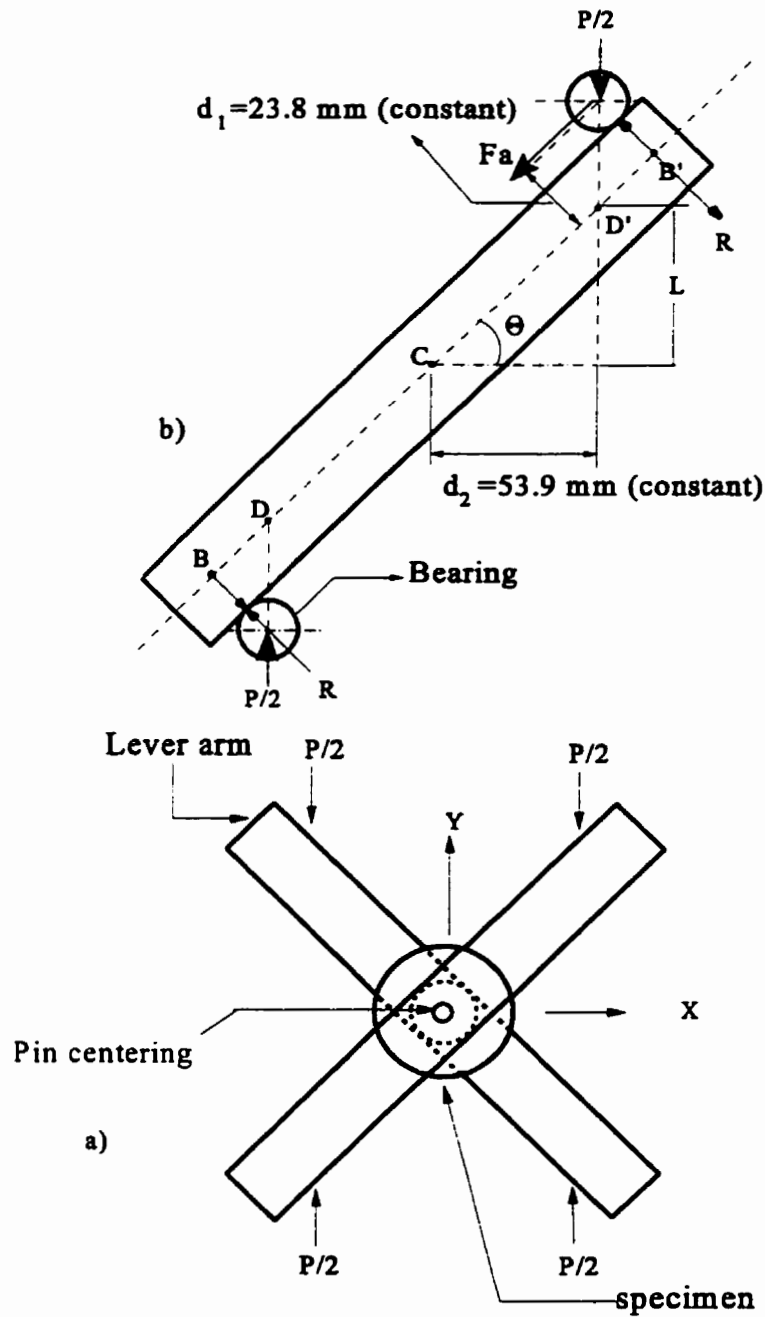


Figure 2.12 Diagram showing the mechanism of the proposed torsion fixture [71]

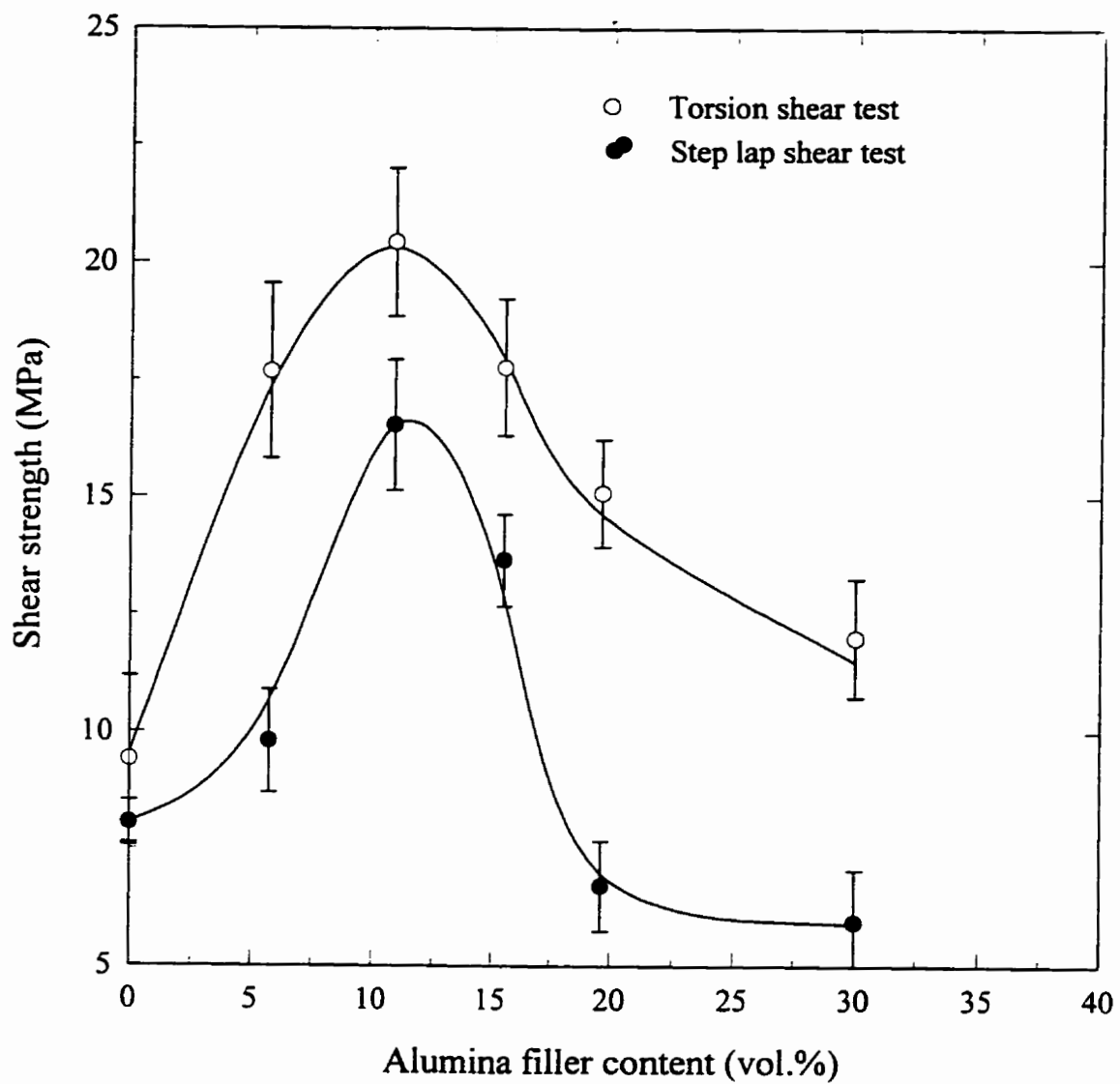


Figure 2.13 Shear strength as a function of filler content in the case of alumina filler [71].

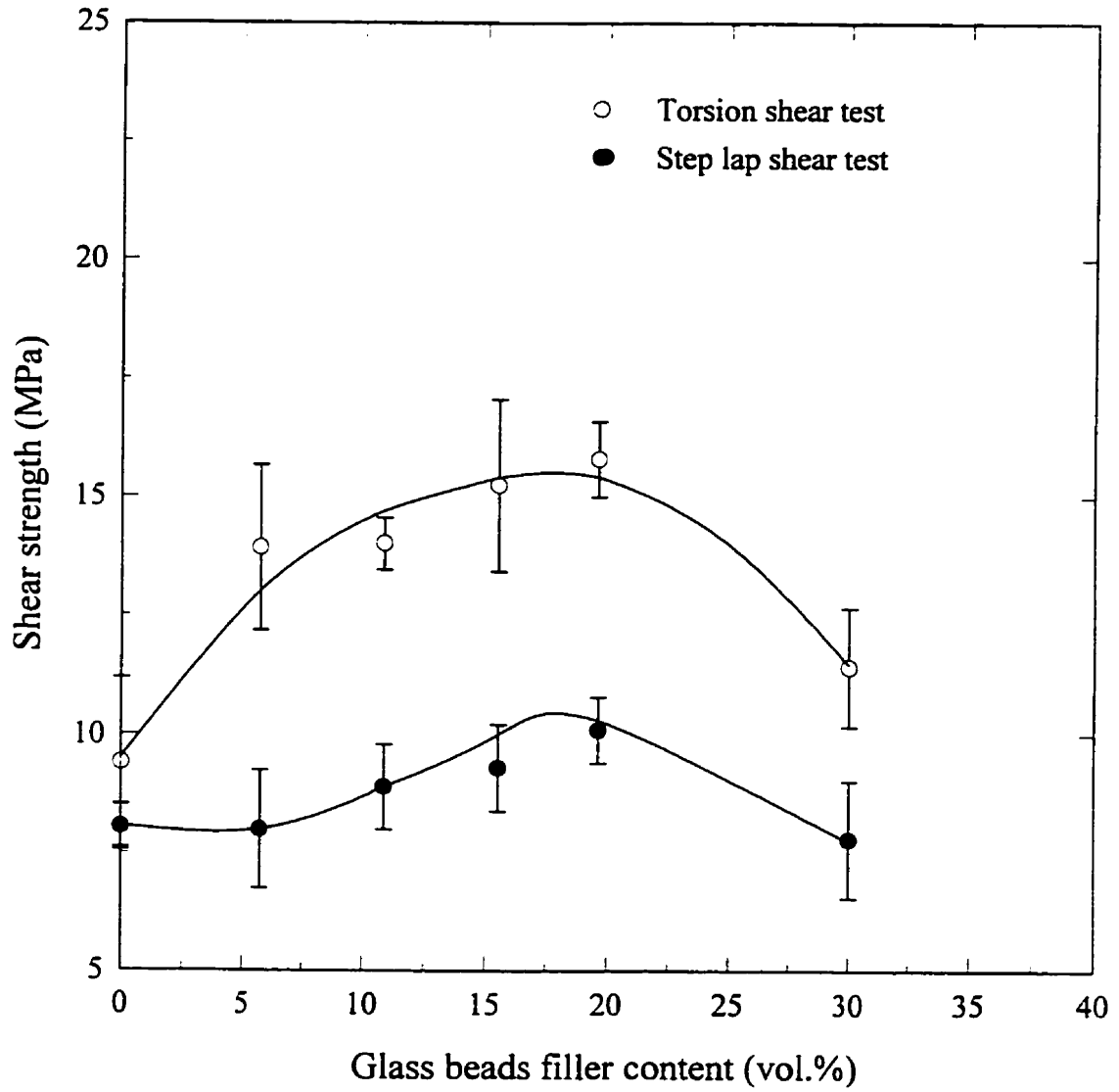


Figure 2.14 Shear strength as a function of filler content in the case of glass beads filler [71].

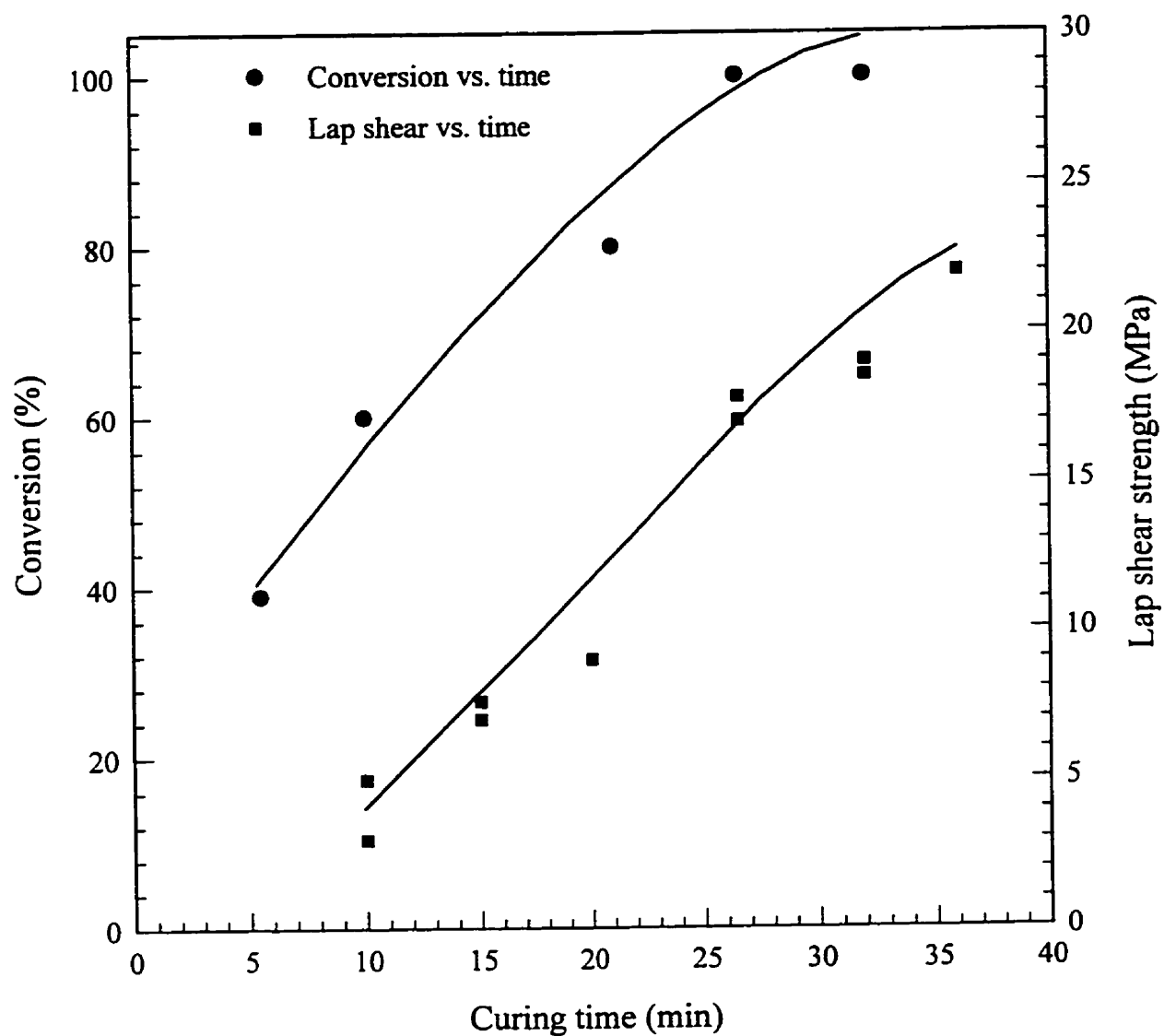


Figure 2.15 Conversion and lap shear strength of adhesive Evo-Tech TE as a function of curing time at 120°C [78].



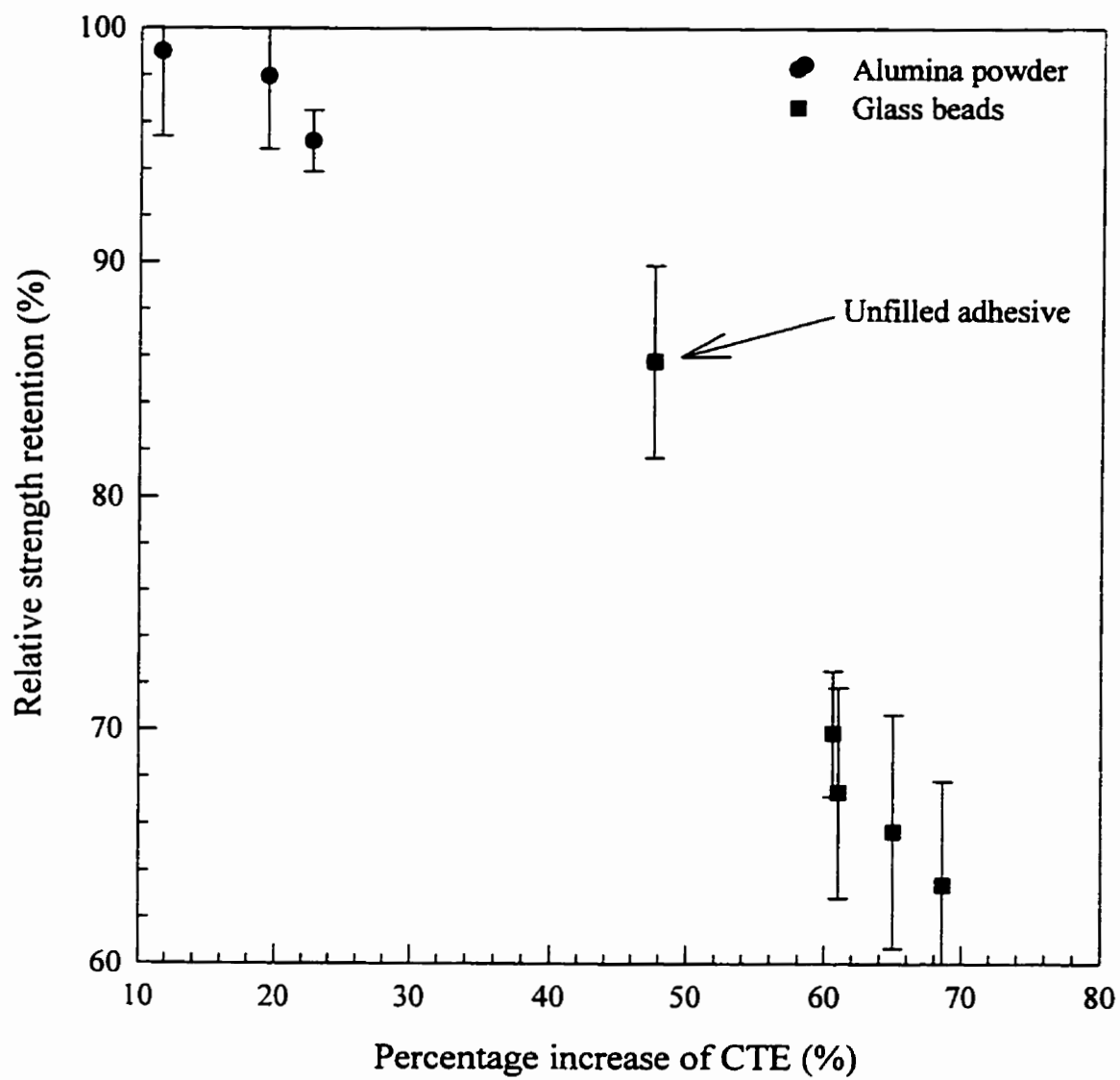


Figure 2.16 Relative strength retention vs. percentage increase of CTE [87]

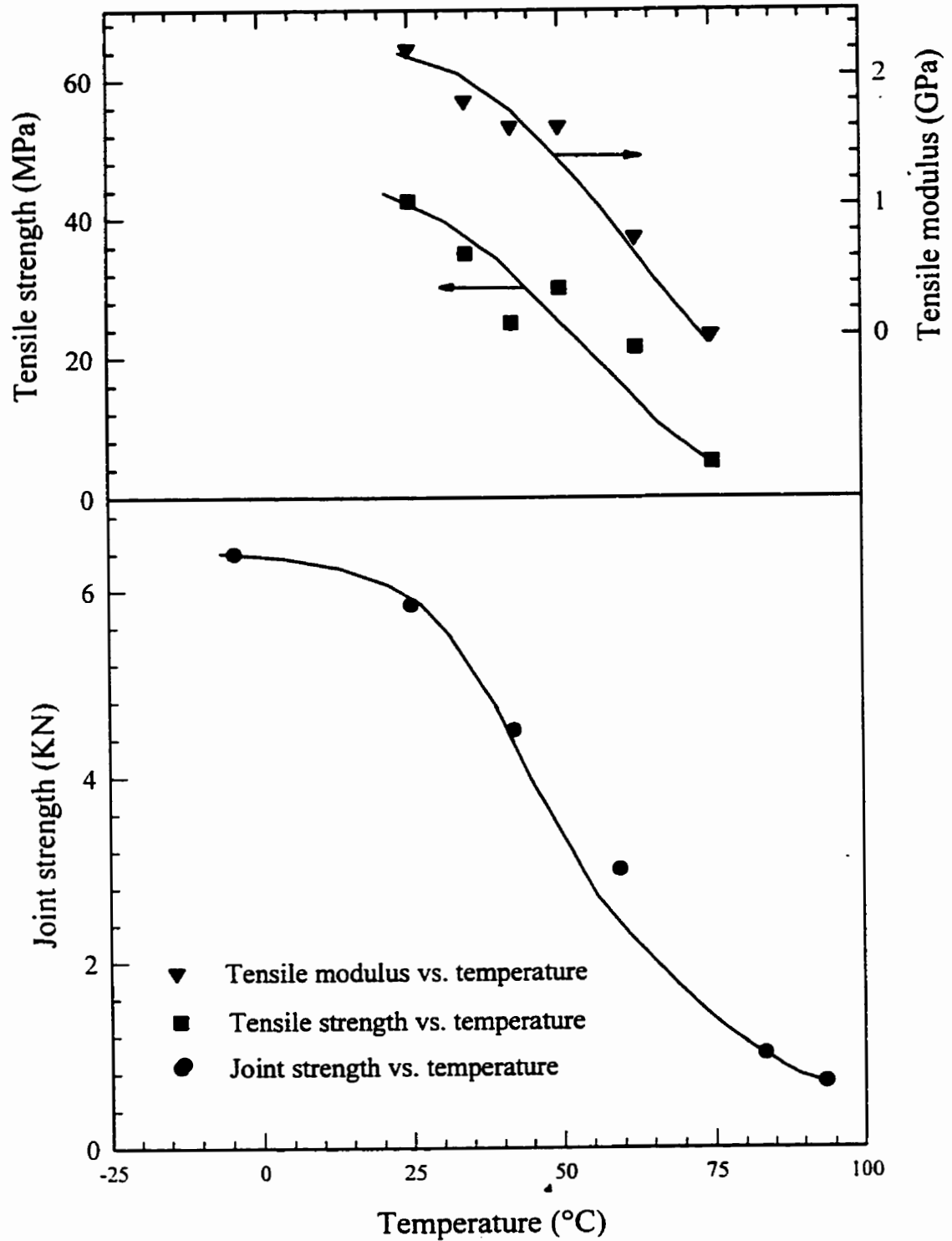


Figure 2.17 Temperature dependence of strength of aluminium lap joint using epoxy adhesive compared to mechanical properties of the adhesive [90].

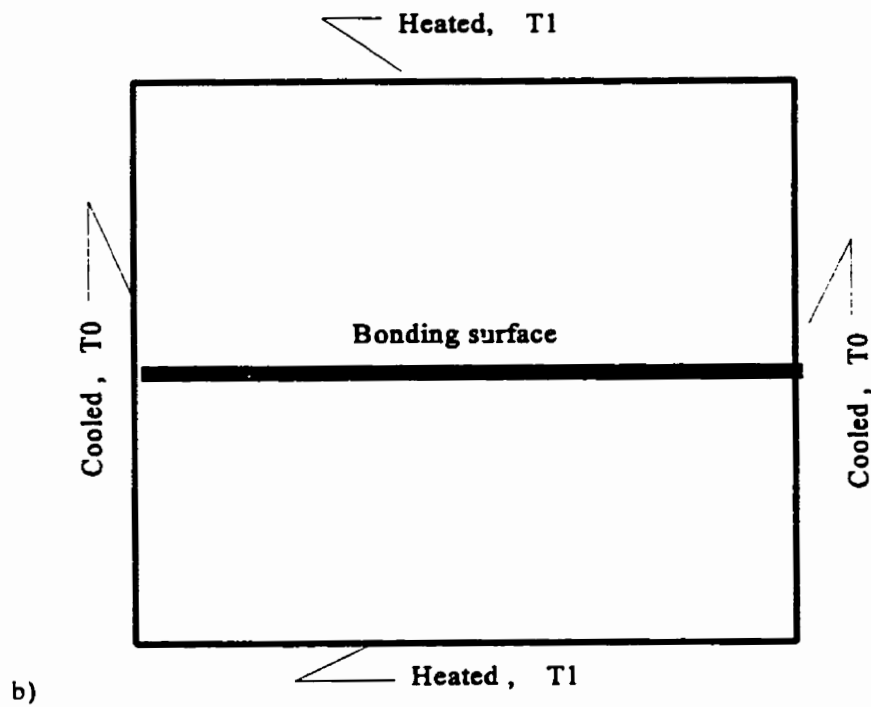
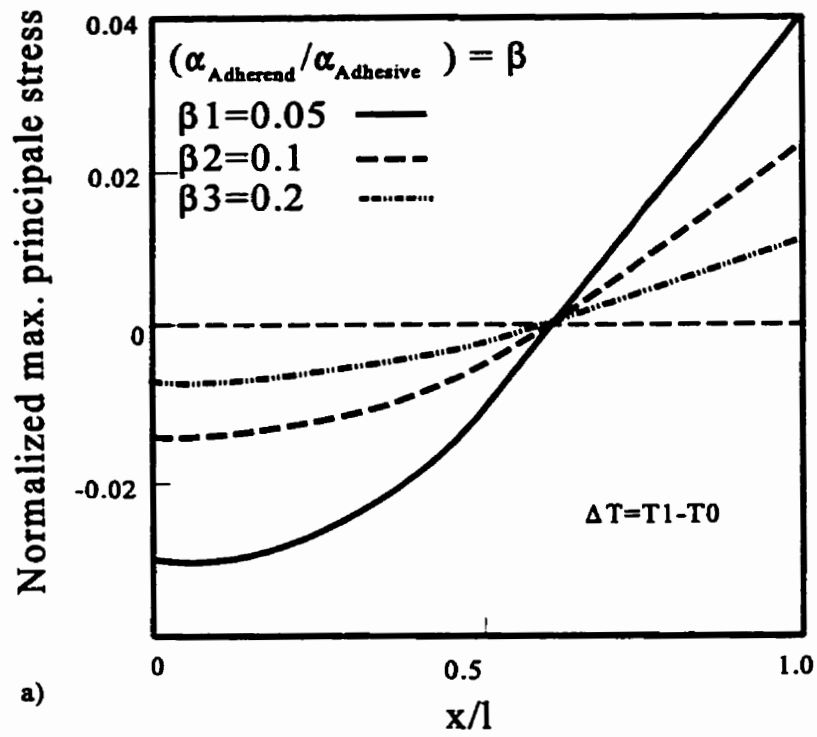


Figure 2.18 Effect of coefficient of thermal expansion ratio's on principle stress distribution in adhesive rectangular butt joint [100].

## CHAPITRE III

### PROPOSAL OF A TORSION SHEAR FIXTURE FOR BONDED JOINTS

#### 3.1 Abstract

The aim of the present work is to design a simple torsion fixture for bonded joints that is adaptable to conventional testing machines and at the same time gives reliable results. This is achieved by transforming a traction or compression movement of a conventional machine to a torsion one on the bonded joints. In the present study, a full description of the mechanism of transferring a compression/traction movement to a pure torsion is explained, and the validation approach is outlined. Finally, experiments on bonded joints are performed and compared to step lap shear test. The results showed that the proposed torsion apparatus is very promising in measuring the strength of bonded joints.

**Key words:** Torsion shear fixture, mechanical properties, adhesives, shear strength, step lap test.

### 3.2 Introduction

When measuring the shear strength of bonded joints, two fundamental requirements are needed, the simplicity of testing and reliability of the results. However, these requirements seem to be irreconcilable in bonded structures. The shear strengths measured using standard methods such as lap shear specimens give rise to non-uniform shear stresses that affect the reliability of the results, but can be performed easily using conventional standard testing machines. On the other hand, measuring the torsion shear strength requires particular testing apparatus, which is not available for all laboratories. In the following a brief review on adhesively bonded joint testing is given in order to appreciate the relevance of torsion testing of these joints.

The mechanical performance of adhesives is usually determined on bulk specimens or adhesively bonded joints, or both. Testing of bulk adhesives is easier than testing films because much larger deformations can be attained, and are much easier to measure. On the other hand, mechanical testing of adhesive bonded constructions is the most straightforward method to measure the strength of a joint. In the design and strength analysis of bonded joints, the major requirements are the elastic shear and tensile moduli. Also necessary are Poisson's ratio, ultimate shear strain, and ultimate shear stress. The difficulties in achieving reliable results on adhesive bonded joints is related to many factors, the most important being: specimens configuration, strain measurements, stress state to which the bondline is subjected and thickness of the bondline [1-2].

There are four basic types of loading an adhesive joint: tensile, shear, peel and

cleavage. Tensile shear strength is most widely adopted as a measure of the ultimate shear strength of an adhesive bond loaded in tension. In this type of loading, the forces act in the plane of the adhesive layer. The single lap joints are the most commonly used adhesive joints and have been the best studied so far. A review of the published literature related to the analysis of bonded joints suggests that there are three widely accepted methods for predicting the strength: closed form solutions [3], finite element method (FEM) [4-5] and linear elastic fracture mechanics (LEFM) concept [6-7]. More recently, a new approach based on an interface corner stress intensity factor has been investigated within the context of elasticity theory [8]. The precise analysis of simple lap is very complex. First, because the stress distribution along the overlap length and through the thickness is non uniform [4, 9-16]. In addition there are interaction between each of the three potential failure modes: adherent yielding, adhesive peel, and adhesive shear. Consequently, the joint strength reliability is affected. Another factor affecting the simple lap joint strength is the existence of a bending moment in addition to the in plane tension arising from the two non collinear forces. The use of step lap joint is an alternative test method of the single lap joint, in which the undesirable bending effect is avoided. However, the stress distributions are almost unchanged [17-18].

In terms of load transfer between two members, double lap joints are probably the most desirable joints. The loads in the adherent parts can be in tension, compression, or in plane shear. However, there is a further difficulty of making two uniform bondlines of the same thickness [19].

Peeling tests are the most selective for measuring the surface treatment quality differences. Uniformity of peel strength values for a given adhesive in contrast to lap shear

strength made the peel test attractive to measure the properties of adhesive bonded joints. Various forms of peel tests are used to assess the performance of structural adhesives. In fact, this form of test deliberately stresses the adhesive in a very small region, subjecting it to a large tensile stress, although a complex stress situation is usually present. This situation is not easily assessed, and peel is normally used to compare adhesives rather than to measure their properties [18, 20].

Cleavage strength is very rarely quoted in reference works. In this type of test severe localized loading occurs on one side of the joint, while the other side is merely loaded. This type of test is usually performed to investigate the ability of the bonded joint to withstand further processing after assembly [21]. Axisymmetric joints also with square or rectangular adherents, are widely used specimens for testing the response of adhesives to shear, tensile and compressive stresses. Butt joints or napkin ring, as specified by ASTM E229, can provide an apparently convenient means for determining the mechanical properties of structural adhesives. The test is used to measure the moduli of rigidity, elasticity and Poisson's ratio [22]. The advantage of using butt joints is that the adhesive is tested in the thin film form as used in most joints, thus overcoming any possible objection to bulk specimen. Although the stress distribution is simple, end effects are once again a problem. As stated by Adams and Wake [4], "if joints are to be loaded to failure and if the failure stress is to mean anything, then it must be true stress and not a convenient but misleading approximation".

It should be mentioned also that in practice, most structural adhesives exhibit considerable plastic deformation when subjected to shear stress, and it is quite probable

that the presence of a spew fillet will yield without causing premature failure of the joint when loaded in torsion and this would lead to an overestimation of the shear modulus of the adhesive [23-24].

Finally, one should mention the torsion shear fixture needed to investigate the mechanical properties of adhesive bonded joints. Historically, the torsion apparatus has been developed by Bossler et al. in 1968 [22]. Other designs have been also proposed in ASTM known as ASTM E229 [25]. The torsion shear apparatus is designed to ensure that no bending or cleavage loads are imposed on the napkin ring specimens that must be subjected to a pure shear.

The reason that, the shear testing of adhesive bonded joint is mainly performed under tension or compression loading of either single or step lap joints is due to the fact that this approach meets the requirement of ease of testing. However, the reliability of the tests is questionable because of the non-uniform stress distribution. The contrary is seen for the torsion testing method, i.e., the method is reliable but the experiment is difficult which has prevented its widespread popularity. The main feature of the proposed torsion apparatus in this paper is its simplicity, moderate cost and adaptability to universal testing machines.



### 3.3 Proposal of a torsion fixture

Figure 3.1 shows the mechanism of the proposed torsion fixture. This fixture is designed to be fitted to any uniaxial testing machine with the aid of some clamping accessories (figure 3.2). The mechanism to create a torsion loading on a bulk specimen or a bonded joint is based on the torque generated by two lever arms in a cross configuration moving in opposite rotational directions. The rotation of the lever arms is provided by the axial displacement of the cross-head of the uniaxial testing machine. In order to easily describe the operation of the proposed fixture, let take the specimen configuration shown in figure 3.3 and consider the measurement of its shear stress-shear strain response. The specimen is inserted between the two lever arms through cross grooves and a centering pin as shown in figure 3.1.a. To accomplish a perfect rotation movement, the lever arms are laid on needle bearings hold by lower and upper shafts (figure 3.2). The shafts came with a lower and upper steel frames that can be connected to an uniaxial testing machine. Moreover, clamping accessories are designed to hold the upper and lower frames aligned and at the same time avoid the frames to rotate during loading. In figure 3.1.b a detailed mechanism of equilibrium forces acting on the system is shown. The force applied by the uniaxial machine is transferred to the needle bearings supported by the steel shafts and give rise to two concurring forces:

$$\begin{aligned} R &= P/2 \cos \theta \\ F_a &= \mu (P/2 \sin \theta) \end{aligned} \quad (3.1)$$

where  $\mu$  is the coefficient of friction,  $P/2$  is the half force applied by the machine and  $\theta$  is the angle between the segment BC and the horizontal. To ensure pure torsion and avoid

bending and cleavage, the axial force,  $F_a$ , should be negligible. Since the needle bearing is free to displace on the steel shaft and free to rotate, this requirement is satisfied, therefore, we can write the following:

$$R \gg F_a \rightarrow \mu \ll 1 \quad (3.2)$$

The determination of the torsion moment is easily obtained from the diagram forces acting on the lever arm of the torsion apparatus shown in figure 3.1.b. The half distance of the lever arm is represented by the segment BC and is given by:

$$BC = \left( \frac{d_2}{\cos \theta} \right) + (d_1 \cdot \operatorname{tg} \theta) \quad (3.3)$$

Since the length L decreases during the experiment, the angle  $\theta$  then should be expressed by the following:

$$\theta = \operatorname{arctg} \left( \frac{L}{d_1} \right) \quad (3.4)$$

$$L = d_1 - (d/2) \quad (3.5)$$

where d is the displacement of the head of the machine. Hence, the torsion moment M induced by the two lever arms is expressed by:

$$M = 4R \cdot BC \quad (3.6)$$

Therefore, the maximum shear stress, acting on the extreme edge radii of the validation specimen shown in figure 3.3 is obtained from the following relationship:

$$\tau_{r,\theta \max} = \frac{M r_o}{J} = \frac{M r_o}{\pi (r_o^4 - r_i^4) / 2} \quad (3.7)$$

where  $r_o$  is the outer radii of the necked region of the validation specimen,  $r_i$  is the inner radii and  $J$  is the polar inertia moment.

The shear modulus is then given by equation 3.8 and is determined by the secant modulus method.

$$G = \frac{\tau_{r,\theta}}{\gamma_{r,\theta}} \quad (3.8)$$

$\gamma_{r,\theta}$  is measured by the strain gages response.

It should be noticed that the condition of thin walled torsion specimen are not encountered for the validation specimen. However, this will be the case for bonded joint in section 3.6. In other terms, if extraneous stresses are to be induced in the torsion region, they would be amplified in the validation specimen compared to the napping ring joints in which this fixture is intended.

Experimental tests with the proposed torsion fixture were performed using a cross head speed of 5 mm/min. Actually, it is more relevant to consider the angular speed rather than the cross head speed. To achieve this objective, the following expression has been established on the basis of cinematic relationships.

$$\omega = \frac{V_m \cdot \cos^2 \theta}{d} \quad (3.9)$$

Where  $\omega$  is the rotational speed and  $V_m$  is the cross head speed of the machine.

The recommended time to failure of the napkin ring specimens given by ASTM E 229 should be between two to five minutes. In the present study, the rotational speed was almost constant during the four minutes of the test experiment (0.047 rad/min at the start of the experiment to 0.055 rad/min at the failure of the specimen).

### 3.4 Experimental validation of the proposed torsion fixture

Even though the preceding analysis predicts a quasi-pure torsion loading, extraneous stress components can be generated by the loading mechanism and inflect the results reliability. The validation procedure is intended to verify if the proposed torsion fixture induces extraneous stresses other than pure torsion. Probably, the best validation approach is to compare results from the proposed fixture to those obtained on proven standard equipment such as that proposed by Bossler or ASTM E229 [22, 25]. Unfortunately, such equipment is not available and an alternative validation approach is proposed. First as shown in figure 3.3, a specimen configuration with appropriately mounted strain gages capable of detecting the principal strain components during loading is proposed. This permits the measurement of axial, transverse and shear strains. The magnitude of these strains components will show to what extent extraneous stresses, other than torsion, are present. From the same test, the shear modulus  $G_A$  can be determined.

Secondly, independent standard tensile tests will be performed on the same material. Strain gages for the tensile tests will be used in order to determine the shear modulus of the material using the Timoshenko formula  $G_T = (E/2(1 + \nu))$ . If the proposed torsion test is reliable,  $G_A$  and  $G_T$  should be comparable.

The specimens used to validate the proposed torsion apparatus were casted in a steel mold laboratory made to fit the lever arms in a cross shape form (figure 3.1). The material used is a general purpose thermoset vinylester resin, the same one used for the standard tensile specimens. To avoid subjection of the validation specimen to any stress concentration especially at the extreme edges, it was decided to reinforce this part with chopped fibers (figure 3.3). As stated earlier, to accomplish the validation two types of strain gages are used. First, strain gage rosettes ( $0^\circ/90^\circ$ ) are bonded onto the validation specimen along the y and z directions. In addition ( $\pm 45^\circ$ ) strain gage rosettes were also used to measure the shear strain in the main direction of the specimen (z). In all the experiments, three specimens were tested to detect the bending in the yz plane and other three to detect the bending in the xz plane.

### 3.5 Results and Discussions

Figure 3.4 shows a finite element computation of a typical validation specimen. It is clearly seen that any applied force P on the lever arm induces a stress concentration on the necked region of the specimen. Mechanical tests performed on specimens show that all specimens present a typical torsion failure at a  $45^\circ$  direction (figure 3.3).

The results of the torsion test are shown in figures 3.5 and 3.6. Both figures illustrate the extraneous strains in  $xz$  and  $yz$  planes. Since only the elastic domain is of interest, the shear strains greater than 1% were not taken into consideration. Table 3.1 summarizes the results of both the torsion and tensile results.

It can be seen from the figures 3.5-3.6 that the axial and transverse strains measured up to  $\gamma_{r\theta}$  of 1% are negligible. This represent, in the extreme case, 3% of the shear strain in the  $xz$  plane and 4% in the  $yz$  plane respectively. A careful analysis of the experiment shows that most of the contribution to the experimental error came from the instabilities in the Wheatstone bridge. On the other hand, the lower and upper frame alignment can be improved so that the extraneous stress effects no more exit or at least very negligible. The specimen porosity observed during preparation may also interfere in the scattering shown in the results.

Table 3.1 Results of the torsion and tensile tests.

Tests	Ultimate strength $\tau_{r\theta}$ (MPa) or $\sigma_{ult}$ (MPa)	Tensile modulus E (GPa)	Poisson's ratio $\nu$	Shear modulus $G_T$ or $G_A$ (MPa)
Torsion test	$32.0 \pm 8.1$	-	-	$958 \pm 39$
Tensile test	$43.5 \pm 6.7$	$2.9 \pm 0.2$	$0.40 \pm 0.02$	$1059 \pm 60$

It is shown from the figures 3.7 and 3.8 that the vinylester is relatively a brittle material and has a relatively linear behavior up to the nominal axial strain of

1%. Viscoelastic behavior was more evident at higher strains approaching the limit of failure.

The shear modulus obtained in both experiments showed a good agreement, the average values thus obtained of 1059 MPa for the tensile test and 958 MPa for the torsion test are of the same magnitude. A relatively small error of 9% mainly caused by the non recorded friction losses of the forces arising in the needle bearings and the accessory block alignments is quite acceptable. Equally, the undesirable bending effects, even as small as recorded may contribute to this difference. Although, the small values of the standard deviation for the torsion experiments show a consistency in the obtained results.

As a summary, the results obtained in the both tensile and torsion experiments on the validation specimens are in agreement. The fact that a small variation of 9% difference in shear modulus is found between both experimental tests suggests that the proposed torsion apparatus is very promising. It is obvious that the small extraneous bending stresses recorded in the case of the validation specimens would vanish almost completely for the type of napkin ring specimens mainly due the small region of the adhesive thickness and the larger aspect ratio of the ring. Moreover, a minor modification is done on the lever arms which are brought to a round shaped form to minimize the contact and thus minimizing the bending stresses.

## **3.6 Application to the case of bonded joints**

### **3.6.1 Materials**

The materials used in the present study are an epoxy resin of a chemically pure bisphenol A diglycidyl ether (DGEBA) (DER 331) from Dow chemicals, a polyamide resin (V125) from Henkel Co. as an amine hardener and a tertiary amine (2,4,6 diphenyl amine) Epi-cure 3253 from Shell chemicals as a catalyst. Two types of fillers are used, silane treated glass beads CP3003 with a diameter less than 45 $\mu$ m, and ceramic filler (pure alumina powder) with a diameter less than 100 $\mu$ m. Also are used aluminum T6061-T6 plates and napkin ring as adherents.

### **3.6.2 Specimens preparation**

The surface treatment of the aluminum plates is performed according to a recommended ASTM D2651 procedure (hot etching mixture of dichromate-sulfuric acid, referred as FPL etch). In performing the surface treatment, care should be made in order to obtain uniform results. It was reported that variation of the surface treatment parameters has a drastic effect on shear and peel strength properties [26]. The adhesive composites are prepared by mixing the epoxy resin, curing agent, catalyst and fillers. The mixture is stirred completely and placed into the plates to be joined. It has to be mentioned that because of the high viscosity of the adhesives, no air bubble removal is undertaken. The adhesive thickness between the two plates of the step lap shear samples was 0.2 mm and this is done by placing



a thin shim of steel at both ends of the plate as shown in figure 3.9. To prevent any excess epoxy adhesive from sticking on the edges of the specimen (spew fillet), a 3 mm free space is coated with grease and removed before curing takes place. On the other hand, napkin ring specimens as shown in figure 3.10 are also joined with the same mixtures under the same conditions.

### 3.6.3 Shear test procedures

Step lap shear specimens inspired by ASTM D1002 are held to grips of an universal testing machine MTS 810 coupled to a data acquisition system. A 1.3 mm/min cross head speed is set for all the experiments. At least five specimens were tested for reproducibility. Similarly, napkin ring samples are also tested at a 5 mm/min cross head speed with the proposed laboratory torsion fixture. It should be noted that the above analysis of section 3.3 is also valid in the case of bonded joint. Furthermore, the shear strain  $\gamma_{r\theta}$  can be expressed as follow:

$$\gamma_{r\theta} = \frac{r}{2e} d\theta \quad (3.10)$$

where  $d\theta$  is the angular displacement of the two adherent surfaces,  $e$  is the adhesive thickness,  $r$  is radial distance to the center line of the joint.

### 3.7 Bonded joint results and discussion

A more detailed analysis of the effect of filler content on the mechanical properties of adhesive bonded joints is given in the second part of this research work [27]. Concisely, this part of work is intended to verify the reliability of the proposed torsion apparatus. Figures 3.11 and 3.12 compare the two types of experiments on samples of various filler type and filler content. It is shown from these figures that the general trend of the shear strength in both experiments increases with filler content, reaches a maximum and then starts to decrease. It is clear that the shear strength measured with the proposed torsion shear fixture is higher than that measured with the conventional step lap specimen. It is well known that step lap joints produce underestimated joint strengths [10]. This is confirmed by the results of figure 3.11 and 3.12 which at the same time confirms the reliability of the proposed torsion fixture.

Additional evidence of the reliability of the torsion measurements made with the proposed torsion fixture is given by comparing the relative modulus ( $G'_c/G'_a$ ), where  $G$  is the shear modulus and the subscripts  $c$  and  $a$  represent filled adhesive and matrix respectively; measured on the napping ring specimen and the relative modulus measured on the bulk materials by DMA. The results are shown in figures 3.13 and 3.14. Even though, no extensometers were used to measure with accuracy the shear strain of the adhesive bonded joints, a good agreement between both results is found. If the fracture has to occur in the adhesive i.e., 100% cohesive failure, the strength of the joint can be predicted

easily. However, if this is not the case, a comparison of the shear strength of both bulk adhesive and bonded joint (figure 3.15), it is clearly seen that the fracture occurred earlier in the bonded joint, resulting in lower strength. Whereas, a good agreement of the shear modulus is observed between both results. Moreover the torsion shear results showed that the epoxy based adhesives as illustrated in figures 3.16 and 3.17 are relatively brittle materials. They showed a relatively linear behavior up to fracture.

### **3.8 Conclusion**

As a summary, numerous mechanical testing methods have been designed to evaluate specific mechanical properties of adhesive bonded joint. The aim of the present study was to design a simple torsion fixture for bonded joints that is adaptable to conventional testing machines and at the same time gives reliable results. It is convincing from the results of the validation work that the proposed torsion apparatus is quite acceptable for measuring the shear properties of bonded joints. Taking into consideration the small inconveniences encountered during the experimental work, it is recommended to improve the block alignment for ease of testing. Regardless of the above mentioned statements, it is shown that the torsion shear strength results are more reliable than those obtained by the standard lap shear test. The improvement is mainly due to the fact that step lap test induces non uniform stresses that affect the reliability of the results contrary to torsion shear experiments.

### **3.9 Acknowledgment**

This research was financed partly by Natural Sciences and Engineering Research Council of Canada (NSERC) and Fonds pour la Formation des Chercheurs et de l'Aide à la Recherche (FCAR). The authors thank Mr. B. Goulet (M.ing student) for his contribution on doing the validation work and his precious suggestions.

### 3.10 References

- 1 E. J. Hughes, W. Althof and R. B. Krieger, "Adhesive Bonding of Aluminum Alloys", (E. W. Thrall and R. W. Shanon Marcel Dekker, 1985) p.141.
- 2 S. Semerdjier, " Metal to Metal Adhesive Bonding ", (S. Semerdjier Business Books London, 1970) p.55
- 3 L. J. Hart-Smith, Technical report, NASA CR1122 36, Langley Research Center, Hampton Virginia, January 1973.
- 4 R.D. Adams and William C.Wake, " Structural Adhesive Joint in Engineering ", (Elsevier Applied Science London and NY, 1984) p.14.
- 5 J.N. Reddy and S. Roy, " Adhesive bonding ", (L. H. Lee, Plenum Press NY, 1991) p.359.
- 6 K. M. Liechti, " Engineered Materials Handbook ", ASM Int. 3, (1990) 335.
- 7 G. P. Anderson and K. L. De Vries, Int. J. Fract. 39 (1989) 191.
- 8 E. D. Reedy, JR., Int. J. Sol. Struc. 30, 6 (1993) 767.
- 9 O. Volkersen, Construction Métalique 4 (1965) 3.
- 10 J. M. Giraud, Matériaux et Techniques (1980) 255.
- 11 M. Halioui and J. P. Lieurade, Matériaux et Techniques, 1991, p. 17
- 12 C. Kassapoglou and J. C. Adelman, SAMPE Quart. 24, 1 (1992) p.19 .
- 13 M. Y. Tsai and J. Morton, J. Strain Analy. 29, 1 (1994) p.137.
- 14 M. Goland, E. Reissner, J.Appl. Mech. 11 (1944) A17.
- 15 O. Volkersen, Luftfahrtforschung 15 (1938) p.41.

- 16 F. Erdogan and E. W. Thrall, " Adhesive Bonding of Aluminum Alloys " ( E. W. Thrall and R. W. Shanon Marcel Dekker, 1985) p.
- 17 K. Mori and T. Sugibayashi, JSME Int. Journal, Series:1 **33**, **3** (1990) p.349
- 18 T. A. Osswald, "Engineered Materials Handbook", ASM Int. **3** (1990) p.325
- 19 L. J. Hart-Smith and E. W. Thrall, Adhesive Bonding of Aluminium Alloys, ( E. W. Thrall and R. W. Shanon, Marcel Dekker, 1985) p.
- 20 A. Marceau and E. W. Thrall, *ibid.* (1985) p.177.
- 21 R. D. Adams, " Engineered Materials Handbook ", ASM Int. **3** (1990) p.325.
- 22 R. C. Bossler, M. C. Franzblau and J. L. Rutherford, J. Sci. Instr.: J. Phys. E. **21** (1968) p.829.
- 23 R.D. Adams, J. Coppendale and N.A. Peppiatt, J. Strain Analy. **13**, **1** (1978) p.1.
- 24 M. P. Zanni-deffarges and M.E.R., Int. J. Adhes. Adhes. **13**, **1** (1993) p.41.
- 25 Standard Test Method for shear strength and modulus of structural adhesives, **E229-70**.
- 26 M.C. Ross, R.F. Wegman, M.J. Bodnar and W.C.Tanner, SAMPE J. **10**, **3** (1974) p.5.
- 27 M. Ouddane, R. Boukhili and R. Gauvin, submitted to J. Mater. Sci., May (1997)

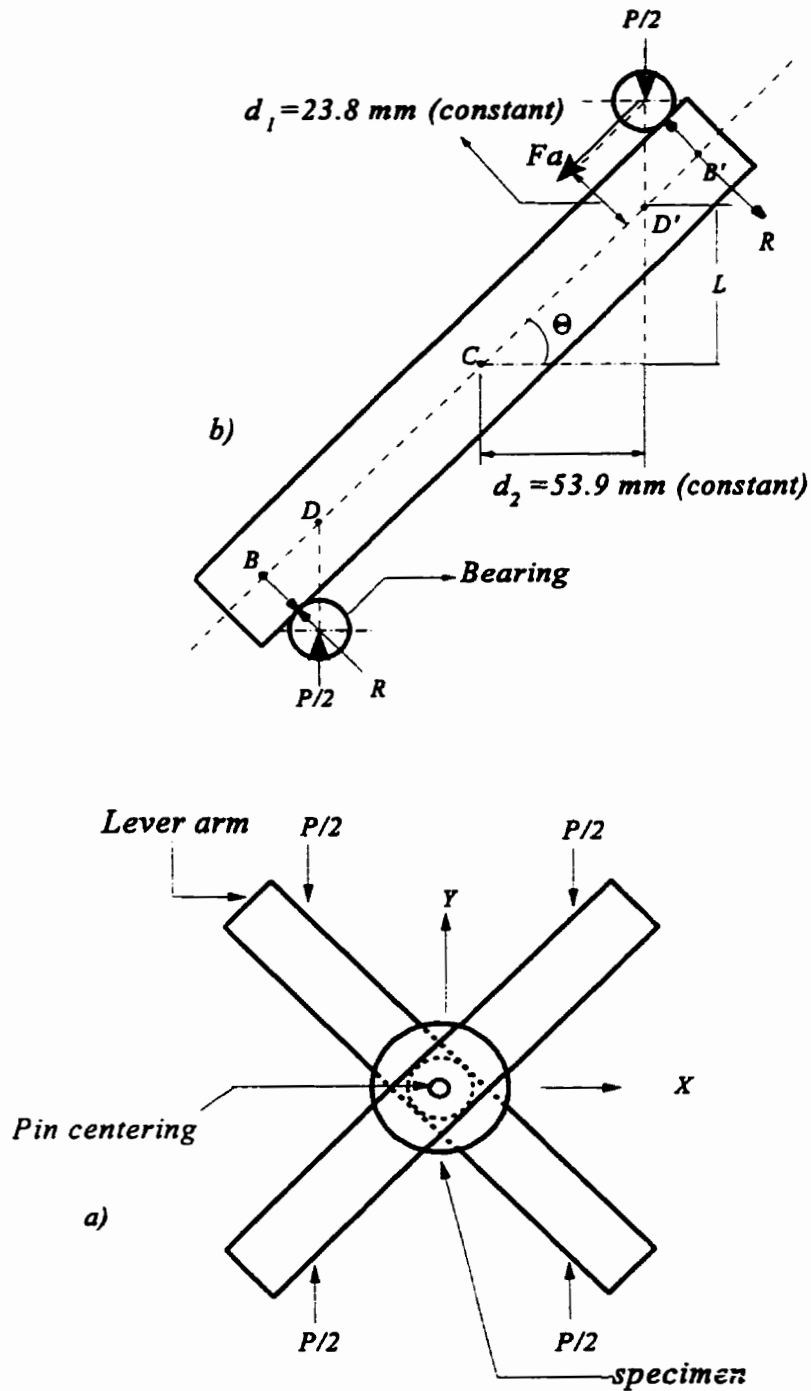
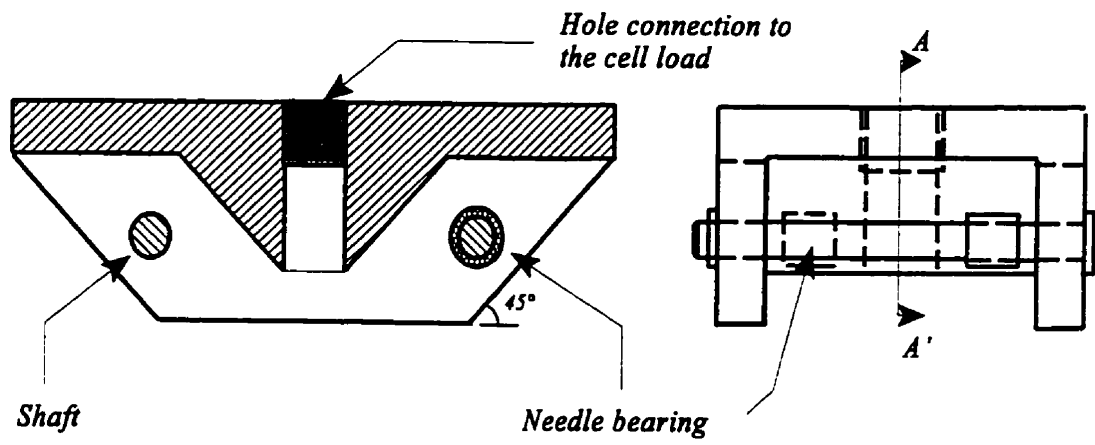


Figure 3.1 Diagram showing the mechanism of the proposed torsion fixture.



Section "A-A"

Figure 3.2 Upper steel frame diagram.





Figure 3.3 A photograph showing the strain gages mounted on the validation specimen also shown a 45° failure direction.

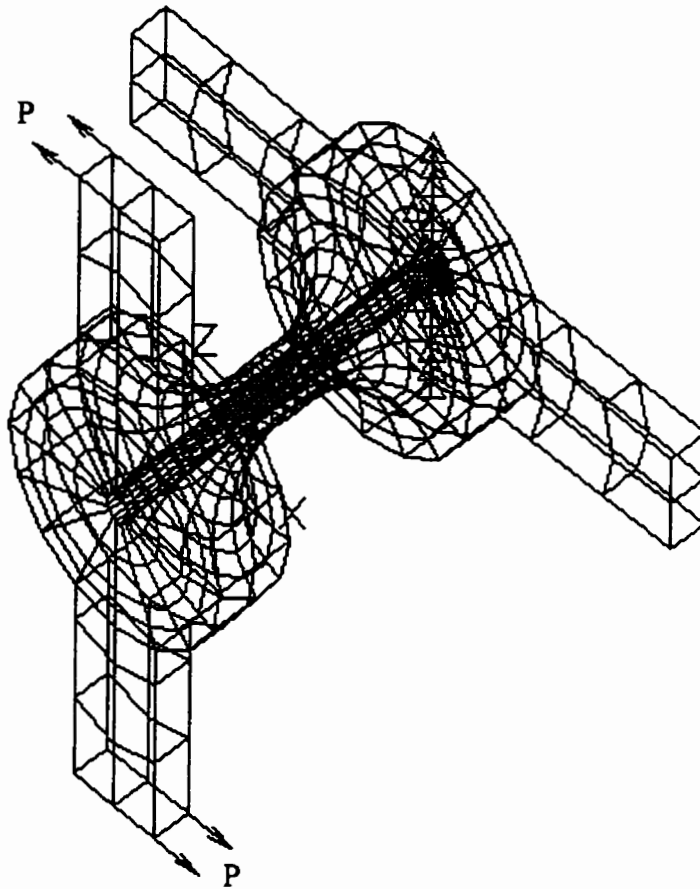


Figure 3.4 Finite element model of the validation specimen.

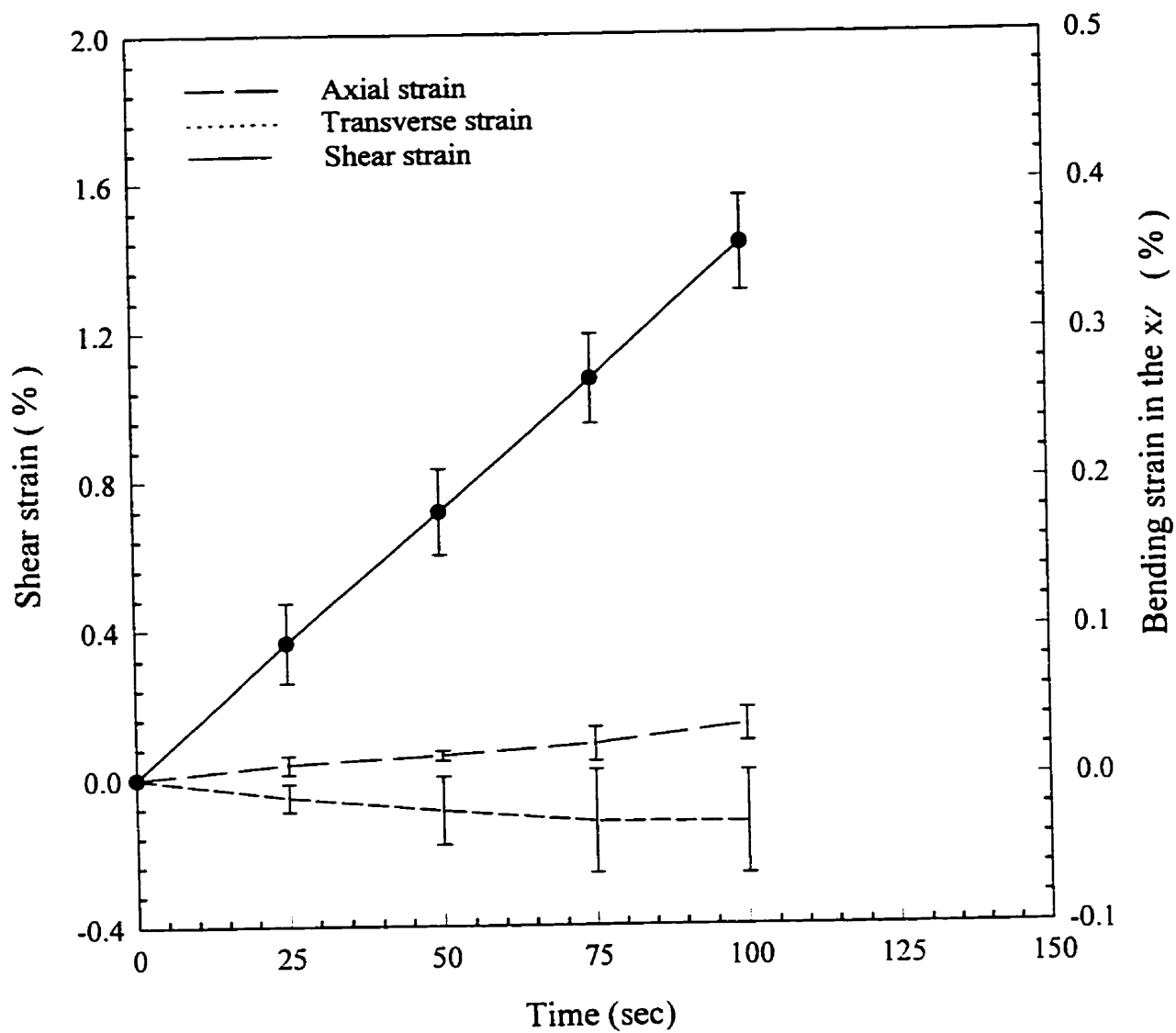


Figure 3.5 Axial, transverse and shear strains as a function of time (bending in the  $xz$  plane).

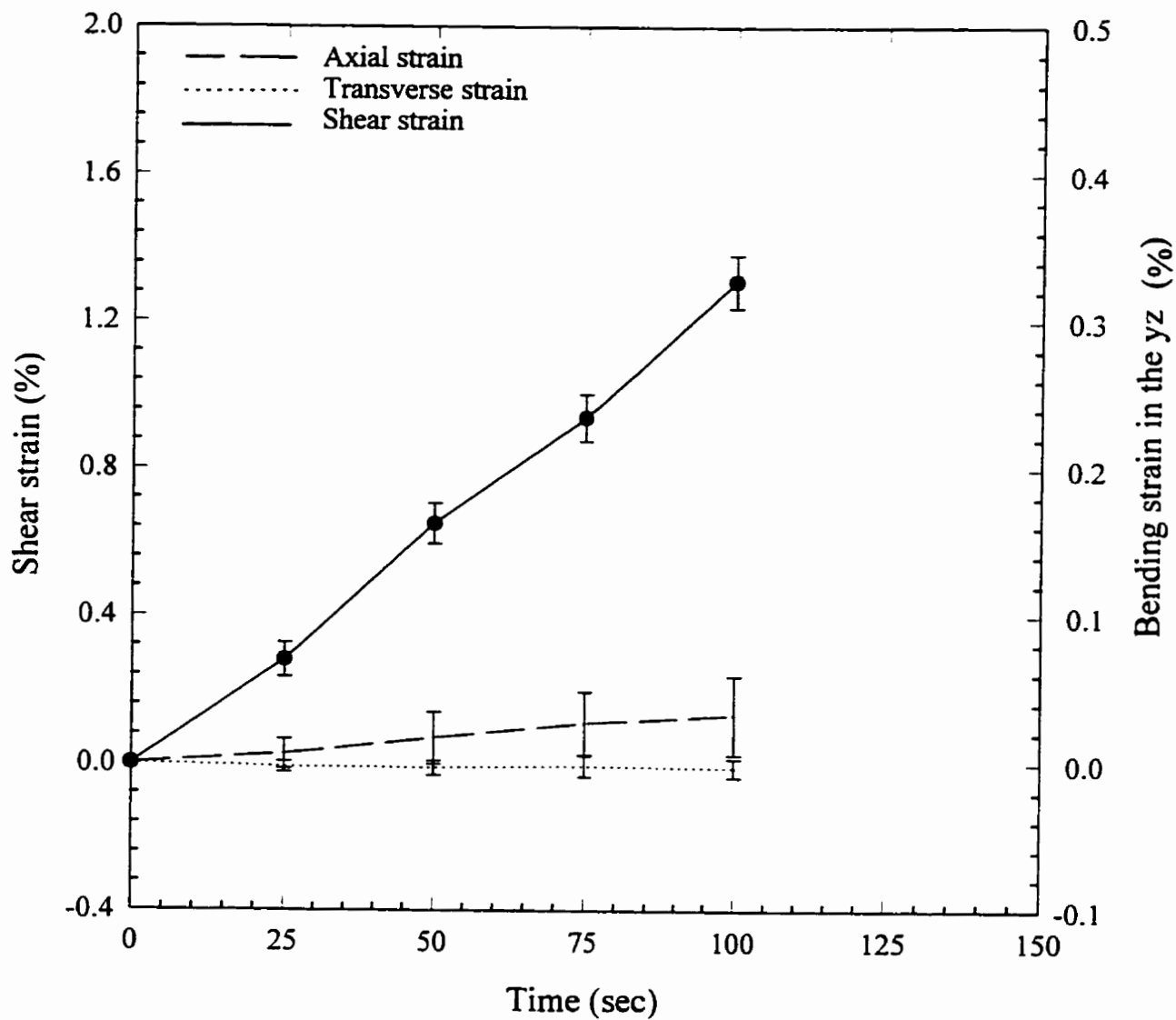


Figure 3.6 Axial, transverse and shear strains as a function of time (bending in the yz plane).

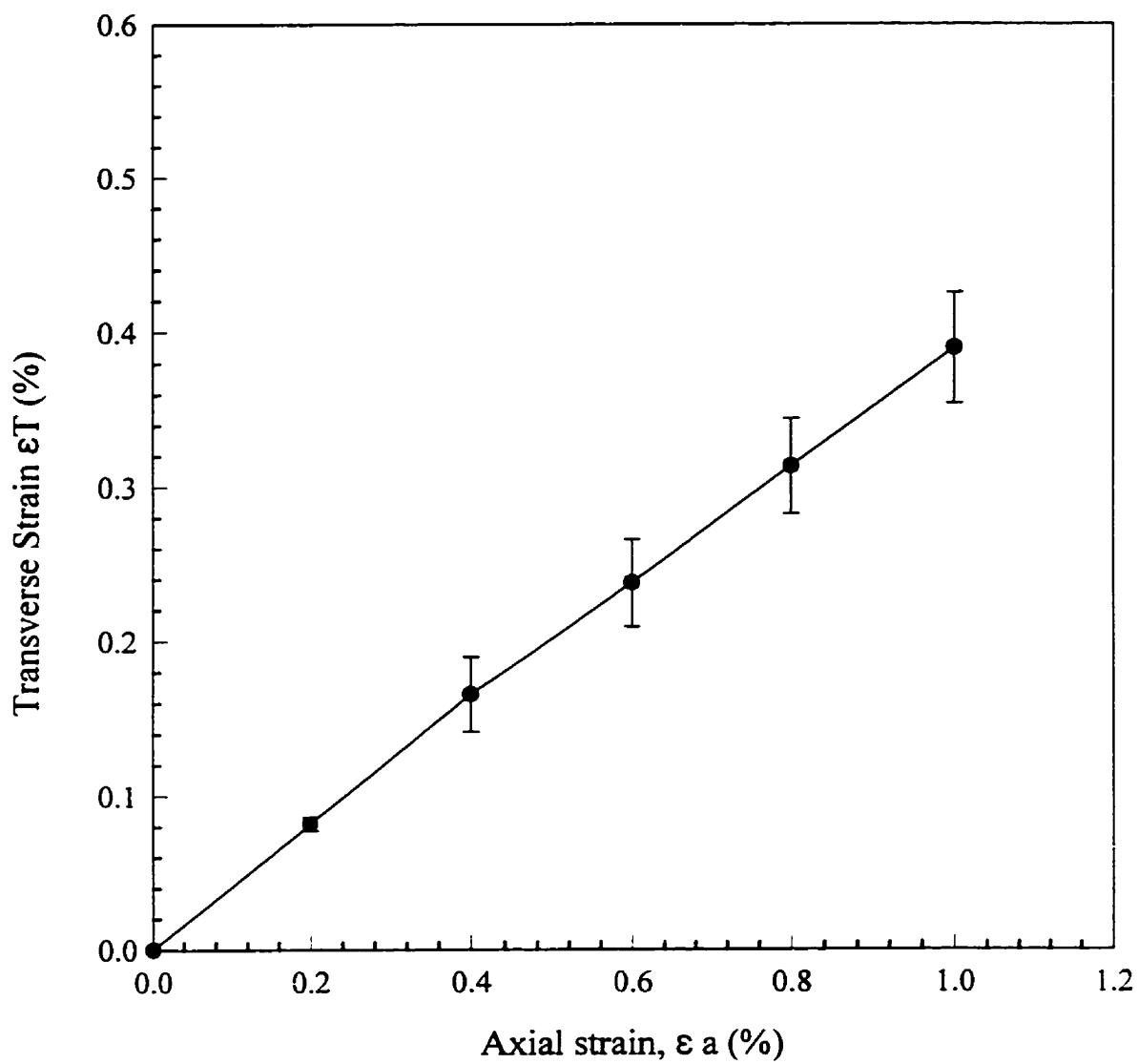


Figure 3.7 Transverse strain vs. axial strain curve.

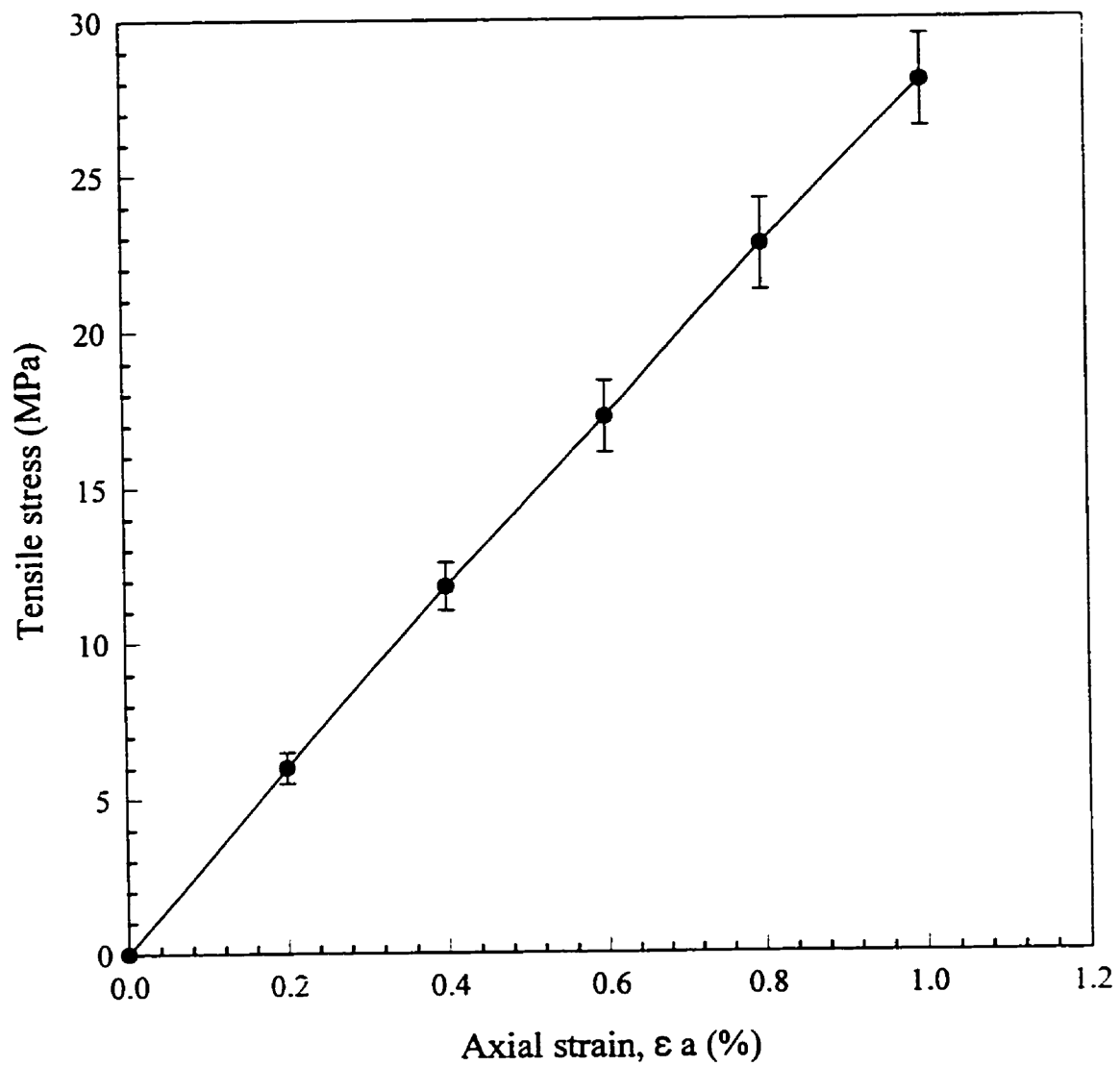


Figure 3.8 Tensile stress vs. strain curve.

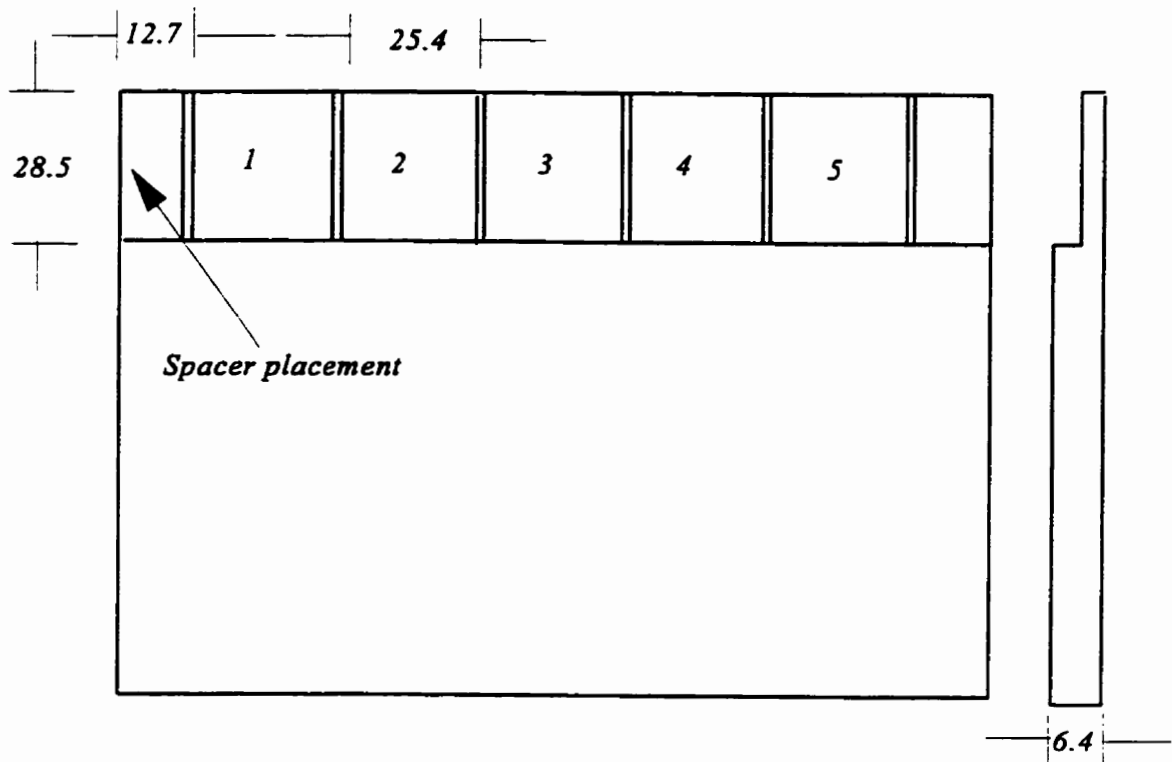


Figure 3.9 Step lap specimens (all dimensions are in mm).

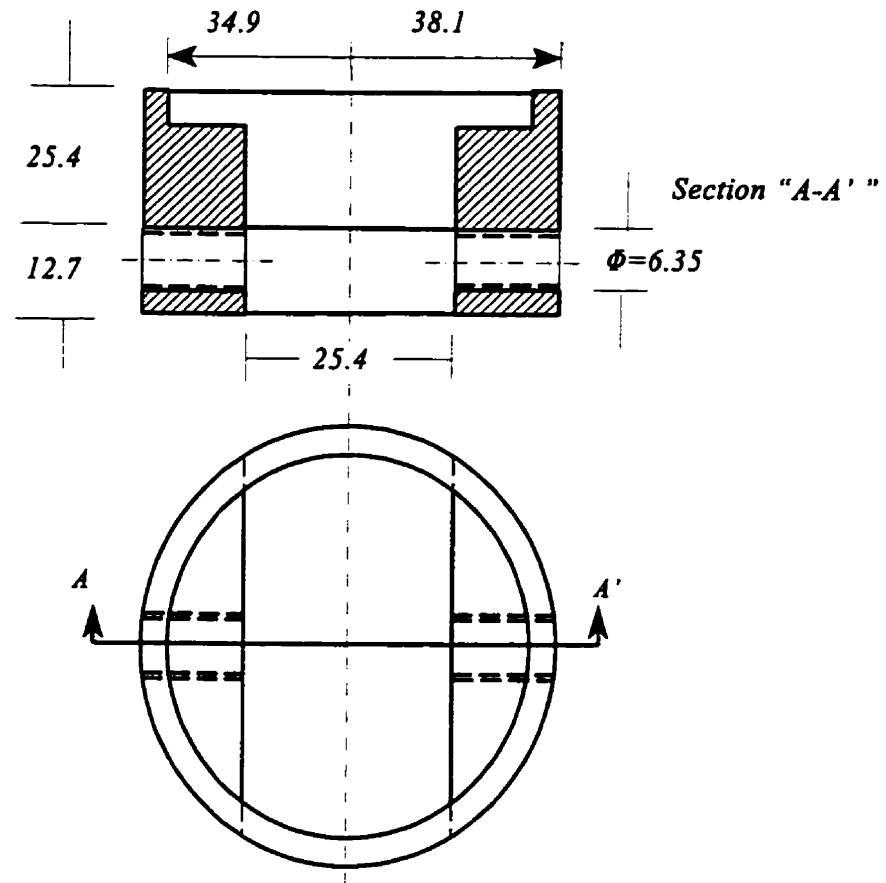


Figure 3.10 Napkin ring specimen (all dimension are in mm).



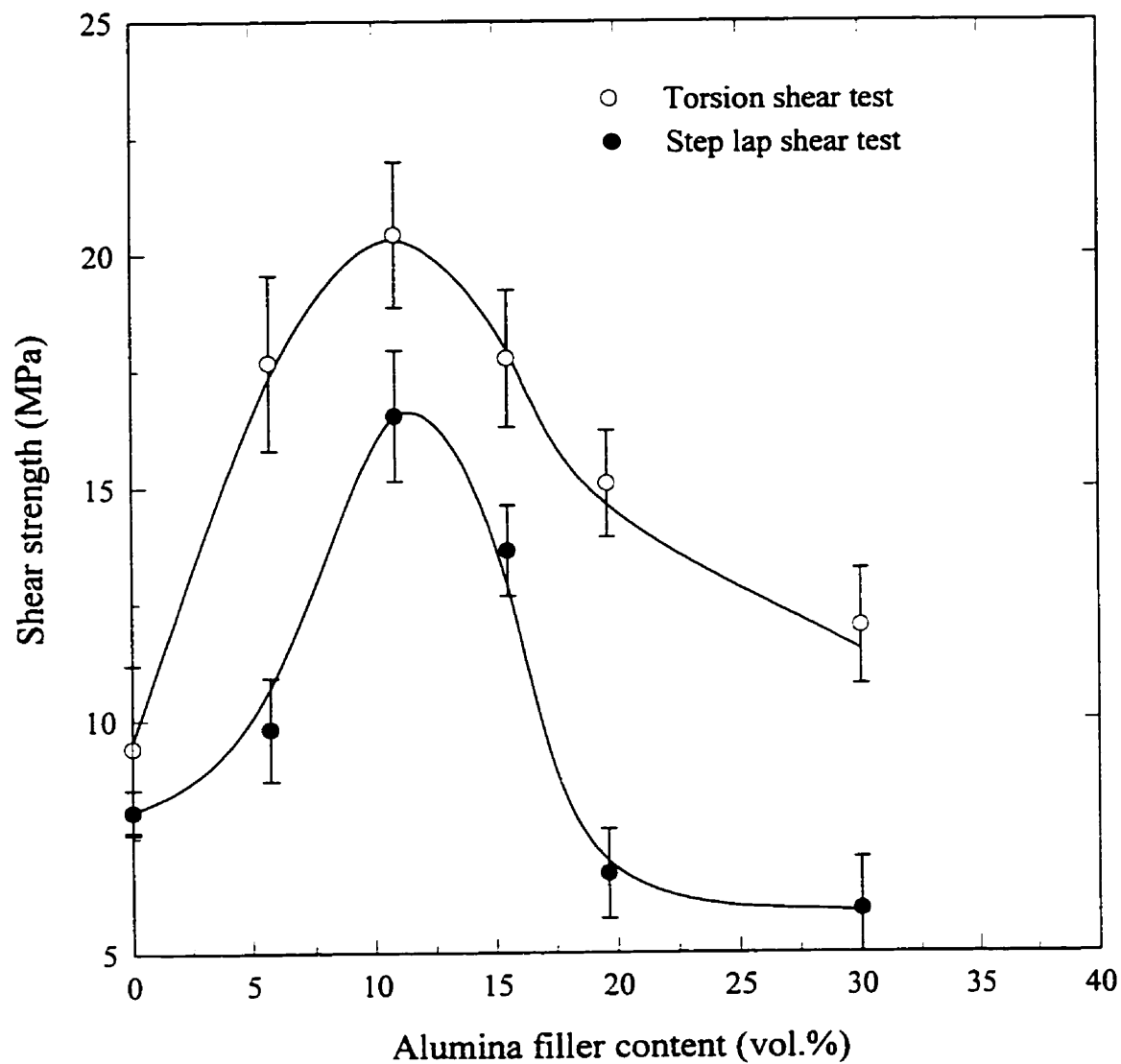


Figure 3.11 Shear strength as a function of filler content in the case of alumina filled adhesive.

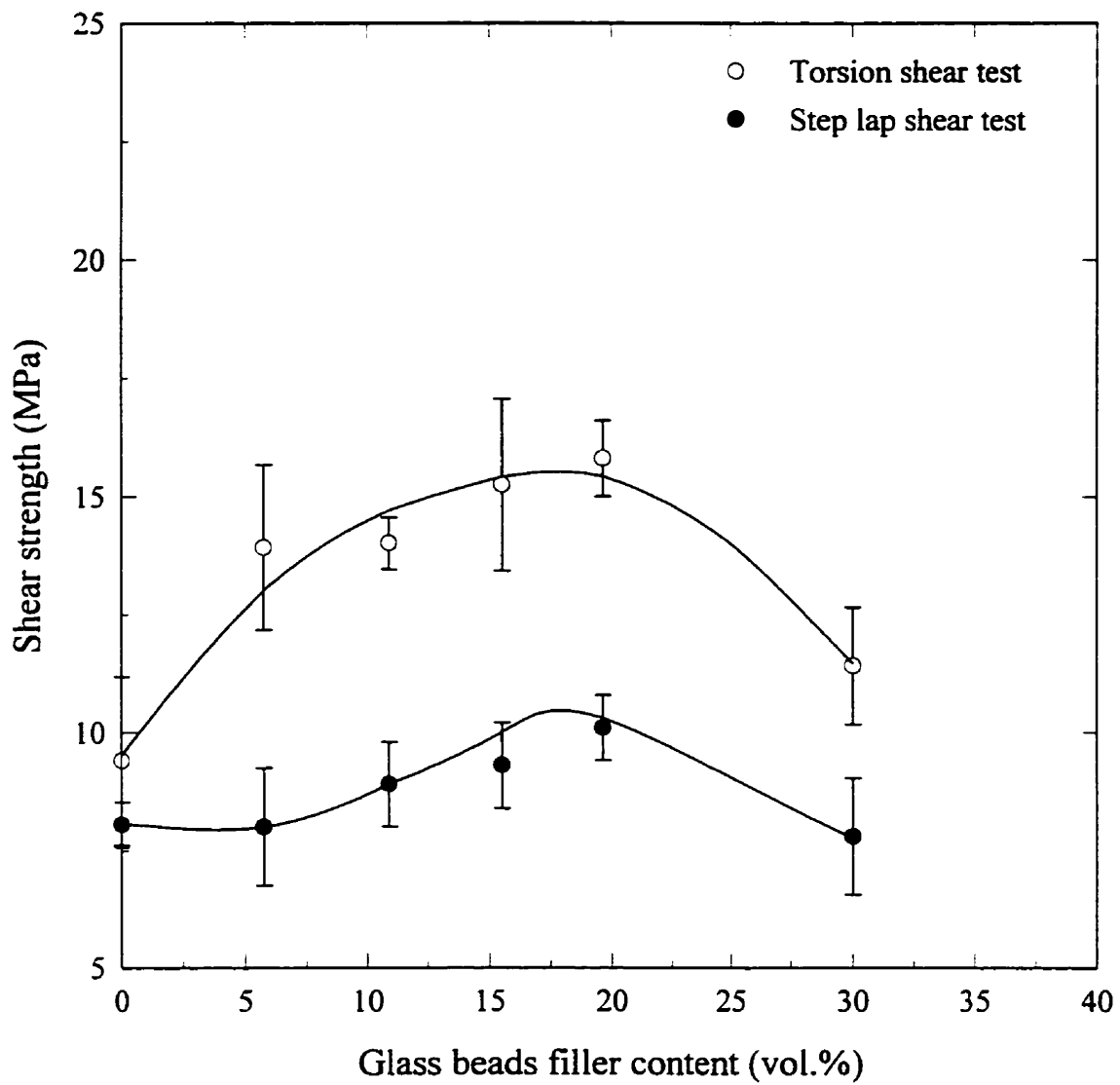


Figure 3.12 Shear strength as a function of filler content in the case of glass beads filled adhesive.

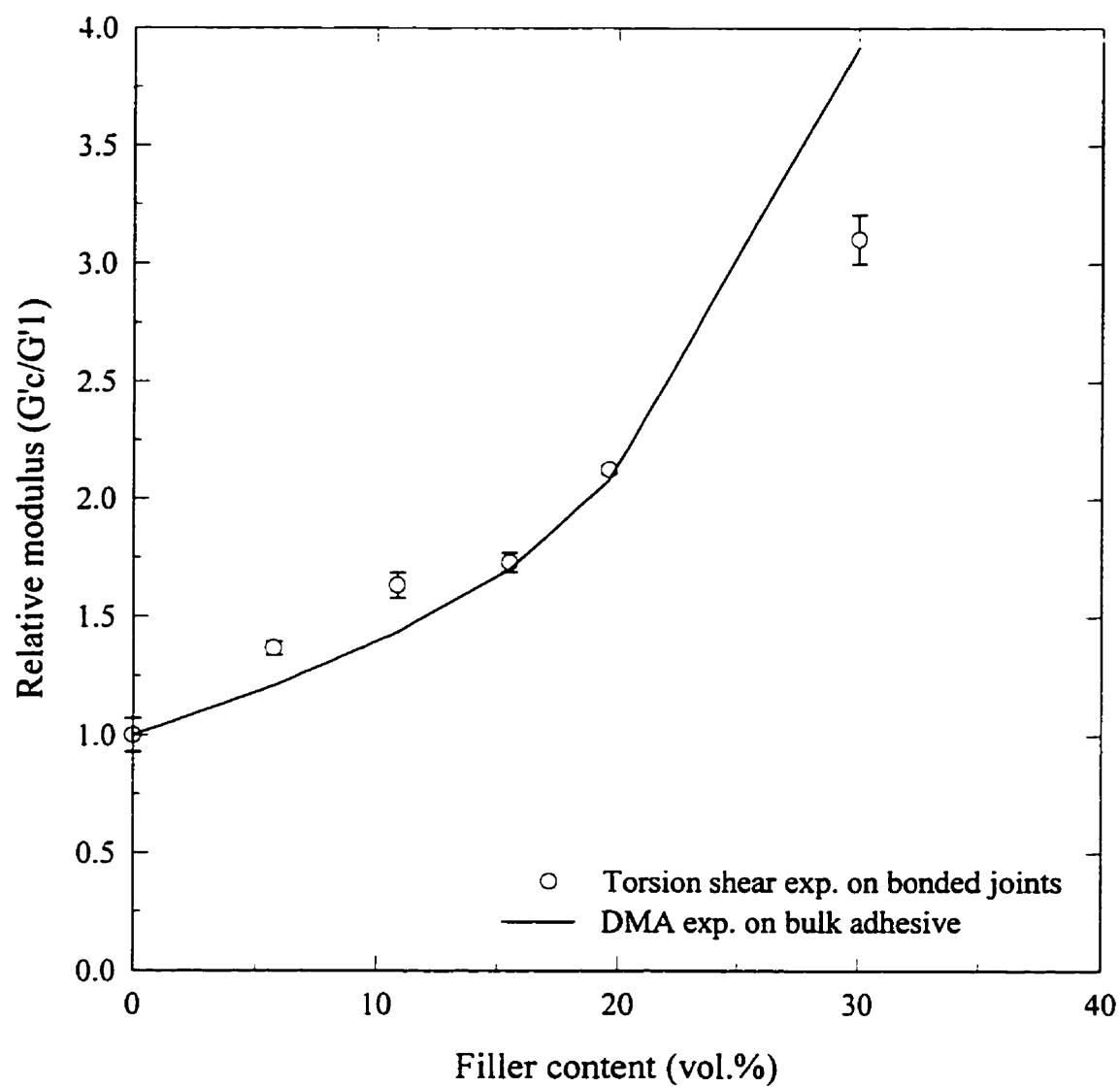


Figure 3.13 Relative modulus as a function of filler content in the case of alumina filled adhesive.

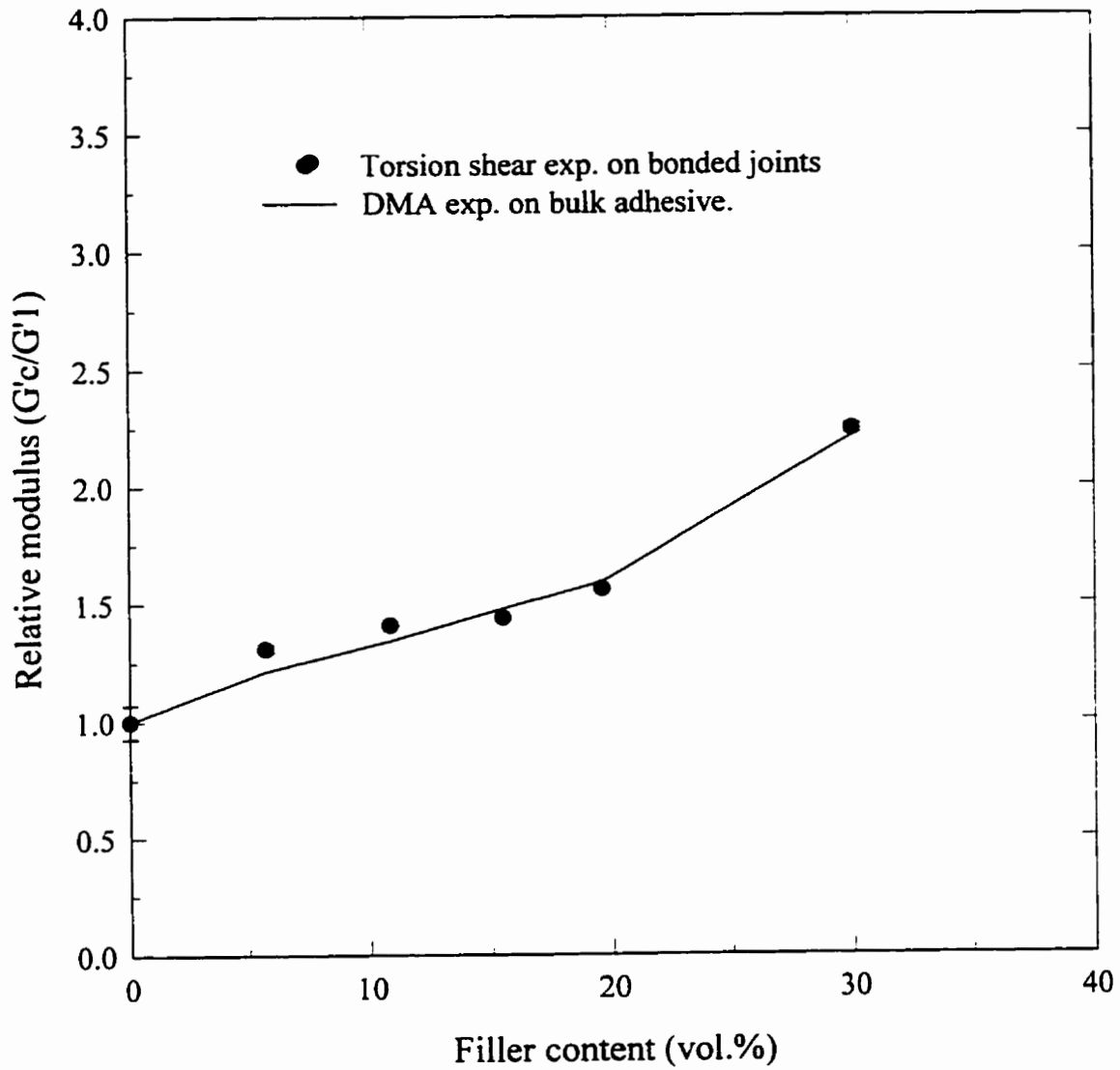


Figure 3.14 Relative modulus as a function of filler content in the case of glass beads filled adhesive.

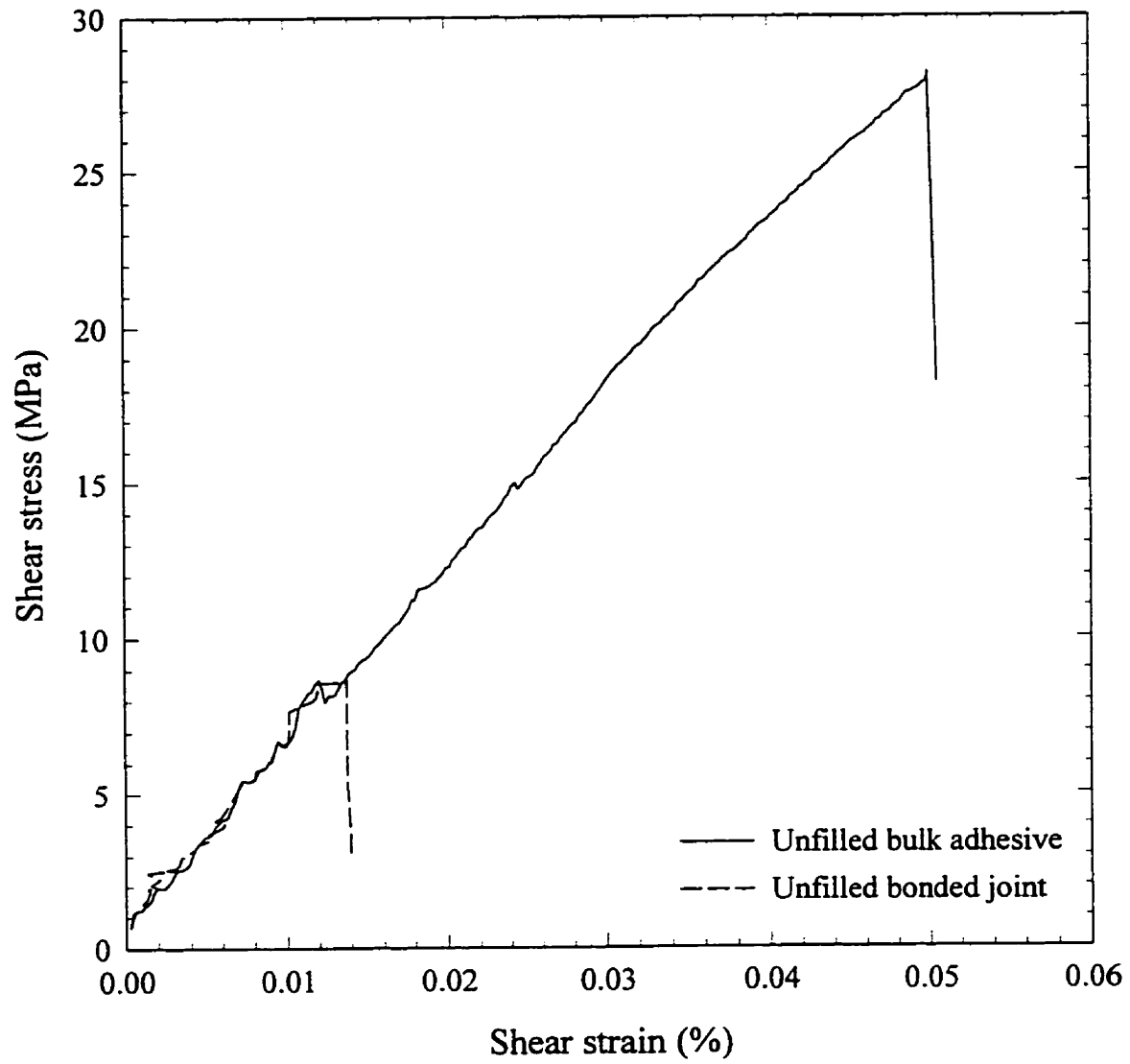


Figure 3.15 Torsion shear stress versus shear strain (comparison between bulk adhesive and bonded joint).

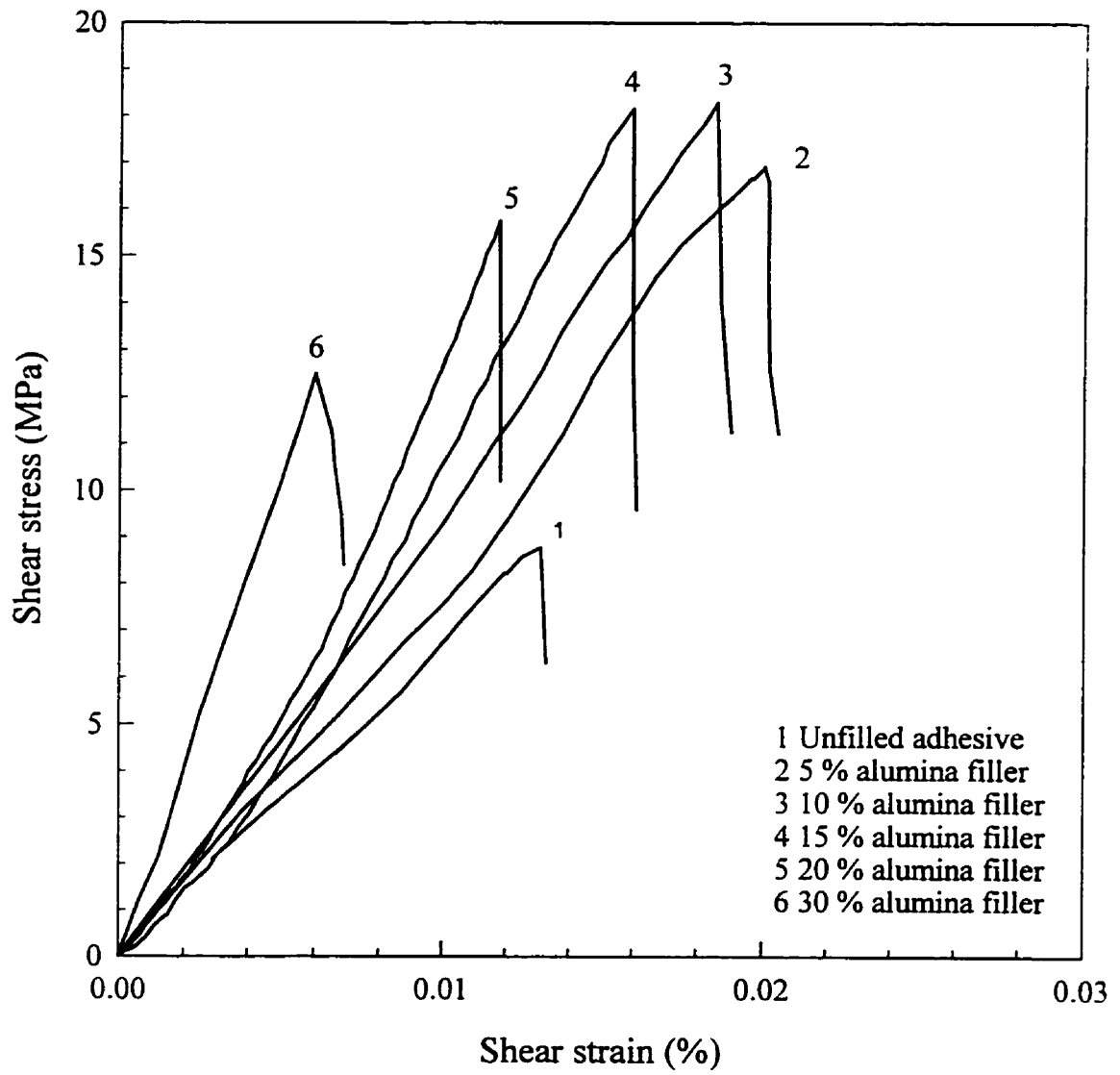


Figure 3.16 Torsion shear stress vs. torsion shear strain in the case of alumina filled adhesive.

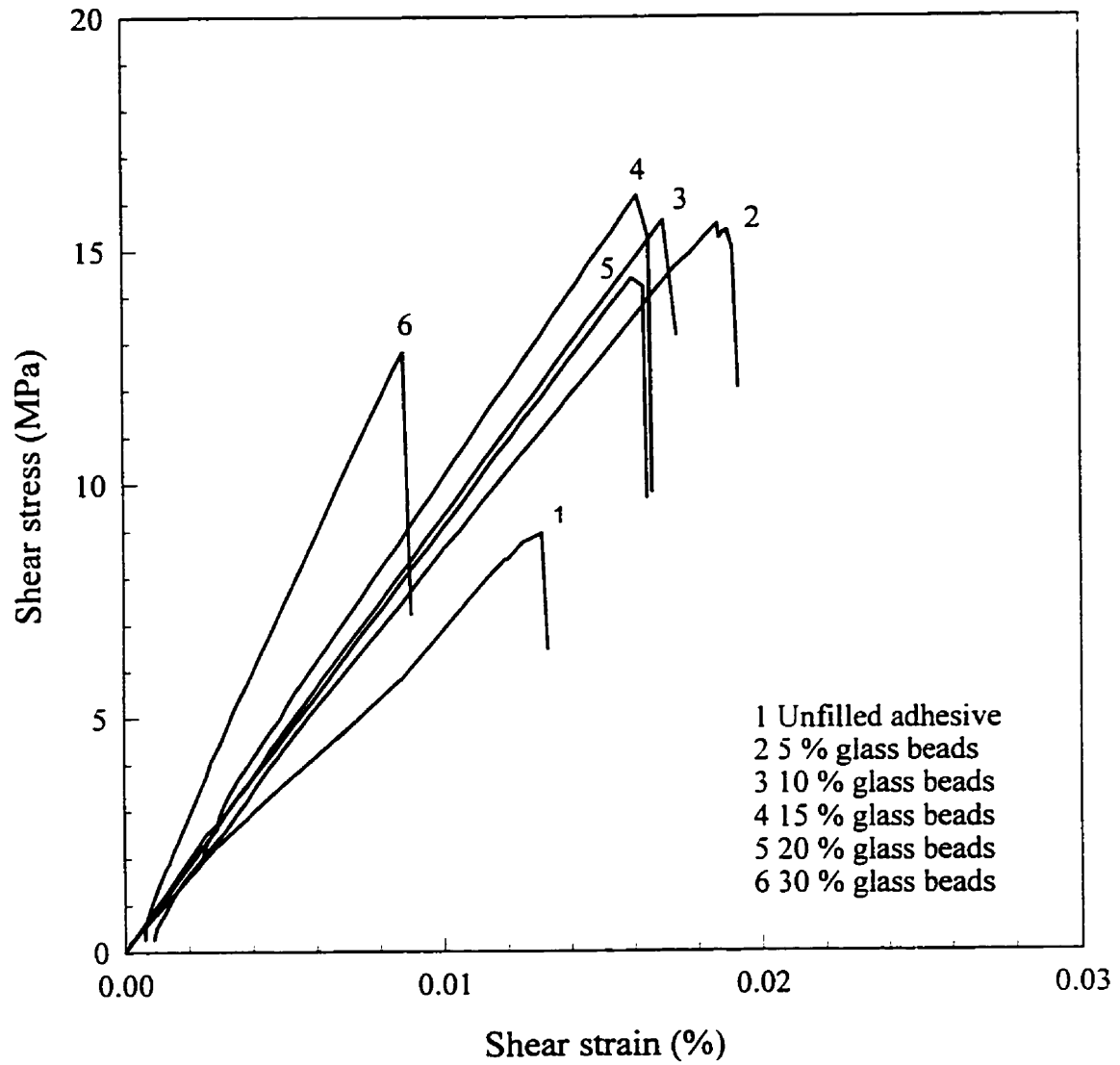


Figure 3.17 Torsion shear stress vs. torsion shear strain in the case of glass beads filled adhesive.

## CHAPITRE IV

### THE EFFECT OF FILLER CONTENT ON THE MECHANICAL PROPERTIES OF EPOXY BASED ADHESIVES

#### 4.1 Abstract

Dynamic mechanical analysis (DMA), tensile, step lap and torsion shear tests are used concurrently to investigate the effect of filler content on the bulk and adhesive joints properties of an epoxy based adhesive. A general purpose epoxy adhesive is filled with alumina ceramic powder (ACP) or glass beads (GB) with volume content ( $V_f$ ) varying from 0 to 30%. The DMA results show that the storage modulus,  $E'$ , and glass transition temperature,  $T_g$ , of the bulk material increase with filler content, while the maximum damping capacity,  $\tan \delta$ , decreases significantly. Except for  $T_g$ , these trends are more pronounced for the ACP fillers. As expected, the tensile modulus increases and the tensile strength decreases as the filler content is increased. However, the shear strength as measured by aluminum/adhesive/aluminum step lap and torsion joint tests is significantly improved with the introduction of fillers. This improvement reached a maximum at intermediate filler content and then started to vanish. This behavior is clearly more pronounced with ACP fillers. The observed behaviors are discussed in terms of adhesive versus cohesive failure.

**Key words:** Adhesives, Filler effect, Mechanical properties, DMA, Shear strength, Adhesive/cohesive failure.



## 4.2 Introduction

Adhesives, which existed for thousands of years, have become much more important only in the past few decades. Recognition of the merits of adhesive bonded joints has led to an ever increasing amount of interest in adhesive bonding. Consequently, adhesion science is an extremely active area of research today. In industry, many experts predict as reported by Irving [1], it would be only a matter of time before adhesive bonding would be used much more extensively than it is now. The subject of adhesive bonding is truly multi disciplinary involving aspects of surface chemistry and physics, polymer chemistry and stress and fracture analysis. A general review of the subject is given by Kinloch [2-4], Adams and Wake [5] and more recently by Lee [6]. There is a convergence of opinion among researchers to reduce the thermal stresses in bonded joints. Many solutions were presented which take into account the differences in mechanical and thermal properties between the adhesive and the adherents. Decreasing the thickness of the adhesive would appreciably reduce the thermal stresses [7-9].

Four different types of fillers have been added to adhesives: filler particles, fibers, flakes, and fabrics. Each type of filler is chosen according to a specific application. Particulate fillers have been used either for surface finish for aerospace components, to reduce the cost or reduce shrinkage or more likely to reduce the CTE (coefficient of thermal expansion) of the adhesive [10-12]. Sometimes, filler particles might be brought to the adhesive to achieve a better heat resistance, improved dimensional stability and resistance to chemical attacks. The most used fillers to achieve the above mentioned features are inert fillers such as

asbestos,  $\text{CaCO}_3$ , talc, carbon black etc. To impart a desired property characteristic to the adhesive to meet a specific requirement such as conductivity in electronic components, it is recommended to add metal filler such as silver or copper which fit the needs best without reducing the mechanical performance [11-14]. The effect of fillers on the mechanical properties of adhesives and bonded joints has been first reported by Young [15].

More recently Halioui et al. [16] also reported a review of the effect of filler content on the shear strength of bonded joints. Usually, it is shown that the shear strength decreases as the filler content increases. The past decade has brought forth a considerable work on the effect of reinforcing filler on the bulk properties of polymeric composites [17-25]. Investigators found changes in thermodynamic and mechanical properties due to the presence of filler. However, very little is known about the effect of filler's type on the adhesion affinity between the adhesive and the adherent. The need to investigate such feature as well as filler content on the performance of adhesive bonded joints led to an increasing interest. Therefore, this work is devoted to the study of the effect of filler content (alumina powder and glass beads) on the mechanical properties of epoxy based adhesives. DMA, tensile tests, torsion and step lap shear experiments will be used concurrently to investigate the above mentioned features on the mechanical properties.

### **4.3 Experimental procedure**

#### **4.3.1 Materials**

The materials used in the present study are an epoxy resin of a chemically pure bisphenol A diglycidyl ether (DGEBA) (DER 331) from Dow chemicals, a polyamide resin (V125) from Henkel Co. as an amine hardener and a tertiary amine (2,4,6 diphenyl amine) Epi-cure 3253 from Shell chemicals as a catalyst. Two types of commercial fillers are used, silane treated glass beads CP3003 with a size diameter less than 45 $\mu$ m and an available ceramic filler (pure alumina powder) of size diameter less than 100 $\mu$ m . Also used an aluminum T6061-T6 plates and napkin ring as adherents to be joined.

#### **4.3.2 Specimens preparation**

The surface treatment of the aluminum plates to be joined is performed according to the recommended ASTM D2651 procedure (hot etching mixture of dichromate-sulfuric acid, referred as FPL etch). In performing the surface treatment, care should be made in order to obtain uniform results. It was reported that variation of the surface treatment parameters has a drastic effect on shear and peel strength properties [26]. The adhesive composites are prepared by mixing the epoxy resin, curing agent, catalyst and fillers. The mixture is stirred completely, part of it is placed into the plates to be joined, the other part is cast into a steel mold for standard tensile tests according to ASTM D638 and DMA samples. It has to be mentioned that because of the high viscosity of the adhesive investigated no air bubble

removal is undertaken. The adhesive thickness between the two plates of the step lap shear samples is 0.2 mm and this is done by placing a thin shim of steel at both ends of the plate as shown in figure 4.1.a. To prevent any excess epoxy adhesive from sticking on the edges of the specimen (spew fillet), a 3 mm free space is coated with grease and removed before curing takes place. On the other hand, napkin ring specimens [27] are joined with the same mixtures under the same conditions (figure 4.1.b).

### 4.3.3 Mechanical Evaluation

Step lap shear specimens inspired by ASTM D1002 are held to grips of an universal testing machine MTS 810 coupled to a data acquisition system. A 1.3 mm/min cross head speed is set for all the experiments. At least five specimens are tested for reproducibility. Similarly, napkin ring samples are also tested at a 5mm/min cross head speed with a recently developed laboratory torsion apparatus [27]. Tensile tests on the bulk adhesive are also carried out under the same conditions. To estimate the surface ratio of cohesive versus adhesive failure, a transparent grid with 1 mm<sup>2</sup> cells is opposed to the both sides of the joint fracture surfaces of each specimen. The results are believed to be reliable since each test is repeated five times and each measurement performed twice.

For the DMA tests, rectangular samples (60 x 12 x 2.5mm) are cut from a cast plate prepared from the same mixture of filled epoxy/polyamide formulations. The experiments are carried out using a Dupont DMA 983 instrument to determine the viscoelastic properties of the bulk adhesive. A heating rate of 2°C/min from ambient temperature to around 100°C

is set for all the samples. The specimens are clamped between two parallel arms and subjected to a uniform sinusoidal displacement of the constant maximum strain  $\epsilon=2 \times 10^{-4}$ . The oscillation frequency is fixed at 1 Hz. More details on the use of this apparatus is given by Elomari et al. [28].

## 4.4 Results and Discussion

### 4.4.1 DMA results

To assure confidence in the DMA results, five tests are performed for each filler content. Figures 4.2 and 4.3 show representative DMA curves obtained with different concentration of ACP and glass beads. The test reproducibility is within  $\pm 10\%$  for the storage modulus  $E'$  and  $\pm 12\%$  for the damping capacity  $\tan \delta$ . The glass transition temperature,  $T_g$ , is estimated to the temperature corresponding to the intersection of an initial tangent line with a final tangent line.

Figure 4.4 shows an increase in  $T_g$  as function of filler content along with the error bars. This behavior has been extensively treated previously [20-21]. However, it should be noted that  $T_g$  is not affected by filler type (ACP or glass beads) contrary to  $E'$  and  $\tan \delta$  as shown in figure 4.2 and 4.3. Moreover, the sensitivity to the type of filler as well as the filler content can be also seen more clearly from the values of the loss modulus  $E''$  as shown in figures 4.5 and 4.6. The larger difference between the two type of filler is seen at higher filler content. The loss modulus of ACP filled adhesive being almost two times higher than that

of glass beads filled one. The larger increase in  $E'$  as function of filler content with ACP compared to that with glass beads can be understood in terms of micromechanics i.e., the contribution of the modulus of the filler to that of the filled material.

Theoretically, micromechanical models can be used to predict the contribution of a filler to the modulus of the filled material. However, these models require the knowledge of the mechanical properties of the fillers, their size and distribution and all these parameters are difficult to measure directly. In this paper the required data are taken from [19, 29] and shown in Table 4.1. The modulus of the ACP being at least five times higher than that of the glass beads for the same filler content, the modulus of ACP filled epoxy is quite larger than that of glass beads filled epoxy. In the following, it is shown that the effect of filler content on the storage modulus,  $E'_c$ , can be predicted reasonably using the modified Kerner model. The relative modulus ( $E'_c/E'_1$ ) of filled to unfilled matrix is compared to the theoretical prediction through equation 4.1 [19].

$$\frac{G_c}{G_1} = \frac{1 + A B \phi_2}{1 - B \psi \phi_2}$$

$$A = \frac{7 - 5 \nu_1}{8 - 10 \nu_1} \quad (4.1)$$

$$B = \frac{G_2/G_1 - 1}{G_2/G_1 + A}$$

$$\psi = 1 + \frac{1 - \phi_m}{\phi_m^2} \phi_2$$

Where  $\nu_1$ =Poisson's ratio of the matrix. G is the shear modulus and the subscripts 1, 2, c

present the matrix, particulate filler and composite respectively. The parameter  $\phi_2$  is the volume fraction of the filler particles and  $\phi_m$  is the maximum packing fraction. Table 4.1 shows the properties of both fillers and the matrix used to calculate the relative modulus. Since the approximative equality shown by equation 4.2 can be verified using Tomishinko equation ( $G=E/(2(1+\nu))$ ), then the terms ( $G'_c/G'_1$ ) and ( $G_2/G_1$ ) can be changed by ( $E'_c/E'_1$ ) and ( $E_2/E_1$ ). Such results are displayed in figure 4.7, and it can be argued that both results are quite similar. This agreement is not surprising between both results, since the Kerner equation was developed for systems with spherical particle symmetry and continuous stress transfer at the phase boundaries.

$$\frac{G_c}{G_1} \approx \frac{E_c}{E_1} \quad (4.2)$$

Table 4.1 Properties of fillers and the matrix.

Material	Modulus E (GPa) <sup>[29]</sup>	Poisson ratio $\nu$ <sup>[29]</sup>	Maximum Packing fraction $\phi_m$ <sup>[19]</sup>
ACP filler	380	0.22	0.4
Glass beads	71	0.17	0.632
Epoxy/Polyamide	1.76 <sup>a</sup>	0.33	---

a: measured value by DMA.

Probably, the most interesting feature for the DMA results of figures 4.2 and 4.3 is the change in Tan  $\delta$  with filler content particularly above the glass transition temperature. Even though the adhesives studied in this paper are not intended for high temperature

application, considering the change in  $\tan \delta$  at relatively high temperature is worthwhile since it is an indication of the microstructural arrangement between the particles and the polymer. Microstructural arrangement means in this case filler/polymer interface and filler agglomerates. An improved filler/polymer interface restricts motion at the interface and results in a decrease of  $\tan \delta$ . Formation of filler agglomerates favors particle/particle friction and results in increase in  $\tan \delta$ . For the two types of filler studied it can be seen that  $\tan \delta$  decreases in both cases with filler content. This decrease is more pronounced in the case of ACP. For a given filler content, the lower  $\tan \delta$  observed for ACP/epoxy compared to glass beads/epoxy can be explained looking to the definition of  $\tan \delta = E''/E'$ . More rigid ACP filler contribute to lower  $\tan \delta$  by increasing  $E'$ . However, qualitatively speaking, this consideration alone do not explain the difference in  $\tan \delta$  observed between the two types of filler. Consequently, it can be postulated that excess damping obtained with glass beads is the results of poor particle/epoxy interface and/or existence of filler agglomerates. Actually, the later reason has to be dropped since at a filler content of 5.7%, while no filler agglomerate is seen in both cases,  $\tan \delta$  is quite larger for glass beads than ACP.

#### 4.4.2 Lap shear vs. Torsion shear results

Figure 4.8 indicates the behavior of step lap joints as function of filler content. The shear strength of aluminum/adhesive/aluminum joints increases with the filler content, reaches a maximum and then starts to decrease. The same observation is outlined in the literature without explanation [10]. Interestingly, it is seen from figure 4.8 that the maximum reached depends on the type of filler incorporated. It is approximately at 10% volume for



ACP and nearly at 20% volume for treated GB. In similar manner, this behavior is confirmed by the napkin ring experiments as illustrated by figure 4.9. Moreover, the improvement is significantly better with alumina than with glass beads fillers. It is clear that the shear strength measured with the proposed torsion shear fixture is higher than that measured with the conventional step lap specimen. It is well known that step lap joints produce lower joint strengths [30]. In order to explain the observed behavior, an adhesive versus cohesive failure concept is used. Figures 4.10 and 4.11 represent the fraction of cohesive fracture surface as a function of filler content, and it can be seen that the general pattern of the curves is comparable to the ones of the shear strength versus filler content. The fraction of cohesive fracture surface increases with increasing filler content, reaches a maximum and then starts to decrease. This result confirms that the magnitude of the shear strength is related to the fraction of cohesive failure involved. Consequently, the better improvement with ACP fillers compared to GB fillers can now be explained by the fact that at the same filler content, ACP contributes more to cohesive failure than GB. However, this statement rises two questions:

- 1) What considerations make ACP contributes more than GB to promote cohesive failure?
- 2) For a given adhesive does the shear strength depends only on the fraction of cohesive failure surface or also depends on the physical properties of the filler involved i.e., ACP or GB. Probably, better adhesion of ACP filled adhesive to the aluminum adherents can be explained from one side by the adhesion affinity of this filler to aluminum surfaces, i.e., higher interaction forces develop at the interface between the two. It was stated that FLP surface treatment made on aluminum adherents promote the formation of alumina oxide [31-32] and this affinity between the ACP and the treated surface may favors better adhesion.

The concept of cohesive versus adhesive failure is extensively employed and it is a controversial subject in the literature [30,33]. It is stated that adhesive/cohesive failure is related to the thickness of the adhesive. For thicker adhesive joints, the peeling stresses are so high that cause adhesive failure. However, for thinner adhesive joints the shear stresses predominate and consequently produce cohesive failures [30]. Other researchers have attributed the cohesive/adhesive failure to factors such as weak boundary layer and that adhesion results from molecular interactions [32].

The fact that the addition of a certain amount of filler results in an increase of the shear strength by promoting cohesive fracture needs explanation. This is particularly important since it is well known that addition of filler such as ACP and GB will lower the bulk strength of polymeric materials. To verify this later statement for the materials used, standard tensile tests were performed on the bulk adhesive filled with ACP and GB, and typical results is shown in figure 4.12. It can be seen that, as expected, the tensile strength decreases as the filler content of ACP increases and a similar behavior is observed with glass beads. The reverse trend is seen when dealing with the same material as an adhesive (figures 4.8 and 4.9). To explain these facts, the following mechanisms represented schematically in figure 4.13 is proposed: the unfilled adhesive contain a large amount of air bubbles which emerge to the interface during the processing of the joint (figure 4.13.a). These air bubbles at the interface will lower the shear strength by two mechanisms: 1) By lowering the effective bonded joint surface, 2) by serving as preferential fracture initiation sites. When fillers are added to the adhesive, it is likely that the filler particles will occupy the space of the air bubbles. These particles being wetted by the adhesive are able to adhere to the joint

interface (figure 4.13.b). In this case the effective bonded joint surface is greater than for the unfilled one. This process continues until it reaches a saturation point which corresponds to the maximum shear strength. Above this maximum oversaturation of the adhesive by fillers causes the particulate fillers to rub against the adherent surfaces (figure 4.13.c). This is the step in the process, where the adhesive failure and lower strengths predominate.

Ideally, it is more suitable to obtain cohesive failures when dealing with bonded joints, since only the performance of the adhesive is tested. Therefore the use of the concept cohesive/adhesive failure in the adhesion science is an important facet. In fact, if a plot of cohesive fracture surface of the bonded joints is performed as a function of the shear strength, one should obtain the ideal case of 100% cohesive that corresponds to an ideal material without defects, i.e., obtaining the performance of the adhesive that should have a maximum strength. This can be done by a simple extrapolation of the linear curve of shear strength versus cohesive fracture surface. Figures 4.14 and 4.15 illustrate the observed linear relationship between the shear strength and the cohesive fracture surface. According to this linear relationship, the 100 % cohesive failure of an ideal adhesive should have a shear strength of approximately 31 MPa and 40 MPa for both step and napkin ring experiments respectively. It is well known that the extraneous stresses developed in the step lap shear are the main cause of the discrepancy between these two results. In order to predict the shear strength of the bulk adhesive using the results of figure 4.15 or the reverse is true, i.e., obtain the shear strength of the bonded joints from the bulk adhesive, the following approach is presented. The torsion shear strength of the bulk adhesive is performed with the recently developed torsion fixture and the results are shown in figure 4.16 which compares the

bonded joints to the bulk adhesive. Broadly speaking, the modulus of both bulk and bonded joints are of the same magnitude, whereas, the shear strength of the bonded joints is much lower than that of the bulk adhesive. It should be mentioned that an ideal material without defects would show a higher shear strength closer in magnitude to the shear strength of 100% cohesive failure obtained from the extrapolated curve of figure 4.15. Even though no experimental evidence shows this tendency, it can be argued that the results are satisfactory to predict the shear strength of an ideal bulk adhesive when the failure is within the adhesive.

#### **4.5 Conclusion**

Particulate fillers are added to adhesives for many purposes such as the reduction of the thermal expansion, improvement of the heat resistance and dimensional stability, and so on. However, based on the fact that addition of fillers to polymers tends to decrease their mechanical properties, it is believed that the same behavior will occur when dealing with polymeric adhesives. This study shows that if fillers are used in adequate proportions the overall mechanical properties can be improved. These adequate proportions or filler content depend on the type of filler used. For instance, for the materials used in the present study, it is found that the optimum filler content with respect to the shear strength is 10% volume for alumina powder and 20% volume for glass beads. This trend is confirmed using two different mechanical tests, i.e., step lap shear and torsion shear experiments. Moreover, it is shown that the shear strength as function of filler content is directly related to the fraction of adhesive versus cohesive fracture surface. A tentative explanation for the

improvement of the adhesive shear strength with filler addition is given based on the fact that the filler particles will occupy a space which otherwise would be occupied by air bubbles. These air bubbles are inevitable in the case of very high viscosity adhesives as the one used in this investigation.

#### **4.6 Acknowledgment**

The authors wish to thank the Natural Sciences and Engineering Research Council of Canada (NSERC) and Fonds pour la Formation des Chercheurs et de l'Aide à la Recherche (FCAR) also we would like to thank Mr. D. Mammoliti and Mr. R. Borssessa of Shell chemicals for providing us materials and supports.

#### 4.7 References

1. B. Irving, *J. Welding* , **73**, **9** (1994) 51
2. A. J. Kinloch, *J. Mater. Sci.* **15** (1980) 2141
3. A. J. Kinloch, “ Development in Adhesive 2 ”, (A. J. Kinloch, 1981) p.83
4. A. J. Kinloch, *J. Mater. Sci.* **17** (1982) 617
5. R.D. Adams and William C.Wake, “ Structural Adhesive Joint in Engineering ”, (Elsevier Applied Science Publication, London and NY, 1984).
6. L. H. Lee, *Adhesive bonding*, (L. H. Lee, Plenum Press NY, 1991).
7. H.P. Kirchner, J.C. Comway, JR., and A. Esegall, *J. Americ. Ceram. Soc.*, **70**, **2** (1987) 104.
8. W.A. Zdanienski J.C. Comway, JR., and H.P. Kirchner, *J. Americ. Ceram. Soc.*, **70**, **2** (1987) 110.
9. D.M. Mazenko, G.A. Jensen and P.J. McCormick, *J. SAMPE*, **23**, **3** (1987) 28.
10. A.M. Zihlif, L. Feldman and R.J. Farris, *J. Mater. Sci.*, **24**, **9** (1989) 3267.
11. T. Plaszczynski, “Advanced composite Materials: New developments and applications”, (ASM International ESD Materials Park, OH, 1991) p.123.
12. H.F. Rush and G.C. Firth, “ Welding and Fastening Symposium ”, (1984) 465 also in NASA report N85-18069.
13. J. Comyn, “ Engineered Materials Handbook ”, Vol.3 (ASM International, New York, 1990) p.616.
14. A. Bjornklett and H. Kristiansen, *Hybrid Circuits Symposium*, **33**, (1994) 28.

15. L.O. Young, *Adhesive Age*, **2**, (1959) 39.
16. M. Halioui and J. P. Lieurade, *Matériaux et Techniques*,(1991) 17.
17. T. Morayama, “Dynamic Mechanical Analysis of Polymeric Materials”, **2** (Elsevier Science Publishers, New York, 1978) p.130.
18. J.A. Manson and L.H. Sperling, “Polymer Blends and Composites”, (Plenium Press New York, 1976) p.373.
19. L.E. Nielson and R. F. Lendel, “ Mechanical Properties of Polymers and Composites ”, (2<sup>nd</sup> edition,Marcel Dekker Publishers New York, 1994) p.377.
20. D.H. Droste and A.T. DiBenedetto, *J.Appl. Polym. Sci.*, **13** (1969) 2149.
21. E.H. Chiu, Ph.D Thesis, Lehigh University, June 1973.
22. E.H. Kerner, *Proc. Phys. Soc.* , **69B** (1956) 808.
23. Z. Hashin, *J. Appl. Mechan.*, **29** (1962) 143.
24. T.B. Lewis and L.E. Nielsen, *J. Appl. Polym. Sci.*, **14** (1970) 1449.
25. L.E. Nielsen and T.B. Lewis, *J. Polym. Sci.*, **A-27**(1969) 1705 .
26. M.C. Ross, R.F.Wegman, M.J.Bodnar and W.C.Tanner, *SAMPE J.* **10** (1974) 4.
27. M. Ouddane, R. Boukhili, R. Gauvin, Submitted to *J. Mater. Sci.*, (May 1997)
28. S. Elomari, R.Boukhili, M.D.Skibo and J. Masounave, *J. Mater. Sci.* **30**, (1995) 3037
29. J.F. Shackelford, W. Alexandre and J.S. Park, “CRC Materials Science and Engineering Handbook”, (CRC Press Inc. 1994).
30. J. M. Giraud, *Matériaux et Techniques*, (1980) 255
31. J.S. Ahearu, G.D. Davis, T.S. Sun and J.D.Vanables, “ Polymer Bonds, in Adhesion

Aspects of Polymeric Coatings ", (K.L. Mittal, Plenum Press, 1983) p.288

32. N.Ho Sung, " Engineered Materials Handbook ", Vol.3 (ASM International, New York, 1990) p.622.
33. J. D. Minford, " Adhesive Bonding ", (L.H. Lee edition, Plenum Press, New York, 1991). p.239.



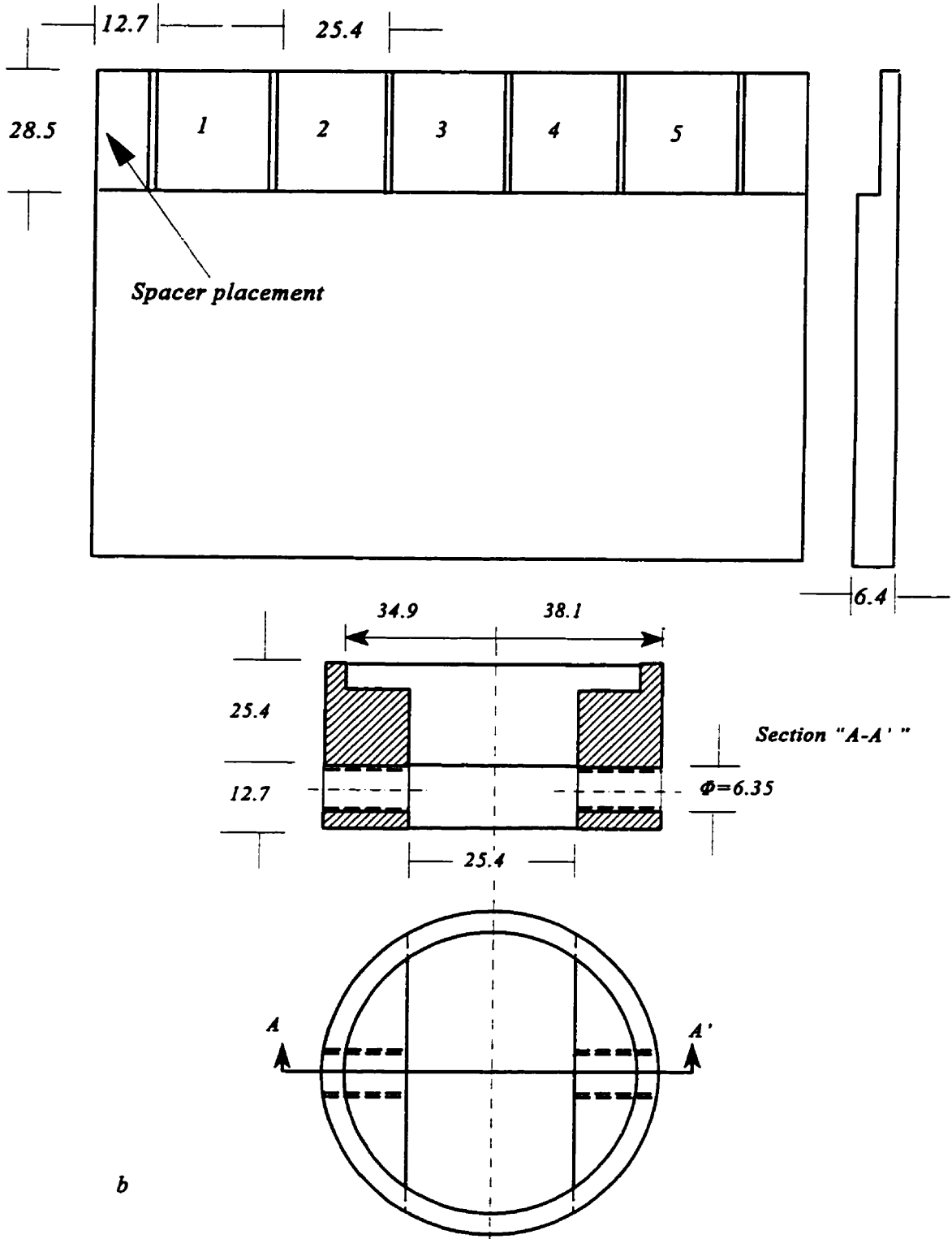


Figure 4.1 Step lap shear and napping ring specimens.

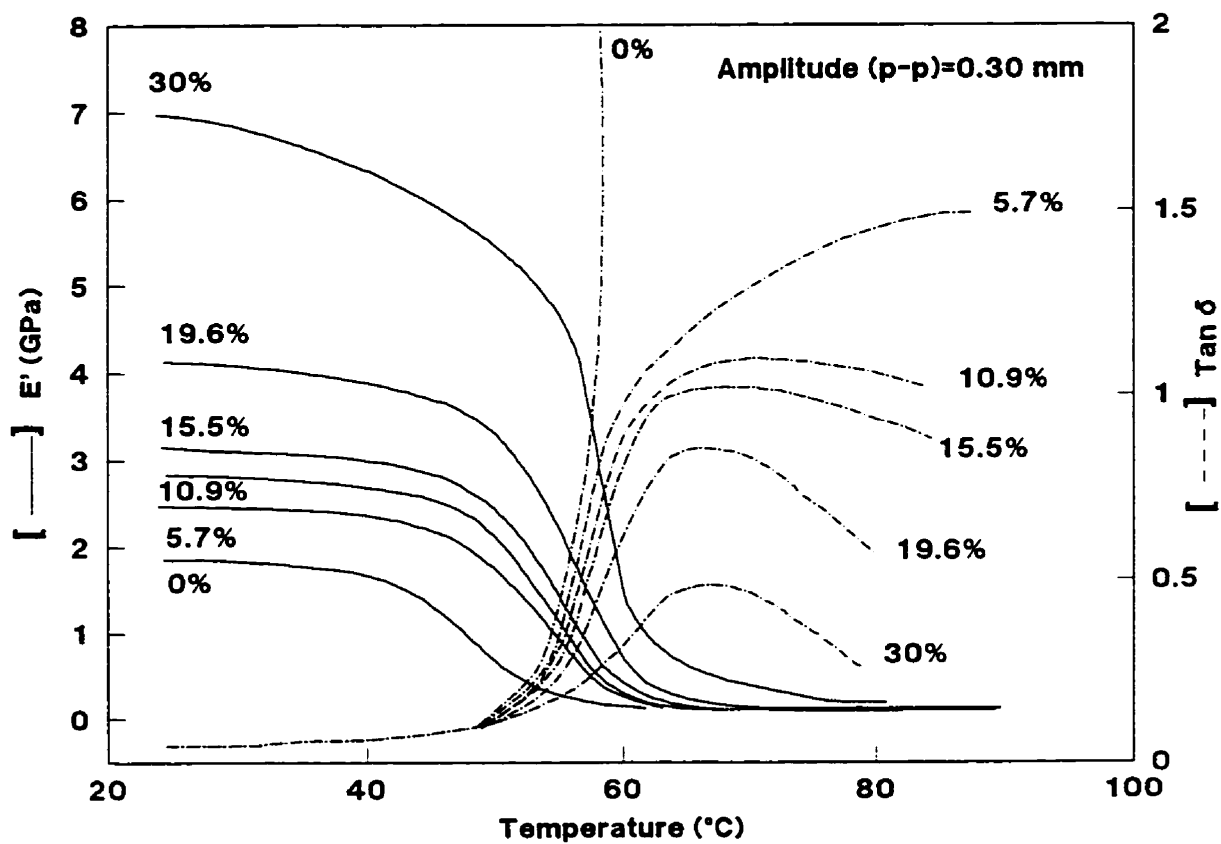


Figure 4.2 Storage modulus and damping capacity as a function of temperature for alumina filled adhesive.

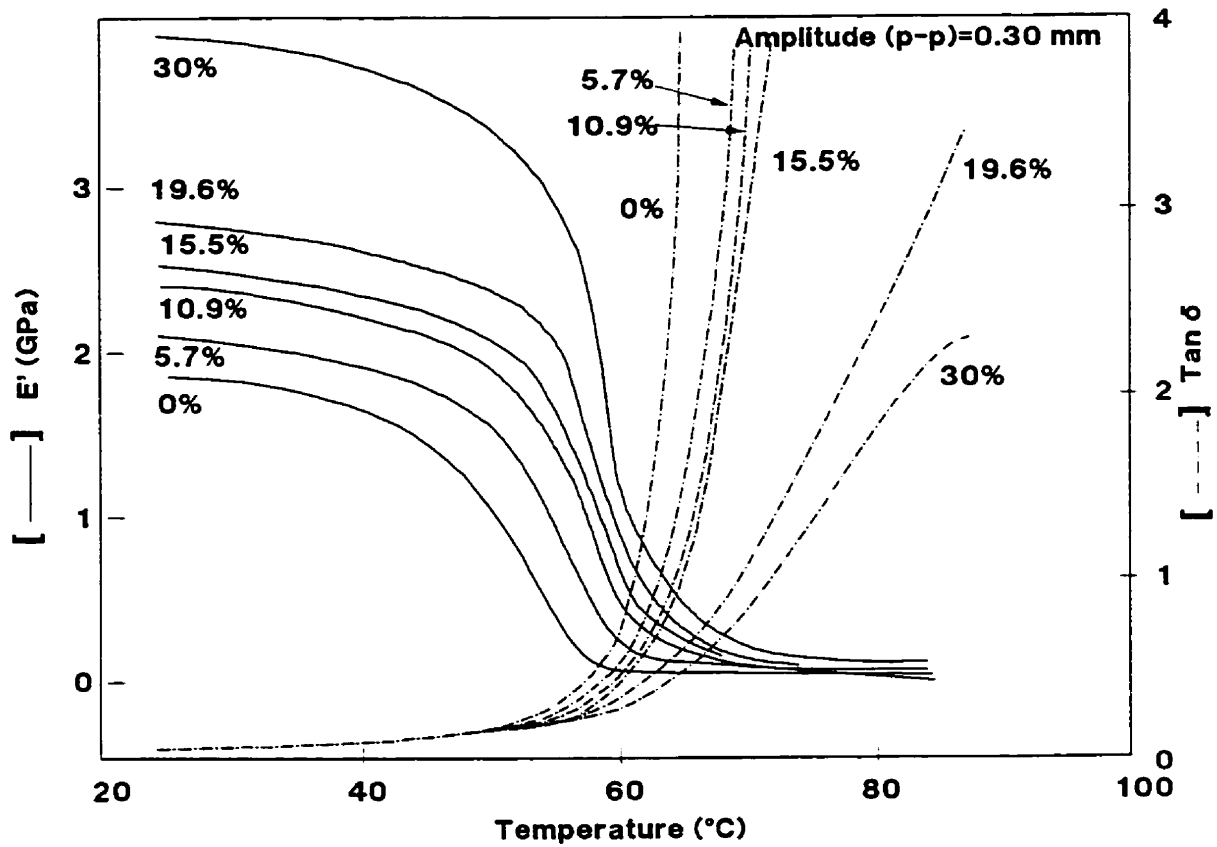


Figure 4.3 Storage modulus and damping capacity as a function of temperature for glass beads filled adhesive.

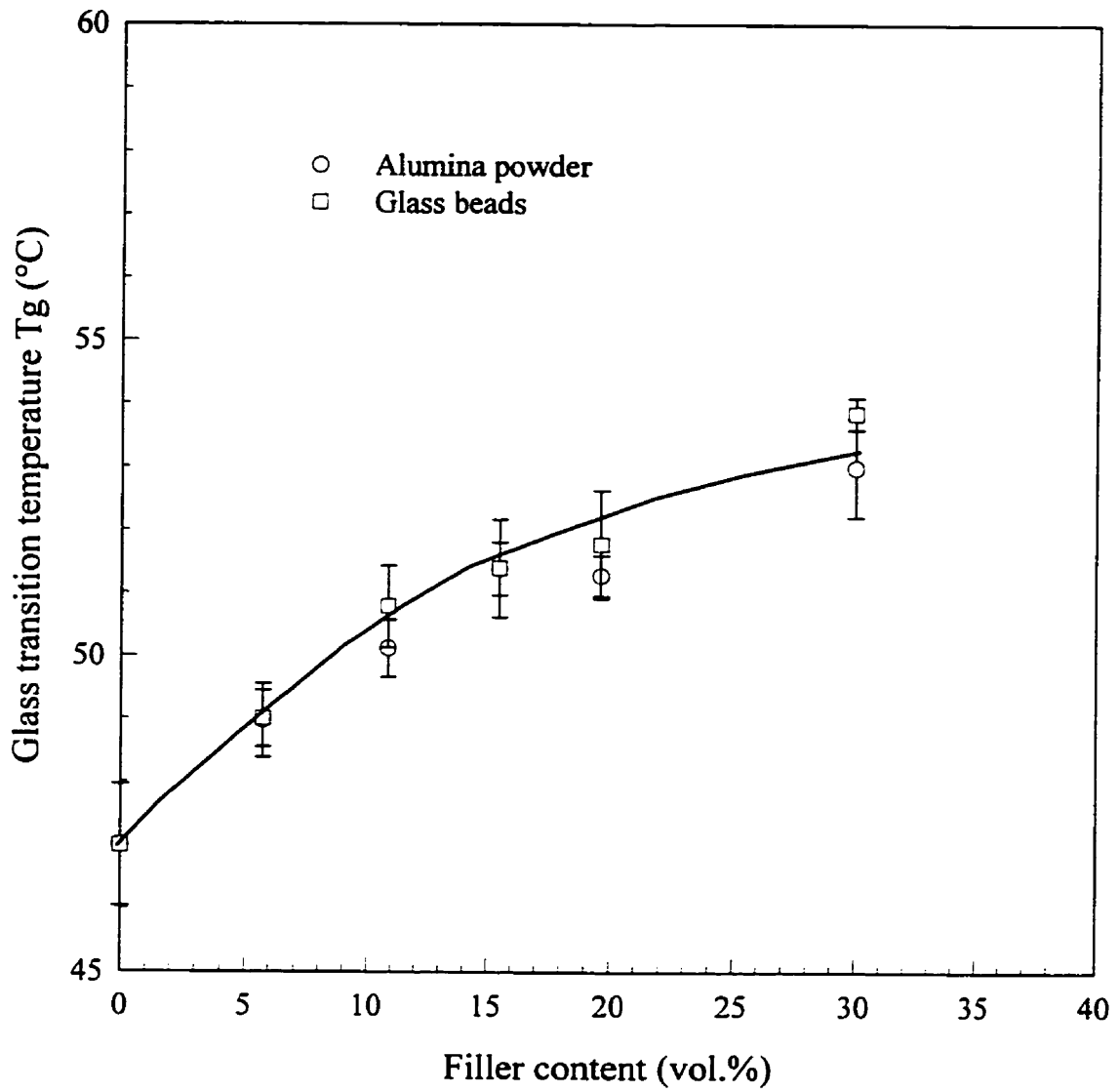


Figure 4.4 Glass transition temperature of epoxy adhesives as a function of filler content.

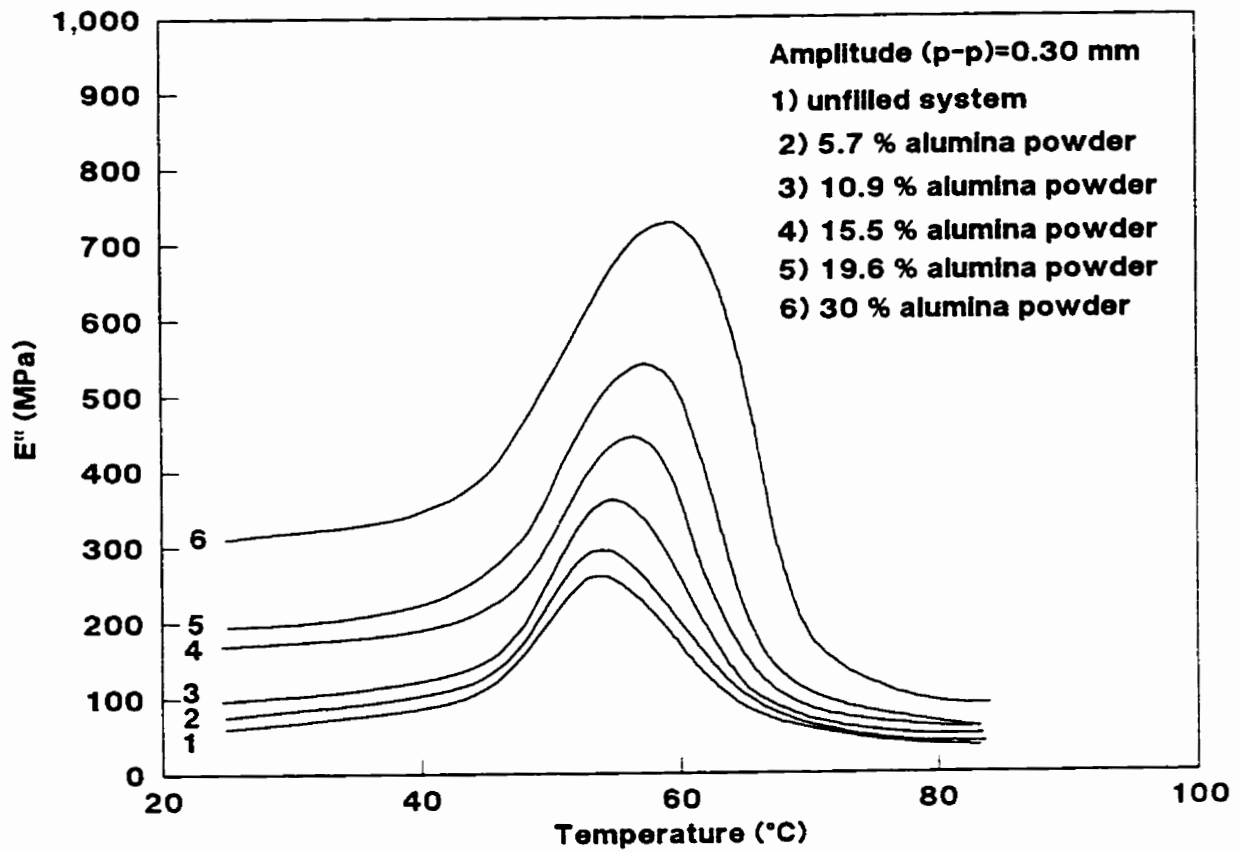


Figure 4.5 Loss modulus as a function of temperature for alumina filled adhesive.

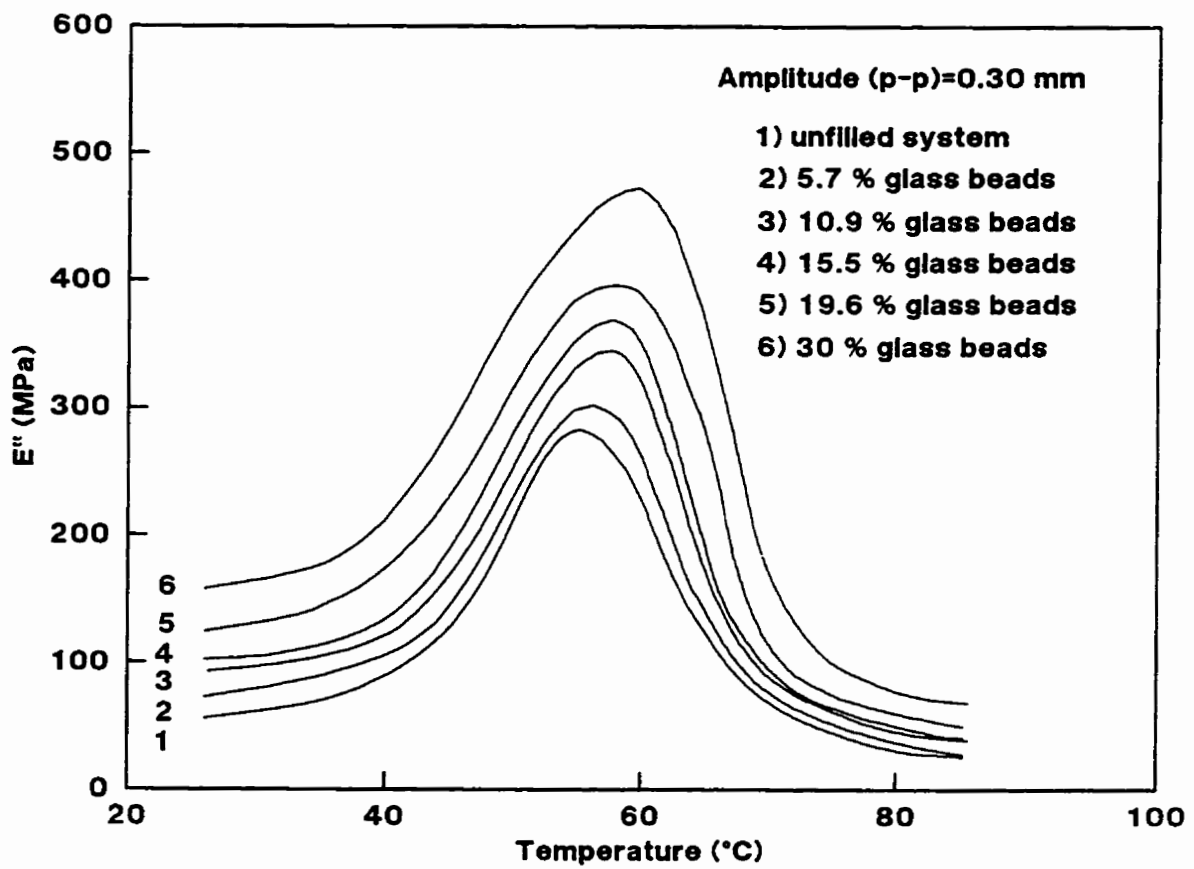


Figure 4.6 Loss modulus as a function of temperature for glass beads filled adhesive.

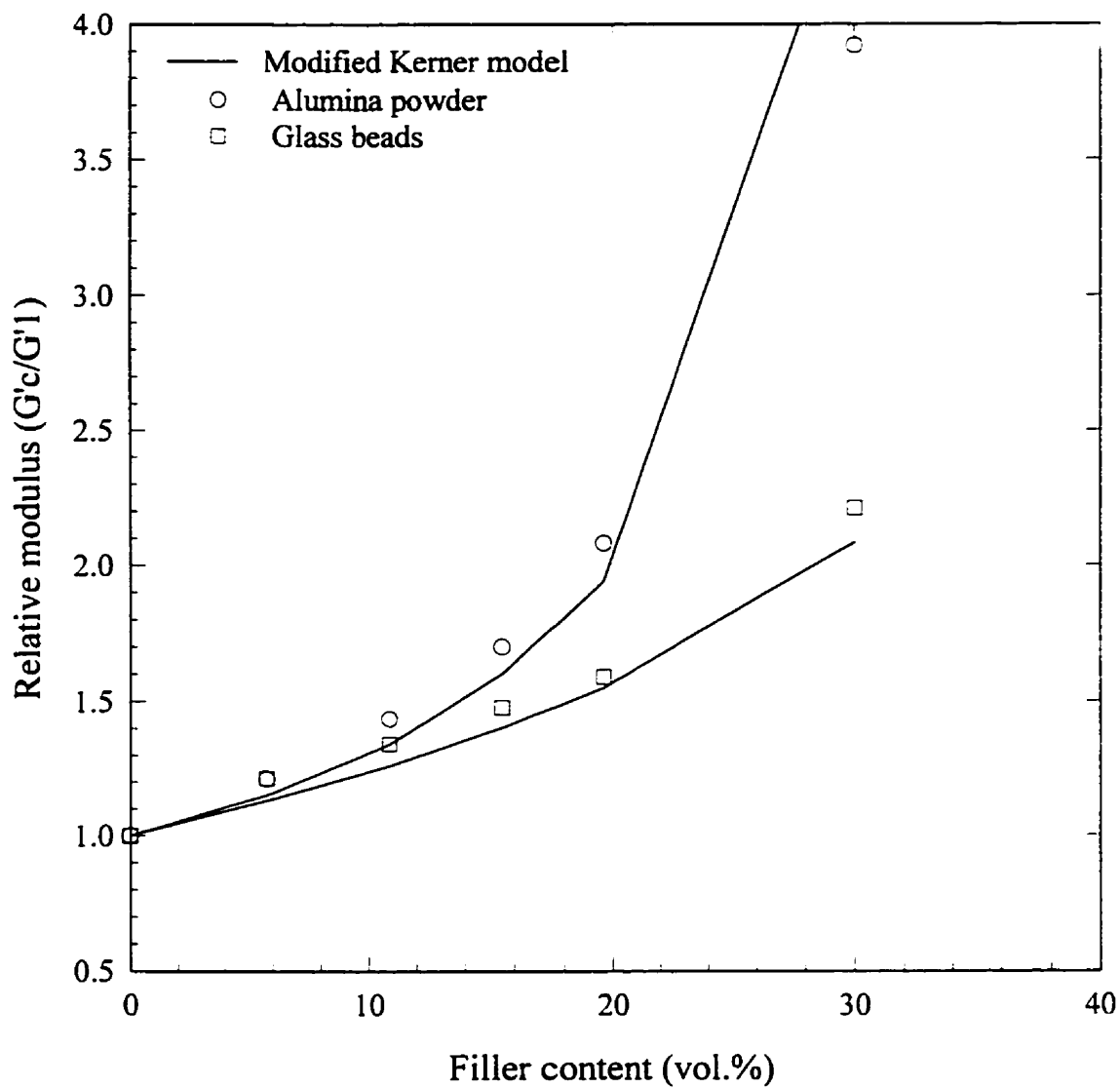


Figure 4.7 Relative modulus as a function of filler content (comparison between the theoretical prediction and experimental results) .

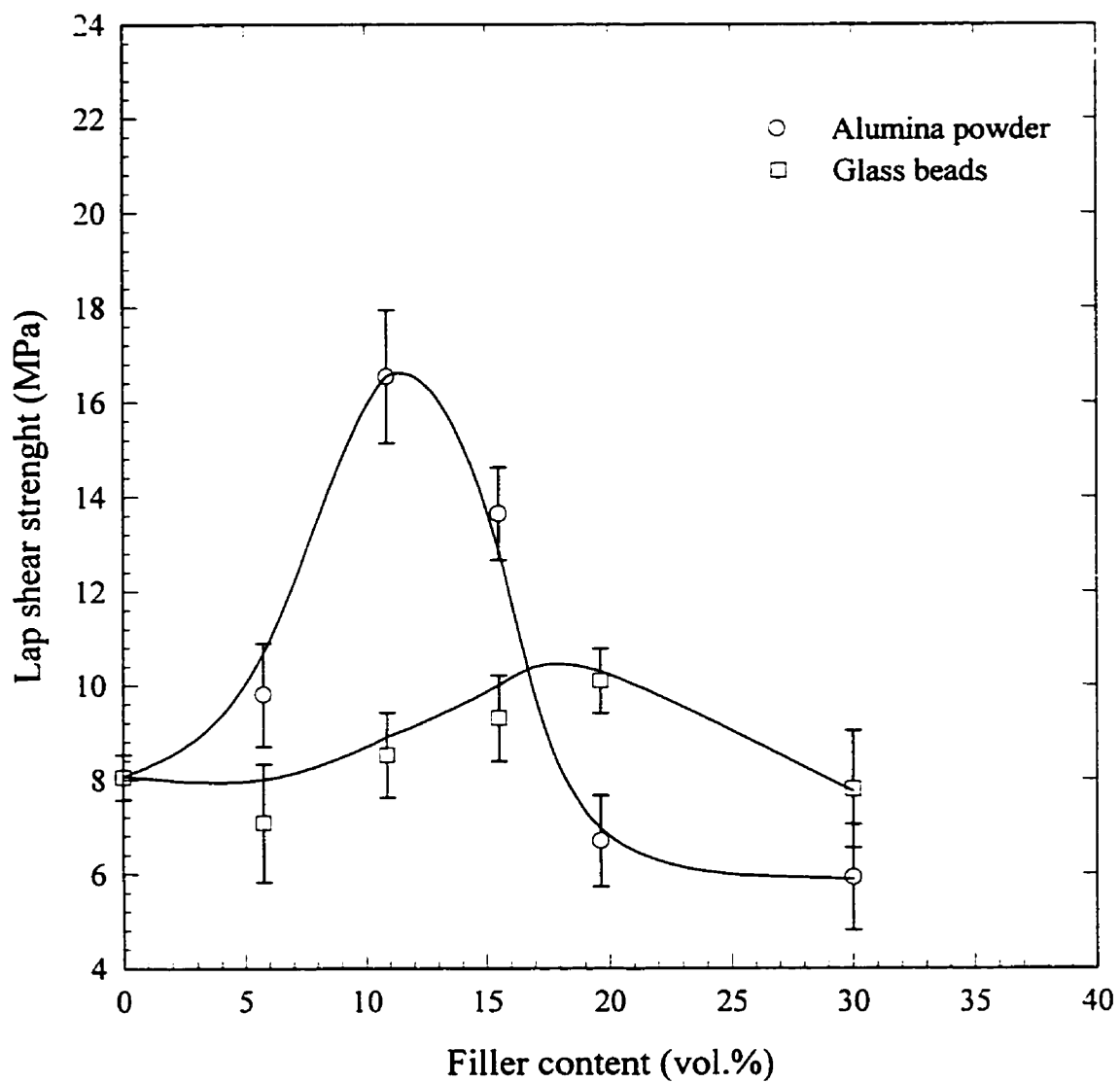


Figure 4.8 Step lap shear strength as a function of filler content.



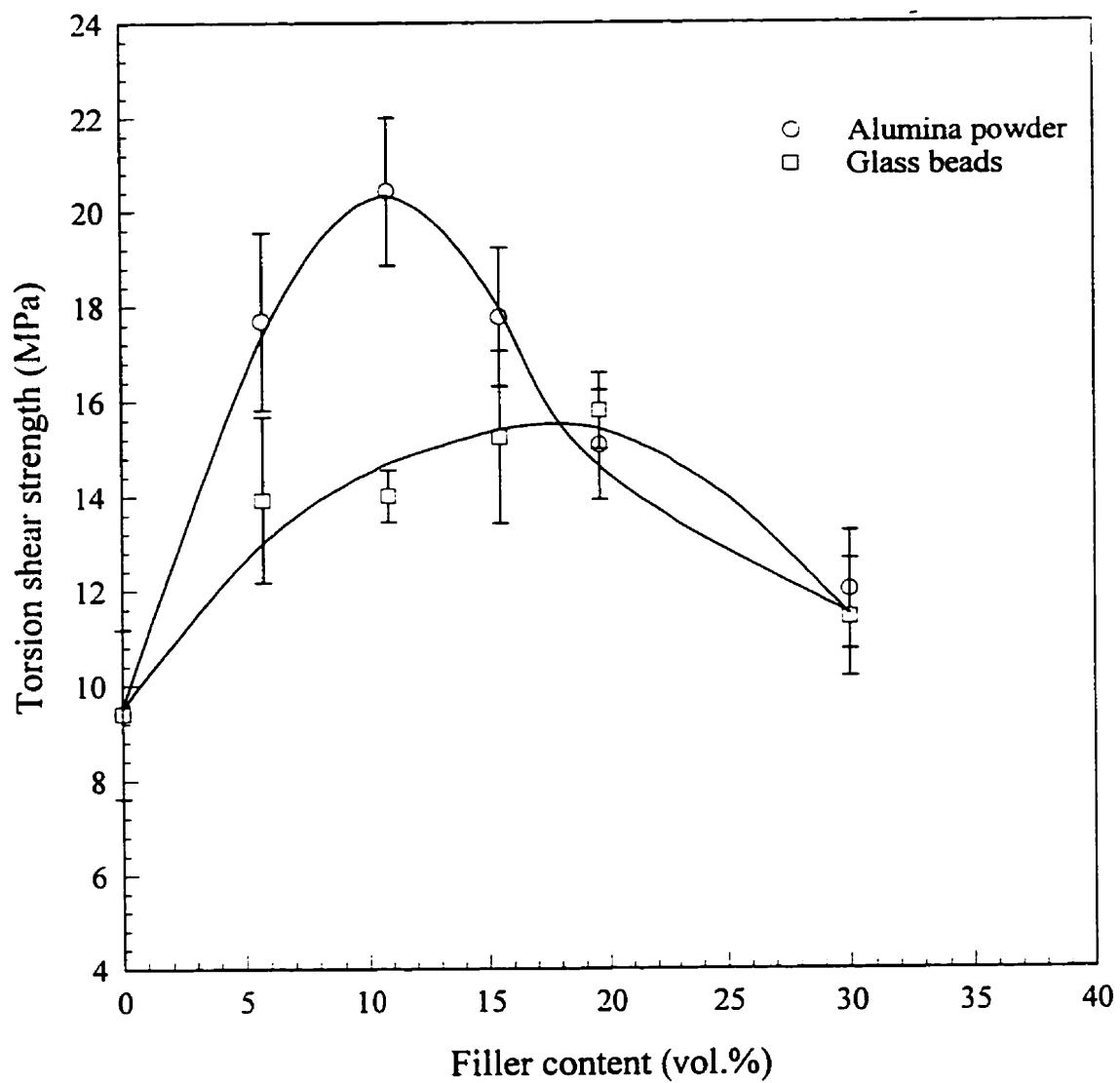


Figure 4.9 Torsion shear strength as a function of filler content.

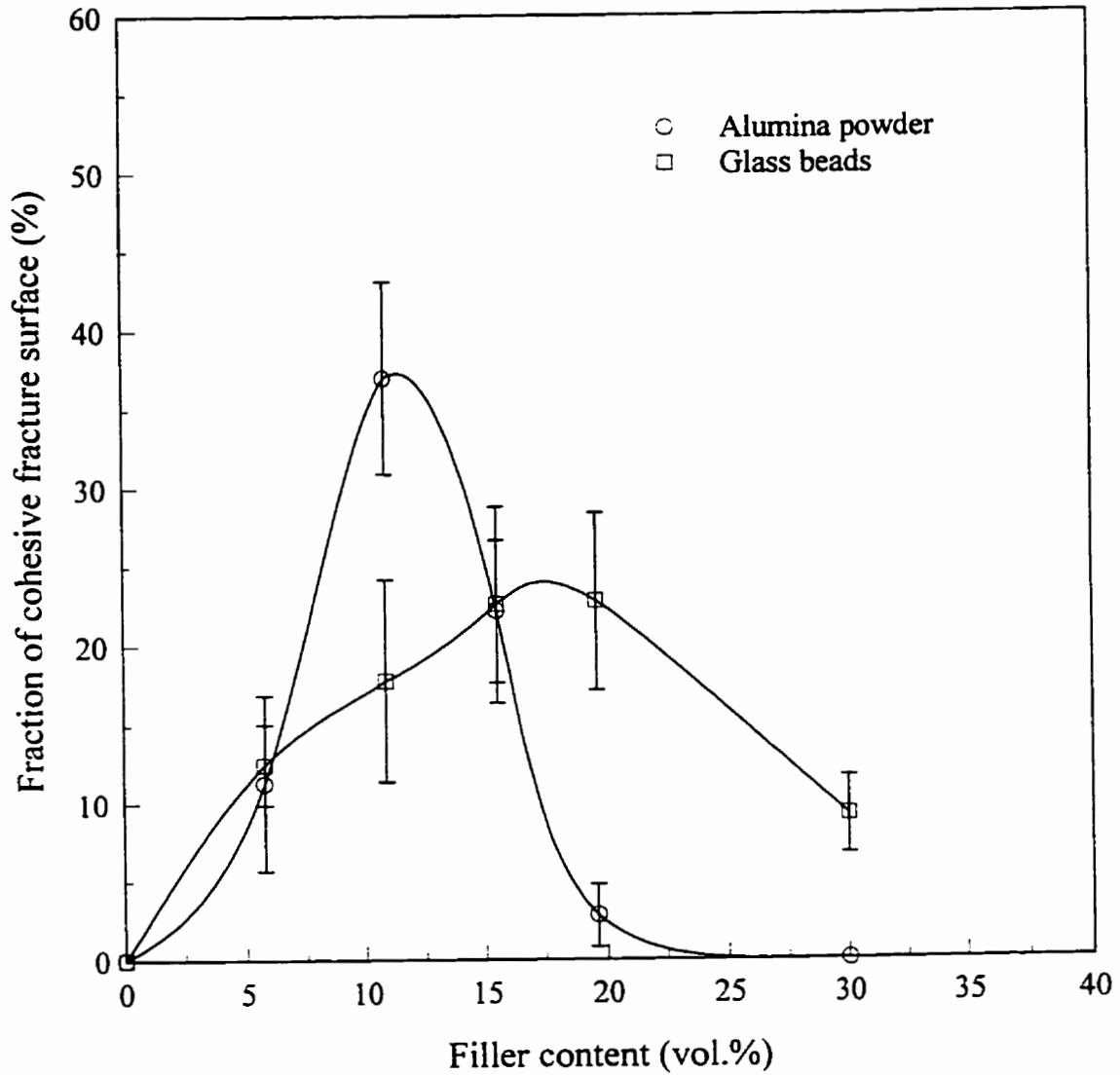


Figure 4.10 Fraction of cohesive fracture surface as a function of filler content (step lap shear test).

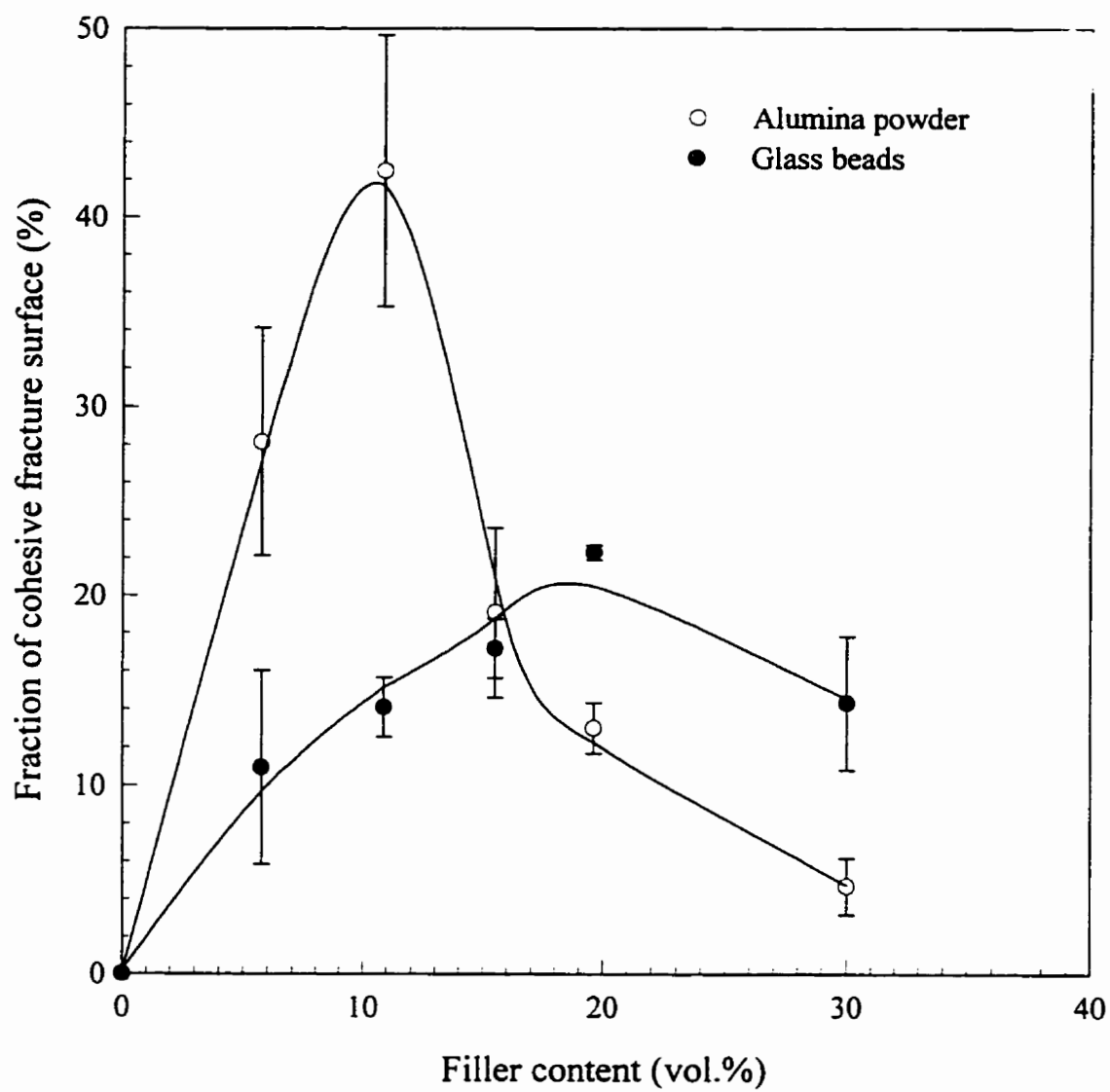


Figure 4.11 Fraction of cohesive fracture surface as function of filler content (torsion shear test).

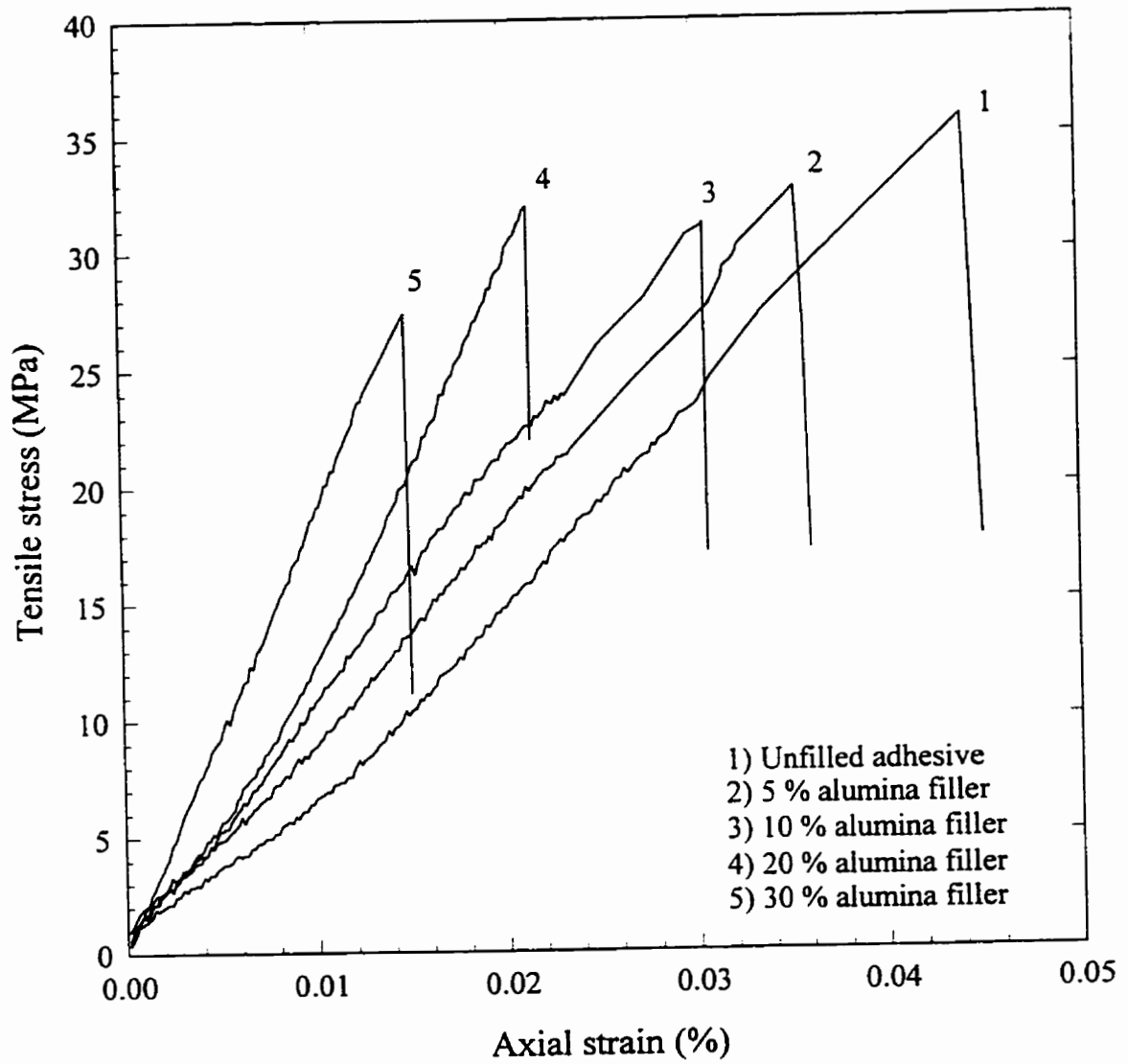


Figure 4.12 Tensile stress versus tensile strain obtained from bulk adhesives.

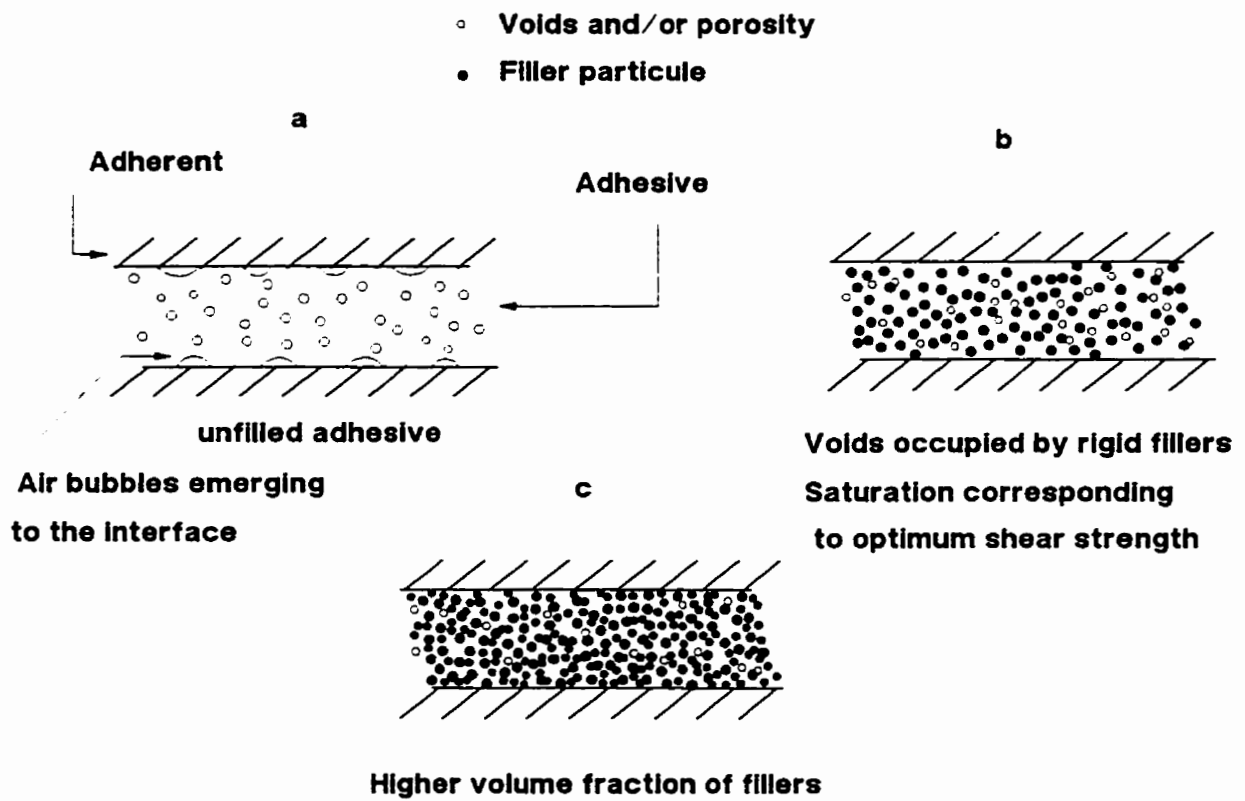


Figure 4.13 Schematic drawing showing how fillers affect adhesion.

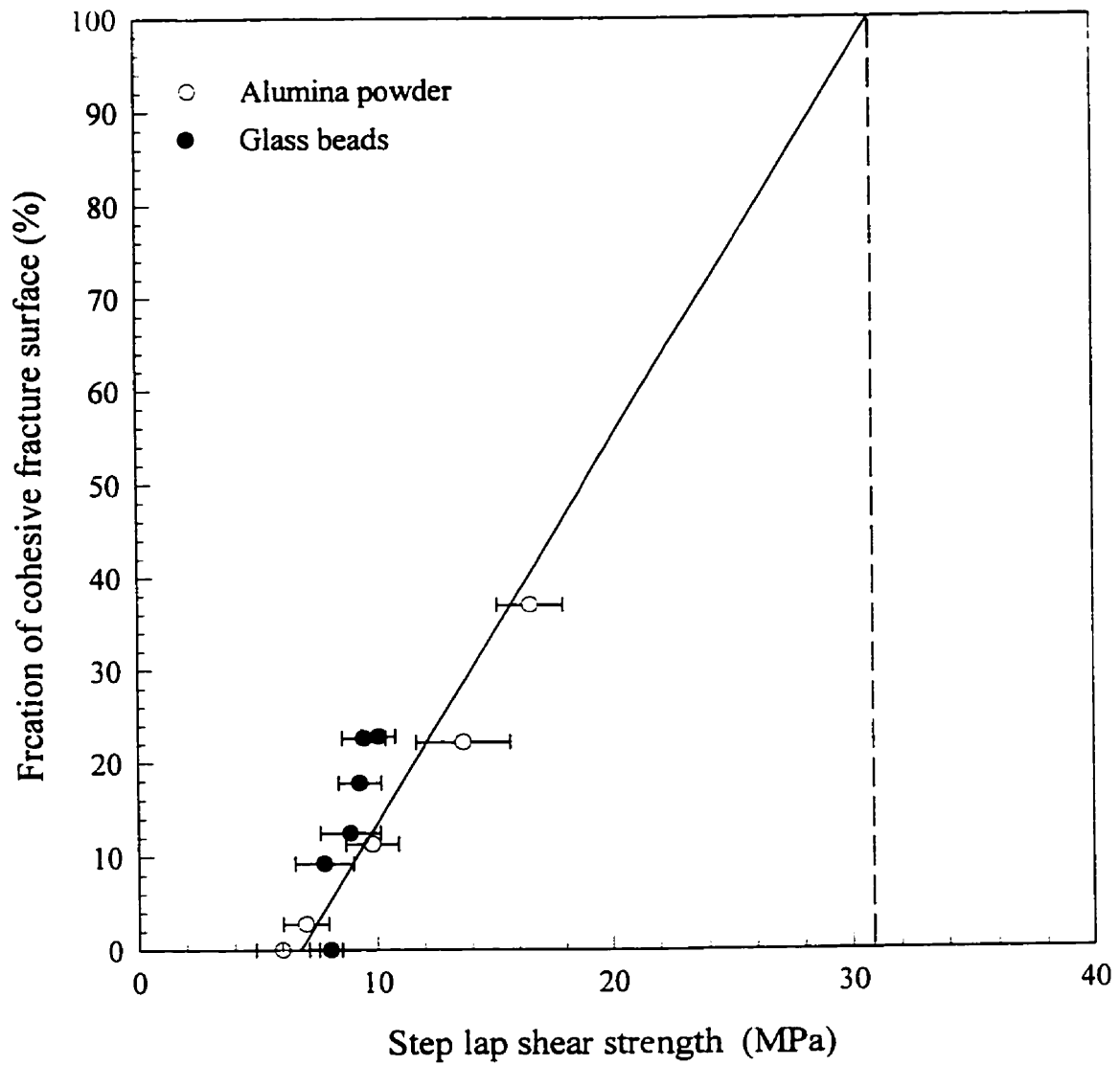


Figure 4.14 Fraction of cohesive fracture surface versus step lap shear strength.

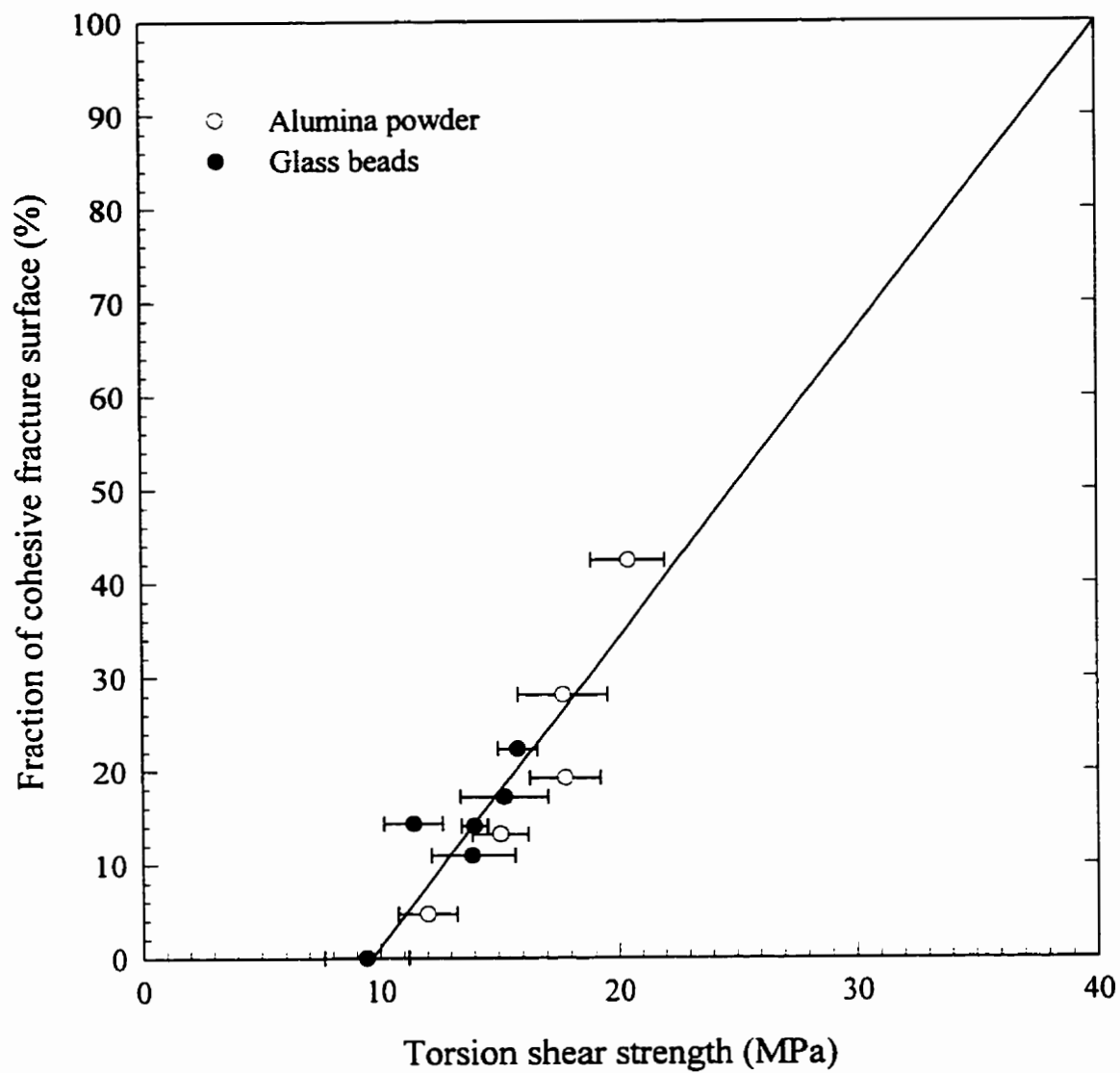


Figure 4.15 Fraction of cohesive fracture surface versus torsion shear strength.

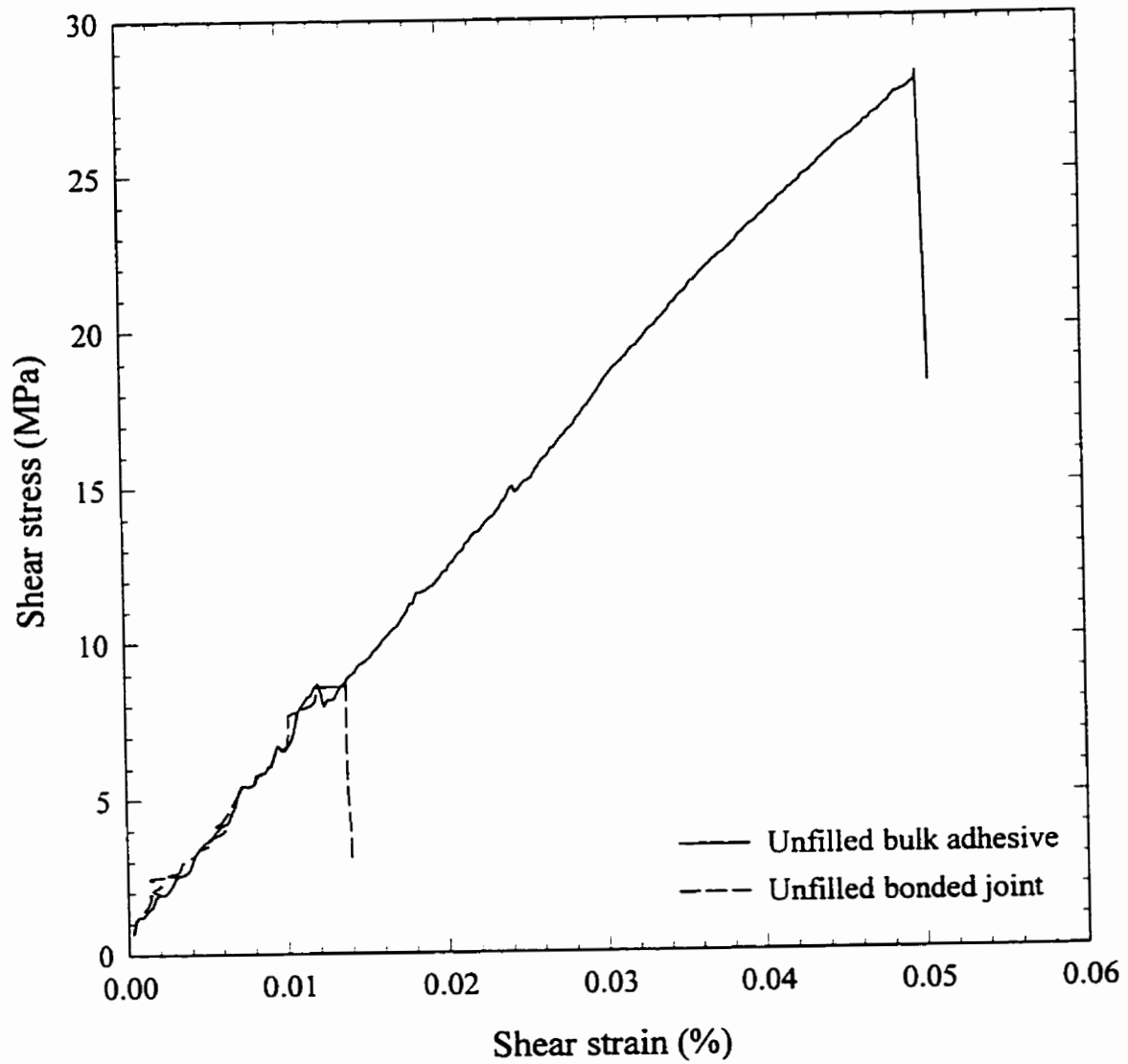


Figure 4.16 Torsion shear stress versus torsion shear strain (comparison between bulk adhesive and bonded joint).



## CHAPITRE V

### MOISTURE ABSORPTION EFFECT OF ADHESIVE FILLED BONDED JOINTS

#### 5.1 Abstract

The effect of filler type and content on the performance and durability of adhesive bonded joints upon exposure to damp heat (water immersion ) is investigated using concurrently step lap shear and thermo mechanical analysis (TMA) experiments. A TMA based approach is developed in order to predict the strength of the bonded constructions. Two types of fillers, glass beads (GB) and Alumina powder (ACP), are used in order to achieve the objectives. It is shown that ACP filled adhesives have higher strength retention compared to GB filled ones. It is also demonstrated that valuable information can be extracted from TMA measurements. Generally, the increase of the coefficient of thermal expansion CTE of the bonded joints are found to be in agreement with the decrease of the step lap joint strengths after exposure. The increase of the CTE of the bonded joints resulting from exposure to hot water seems to increase the stresses which in turn affect the overall strength. Similarly, bulk adhesive results showed that GB filled systems are more susceptible to water than ACP filled ones, which confirmed the decrease in strength of GB filled bonded constructions.

**Key words:** Moisture effect, fillers, mechanical properties, step lap shear, TMA.

## 5.2 Introduction

Adhesives are being increasingly used in structural engineering applications but a problem frequently encountered is that the mechanical properties of the bonded joints may rapidly deteriorate upon exposure of the joint to aggressive environment conditions involving heat and humidity. Several reviews have been written which address this aspect [1-5]. Diffusion of water into the interfacial region can reduce the strength of the bonded joints by a number of different mechanisms [5-9]. Kinloch [1] stated that the overall mechanics of failure of the bonded joint may be identified from basic fracture mechanical considerations. The first stage is the accumulation of a critical concentration of water in the interfacial regions which must be exceeded for environmental attack to occur. The second stage involves a loss in the integrity of the interfacial regions due to: 1) the rupture of interfacial secondary bonds 2) subtle changes occurring in the oxide structure, e.g., hydration, which causes a mechanical weakening of the oxide layer. The same conclusion, i.e., the formation of weak oxide layer, has been drawn by some authors [10-13]. The third stage concerns the ultimate failure of the adhesive joint.

When adhesive joints are exposed to wet environments, water molecules will migrate and be preferentially adsorbed into the interface where a high-energy surface adherent is present. Water can enter either by diffusion through the bulk adhesive layer or by wicking along the adhesive/adherent interface. However, it is believed that in a typical structural joint, such as epoxy-metal, the water generally enters a joint system by diffusion through the epoxy rather than by passage along the interface [2,6,14].

The selection of a polymer having low values of permeability and diffusivity as an adhesive is an obvious approach to delay or reduce water migration into joints. However, it must be balanced with the other properties an adhesive should have. The durability of the bonded joints can considerably be enhanced by applying silane primers [1]. In this case, the primer layer itself will be the weakest part of the joint and fracture may occur by cohesive failure of this layer. It is also believed that incorporation of inert or metallic fillers would reduce the permeability assuming that water cannot easily debond the second phase. [15-16]. This simplistic assumption was not confirmed by experimental evidences. Many investigations dealing with metal filled adhesives related to electronic components can be found in refs [17-20]. However, these investigations were focused on the electrical performance rather than the mechanical aspects. This paper is aimed to investigate the effect of filler type and content on the performance and durability of adhesive bonded joints upon exposure to damp heat (water immersion). A TMA based approach is developed in order to predict the strength of the bonded joints. Step lap shear and TMA experiments are used concurrently to investigate the effect of moisture on bulk and bonded joint.

### **5.3 Experimental procedure**

#### **5.3.1 Materials**

The materials used in the present study are an epoxy resin of a chemically pure bisphenol A diglycidyl ether (DGEBA) (DER 331) from Dow chemicals, a polyamide resin (V125) from Henkel Co. as an amine hardener and a tertiary amine (2,4,6 diphenyl amine)

Epi-cure 3253 from Shell chemicals as a catalyst. Two types of commercial fillers are used, a silane treated glass beads CP3003 with a size diameter less than  $45\mu\text{m}$  and an available ceramic filler (pure alumina powder) of size diameter less than  $100\mu\text{m}$ . Also used is aluminum T6061-T6 plates as adherents.

### 5.3.2 Specimens preparation

In the present study three types of specimens are tested. The bulk specimens are intended to be used to measure the diffusivity of water. Square samples are cut from cast plates and the initial masses in the dried conditions are recorded and their initial dimensions obtained with a micrometer. Three samples of bulk adhesives for each formulation are transferred to the boiling water bath ( $100^{\circ}\text{C}$ ). In each case, the moisture absorption as a function of time is monitored by weighing the samples periodically on a micro-balance which enabled masses to be determined to within  $\pm 0.1$  mg. Other bulk adhesive specimens are used for CTE measurements. The samples are  $2.5 \pm 0.1$  mm thickness to avoid any subjection to non-uniform temperature distribution when heating the samples. The last samples being bonded joints of either step lap shear and TMA specimens have both the same dimension ( $10 \times 10$ ) mm (figure 5.1) and are intended for comparison purposes. Both TMA samples and step lap bonded joints are then immersed in accelerated ageing tests: damp heat (DH) at  $100^{\circ}\text{C}$  and 100% RH (water immersion) for three weeks. Step lap shear specimens inspired by ASTM D1002 are held to grips of an universal testing machine MTS 810 coupled to a data acquisition system. A  $1.3$  mm/min cross head speed is set for step lap shear tests. At least five specimens are tested for reproducibility for both not aged and aged

samples.

### 5.3.3 TMA procedure

A Dupont 2100 Thermo mechanical analyzer (TMA) instrument is used to measure the CTE of both bulk adhesives and bonded joints. The experimental procedure used for bulk adhesives is that described by Ennis et al. [21], which consist of preheating the samples with a heating rate of  $5^{\circ}\text{C}/\text{min}$  through  $T_g$  followed by a slower cooling  $\leq 1^{\circ}\text{C}/\text{min}$  to room temperature, while the probe is not removed from the sample, it is reheated again at a heating rate of  $10^{\circ}\text{C}/\text{min}$  from  $-60^{\circ}\text{C}$  to  $100^{\circ}\text{C}$ . It should be mentioned that two different probes are used in the experiment, (standard probe of 2.5 mm diameter and macro-expansion probe of 6.4 mm diameter). In the case of TMA bonded joints, they are tested with the standard probe at  $10^{\circ}\text{C}/\text{min}$  from  $-60^{\circ}\text{C}$  to  $200^{\circ}\text{C}$ .

## 5.4 Results and discussion

### 5.4.1 Bulk adhesive:

The results for the percentage weight gain ( $M_m$ ) as function of square root of time ( $t^{1/2}$ ) are shown in figures 5.2 and 5.3. These results, illustrate the effect of varying the filler content and type of filler on the moisture absorption characteristics expressed by the weight gain. The weight gain of all the samples has been characterized by an apparent diffusion coefficient,  $D$ , and an apparent maximum moisture content,  $M_m$ . The diffusion coefficient

is calculated from the initial linear increase of weight change  $M$  with  $t^{1/2}$  according to Fickian theory [22]. At least 3 specimens are tested for reproducibility.

$$D = \pi \left( \frac{h}{4 M_m} \right)^2 \left[ \frac{\Delta M}{\Delta(t^{1/2})} \right]^2 \left( 1 + \frac{h}{a} + \frac{1}{b} \right) \quad (5.1)$$

Where  $h$  is the sample thickness and  $a$  and  $b$  are the other two sample dimensions.  $\Delta M$  and  $\Delta(t^{1/2})$  are small increments.

From figure 5.4, which shows the effect of filler content on the diffusion coefficient, it can be seen that GB filled adhesives are more permeable to water than ACP filled ones. The effective diffusion coefficient of a composite consisting of spherical particles in a matrix has been determined using the Maxwell theory [23] and is given by:

$$D = D_m \left[ \frac{2 - 2V_f + (1 + 2V_f) D_p/D_m}{2 + V_f + (1 - V_f) D_p/D_m} \right] \quad (5.2)$$

where  $V_f$  is the volume fraction of the particulate fillers,  $D_p$  and  $D_m$  are the diffusion coefficient of the particles and matrix respectively. In the case of small values of  $V_f$  and in the limit that  $D_p/D_m$  is very small, equation 5.2 can be approximated by:

$$D = D_m \left[ \frac{2 - 2V_f}{2 + V_f} \right] \quad (5.3)$$

Equation 5.3 predicts that the diffusion coefficient will decrease with increasing filler content. This is logical since water absorption by ACP and GB particles is negligible and this

model assumes perfect bonding at the particle/matrix interface. However, the experimental results in figure 5.4 show an opposite behavior to the prediction of equation 5.3 and this disagreement is more pronounced in the case of GB than ACP fillers. The apparent reason is that incorporation of fillers is accompanied by air bubbles and also the filler /matrix interfaces can serve as preferential sites for water diffusion. According to this explanation ACP filled adhesives must have better filler/matrix interface and this fact is in agreement with the previous work [24] with the same materials and dealing with the mechanical properties.

Figure 5.5 represents the volume increase (swelling) as function of the filler content for both types of filled bulk adhesives subjected to water immersion until saturation. It can be seen from the figure 5.5 that the volume change of bulk adhesives increases as the filler content increases and it is more pronounced in the case of GB filled adhesives than ACP filled ones. However, the volume increase of GB filled adhesive rises a question: why the volume change and the weight gain does not show the same level, since the water absorption is the same for both ? Probably, this is the result of the pronounced micro cracking observed in the thickness direction of the GB filled adhesives. This phenomenon is found to occur at saturation only in the case of higher volume of GB filler content. The reason of such micro cracking is the results of poor particle/matrix interface and the presence of filler agglomerates in small regions favors this phenomenon.

#### 5.4.2 TMA results

The present TMA technique was used very efficiently with pure aluminum and metal matrix composites [25]. TMA is intended to be used with polymeric materials, however so far the best results were obtained with metals and metal matrix composite [26]. Investigations using epoxy adhesive formulation with the TMA instrument showed discrepancies in the real behavior of the dimension change vs. temperature as shown in figure 5.6. The use of 2.6 mm probe diameter shows a pronounced penetration near the glass transition temperature  $T_g$ . Therefore, it is decided to use a 6.4 mm probe diameter for the rest of experiments. Curves a and b in figure 5.6 illustrate the dimensional change of bulk adhesives before and after conditioning. It is clearly seen that the behavior of the dimensional change of the unconditioned sample shows penetration near  $T_g$  and this behavior is avoided using the recommended conditioning proposed by Enis et al.[21]. More details about these procedural variables can be found in the previous work of Ennis and Prime [21,27]. Curve c in figure 5.6 shows the dimensional change vs temperature for the TMA bonded joint specimen. In this case no penetration is observed near  $T_g$  and the application of the recommended correction [21] is not necessary. Figures 5.7 and 5.8 compare the  $T_g$  obtained on bulk adhesive and bonded joint for ACP and GB filled adhesives. In fact, the same trend is observed for bulk adhesive and bonded joint present an evidence of the reliability of using small scale bonded joints. The obtained glass transition temperatures,  $T_g$ 's, are in agreement with those obtained in the previous work with DMA [24]. It is also shown from figures 5.7 and 5.8 that  $T_g$  of bonded joints is slightly higher than that of bulk specimens. This is probably related to the fact that the adhesive in film form (joint) achieves a higher degree of



cure than in the bulk form.

Figures 5.9 and 5.10 show the glassy CTE, i.e., below the glass transition temperature, for both ACP and GB filled adhesives as function of filler content. As expected, the CTE of both filled epoxy adhesives decreases as the filler content increases. Many of the expressions which have been proposed to take into account the mechanical interaction between phases are discussed in the literature [28-29]. As a matter of fact, these micro mechanical models can be used to predict the contribution of a filler to the CTE of filled adhesives. However, these models require the knowledge of the mechanical properties of the fillers as well as their physical properties, their size and distribution and all these parameters are not available for the commercial fillers used. Some of the needed properties are taken from the literature [30]. The comparison between the theoretical predictions of some of these models is illustrated in both figures 5.9 and 5.10. It can be seen that below the glass transition temperature, a good agreement of the glassy CTE is found to be satisfactory between the experimental results and the well known Kerner model. This agreement is not surprising between both results, since the Kerner equation was developed for systems with spherical particle symmetry and continuous stress transfer at the phase boundaries.

**Kerner model:**

$$\alpha_c = V_m \alpha_m + V_f \alpha_f + \left( \frac{4G_m}{K_c} \right) \left[ \frac{(K_c - K_f) (\alpha_m - \alpha_f) V_f}{4G_m + 3K_f} \right] \quad (5.4)$$

where

$$K = \frac{E}{3(1 - 2\nu)}$$

$$G = \frac{E}{2(1 + \nu)}$$

**Tummala and Friedberg model:**

$$\alpha_c = \alpha_m - V_f (\alpha_m - \alpha_f) \theta \quad (5.5)$$

where

$$\theta = \frac{(1 + \nu_m)/2E_m}{(1 + \nu_m)/2E_m + (1 - 2\nu_f)/E_f}$$

**Wang and Kwei model:**

$$\alpha_c = \alpha_m - V_f \theta (\alpha_m - \alpha_f) \quad (5.6)$$

where

$$\theta = \frac{(3E_f/E_m)V_f}{(E_f/E_m)(2V_f(1 - 2\nu_m) + (1 + \nu_m)) + 2V_m(1 - 2\nu_f)}$$

where  $\alpha$  is the coefficient of thermal expansion, E is the modulus, V is the volume fraction,  $\nu$  is the Poisson ratio, and the subscripts c, m, f represent the filled adhesive, the matrix and the filler particles respectively. It should be mentioned that other models (Blackburn and Turner models) were also applied. However, these models are not applicable to the studied systems, since they showed discrepancies between the experimental results and the predictions.

Figures 5.11 and 5.12 show the effect of filler type and content on the CTE in the rubbery state. None of the preceding theoretical model has been found to fit with these results.

On the other hand, upon exposure to hot water, bulk adhesives of both ACP and GB filled systems gave non exploitable results when tested with the TMA instrument, since the curves dimensional change vs. temperature showed irregular bumps along the temperature increase.

### **5.4.3 Bonded joint**

In order to measure the CTE of bonded joints, small scale bonded joints are tested with TMA instrument. At least five samples are tested for repeatability for each formulation. Figures 5.13 and 5.14 illustrate the CTE of the bonded joints before ageing. Since the CTE of the bonded joint below and above the glass transition temperature depends mainly on the thickness of the adhesive, the present study have taken into consideration the bondline thickness variation. It can be seen from both figures that the CTE of bonded joints decreases as the filler content increases. As expected, it increases as the bondline thickness of the adhesive is increased. The theoretical predictions based on the law of mixtures (equation 5.7) show a good agreement with the experimental results (figures 5.13.a and 5.14.a) for the glassy CTE.

$$\alpha_g^J = \alpha_g^{Al} \frac{t_{Al}}{t_T} + \alpha_g^{adh.} \frac{t_{adh.}}{t_T} \quad (5.7)$$

However, the predicted rubbery CTE values from equation 5.7 are lower than the measured results. In order to fit the experimental results, a modified law of mixture is proposed (equation 5.8) which takes into account the increase of the CTE for the rubbery state.

$$\alpha_L^J = \alpha_L^{Al} \frac{t_{Al}}{t_T} + k_f \alpha_L^{adh.} \frac{t_{adh.}}{t_T} \quad (5.8)$$

where  $\alpha_g^{Al} = \alpha_L^{Al}$  is the CTE of Aluminum and  $\alpha_g^{adh.}$  and  $\alpha_L^{adh.}$  are the CTE of the adhesive in the glassy and rubbery states respectively and  $t_{adh.}$   $t_{Al.}$  are the thickness of adhesive and aluminum adherent respectively. A correction factor  $k_f$  is introduced into the law of mixture to fit best the measured CTE. Upon numerous calculation using curve fittings, the best value for the correction factor is found to be 2.7, which fit best both ACP and GB filled adhesives. The results are shown in both figures 5.13.b and 5.14.b.

Previous studies [31-32] attempted to relate the bonded joints strength to the damaged area after exposure to water. The estimation of the joints strength is based on the model of the rate of water diffusion into the laminated area of a joint. In the present study, the evaluation of the amount of the residual strength after exposure to hot water is made by testing five samples before and after ageing. The results of the relative residual strength after exposure is given by the following expression and are shown in figure 5.15.

$$\text{Strength retention} = \frac{\text{strength}_{\text{After ageing}}}{\text{strength}_{\text{Before ageing}}} \times 100$$

From figure 5.15, it can be seen that after 3 weeks in hot water:

- The unfilled system retain about 85% of its initial strength.
- Introduction of ACP fillers improves the strength retention to almost 100%.
- Introduction of GB fillers decreases the strength retention to about 65%.

In order to explain such behavior, the CTE of the small scale bonded joints are measured in the same conditions. The adhesive bondline thickness for both step lap and small scale bonded joints was  $0.2 \pm 0.05$  mm. Figure 5.16 illustrates the percentage increase of CTE compared to the original CTE, i.e., before ageing. It is shown that GB filled systems indicate a higher increase of CTE compared to ACP filled bonded joints.

Actually, a simultaneous analysis of figures 5.15 and 5.16 show clearly that the effect of the fillers on the strength retention after ageing is closely related to their effect on the CTE. Figure 5.17 combines the results of figures 5.15 and 5.16 in a plot of the residual strength retention versus the percentage increase of CTE. In the middle of figure 5.17, it can be seen that about 46% CTE increase of the unfilled adhesive results in nearly 85% strength retention. On the left side of the unfilled adhesive, the ACP filled adhesives which have less increase in their CTE show a better strength retention and the reverse is seen with GB filled adhesives. It is clearly shown from figure 5.17 that both properties are proportionally linked. It is obvious that the higher increase of CTE in these joints specially in the case of GB filled

bonded joints, produce higher stresses expressed by equation 5.9, which in turn generate lower residual strengths.

$$\sigma_x = \sigma_y = \int_{T_r}^{T_s} \frac{E(T) \alpha^j dT}{1-\nu(T)} \quad (5.9)$$

and  $\sigma_z = 0$ .

where  $\alpha^j$  is the CTE of the bonded joint in the glassy and/or rubbery state, E is the modulus,  $\nu$  is the Poisson ratio and T is the temperature.

## 5.5 Conclusion

Addition of a given type of filler to an adhesive is usually motivated by specific purposes. However, the overall physical and mechanical properties will be affected in a positive or negative manner. This investigation deals with the effect of moisture absorption in filled adhesives on the thermal expansion as well as on the strength of bonded joints. Study of the bulk adhesive properties for the same conditions is undertaken as a reference. It is shown that simplistic assumption based on the fact that, if filler is water resistant, the filled adhesive will be the same can be misleading. It is clearly shown that filled adhesives absorb more water than unfilled ones and the amount of absorbed water depend on the type and amount of filler used.

In the second part of this investigation, a qualitative relationship is drawn between

CTE and shear lap strength measurements of bonded joints. Higher values of the bonded joints CTE's in the case of glass beads filled adhesives resulted in low strength retention. The opposite is seen with alumina ceramic particulate filled adhesives. This concordance between the two measured properties is an indication of the reliability of the CTE measurement made on bonded joints.

### **5.6 Acknowledgments**

The authors wish to thank the Natural Sciences and Engineering Research Council of Canada (NSERC) and Fonds pour la Formation des Chercheurs et de l'Aide à la Recherche (FCAR).

## 5.7 References

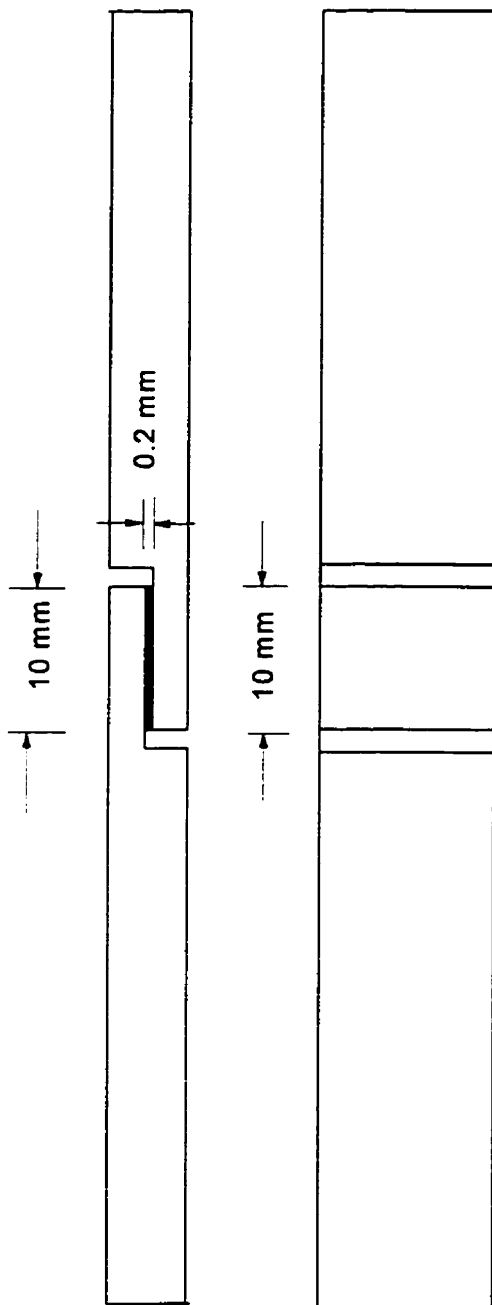
- 1 A. J. Kinloch, *J. Adhes.* V.10. 1979, p.193
- 2 D.M. Brewis, J.Comyn, and J.L. Tegg, *Int.J. Adhes. Adhes.*, v.1, 1980,p.35
- 3 J.D. Venables, *J. Mater. Sci.*, v.19,1984, p.2431
- 4 R.G. Schmidt and J.P. Bell, in *Adv. Polym. Sci.*, V.75, (K. Dusck Ed.) Springer Verlag, Berlin,1986, p.33
- 5 J. D. Minford, " Adhesive Bonding ", (L.H. Lee edition, Plenum Press, New York, 1991) p.239.
- 6 R. A. Gledhill and A.J. Kinloch, *J. Adhes.*, 6, 1974, p.315
- 7 J.D. Venables, D.K. McNamara, J. M. Chen, and T.S. Sun, *Appl. Surf. Sci.*, v.3, 1979, p.88
- 8 H. Leidheiser, Jr. and M.W. Kendig, *Ind. Eng. Chem. Prod. Res. Dev.*, V.17, 1978 p.42
- 9 J.W. Holubka, J.E. deVries and R.A. Dickie, *Ind. Eng. Chem. Prod. Res. Dev.*, V.23, N.1, 1984, p.63
- 10 A. Pattnaik and J.D. Meakin, *J. of Appl. Polym. Sci: Appl. Polym. Sympos.*, 1977, p.145
- 11 T. Smith, *J. Appl. Polym. Sci.: Appl. Polym. Sympos.*1977, p.11
- 12 B.B. Bowen, "Sympos. Adhes. Adhes. State Art", University of pittsburgh, May 1974
- 13 J.S. Noland *Adhesion Science and Technology*, Ed. L.H. Lee, Plenum Press, new York, 1975, p.413
- 14 A.W. Bethune, *SAMPE J.*, v.11,N.4,1978,p.4



- 15 Handbook of fillers and Reinforcements for Plastics, H.S. Katz and J.V. Milewski, Ed., Van Nostrand, 1978
- 16 N.Ho Sung, " Engineered Materials Handbook ", Vol.3 (ASM International, New York, 1990) p.622
- 17 G.F.C.M. Lijten, H.M.Van Noort and P.J.M. Beris, Journal of Electronics Manuf., V.5, N.4, 1995, p.253
- 18 J.C. Jagt, P.J.M. Beris and G.F.C.M. Lijten, IEEE Trans.Comp., Pack. Manuf. Tech.B18, N.2 1995, p.292
- 19 Z.Lai and J.Liu, IEEE Trans.Comp.Pack.Manuf. Techn.-part B, v.19, N.3, 1996, p.644
- 20 J.Liu, L. Ljungkrona and Z.Lai, IEEE Trans.Comp., Pack. Manuf. Tech. B18, N.2 1995, p.313
- 21 B.C. Ennis and J. G. Williams, Thermochemica Acta, V.21, 1977, p.355
- 22 C.H. Shen and G.S. Springer, J.compos. Mater. V.10, 1976, p.2
- 23 L. EL -Sa'ad, M.I. Darby and B. Yates, J. Mater. Sci., V.24, N.5, 1989, p.1653
- 24 M. Ouddane, R. Boukhili and R. Gauvin, submitted to J. Mater. Sci., (1997)
- 25 S. Elomari, R.Boukhili, D. J. Lloyd, Acta Materialia, v.44, N.5, 1996, p.1873
- 26 S. Elomari, R.Boukhili, D. J. Lloyd, C.S. Marchi and A. Mortensen, J. Mater. Sci, V.32, N.8,1997, p.2131
- 27 R.B. Prime, Thermal characterisation of polymeric materials, ed. E.A. Turi, Academic Press NY, 1985, p.435
- 28 L. Holiday and J. Roberson, J. Mater. Sci., V.8, 1973, p.301
- 29 R. S. Raghava,, Polym. Composites, V.9, N.1, 1988, p.1

- 30 J.F. Shackelford, W. Alexandre and J.S. Park, "CRC Materials Science and Engineering Handbook", (CRC Press Inc. 1994).
- 31 J.W. Williams and F.J. Boerio, 37th Annual Conf., Reinf. Plast./Compos. Inst., The Soc. Plast.Ind., Session 2-D, 1982, p.1
- 32 A. Kaul, N.H. Sung, I. Chin and C.S.P. Sung, Polym. Eng. Sci. V.24, N.7, 1984, p.493

## Step lap shear specimen



## TMA Specimen

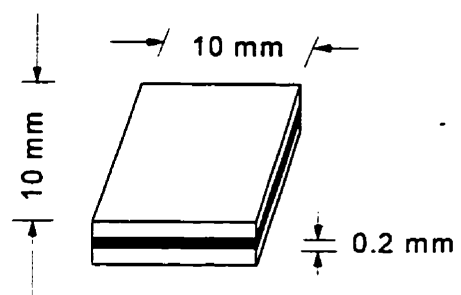


Figure 5.1 Step lap shear and TMA specimen geometries.

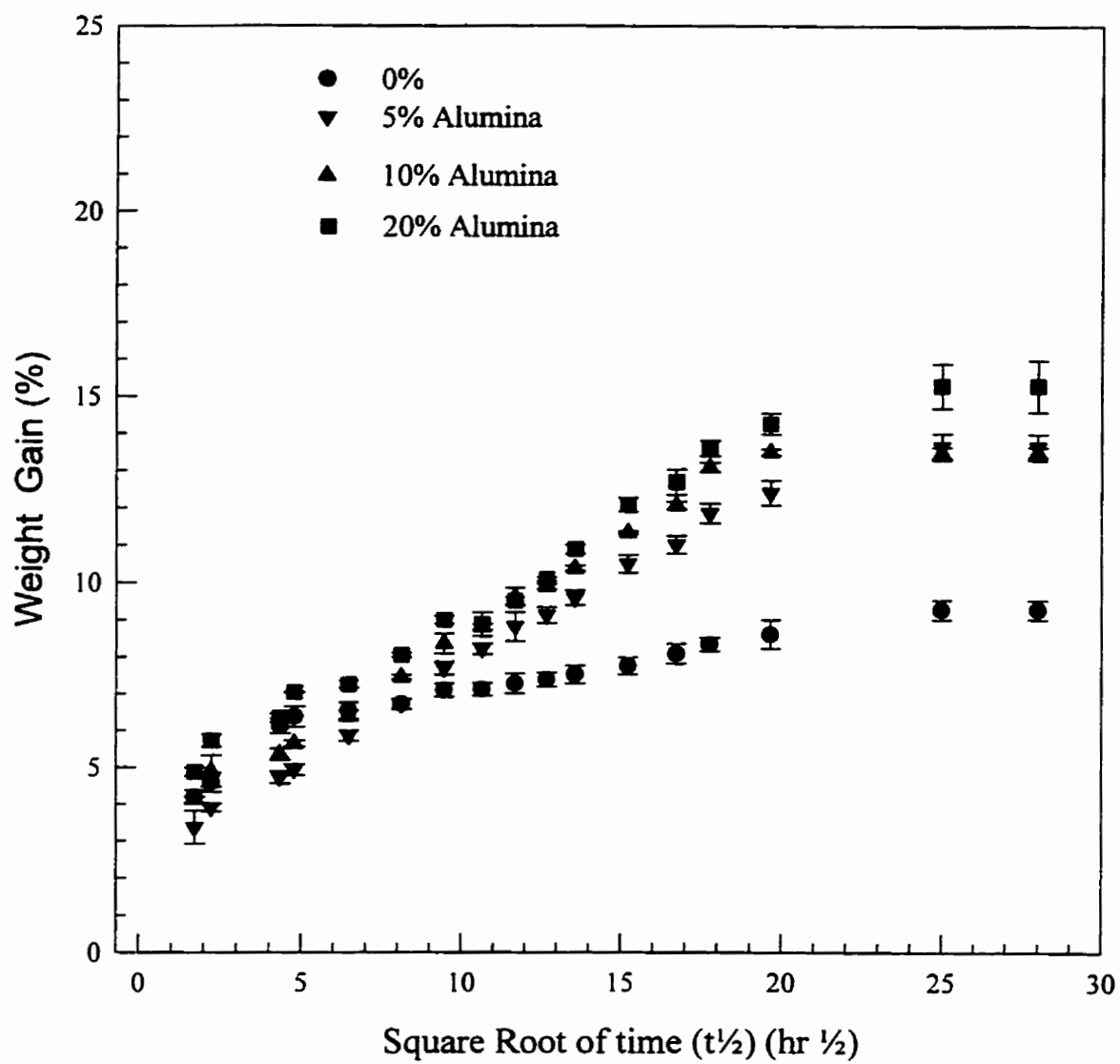


Figure 5.2 Percentage weight gain vs. square root of time for ACP filled bulk adhesives.

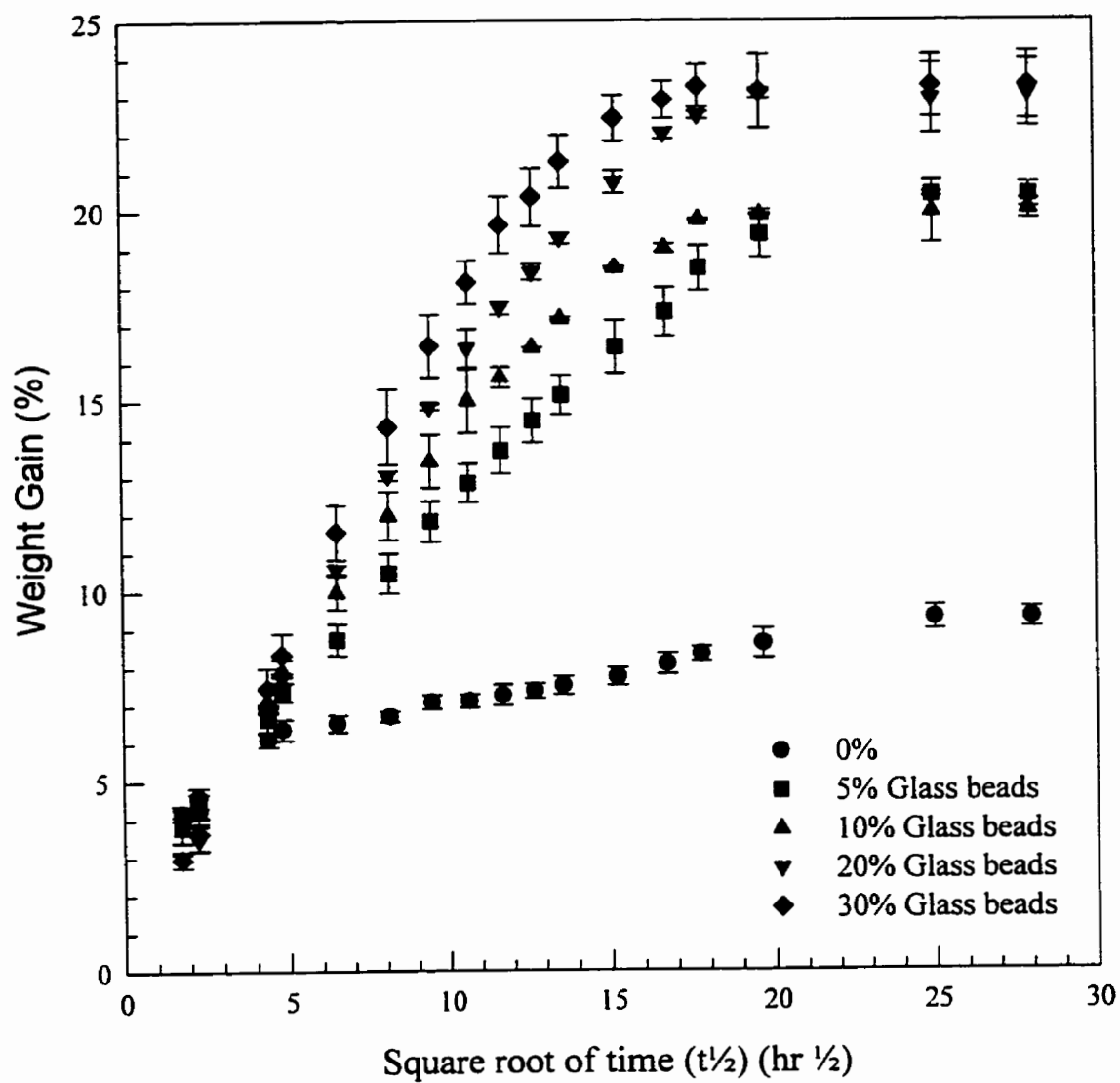


Figure 5.3 Percentage weight gain vs. square root of time for GB filled bulk adhesives.

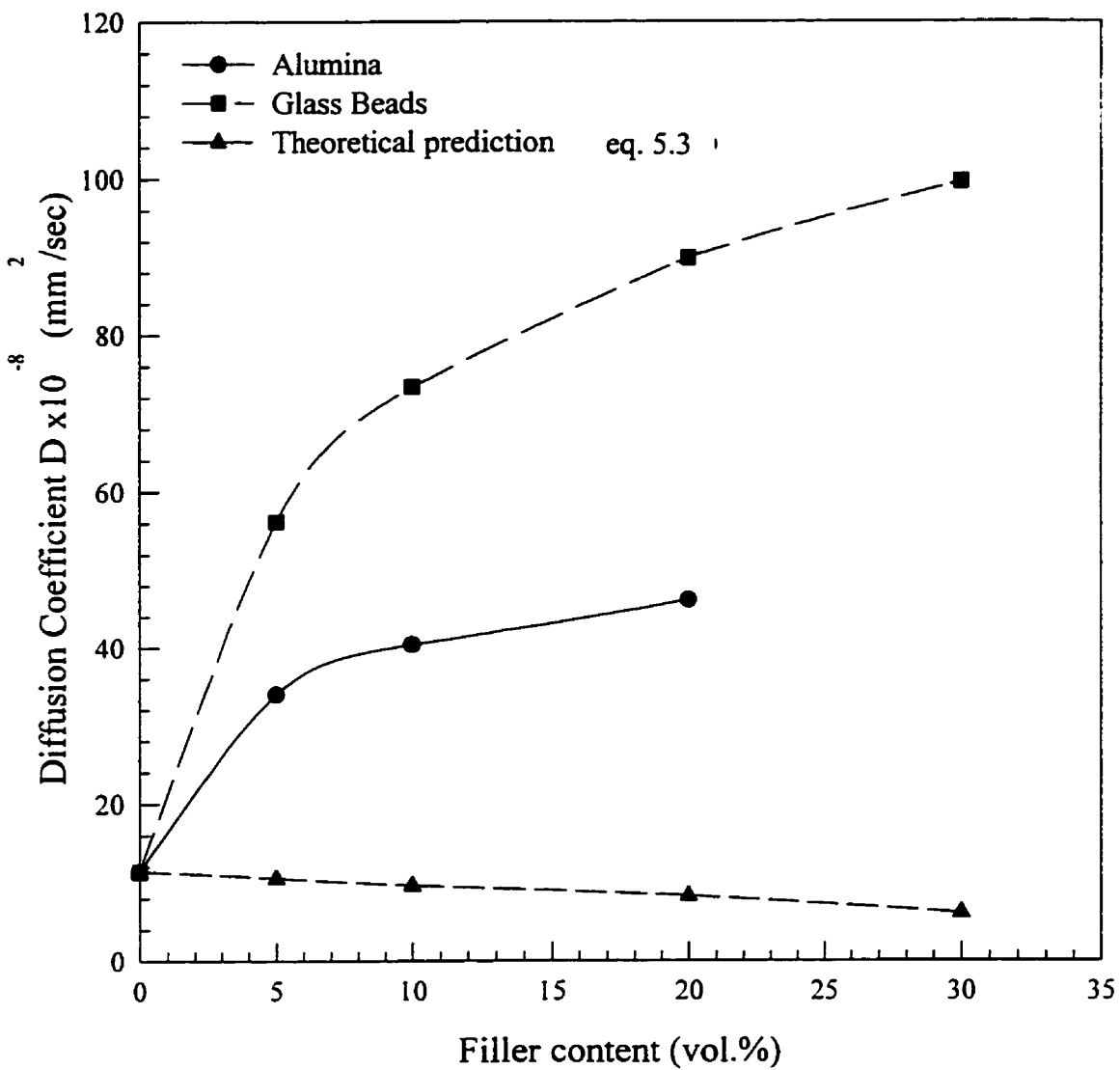


Figure 5.4 Apparent diffusion coefficient as a function of filler content for bulk adhesives.

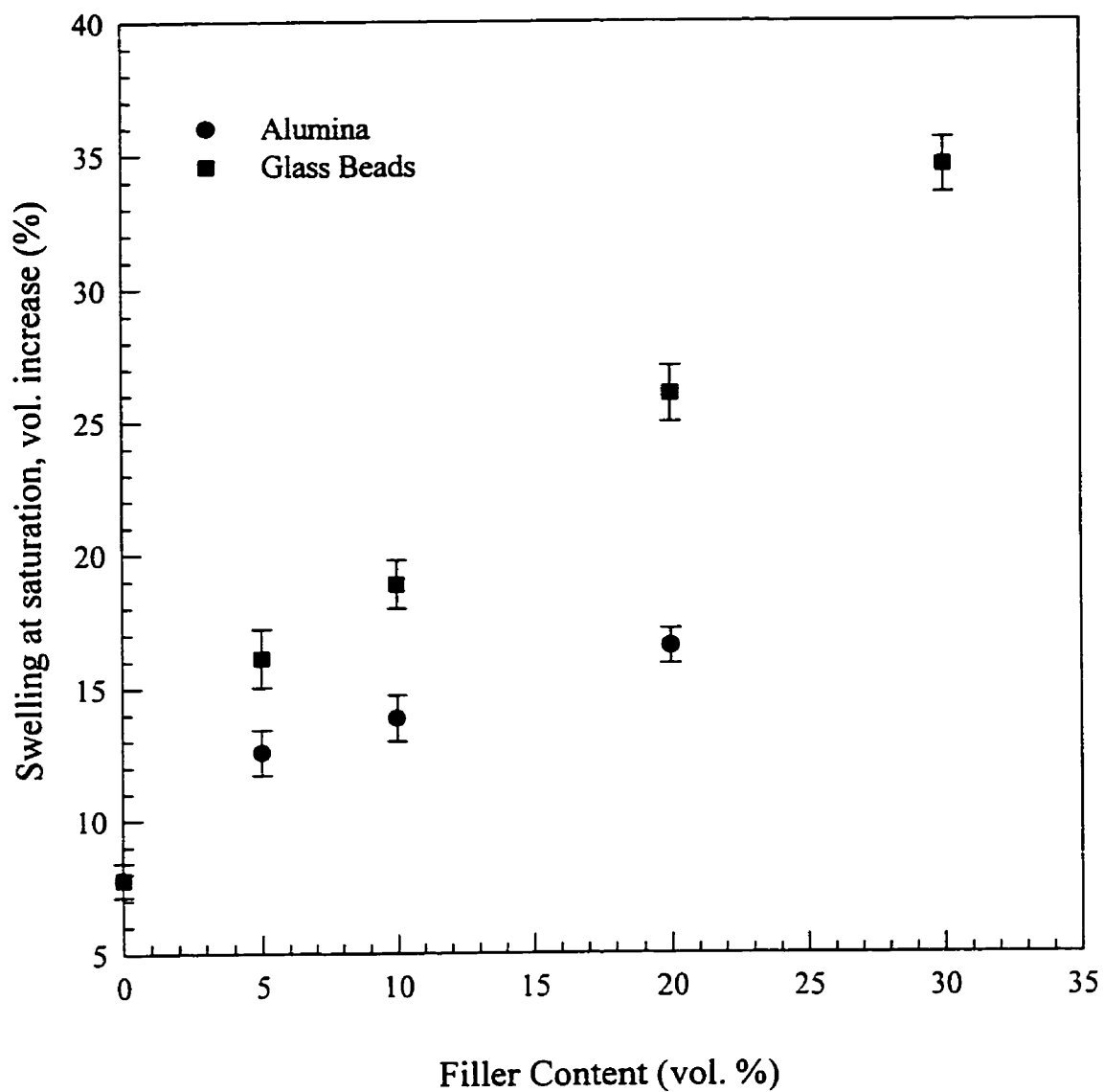


Figure 5.5 Volume increase of bulk adhesives as a function of filler content for bulk adhesives.

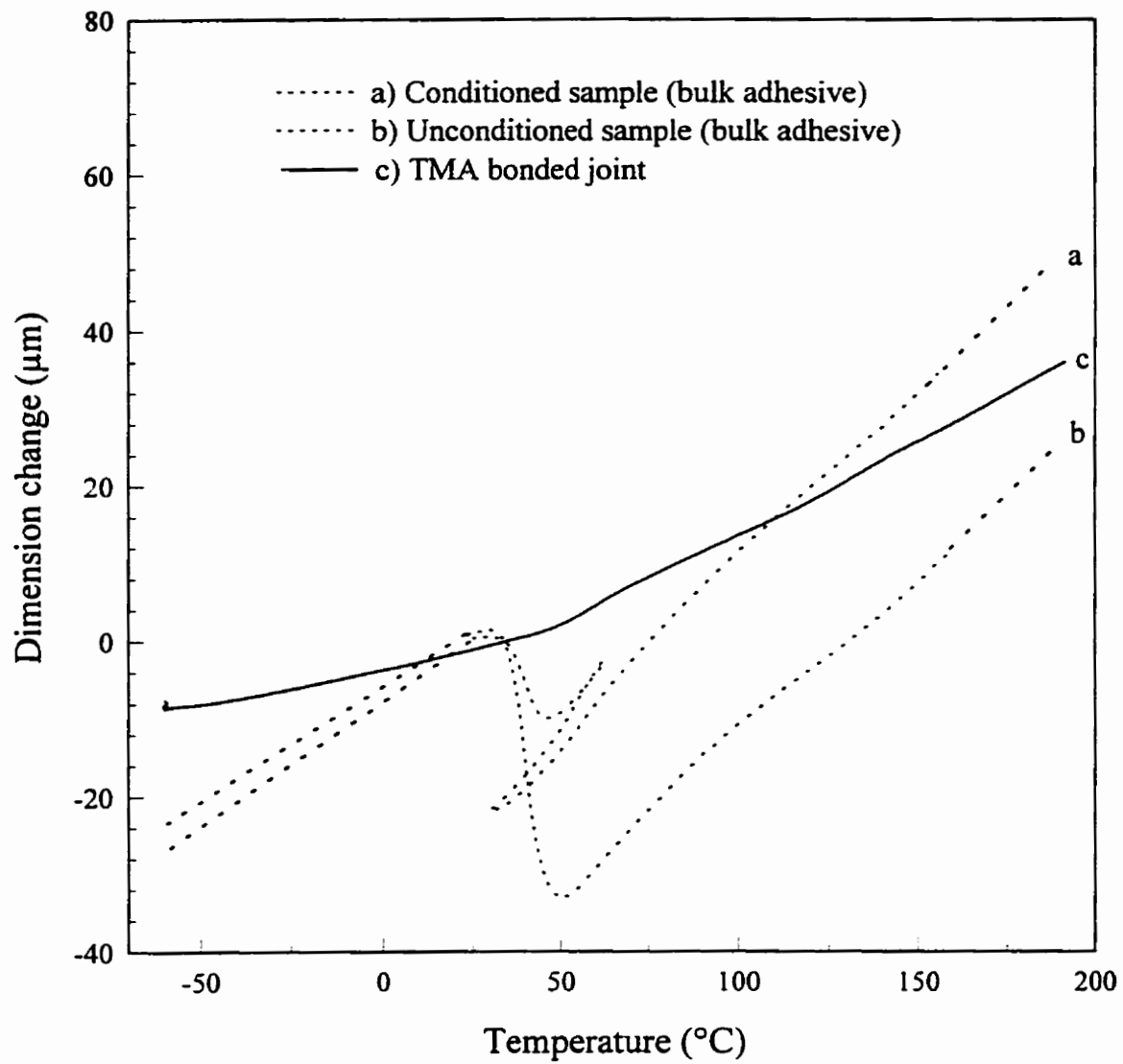


Figure 5.6 Dimension change as function of temperature



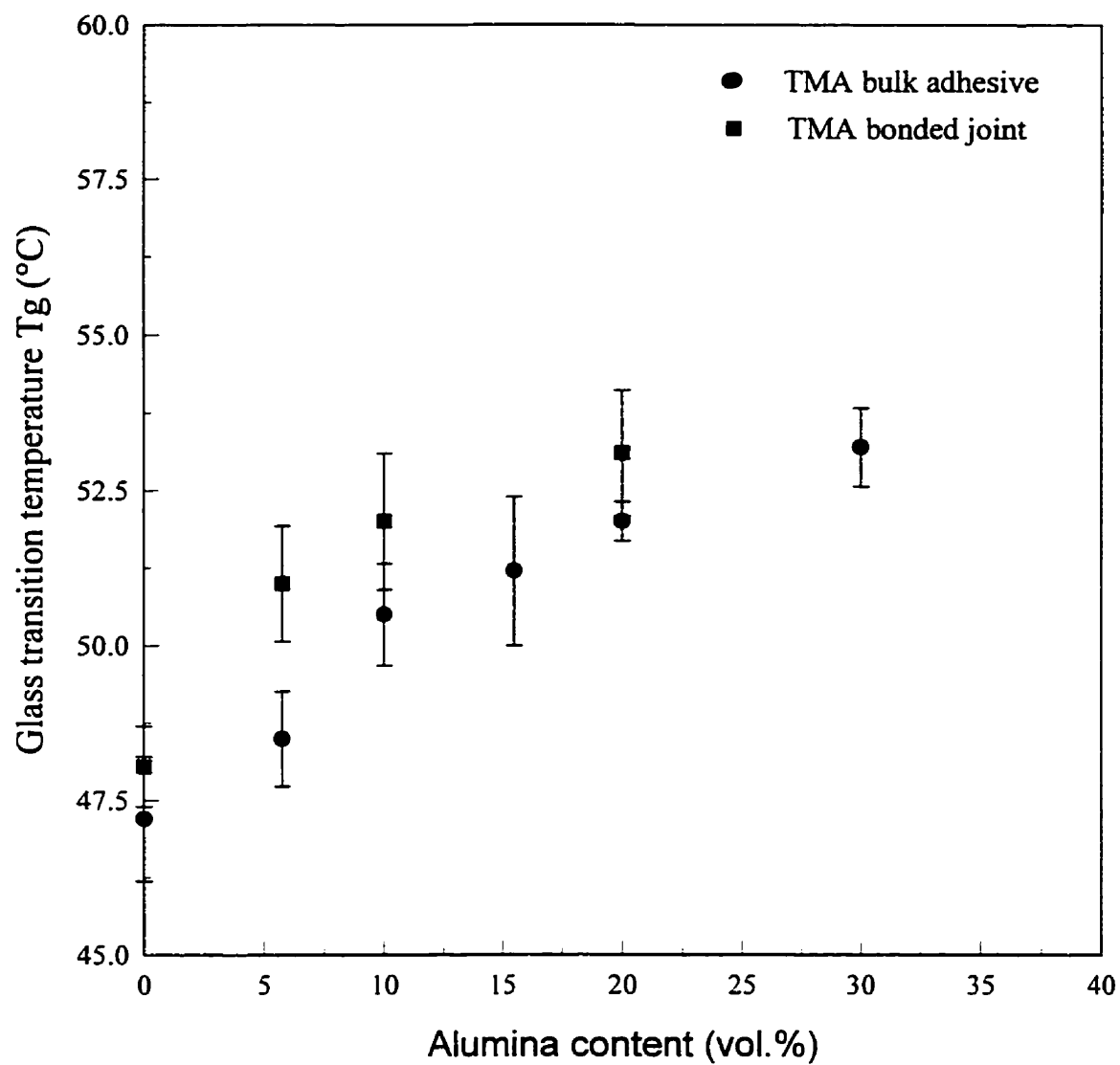


Figure 5.7 Glass transition temperature of filled adhesives as a function of alumina filler content.

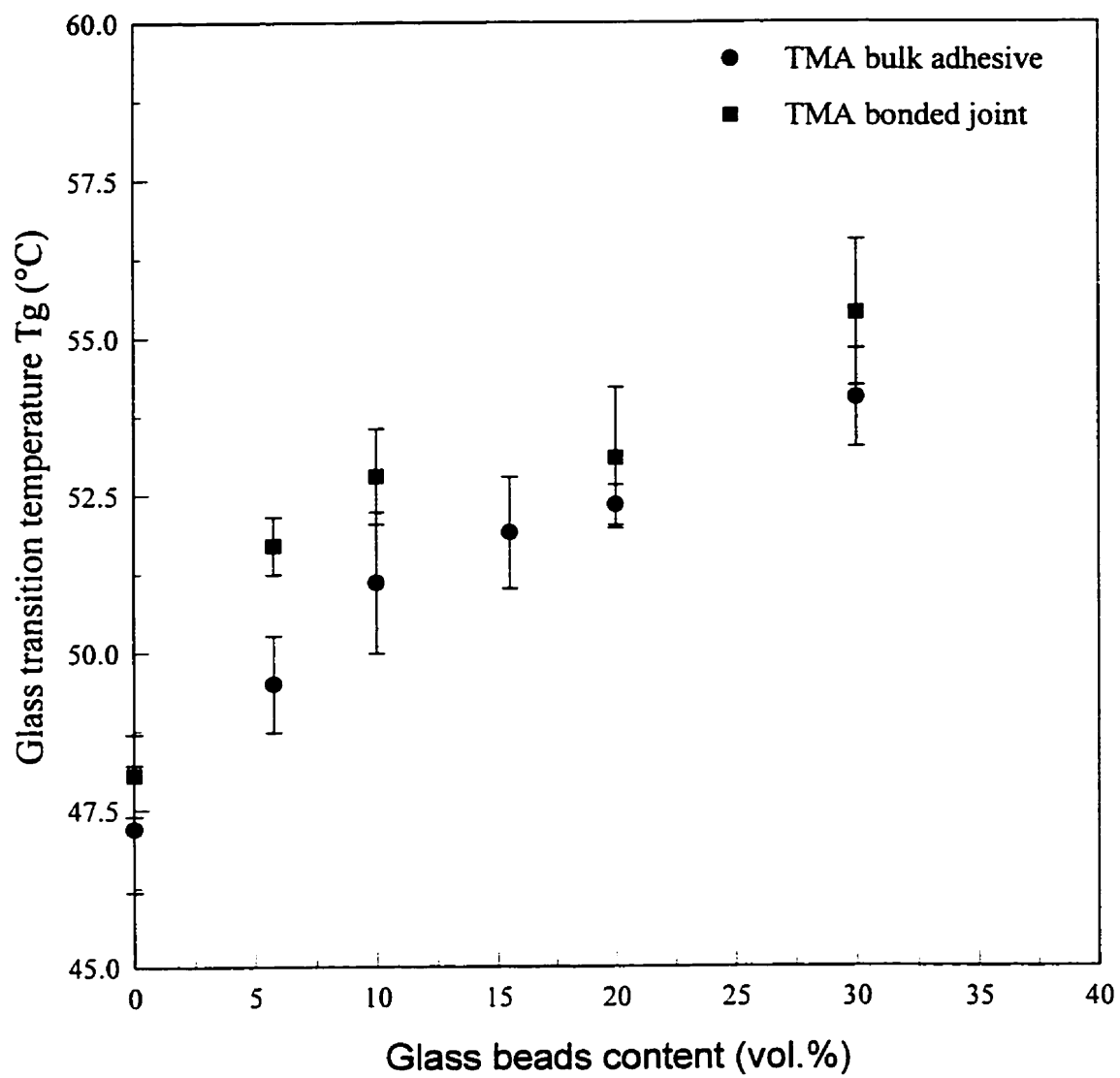


Figure 5.8 Glass transition temperature of filled adhesives as a function of glass beads filler content.

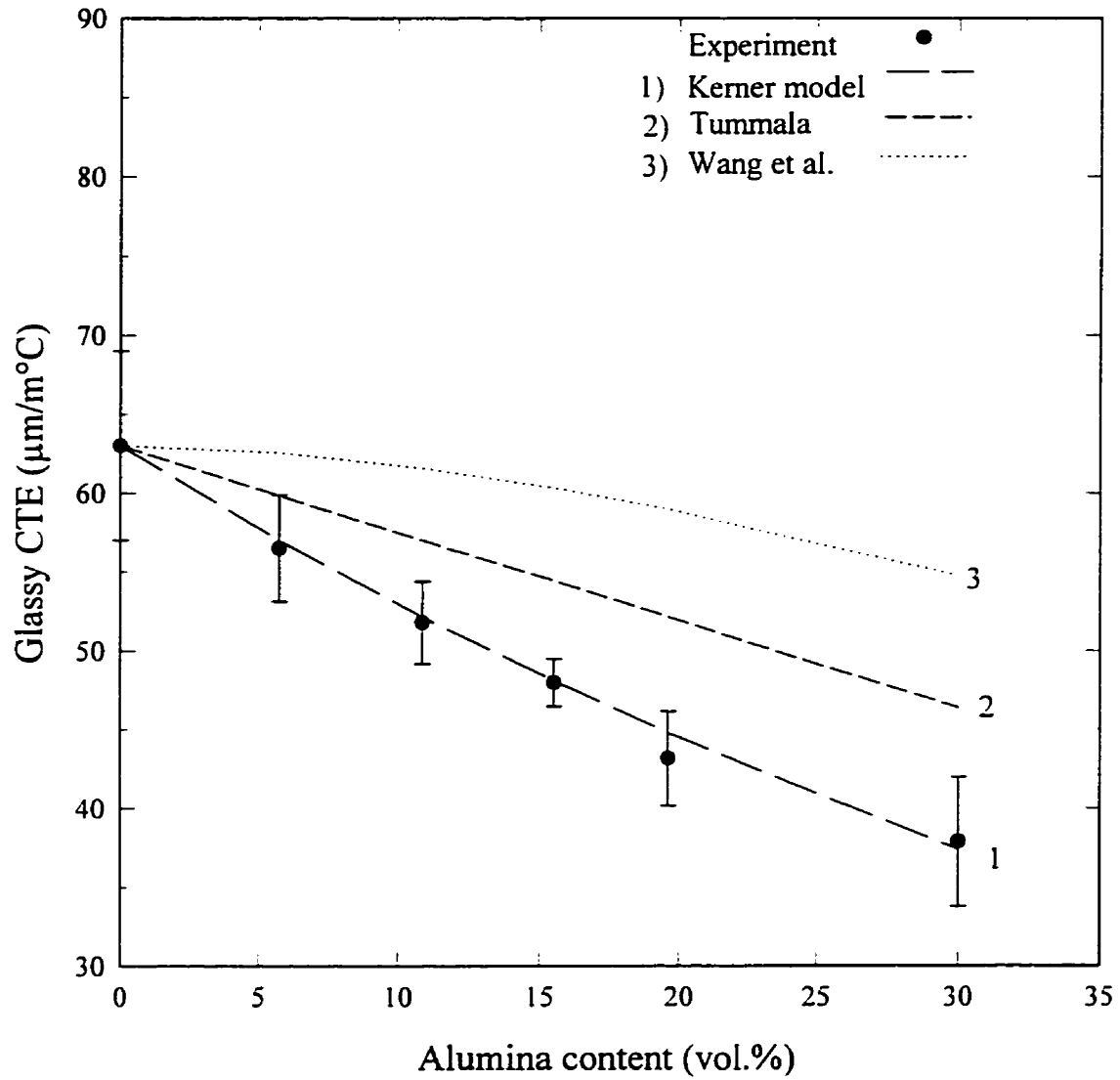


Figure 5.9 Glassy coefficient of thermal expansion (CTE) as a function of alumina filler content (Bulk adhesives).

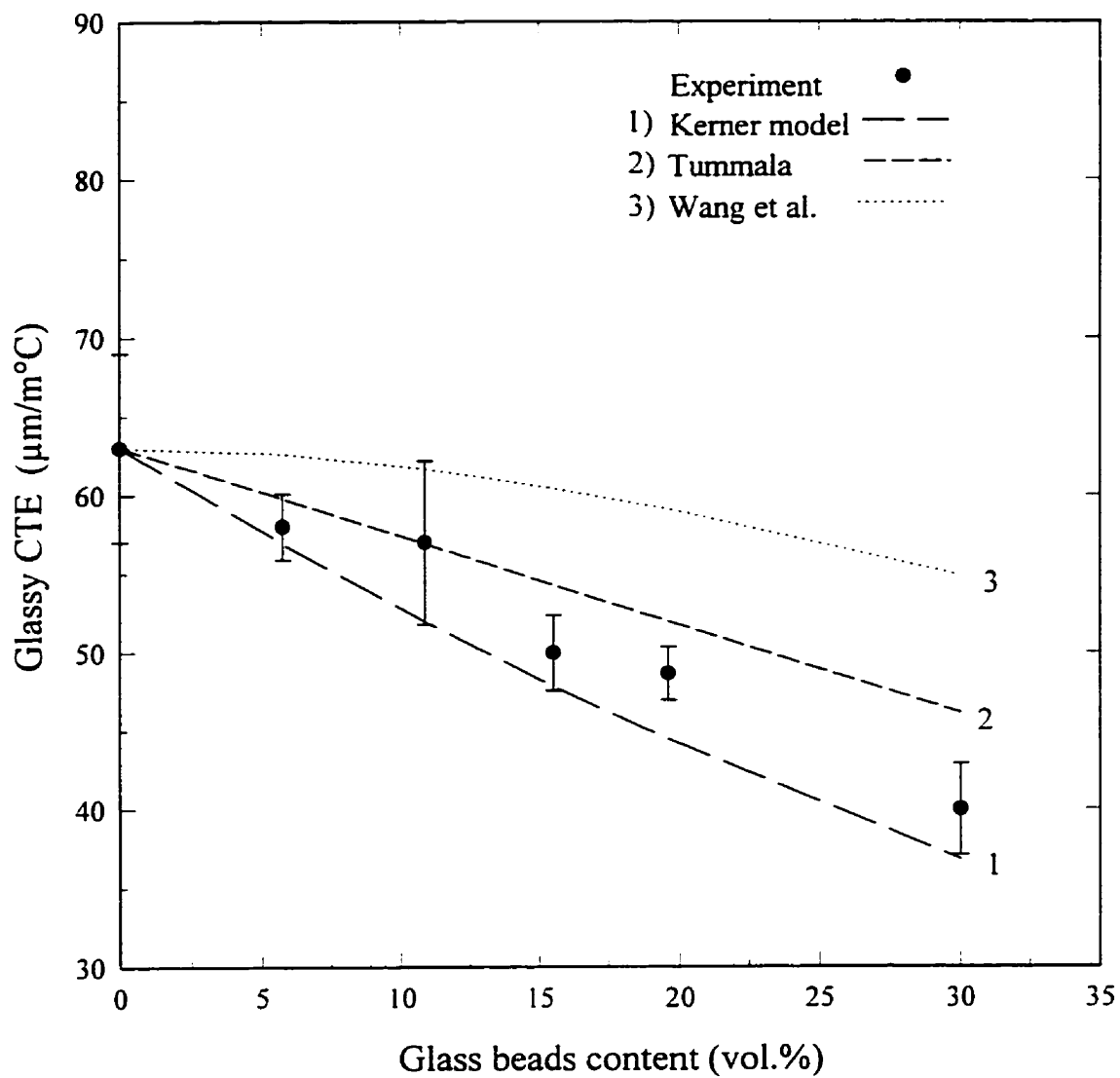


Figure 5.10 Glassy coefficient of thermal expansion (CTE) as a function of glass beads filler content (Bulk adhesives).

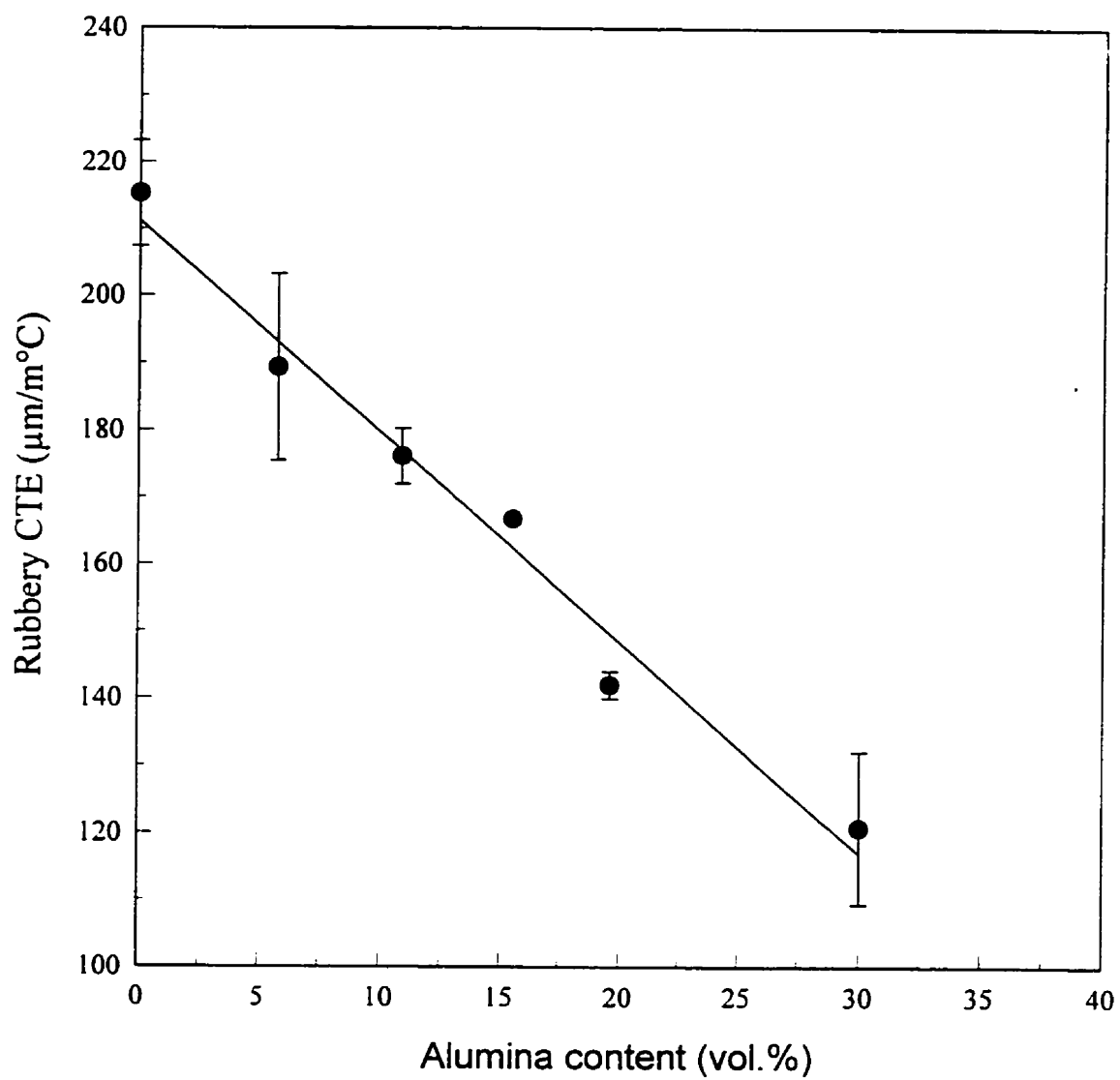


Figure 5.11 Rubbery coefficient of thermal expansion (CTE) as a function of alumina filler content (Bulk adhesives).

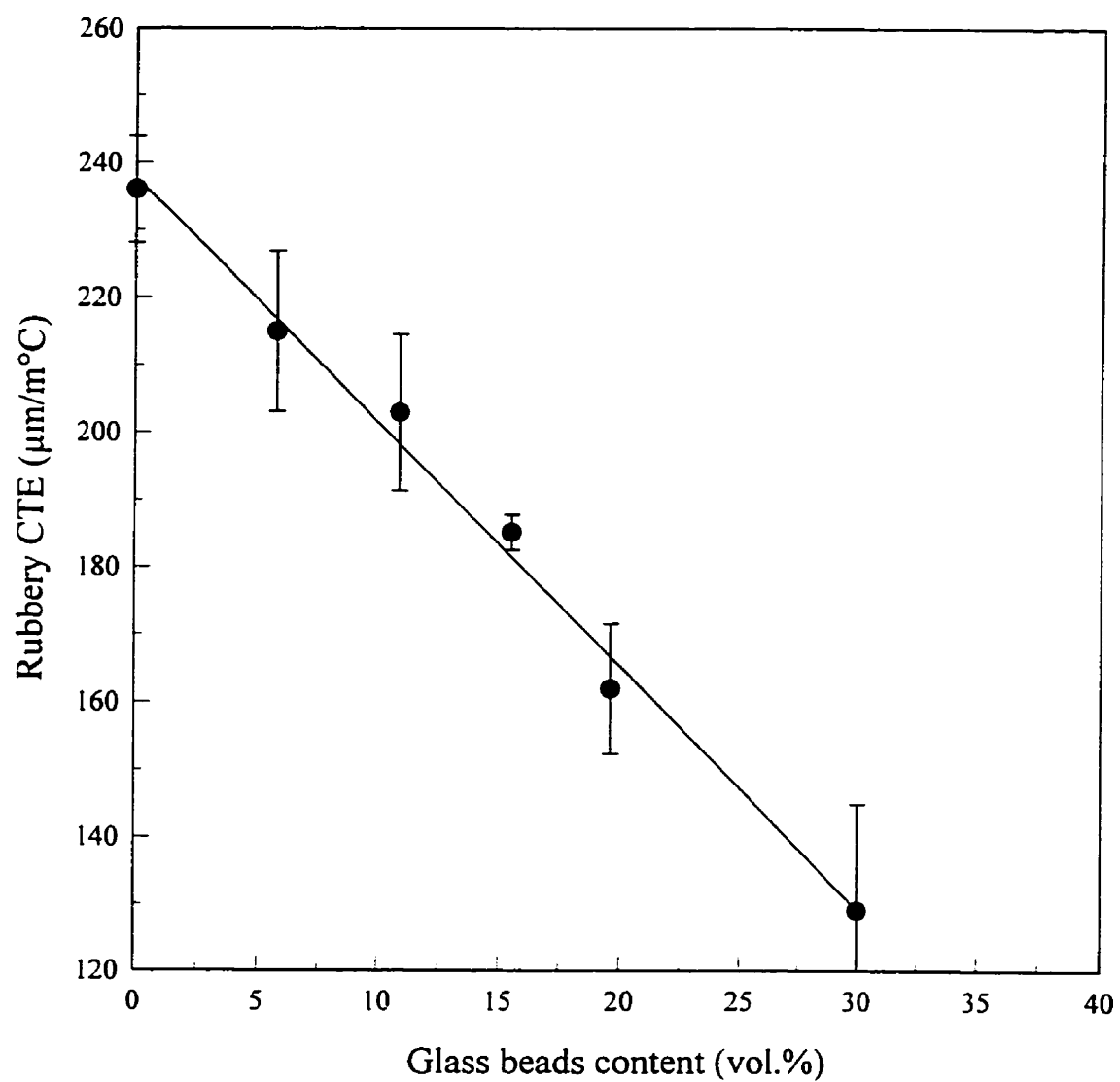


Figure 5.12 Rubbery coefficient of thermal expansion (CTE) as a function of glass beads filler content (Bulk adhesives).

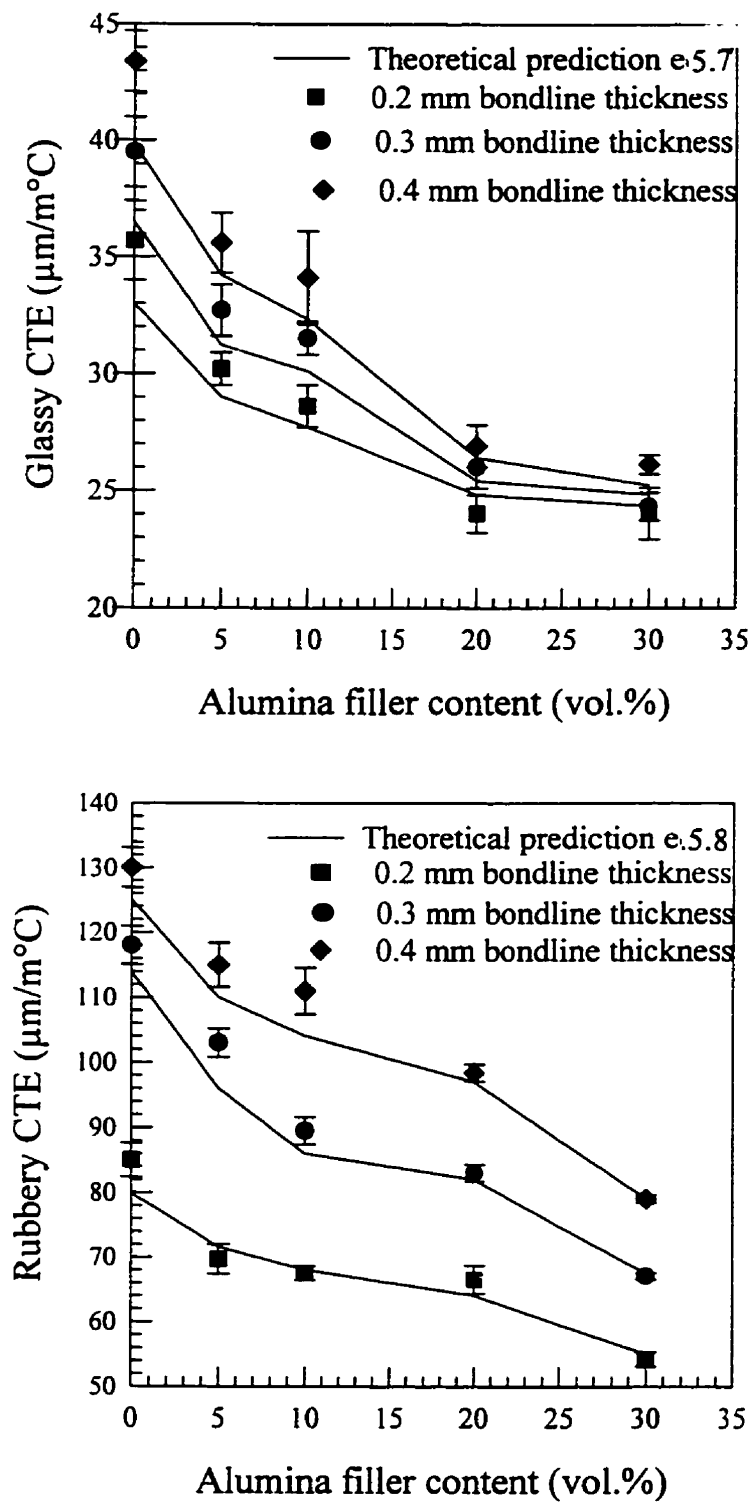


Figure 5.13 Coefficient of thermal expansion as a function of alumina filler content for various bondline thicknesses, a) Glassy CTE, b) Rubbery CTE, (Comparison between theoretical prediction and experiment).

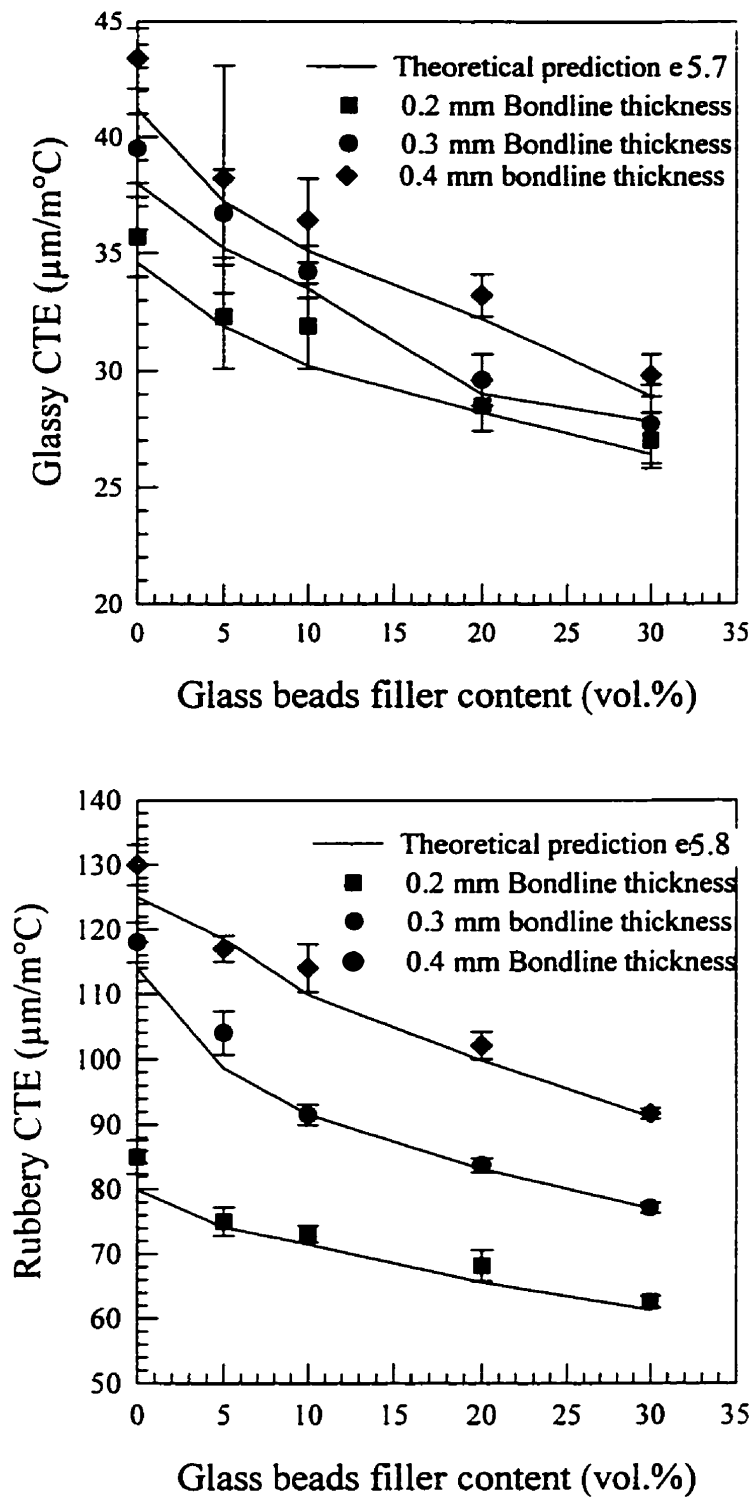


Figure 5.14 Coefficient of thermal expansion as a function of glass beads filler content for various bondline thicknesses, a) Glassy CTE, b) Rubbery CTE, (Comparison between theoretical prediction and experiment).



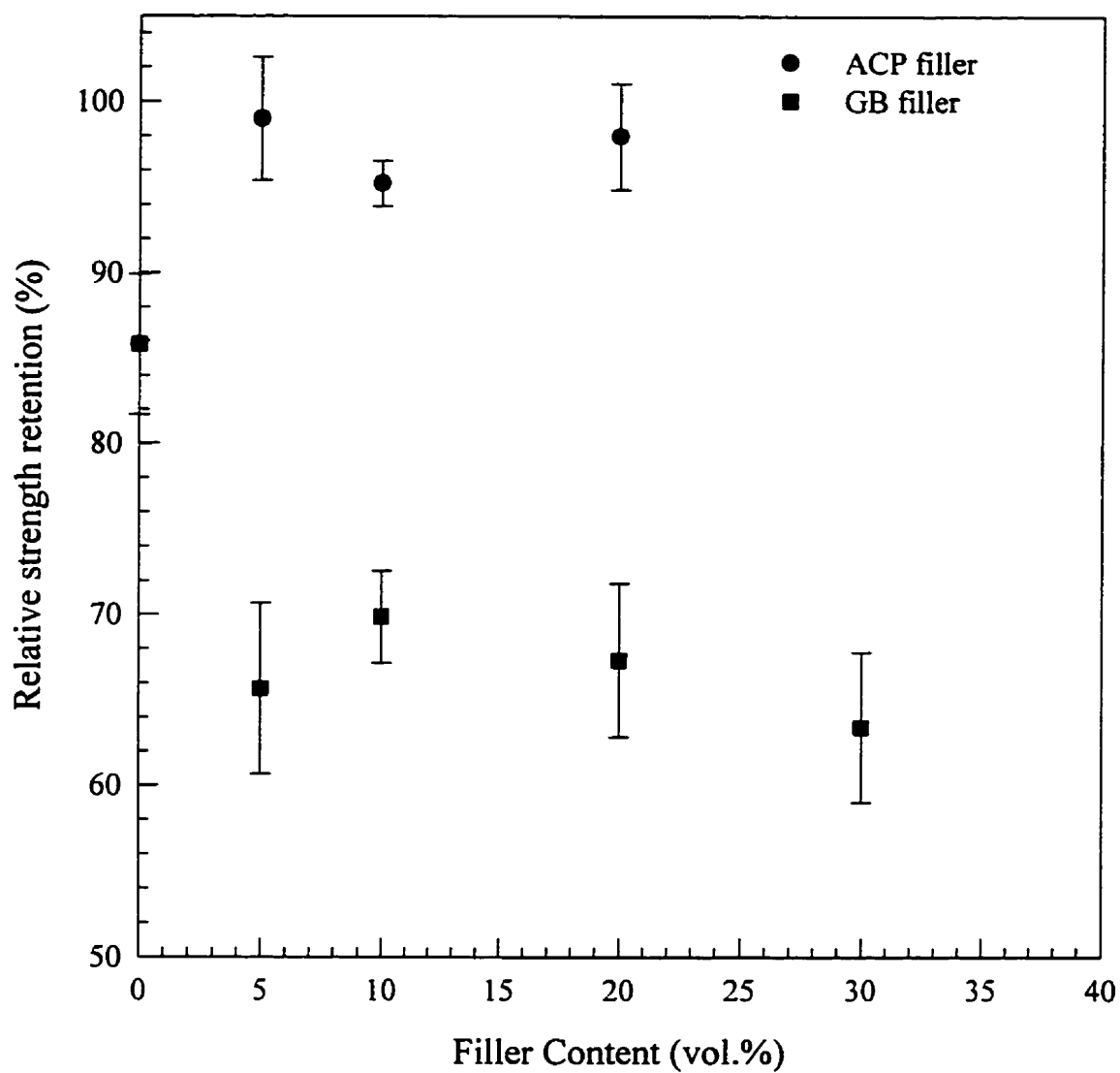


Figure 5.15 Relative strength retention as a function of filler content.

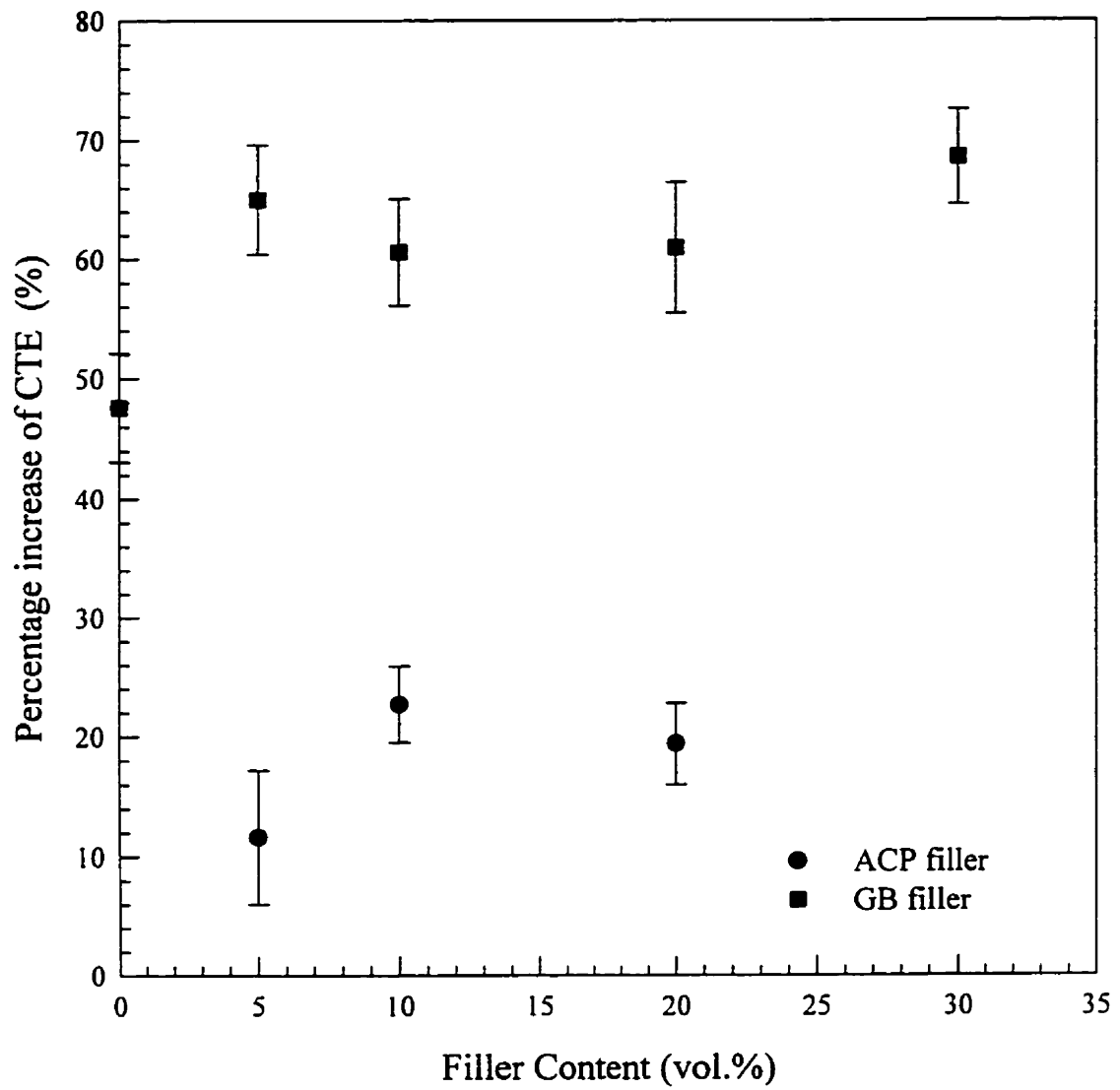


Figure 5.16 Percentage increase of CTE as a function of filler content.

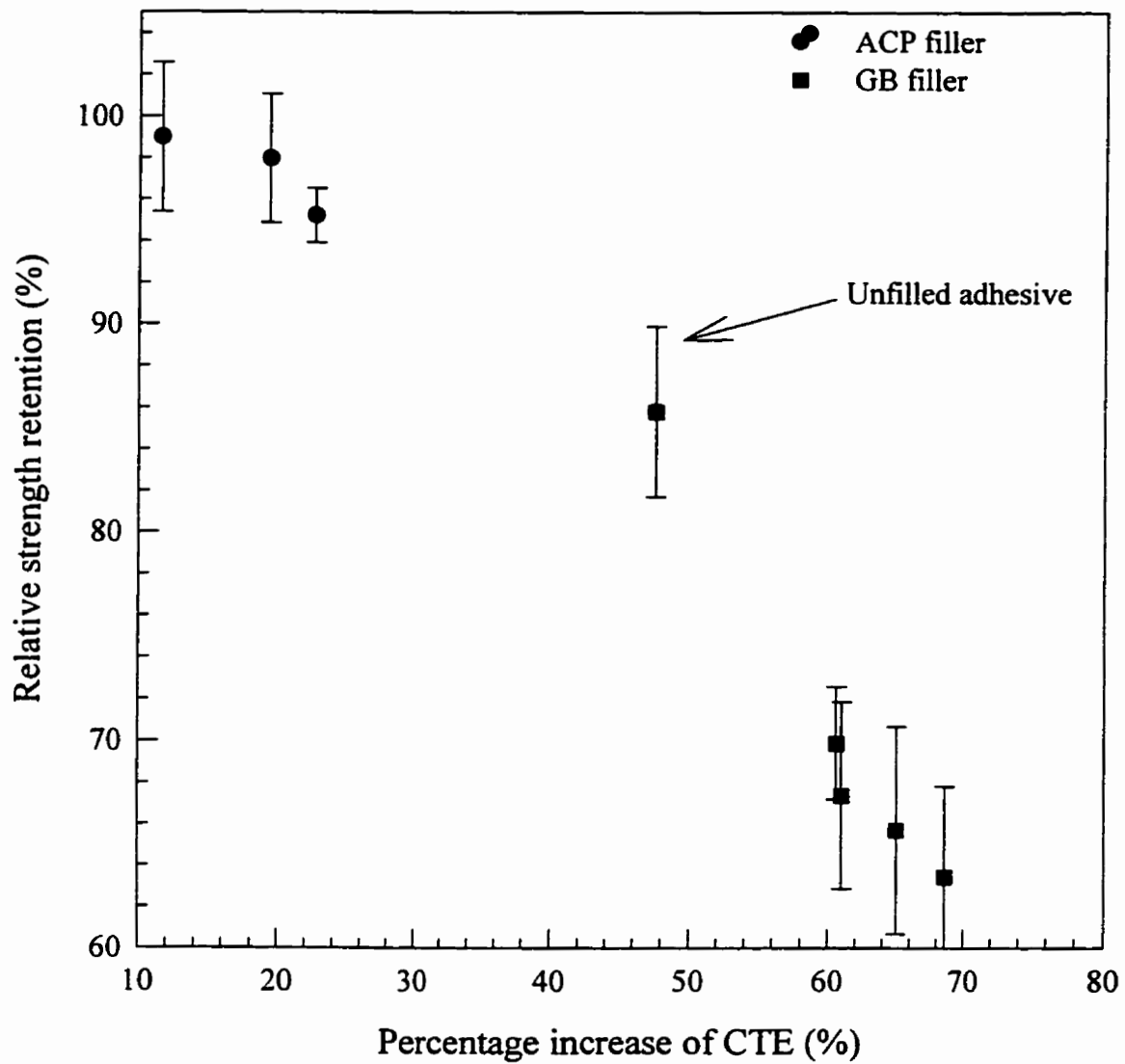


Figure 5.17 Relative strength retention vs. percentage increase of CTE.

## DISCUSSION GÉNÉRALE

Tel que souligné dans plusieurs ouvrages scientifiques, les propriétés des adhésifs font en sorte qu'il est fortement recommandé de solliciter un joint collé en cisaillement et d'éviter la traction. En conséquence, les essais de cisaillement revêtent une importance particulière. En pratique, deux importants critères sont requis dans l'évaluation des assemblages des structures par l'intermédiaire des colles: la fiabilité des résultats expérimentaux et la simplicité de la méthode d'essai. Cependant, ces critères semblent irréconciliables dans les joints collés. La résistance ultime en cisaillement des joints collés est généralement obtenue par le test standard de cisaillement à simple recouvrement. Toutefois, cette méthode d'essai est caractérisée par un cisaillement non uniforme et par la présence d'autres contraintes normales au plan de joint. D'autre part, la détermination de la résistance et de la rigidité en cisaillement des joints collés peuvent également être obtenues par l'essai de cisaillement en torsion. Principalement, l'essai consiste en l'application d'un couple de torsion sur un joint annulaire mince d'adhésif par l'intermédiaire d'une force agissant sur un bras de levier; la contrainte de cisaillement est alors uniforme puisque les effets de bord, associés aux joints à recouvrement, sont éliminés. Cependant, le montage expérimental de torsion n'est pas disponible pour tous les laboratoires, ce qui entrave l'utilisation usuelle de cette méthode d'essai.

La première étape de cette étude a été consacrée au développement d'un montage de torsion pour joints collés. Comme première phase, la validation de montage proposé a été effectuée. Les essais préliminaires sur des spécimens de validation ont permis de déceler

certaines erreurs de design. À la suite des rectifications apportées au montage proposé, il nous est apparu essentiel d'utiliser des jauges de déformation afin de détecter l'existence possible des contraintes parasites pouvant fausser la fiabilité des résultats. Effectivement, cette étape nous a permis de détecter des contraintes de flexion, dans les deux plans xy et xz, très faibles pouvant être omises. En fait, il serait préférable de comparer les résultats obtenus par le montage proposé à ceux d'un montage standard de torsion comme celui proposé par ASTM. Cependant, ce montage n'existant pas, la résistance mécanique des joints annulaires a été comparé à celle des joints à mi-épaisseur. Un comportement similaire a été trouvé entre les deux types d'essais et ce pour les différentes formulations étudiées. Toutefois, les résultats de cette comparaison semblent satisfaisants à en juger la fiabilité du montage proposé.

Quant aux formulations d'adhésifs élaborées, une étude concurrente sur les adhésifs et les joints collés a permis d'éclaircir certaines questions sur le comportement mécanique de ces derniers. L'utilisation de l'analyse mécanique dynamique a clairement établi l'effet du type et de la fraction volumique des charges sur les propriétés mécaniques des adhésifs chargés. Entre autre, la capacité d'amortissement  $\tan \delta$  s'est avérée utile pour la compréhension du phénomène d'adhésion des particules à la matrice époxyde. De basses valeurs de  $\tan \delta$  indiquent un arrangement microstructural à l'interface entre la charge et la matrice. Donc, selon cette explication, le système d'adhésif époxy/ACP possède une meilleure interface. La caractérisation des joints collés à base d'époxy/ACP a manifestement montré que ces derniers sont plus intéressants en terme de résistance mécanique. L'utilisation du concept rupture adhésive versus cohésive a encore démontré l'utilité de ce concept pour

expliquer le comportement des joints collés étudiés. Par contre, une question se pose sur les raisons possibles ou les considérations qui font de l'ACP contribue plus à une rupture cohésive que les billes de verre. Probablement l'affinité d'adhésion du type de la charge d'une part à la matrice et d'autre part à l'aluminium est une des possibilités. L'affinité d'adhésion dans ce cas veut dire les forces d'interaction qui se développent à l'interface entre l'adhésif et le substrat. Ceci est tout à fait en accord avec les travaux effectués sur les traitements de surface d'aluminium. Un traitement de surface avec une solution d'acide chromique favorise la formation d'oxyde d'alumine à la surface qui, à son tour, favorise une bonne adhésion avec le système d'adhésif époxy/ACP.

Définitivement, l'approche utilisée pour prédire la résistance mécanique de l'adhésif en utilisant les résultats des essais de torsion sur les joints collés où vice versa, c'est-à-dire obtenir la résistance mécanique de joint collé à partir des essais sur l'adhésif, s'est avérée valide seulement si la rupture dans le joint collé est cohésive. Toutefois, le module mesuré par les deux types d'expériences est du même ordre de grandeur. Par contre, la résistance mécanique du joint annulaire est beaucoup plus faible que celle obtenue par l'essai de torsion sur l'adhésif. Ceci est logique puisqu'un tel matériau contient des défauts de fabrication et l'approche utilisée est basée sur le fait que le matériau est parfait.

L'étude effectuée pour prédire la durabilité des adhésifs chargés sous un environnement agressif tel que la température humide (immersion à l'eau chaude) a encore montré que le type de la charge est un important facteur pour la réalisation de bonnes colles. L'utilisation de l'analyse thermomécanique dans ce cas a établi l'effet néfaste de la

température humide sur les adhésifs et les joints collés. Les résultats de cette étude ont révélé que les joints collés époxy/GB sont plus sensibles à l'eau que ceux d'époxy/ACP. Les mesures de CTE (coefficient d'expansion thermique) des joints miniatures exposés à une température humide sont plus ou moins liées à la résistance mécanique des joints collés. En résumé, les résultats d'une telle approche concordent bien avec la résistance mécanique relative des joints à mi-épaisseur et l'augmentation de CTE.

## CONCLUSION GÉNÉRALE

Le besoin de caractériser les joints collés pour fonctionner dans des conditions défavorables telles qu'un chargement externe ou un environnement agressif semble de plus en plus intéresser la communauté scientifique. De nombreuses méthodes d'essais ont été développées pour estimer les propriétés mécaniques et physiques des adhésifs et des joints collés. Cependant, il a été trouvé que ces méthodes en soi renferment des inconvénients et des difficultés pour atteindre ces deux principaux critères: facilité de l'essai expérimental et la fiabilité des résultats mécaniques. Présentement, le cisaillement des joints collés est obtenu sous un chargement en traction ou en compression d'un joint à simple recouvrement ou à mi-épaisseur. Quoique cette méthode d'essai est simple, les résultats obtenus ne sont pas fiables dus à la présence des contraintes d'arrachement et de pelage non uniformes sur les deux extrémités du joint. Le contraire est constaté pour l'essai de cisaillement en torsion, c'est-à-dire, la méthode est fiable mais la difficulté des essais expérimentaux entrave la popularité de cette méthode. En d'autres termes, le montage expérimental n'est pas disponible dans la plupart des laboratoires de caractérisation.

Dans la présente étude, un montage de torsion simple et adaptable aux machines d'essais conventionnelles et en même temps générant des résultats fiables a été proposé. Il est convaincant, d'après les essais de validation, que le montage proposé est acceptable pour la mesure des propriétés mécaniques en cisaillement des joints collés. Cependant, il reste que de petits inconvénients se sont manifestés pendant l'expérimentation dus au bloc d'alignement. Donc, il est fortement recommandé de concevoir et d'améliorer cette partie



du montage. Malgré ces petits inconvénients, il a été prouvé que la résistance mécanique des joints annulaires en torsion est plus représentative que celle obtenue avec l'essai standard de joint à mi-épaisseur. L'amélioration est certainement due au fait que le joint à mi-épaisseur induit des contraintes non uniformes qui affectent les résultats mécaniques.

L'ajout des particules de charges dans les adhésifs se fait pour de nombreuses raisons telles que la réduction de l'expansion thermique, l'amélioration de la résistance à la chaleur et la stabilité dimensionnelle et beaucoup d'autres avantages. Cependant, en se basant sur le fait que l'ajout de charges tend à réduire la résistance mécanique, il a été cru que le même comportement se produira avec les joints collés. Ce travail a manifestement établi que si les particules de charge sont incorporées dans des proportions adéquates, les propriétés mécaniques sont généralement améliorées. Définitivement, ces proportions de charge ajoutées dépendent du type de particules utilisées. Actuellement, il a été trouvé que le maximum de résistance mécanique est obtenu pour des volumes de 10% d'alumine et de l'ordre de 20% pour les billes de verre. En fait, cette tendance est confirmée par deux différents essais mécaniques, c'est-à-dire les joints à mi-épaisseur et les joints annulaires. De plus, il a été montré que la résistance mécanique en fonction du volume de la charge ajoutée est proportionnellement liée à la fraction surfacique de la rupture cohésive. Une tentative d'expliquer la raison de l'amélioration de la résistance mécanique avec l'ajout de charges est donnée en se basant sur le fait que les particules de charge occuperont l'espace autrement occupé par les bulles d'air. Ces bulles d'air sont toutefois inévitables à cause de la viscosité élevée des adhésifs élaborés.

Il a été confirmé dans la dernière partie de ce travail que la structure et le comportement des adhésifs à l'égard de la température humide (immersion à l'eau chaude) peuvent être d'une importance vitale pour en juger de la durabilité des joints collés. En effet, la combinaison adhésif/interface est la clé pour le succès des assemblages collés. Quant au choix des particules de charge, on a vu que les systèmes d'adhésifs époxy/alumine sont beaucoup plus intéressants et résistent mieux à l'attaque et la diffusion de l'eau que les systèmes époxy/billes de verre. L'analyse thermomécanique a encore une fois établi que les joints collés qui subissent une forte augmentation de coefficient d'expansion thermique (CTE) montrent une baisse prononcée de la résistance mécanique. L'approche utilisée a démontré que les joints collés à base d'époxy/ billes de verre subissent une dégradation et un endommagement plus marqué que ceux à base d'époxy/alumine.

**BIBLIOGRAPHIE**

**ADAMS R.D. and WILLIAM C.WAKE**, "Structural adhesive joint in engineering", Elsevier Applied Science Pub., London and NY, 1984, p.14

**ADAMS R.D.**, "Failure strength tests and their limitations", Adhesives and Sealants, Engineered Materials Handbook, ASM Int. V.3, 1990, p.325

**ADAMS R.D and HARRIS J.A.**, " The influence of local geometry on the strength of adhesive joints " Int. J. Adhes. Adhes., V. 7, N.2, 1987, p.69

**ADAMS R.D. and COPPENDALE J.**, " Stress Analysis of adhesive bonded tubular lap joints", J. Adhes., V.9, 1977, p.11

**ADAMS R.D., COPPENDALE J. and PEPPIATT N.A.**, "Joints loaded in torsion and tension", J. Strain Analy., V.13, N.1, 1978, p.1

**ADAMS R.D. , COPPENDALE J., MALLICK V. and AL-HAMDAN H.**, " The effect of temperature on the strength of adhesive joints ", Int. J. Adhes. Adhes., V.12, N.3, 1992, p.185

**ADAMS R.D. and MALLICK V.**, " The effect of temperature on the strength of adhesively bonded composite aluminium joints ", J. Adhes. , V.43, 1993, p.17

**ADAMS R.D. and MALLICK V.**, "A method for stress analysis of lap joints", J. Adhes., V.38, 1992, p.199

**AHARONI S.M.**, " Critical exponent equations: Their relation with free volumes at  $T_g$  and  $T_R$  and with the macromolecular domain concept ", J. Macromol. Sci- Phys., V.B10, N4, 1974, p.663

**AHARONI S.M.**, " Thermal dilatation of polymer ", *J. Macromol. Sci. Phys.* V.B9, N4, 1974, p.699

**ALLMAN D.J.**, "A theory for the elastic stresses in adhesive bonded lap joints", *Quart. J. Mech. Appl. Math.*, V.XXX part 4, 1977, p.415

**ALWAR R.S. and NAGARAJA Y.S.**, " Viscoelastic analysis of an adhesive tubular joints", *J. Adhes.*, V.8, 1976, p.79

**ANDERSON G.P. and DEVRIES K.L.**, " Predicting strength of adhesive joints from test results", *Int. J. Fract.*, V.39, 1989, p.191

**ASTM Standard Test Method for Shear Strength and Modulus of Structural Adhesives**, E229-70.

**BJORKLETT A. and KRISTIANSEN H.**, "The effect of the volume fraction of silver on the thermal resistance of die attach adhesives ", *Hybrid Circuits*, V.33, 1994, p.28

**BOSSLER R.C., FRANZBLAU M. C. and RUTHERFORD J. L.**, "Torsion apparatus for measuring shear properties of adhesive bonded joints ", *J. Sci. Inst: J. Phys. E.* , V.21, 1968, p.829

**BRETT C.L.**, " The effect of state of cure and shelf life of epoxy resin system ", *J. Appl. Polym. Sci.*, V.20, 1976, p.1431

**BREWIS D. M. , COMYN J. and SHALASH R.J.A.**, "Effect of moisture and temperature on the properties of an epoxide-polyamide adhesive in relation to its performance in single lap joints", *Int. J. Adhes. Adhes.*, V.2, 1982, p.215

**BREWIS D. M. , COMYN J. and SHALASH R.J.A.**, " Polymer communications ", *Polym.*, V.24, 1983, p.67

**BREWIS D. M. , COMYN J. and TEGG J.L.**, " The durability of some epoxide adhesive-

bonded joints on exposure to moist warm air ", Int. J. Adhes. Adhes., V.1, 1980, p.35

**BURTON B.L.**, " Thermal expansion measurements as a means of screening cured epoxy resins for toughness", SAMPE J., V.24, 1988, p.27

**CHEN D. and SHENG S.**, " Stress distribution in plane scarf and butt joints ", Trans. ASME, J. Appl. Mech., V.57, 1990, p.78

**CHON C.T.**, " Analysis of tubular lap joints in torsion ", J. Compos. Mater., V.16, N.4, 1982, p.268

**CLARK M.T.**, "Definition and Nondestructive detection of critical adhesive bondline flaws", AFML-TR-78-108, U.S. air force materials Laboratory, 1978

**COMYN J.**, " Thermal effects on adhesive joints ", Adhesives and Sealants: Engineered Materials Handbook, ASM Int., V.3, 1990, p.616

**DELMAS Y.**, "Contribution à l'étude théorique et expérimentale du collage de tubes métalliques par l'intermédiaire de résines époxydiques", Thèse de doctorat Université de Reims, 1985.

**DELALE F., ERDOGAN F. and AYDINOGLU M.N.**, " Stresses in adhesively bonded joints-A closed form solution ", J. Compos. Mater., V.15, 1981, p.249

**DE NÈVE B. and SHANAHAN M.E.R.**, " Effect of humidity on an epoxy adhesive ", Int. J. Adhes. Adhesi., V.12, N.3, 1992, p.191

**DROSTE D.H. and DIBENEDETTO A.T.**, "Glass transition temperature of filled polymers and its effect on their physical properties ", J. Appl. Polym. Sci., V.13 1969, p.2149.

**ENNIS B.C. and WILLIAMS J.G.**, " Thermal analysis and dilatometry of cured epoxy

resins ", *Thermochemica Acta*, V.21, 1977, p.355

**EL -SA'AD L., DARBY M.I and YATES B.**, " Moisture absorption characteristics of rubber particulate filled epoxy adhesives ", *J. Mater. Sci.*, V.24, N.5, 1989, p.1653

**ELOMARI S., BOUKHILI R., SKIBO M.D. and MASOUNAVE J.**, "Dynamic mechanical analysis of prestrained  $Al_2O_3$  /Al metal matrix composite" *J. Mater. Sci.*, V.30, 1995 p.3037

**ELOMARI S., BOUKHILI R., and LLOYD D.J.**, "Thermal expansion studies of prestrained  $Al_2O_3$  /Al metal matrix composite" *Acta Metallurgica et Materialia*, V.44, N.5, 1996, p.1873

**ELOMARI S., BOUKHILI R., LLOYD D.J., SAINMACHI C.H. and MORTENSEN A.**, "Thermal expansion responses of pressure infiltrated Al/Sic composites", *J. Mater. Sci.*, V.32, N.8, 1997, p.2131

**ERDOGAN F. and RATWANI M.**, "Stress distribution in bonded joints ", *J. Compos. Mater.*, V.5, 1971, p.378

**GIRAUD J.M.**, " Quelle epaisseur de colle choisir pour un assemblage collé ", *Matériaux et Techniques*, 1980, p.255

**GILIBERT Y. and RIGOLOTT A.**, " Assemblage par adhesion de deux tubes cylindriques sollicités en traction ", *Mech. Res. Comm.*, V.8, N.5, 1981, p.269

**GOLAND M. and REISSNER E.**, " the stresses in cemented joints ", *J. Appl. Mech.*, V.11, 1944, p.A17

**GRAVES S.R. and ADAMS D.F.**, "Analysis of a bonded joints in a composite materials", *J. Compos. Mater.*, V.15, N.3, 1981, p.211

**HAGEMAIER D.J.**, " End product nondestructive evaluation of adhesive bonded metal joints ", Adhesives and Sealants: Engineered Materials Handbook, ASM Int., V.3, 1990, p.743

**HAHN O. and YI X.S.**, " Influence of curing conditions on the mechanical behavior of adhesive joints ", Weld. World, V.25, N.7/8, 1987, p.152

**HALIOUI M. and LIEURADE J.P.**, " Les joints collés à simple recouvrement ", Matériaux et Techniques, 1991, p. 17

**HARISON N.L and HARISON W.J.**, " the stresses in adhesive layer ", J. Adhes., V.3, 1972, p. 195.

**HART-SMITH L. J. and THRALL E.W.**, Adhesive Bonding of Aluminium Alloys, ed. E. W. Thrall and R. W. Shanon, Marcel Dekker, 1985, p.241

**HART-SMITH L.J.**, " Adhesive bonded single lap joints ", Technical report, NASA CR1122 36, 1973.

**HART-SMITH L.J.**, " Further developments in the design and analysis of adhesive bonded structural joints ", Join. Compos. Mater., ASTM STP 749, ed. K. T. Kedward, Philadelphia, PA, 1981, p. 3

**HATTORI T.**, " A stress singularity parameter approach for evaluating the adhesive strength of single lap joints ", JSME Int., Series I:V. 34, N.3, 1991, p.326

**HARWELL**, " A computer program for the non-linear stress analysis of adhesively bonded single lap joints, report AEREG 411, 1986

**HIPOL P.J.**, " Analysis and optimization of a tubular lap joint subjected to torsion ", J. Compos. Mater., V. 18, N.4, 1984, p.298

**HOLIDAY L. and ROBERSON J.**, " Review: The thermal expansion of composites

based on polymers ", *J. Mater. Sci.*, V.8, 1973, p.301

**HU G.K., BAPTISTE D. and FRANCOIS D.**, " BG-P2 thermal residual stress evaluation in adhesive joints ", *Euromat Advanced Structural material*, V.II, combridge UK, 1991, p.493

**HUANG E.W.**, " Thermal stress in a single/metal bond with PR 1578 adhesive ", *SPIE, Advances in Optical Structure Systems*, V.1303, 1990, p.58

**HUGHES E.J., ALTHOF W. and KRIEGER R.B.**, *Adhesive Bonding of Aluminium Alloys*, ed. E. W. Thrall and R. W. Shanon, Marcel Dekker, 1985, p.141

**KASSAPOGLOU C. and ADELMANN J.C.**, " KGR-1 thick adherend specimen evaluation for the determination of adhesive mechanical properties ", *SAMPE Quart.*, V.24, N.1, 1992, p.19

**KAWADA H. and IKEGAMI K.**, " Viscoelastic properties of resin for IC plastic packages and residual stress ", *JSME int. Series 1: Solid Mech., Strength Mater.*, V.35, N.2, 1992, p152

**KEALBLE D.H. and CIRLIN E.H.**, " Chemo-rheology of curing in structural adhesives I: epoxy-phenolic systems ", *J. Polym. Sci., Part C 35*, 1971, p.79

**KEALBLE D.H. and CIRLIN E.H.**, " Chemo-rheology of curing in structural adhesives II: polyimide systems ", *J. Polym. Sci., Part C 35*, 1971, p.101

**KINLOCH A.J.**, " The science of adhesion ", Part 1 surface and inteface aspects, *J. Mater. Sci.*, V.15, 1980, p.2141

**KINLOCH A.J.**, " A fracture mechanics approach to the failure of structural joints ", *Development in Adhesive 2*, ed. A. J. Kinloch, 1981, p.83

**KINLOCH A.J.**, " The science of adhesion ", Part 1 surface and inteface aspects, *J. Mater.*



Sci., V.17, 1982, p.617

**KIRCHNER H.P., CONWAY J.C. JR and ESEGALL A.**, " Effect of joint thickness and residual stresses on the properties of ceramic adhesive joints: I, finite element analysis of stress in joints ", J. Amer. Ceram. Soc., V.70, N.2, 1987, p.104

**KOLLBRUNNER C.F. and BASLER K.**, "Torsion in structures, An engineering approach", Springer-Verlag New York, Heidelberg Berlin 1969, p.1

**KUENZI E.W. and STEVENS G.H.**, " Determination of mechanical properties of adhesives for use in the design of bonded joints ", US Forest products Service Research Note FLP-011, US Dept. of Agric., Madison Wisconsin, 1963

**IRVING B.**, " Applications widen for structural adhesive in metal-to-metal bonding ", Welding J., V.73, N.9, 1994, p.51

**LANDROCK E.H.**, " Introduction", Adhesive Technology Handbook, ed. A. H. Landrock, Park Ridge, New Jersey, Noyes Pub., 1985. p.1

**LANDROCK E.H.**, Adhesive Technology Handbook , ed. A.H. Landrock, Park Ridge, New Jersey, Noyes Pub., 1985, p.54

**LEE L.H.**, "Adhesive Bonding", ed. L. H. Lee, Plenum Press NY, 1991

**LEE C.J.**, " Effect of processing conditions on the UV curable, flip chip adhesives ", 6th Int. SAMPE Electronics Conference, 1992, p.500

**LIECHTI K.M.**, " fracture testing and failure analysis ", Engineered Materials Handbook, Adhesives and Sealants, ASM Int. V.3, 1990, p.335

**LUBKIN J.L. and REISSNER E.**, " Stress distribution and design data for adhesive lap joints between circular tubes ", Trans. ASME, 1956, p. 1213

**LUDBROOK B.D. and WHITWOOD R.J.**, " The use of thermal analysis to investigate

the cure of reactive adhesives ", Int. J. Adhes. Adhes., V.12, N.3, 1992, p.138

**MALLICK V.**, " Stress Analysis of Metal/CFRP Adhesive Joints Subjected to the Effects of Thermal Stress ", Ph.D Dissertation Univ. Bristol, UK, 1989

**MARCEAU A. and THRALL E.W.**, " Environment durability testing ", Adhesive Bonding of Aluminium Alloys, ed. E. W. Thrall and R. W. Shanon, Marcel Dekker 1985, p.177

**MARK H.F.**, " Future improvements in the cohesive and adhesive strength of polymers " Part 1, Adhesives Age, V.22, N.7, 1979, p.35

**MARK H.F.**, " Future improvements in the cohesive and adhesive strength of polymers " Part 2, Adhesives Age, V.22, N.9, 1979, p.45

**MAZENKO D.M., JENSEN G.A. and MCCORMICK P.J.**, " Joint technology for graphite epoxy space structures ", SAMPE J., V.23, N.3, 1987, p.28

**MANSON J.A. and SPERLING L.H.**, " Polymer Blends and Composites ", (Plenium Press New York, 1976) p.373.

**MATSUI K.**, " size effects on nominal ultimate shear stresses of adhesive bonded circular or rectangular joints under torsion ", Int. J. Adhes. Adhes., V.11, N.2, 1991, p.11

**MORAYAMA T.**, " Dynamic Mechanical Analysis of Polymeric Materials ", 2 (Elsevier Science Publishers, New York, 1978) p.130.

**MORI K. and SUGIBAYASHI T.**, " Effect of number of steps on stress distribution and final fracture strength of stepped lap bonded joint ", Nippon Kikkai Gakkai Ronbunshi, PartA V. 55, N.519, 1989, p.2211

**MORI K. and SUGIBAYASHI T.**, " Prediction of strength of stepped lap bonded joint with adhesive resin under tensile shear load ", JSME Int. J., Series 1, V. 33, N. 3, 1990, p.349

**MORI T., YU Q., TAKAHANA S. and SHIRATORI M.**, “ Low temperature strength of metal FRP bonded joints ”, ISME Int., Series I: V.34, N.2, 1991, p.257

**MORI T., YU Q. and SHIRATORI M.**, “ Strength of metal-FRP bonded joints under thermal cycle, Mechanical behavior of materials ”, Part VI, V.3, Kyoto Japan, 1991, p.41

**NAGARAJA Y.R. and ALWAR R.S.**, “ Nonlinear stress analysis of an adhesive tubular lap joint”, J.Adhes., V.10, 1979, p.97.

**NAKAGAWA F., NAKANO Y. and SAWA T.**, “ Two dimensional thermal stress analysis of butt adhesive joints containing rigid fillers ”, ISME Int., Series A: V.37, N.3, 1994, p.238

**NAKANO Y, SAWA T. and NAKAGAWA F.**, “ Two dimensional thermal stress analysis of butt adhesive joints ”, ISME Int., Series I: V.35, N.2, 1987, p.145

**NAKANO Y., SAWA T. and ARAI S.**, “ Stress analysis of an adhesive butt joint under torsional loads ”, Int.J.Adhes.Adhes., V.9, N.2, 1989, p.83.

**NAKANO Y., NAKAGAWA F. and SAWA T.**, “ Thermal stress in bonded joints subjected to uniform temperature change ”, EEP-V.4-1, Advances in Electronic Packaging ASME 1993, p.11

**NIELSON L.E and LENDEL R.F.**, “ Mechanical Properties of Polymers and Composites ”, (2<sup>nd</sup> edition, Marcel Dekker Publishers New York, 1994) p.377.

**NIELSEN L.E. and LEWIS T.B.**, J. Polym. Sci., A-27, 1969, p.1705 .

**O'CALLAGHAN P. and CALLAWAY K.**, “ Fiber orientation sensitivity study for SMC/metal scarf joints ”, 31st AIAA/ASME/ASCE/AHS/ASC Struct., Struct Dyna. Mater. Conference, Part 2, 1990, p.1234

**O'REILLY C.**, “ Designing bonded cylindrical joints for automotive applications ”, SAE

Trans. J. Mater. Manufac., Section 5, V.55, 1990, p.839

**OSSWALD T.A.**, "Measuring constitutive properties ", Adhesive and Sealant Engineered Materials Handbook", ASM Int., V.3, 1990, p.325

**LEWIS T.B and NIELSEN L.E.**, " Dynamic mechanical properties of particulate filled composites ", J. Appl. Polym. Sci., V.14, 1970, p.1449.

**PARKER B.M.**, "Some effects of moisture on adhesive bonded CFRP-CFRP joints ", Compos. Struct., V.6 N.1-3, 1986, p.123

**PENADO F.E. and DROPELE R.K.**, " Adhesives and Sealant Engineered Materials Handbook", ASM Int. V.3, 1990, p.477

**PETRIE E.M.**, " Plastics and adhesives as adhesives ", Handbook of Plastics and Elastomers, ed. C. A. Harper, McGraw-Hill, NY, 1975

**PERKER B.G. and HART-SMITH C.**, "Evaluating cure and shelf life of epoxy prepreps and film adhesive", Modern Plast., 1979, p.58

**PLASCZYNSKI T.**, " Advances in two part epoxy structural adhesives aimed at use on SMC spoilers with visible bond seams ", ASM Int. ESD Materials Park, Ohio, 1991, p.123

**PILAKOUTAS K., HAFEEZ S. and DRITOS S.**, " Residual bond strength of polymer adhesive anchored reinforcement subjected to high temperature", Mater.Struct./ Matériaux et Construction, V.27, N.173,1994, p.527

**PINHEIRO M.DE.F.F. and ROSENERG H.M.**, " Thermal expansion of epoxy resin/particle composites- A size effect ", J. Polym. Sci., Polym. Phys. ed., V.18, 1980, p.217

**PITRONE L.R.**, "Thermal analytical techniques for the determination of structural adhesive cure state and bonded joint performance ", 5th Int. Joint Military/Government Industry

Symposium on Structural Adhesive bonding, Dover New Jersey, 1987, p. 359

**RAGHAVA R.S.**, " Thermal expansion of organic and inorganic matrix composites: A review of theoretical and experimental studies ", Polym. Compos., V.9, N.1, 1988, p.1

**REEDY E.D., JR. and GUESS T.R.**, " Composite to metal tubular lap joints: Strength and fatigue resistance ", Int. J. Fract., V.63, 1993, p.351, also SED-V.14, Wind Energy, ASME 1993

**REEDY E.D., JR.**, " Asymptotic interface corner solutions for butt tensile joints ", Int. J. Solid. Struct., V.30, N.6, 1993, p.767

**REEDY E.D., JR. and GUESS T.R.**, " comparison of butt tensile strength data with interface corner stress intensity factor prediction ", Int. J. Solid. Struct., V.30, N.21, 1993, p.2029

**REEDY J.N. and ROY S.**, " Finite element analysis of adhesive joints ", Adhesive Bonding, ed. L. H. Lee, Plenum Press NY, 1991, p.359

**RENTON W.J. and VINSON J.R.**, " Analysis of adhesively bonded joints between panels of composite materials ", J. Appl. Mech. Trans. ASME, 1977, p.101

**RIDGE D.H.**, " Physical Chemistry of Adhesion ", Willey- Interscience, 1971

**RIX C. and EASTLAND C.**, "Cryogenic and thermal cycling behavior of adhesive materials ", 21st Int. SAMPE, Advanced Materials: The big pay-off, Atlantic city New Jersey, 1989, p.21

**ROSS M.C., WEGMAN R.F., BODNAR M.J. and TANNER W.C.**, " effect of surface exposure time on bonding of aluminum alloys ", SAMPE J., V.10, 1974, p.4

**ROSSETTOS J.N., PENG Y. and NEYEB-HASHEMI H.**, " Analysis of adhesively

bonded composite joints with voids and thermal mismatch ", M-DV.29, Plast. Plast. Compos.: Mater. Proper., Part perform. Proc. Simul. ASME, 1991, p.259

**ROSSETTOS J.N., PENG Y. and NEYEB-HASHEMI H.**, " Comparison of the effects of debonds and voids in adhesive joints ", J. Eng. Mater. Tech., Trans. ASME, V.116, 1994, p. 533

**RUSH H.F JR. and FIRTH G.C.**, Initial investigation of cryogenic wind tunnel model filler materials ", Welding and Fastening, Hampton Virginia, 1984, p. 465, also NASA report N85-18069, 1985.

**SANBORN J.A. and MOREL D.E., JR.**, " Effect of thermal cycling on the mechanical and physical properties of space qualified epoxy adhesive ", J. Reinf. Plast. Compos., V.27, N.2, 1988, p.155

**SATO C. and IKEGAMI K.**, " Tensile strength of adherend shaft joints between CFRP tube and stainless steel at low temperature ", ISME Int., Series A: V.37, N.3, 1994, p.282

**SAWA T., NAKANO Y. and TEMMA K.**, " A stress analysis of butt adhesive joints under torsional loads ", J. Adhes., V.24, 1987, p.245

**SAWYER J.W. and COOPER P.A.**, " Analytical and experimental results for bonded single lap joints with performed adherends ", AIAA J., V.19, N.11, 1981, p.1443

**SEGAL E. and ROSE J.L.**, " Nondestructive testing techniques for adhesive bond joints ", Research Techniques in Nondestructive testing, V. IV, ed. R. S. Sharpe Academic Press Inc. London, 1980, p.275.

**SEMERDJIER S.**, "Metal to Metal Adhesive Bonding", ed. S. Semerdjier Business Books London, 1970, p.55

**SHACKELFORD J.F., ALEXANDRE W. and PARK J.S.**, "CRC Materials Science

and Engineering Handbook", (CRC Press Inc. 1994).

**SHARPE L.H.**, "The materials, processes and design methods for assembly with adhesives", Machine Design, V.38, N.19, 1966, p.179

**SUGIBAYASHI T., MATSUO K., KYOGOKU H. and IKEGAMI K.**, "Strength design of the thin walled butt joint bonded with adhesive resin between dissimilar adherends", Nippon Kikai Gakkai Ronbunshi, Trans. J. Soc. Mech. Eng., Part A, V. 52, N.476, 1989, p.1043

**SUZUKI Y.**, "Adhesive tensile strengths of scarf and butt joint of steel plates (Relation between adhesive layer thickness and adhesive strengths)", JSME Int., Series I: V.30, N.265, 1987, p.1042

**THOMPSON R.B. and THOMPSON D.O.**, "Past experiences in the development of tests for adhesive bond strength", J. Adhes. Sci. Tech., V.5, N.8, 1991, p. 583

**TSAI M.Y. and MORTON J.**, "Three dimensional deformation in a single lap joint", J. Strain Analy., V. 29, N. 1, 1994, p.137

**VOLKERSEN O.**, "Die nietkraftverteilung in zugbeanspruchten nietverbindungen mit konstanten laschenquerschnitten", Luftfahrtforschung, V.15, 1938, p.41

**VOLKERSEN O.**, "Recherches sur la théorie des assemblages collés", Construction Métallique, N.4, 1965, p.3

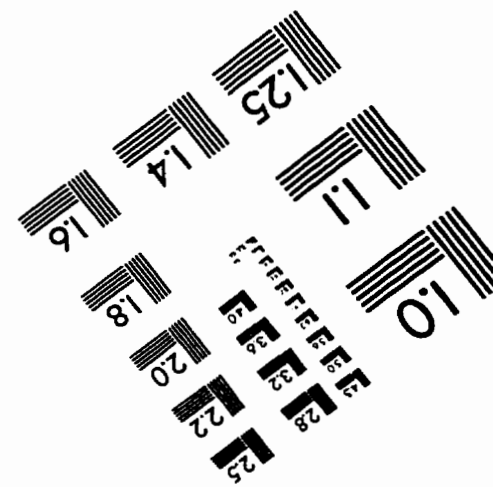
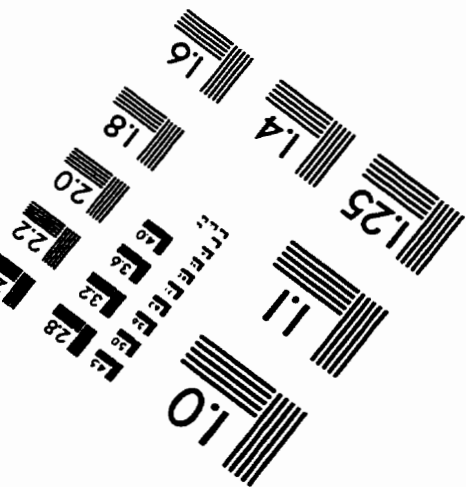
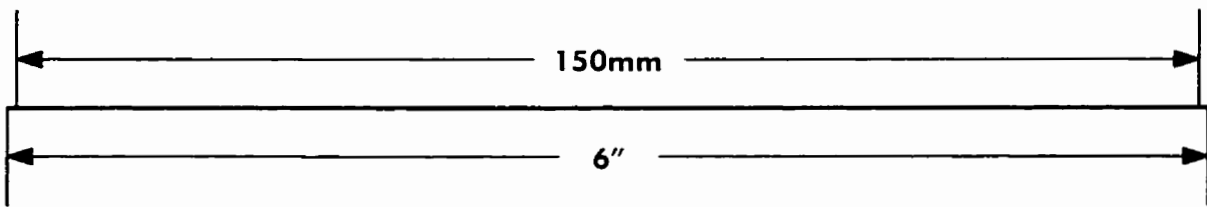
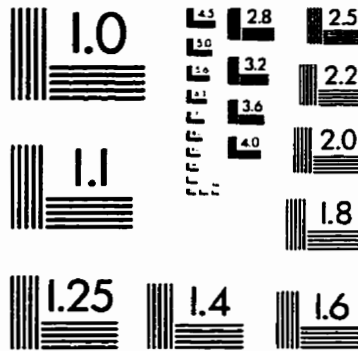
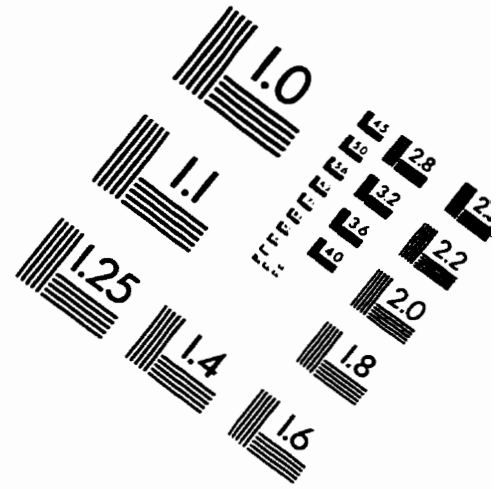
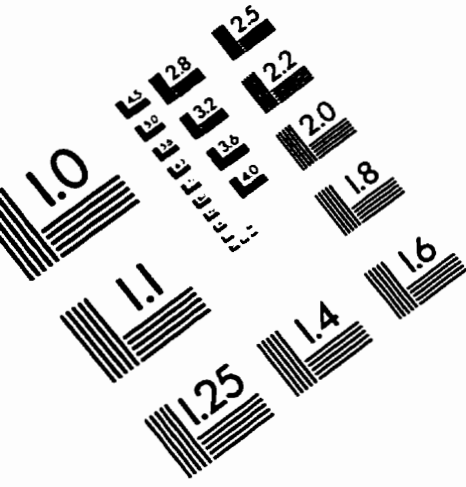
**YU Q., SHIRATORI M. and MORI T.**, "Nonsteady thermal stress analysis and thermal fatigue strength of metal-CFRP bonded joints", JSME Int., Series A: V.36, N.1, 1993, p.43

**ZANNI-DEFFARGES M.P. and SHANAHAN M.E.R.**, "Evaluation of adhesive shear modulus in a torsional joint: Influence of ageing", Int. J. Adhes. Adhes., V.13, N.1, 1993, p.41

- ZDAMIENSKI W.A., COMWAY J.C. and KIRCHNER H.P.**, “ Effect of joint thickness and residual stresses on the properties of ceramic adhesive joints: II, experimental results ”, *J. Amer. Ceram. Soc.*, V.70, N.2, 1987, p.110
- ZISMAN W.A.**, “*Adhesion and Cohesion* ”, ed. P. Weiss, 1962
- ZIHLIF A.M., FELDMAN L. and FARRIS R.J.**, “ Modification of polymer properties to minimize thermal stresses in adhesive joints ”, *J. Mater. Sci.* V.24, N.9, 1989, p.3267
- ZUKAS W.X. and WONG H.H.**, “ Cure monitoring of adhesives ”, *ANTEC 1987*, p.1051
- WILLIAMS H.E.**, “ Asymptotic analysis of the thermal stresses in a two layer composite with an adhesive layer ”, *J. Therm. Stress*, V.8, 1985, p.183
- WILLIAMS J.W. and BOERIO**, “A model for predicting the durability of lap shear joints primed with silanes ”, 37th Annual conference, Reinforced Plastics/Composite Institute Session 2-D, SPE Inc., 1982, p.1



# IMAGE EVALUATION TEST TARGET (QA-3)



APPLIED IMAGE, Inc.  
1653 East Main Street  
Rochester, NY 14609 USA  
Phone: 716/482-0300  
Fax: 716/288-5989

© 1993, Applied Image, Inc., All Rights Reserved